EVALUATION OF NATURALLY OCCURRING OPIOIDS AND SYNTHETIC DERIVATIVES FOR THERAPEUTIC APPLICATION IN ALCOHOL ABUSE AND PAIN

by

Anna Marie Gutridge

A Dissertation

Submitted to the Faculty of Purdue University

In Partial Fulfillment of the Requirements for the degree of

Doctor of Philosophy

Department of Medicinal Chemistry and Molecular Pharmacology

West Lafayette, Indiana

December 2021

THE PURDUE UNIVERSITY GRADUATE SCHOOL
STATEMENT OF COMMITTEE APPROVAL

Dr. Richard van Rijn, Co-chair

Department of Medicinal Chemistry and Molecular Pharmacology

Dr. Andrew Hudmon, Co-chair

Department of Medicinal Chemistry and Molecular Pharmacology

Dr. Susan Sangha

Department of Psychological Sciences

Dr. Benita Sjogren

Department of Medicinal Chemistry and Molecular Pharmacology

Approved by:

Dr. Zhong-Yin Zhang

To all those who have inspired me to see the beauty and magic in life,
for I have found that science is magic made real.

ACKNOWLEDGMENTS

I would like to express my deepest appreciation to my research advisor, Dr. Richard van Rijn, for his guidance and constant mentorship in my graduate studies. I am extremely grateful for his patience, empathy, and dedication towards helping his students, and for his scholarly expertise and constructive feedback that have shaped the scientist and professional I am today. I would also like to extend my gratitude to my advisory committee— Dr. Andy Hudmon, Dr. Susan Sangha, and Dr. Benita Sjogren— for their encouragement and insightful suggestions. Additionally, I am very fortunate to have had wonderful female role models throughout my science education; I would like to thank Dr. Tami Fitzgerald, Dr. Margaret Goodman, Dr. Leanne Petry, and Veronica Betancur for their mentorship— your pursuit and achievement of higher education inspired me in my own.

Thank you to all members of the van Rijn lab with whom I have had the pleasure of working, including Dr. Meridith Doyle, Dr. Meejung Ko, Dr. Alex French, Robert Cassell, Arryn Blaine, Yazan Meqbil, Jinling Yuan, and my past and present undergraduate research assistants Elizabeth Rhoda, Hawk Royer, Maria Shelley, and Haoyue Cui. Your friendship, support, and advice along the way has guided and brightened my graduate experience. I wish you each the best in your future endeavors and, most importantly, I hope your next office space has a window.

Many thanks are owed to my collaborators (and their labs): Dr. Andrew Riley at the University of Illinois Chicago, and Dr. Susruta Majumdar at Washington University in St. Louis, without whom this research would not have been possible. I would also like to thank the American Foundation of Pharmaceutical Research for partial funding of my graduate studies.

To my family (Gutridge, Ferland and Rodgers)— thank you for the support you have provided during this journey. I am most appreciative of the endless coffee whenever I came to visit. To my parents especially, thank for the sacrifices you have made that supported my education and future, and for encouraging me to follow my dreams. The achievements of Katie, Sarah, Paul, and myself are a direct reflection of the work ethic and tenacity you have imbued upon us.

Last and most importantly, I would like to express my gratitude to my husband, Travis Rodgers, for his constant support, love, and unfailing faith my abilities. Thank you joining me on this adventure, and simply for being there, always.

TABLE OF CONTENTS

LIST OF TABLES

LIST OF FIGURES

LIST OF EQUATIONS

LIST OF COMMON ABBREVIATIONS

ANOVA analysis of variance

AUD Alcohol Use Disorder

cAMP cyclic adenosine monophosphate

CNS Central nervous system

CPA conditioned place aversion

CPP conditioned place preference

EtOH ethanol

FDA Food and Drug Administration

GABA γ-aminobutyric acid

GIRK G-protein-coupled inward rectifier potassium channel

GPCR G-protein coupled receptor

GRK G-protein receptor kinase

i.p. intraperitoneal

KO knock-out

MC multiple comparisons

MPE maximum possible effect

MTD maximum tolerated dose

OR opioid receptor

p.o. per os

RM repeated measures

s.c. subcutaneous

SEM standard error of the mean

WT wildtype

βarr1 β-arrestin1

βarr2 β-arrestin2

δOR delta opioid receptor

κOR kappa opioid receptor

μOR mu opioid receptor

ABSTRACT

Historically, natural products from plants, fungi, bacteria and animals have played an important role in the discovery of new drugs. In fact, it has been found that 34% of new FDA-approved drugs over the last 30 years were derived from natural products or their derivatives. Because of the chemical and structural diversity of natural products, they continue to be one of the best options for discovering novel compounds and scaffolds; this is especially true for compounds targeting the μ-, δ-, and κ- opioid receptors. However, traditional opioids such as morphine cause many therapeutically limiting side effects. Therefore, there have been immense efforts to develop opioids that avoid these side effects, with "signal-biased" compounds being an intense area of interest. The research presented here investigates of the biased mechanisms of compounds found in and derived from *Mitragyna speciosa,* also known as kratom, and *Picralima nitida,* also known as akuamma. Kratom and akuamma compounds are examined for their therapeutic potential in treating alcohol abuse and pain, respectively, two prevalent conditions with extreme societal and economic costs.

CHAPTER 1. INTRODUCTION

1.1 G-protein coupled receptors background

1.1.1 Historical relevance of GPCRs

G-protein-coupled receptors (GPCRs), also known as 7-transmembrane receptors, are a ubiquitous and versatile superfamily of receptors that translate extracellular signaling into intracellular signal transduction within cells. The largest family of receptors, the GPCR superfamily consist of over 800 family members identified by the human genome project, with about half of these belonging to the olfactory system (Fredriksson et al., 2003; Lagerström and Schiöth, 2008). These receptors consist of 7 transmembrane helices and make up about 13% of all membrane proteins in the human body (Muratspahić et al., 2019). Corresponding to their expansive expression and distribution, GPCRs regulate many physiological processes and display broad therapeutic application across several diseases (Pierce et al., 2002; Rosenbaum et al., 2009). This therapeutic relevance, as well as their drug-accessibility on cell membranes, has made them key pharmacological targets, and currently about 34% of Food and Drug Administration (FDA)-approved drugs target GPCRs (Hauser et al., 2017). Further underscoring the importance of studying this expansive class of receptors is the award of the 1994 Nobel Prize in Physiology or Medicine to Dr.'s Martin Rodbell and Alfred G. Gilman for their work on G-proteins and their signal transduction, as well as the 2012 Nobel Prize in Chemistry to Dr.'s Brian Kobilka and Robert Lefkowitz for their contributions to the field of GPCR research.

1.1.2 GPCR signal transduction

Analogous to the diversity of this receptor family is the variety of compounds these receptors can be activated by, consisting most commonly of small molecules and peptides. Dependent on the ligand, receptor conformation can change to induce signaling cascades within the cell. The main pathway of signaling at GPCRs occurs through their associated G-protein. G-proteins are heterotrimeric proteins that consist of three subunits: Gα, Gβ, and Gγ, listed in order of decreasing size (Connor and Christie, 1999). This heterotrimeric protein consists of two functional units, the Gα subunit and Gβ-Gγ dimer. In its inactive state, the Gα subunit of the

heterotrimeric protein is bound to guanosine diphosphate (GDP). However, in response to a ligand-induced change in receptor conformation, the Gα subunit exchanges GDP for guanosine triphosphate (GTP) through its inherent guanine nucleotide exchange factor (GEF) activity, and dissociates from the Gβ-Gγ dimer (Oldham and Hamm, 2008). In this activated state, both the Gα subunit and Gβ-Gγ dimer are capable of conducting independent signaling cascades (Khan et al., 2013). The active G-protein is returned to an inactive state when GTP is hydrolyzed to GDP by GTPase activity that is inherent to the Gα subunit, which results in the reassociation of the heterotrimeric subunits (Wettschureck and Offermanns, 2005).

Adding another layer of functional diversity in the GPCR signaling system are the numerous families of Gα-subunits. G-proteins can be divided into four families based on the signaling properties of the Gα subunit: Gαi/o, Gαs, Gαq/11, and Gα12. Additionally there are several subtypes within each family (Cabrera-Vera et al., 2003). The Gαi/o subfamily is comprised of five members: three Gαi subtypes termed Gαi1, Gαi2, and Gαi3, two Gαo subtypes termed GαoA and GαoB, and Gαz. The Gαs subfamily is made up of two Gαs subtypes, Gαs(S) and Gαs(L), and Gαolf. The Gαq family has four members: Gαq, Gα11, Gα14, and Gα15/16, and the Gα12 family has two subtypes: Gα12 and Gα13. Furthermore, there are five Gβ subtypes (Gβ1-5) and twelve Gγ subtypes (Gγ1-12) that can pair into several unique Gβ-Gγ dimers capable of eliciting multifold signaling effects, summarized well in Cabrera-Vera et al. (Cabrera-Vera et al., 2003; Smrcka, 2008).

When activated, Gαi and Gαs have opposing roles in modulating the activity of adenyl cyclase, a ubiquitous enzyme that is responsible for generating cyclic adenosine monophosphate (cAMP). So named for their inhibitory and stimulatory properties, Gαi inhibits adenylyl cyclase resulting in decreased cAMP production, whereas Gαs stimulates adenylyl cyclase to cause an increase in cAMP production (Sunahara et al., 1996; Wettschureck and Offermanns, 2005). The actions of Gαo are less clear, but generally the signaling mediated by this subunit is defined by its Gβ-Gγ dimer (Wettschureck and Offermanns, 2005). When activated, the Gαq/11 subfamily of G-proteins activate β-isoforms of phospholipase C, which increases the production of cleavage products inositol triphosphate and diacylglycerol in the cell (Rhee and Bae, 1997). Lastly, Gα12/13 subfamily has been shown to bind and activate Rho proteins, another class of effectors with GEF activity, and tyrosine kinases (Kozasa et al., 1998). Although not explored in detail here, in addition to the signal transduction through Gα subunits, the Gβ-Gγ dimer can also interact and

regulate activity of adenylyl cyclase, phospholipase Cβ, and K+ and Ca2+ channels, and does so most often through dissociation from Gαi/o subunits in particular due to the relatively higher expression of Gαi families in cells (Ciaraldi and Maisel, 1989; Wettschureck and Offermanns, 2005; Khan et al., 2013; Syrovatkina et al., 2016).

One reason that some favor the name "7 transmembrane receptor" over "GPCR" is that GPCRs do not only couple to G-proteins to initiate intracellular signaling. An increasingly appreciated role in GPCR signal transduction is played by arrestins. Arrestin proteins are effector proteins with four family members: visual arrestin, cone arrestin, and β-arrestin 1 and 2 (sometimes referred to arrestin 2 and 3). Non-visual arrestins (β-arrestin 1 and 2) are of primary focus in this dissertation and from here on will only be referred to as β-arrestin 1 and 2, or generally as β-arrestin proteins. These two proteins are ubiquitously expressed and initially demonstrated the ability to desensitize, internalize, and recycle GPCRs (Seyedabadi et al., 2021), and are thus named for their capacity to "arrest" GPCR signaling (Lefkowitz, 2013). In addition to the properties which defined their initial characterization, β-arrestins are now known to be multifunctional effector proteins that can form interactions with many kinases and other proteins, leading to phosphorylation events for various intracellular targets and initiation of specific signaling cascades (Reiter et al., 2012). The β-arrestin proteins are recruited to the intracellular, C-terminal tail of a GPCR after it has been phosphorylated. This phosphorylation is primarily catalyzed by proteins known as G-protein receptor kinases (GRKs), but other kinases such as protein kinase A and C (PKA and PKC) can also play a role. From here, β-arrestin proteins can be involved in signal termination by contributing to receptor internalization efforts with clathrin and associated adaptor proteins or can initiate aforementioned signal transduction cascades (Claing et al., 2002; Sorkin and von Zastrow, 2009). If internalized, the receptor can be recycled back to the membrane or targeted for degradation via lysosomes. This internalization process is an important regulatory step in controlling receptor desensitization and resensitization (Ritter and Hall, 2009). There is now more and more evidence that receptors can selectively activate signaling pathways associated with G-proteins or β-arrestin proteins via distinct conformational states; this concept is known as functional selectivity or signaling bias and will be explored in more detail in section 1.3 with respect to a specific family of receptors (Urban et al., 2007). These GPCR signaling pathways and their downstream effects are summarized in **Figure 1.1**.

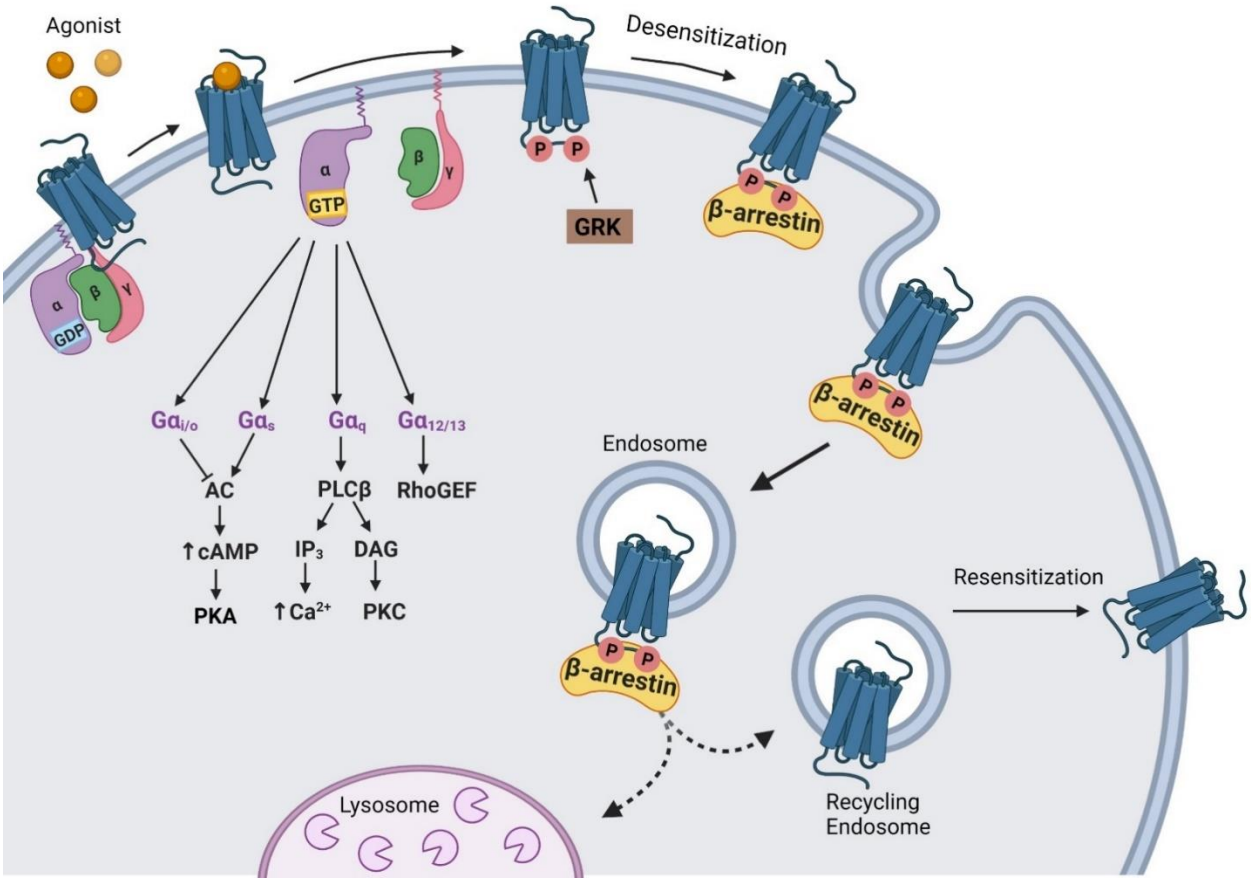

Figure 1.1 General GPCR signal transduction pathways

As described in section 1.1.2, GPCR activation by an agonist can result in several downstream signaling pathways. Gα subtypes can elicit distinct signaling cascades, as well at the Gβ-Gγ dimer (not depicted here). The receptor can be desensitized by receptor phosphorylation by kinases, potentially leading to β-arrestin associated internalization. Depending on the receptor type and interaction with other proteins such as β-arrestins, the receptor can be degraded in lysosomes or recycled back to the membrane. GRK: G-protein receptor kinase, AC: adenylyl cyclase, PKA/PKC: protein kinase A or C, PLCβ: protein lipase Cβ, IP_3: inositol triphosphate, DAG: diacylglycerol, P: phosphorylation. This figure was designed using Biorender.com based on graphics in (Ritter and Hall, 2009).

1.1.3 General GPCR Pharmacology

GPCRs tend to have some level of basal activity in cells, also known as constitutive activity, due to spontaneous adoption of active conformations in the absence of ligand (Berg and Clarke, 2018). Generally, a GPCR ligand is classified as an agonist or antagonist based on the response it produces relative to this constitutive receptor activity. Both ligand types will bind the receptor with good affinity, but agonists will stabilize the receptor in an active conformation to produce an effect

greater than that of the receptor's basal activity. An agonist that elicits the receptor's maximum possible effect, or efficacy, is known as a full agonist. An agonist that displays anything less than full efficacy is known as a partial agonist. In contrast to agonists, antagonists will stabilize the receptor in an inactive conformation to block receptor signal transduction. Because an antagonist blocks receptor response, in this context they do not have efficacy. Like antagonists, inverse agonists will block a receptor effect, but will reduce receptor activity below that of its basal activity (inverse action of a classical agonist.)

Additionally, in the context of constitutive activity, the idea of protean agonists was hypothesized by Kenakin and was named after Greek god Proteus who had shape shifting abilities (Kenakin, 2001). Protean agonists are hypothesized to change behavior based on the system in which they are acting, and the concept of protean agonism is dependent on the assumption that multiple active states of a receptor exist (Kenakin, 2001; Hill, 2006). For instance, in a system with a high proportion of constitutively active, high-efficacy receptors, a protean agonist may lead to activation of active but lower-efficacy receptor forms, with the net effect being inverse agonism. In contrast, in a system with no constitutive activity (quiescent), the protean agonist would increase active forms of a receptor, with the net effect being agonism. The idea of protean agonism and the assumption of multiple active states becomes relevant when describing functional selectivity in section 1.3. In addition to efficacy, potency is another parameter to compare ligand activity, and can be loosely defined as the concentration or dose needed for a ligand to produce its effect. These pharmacological behaviors and parameters are represented graphically in **Figure 1.2**.

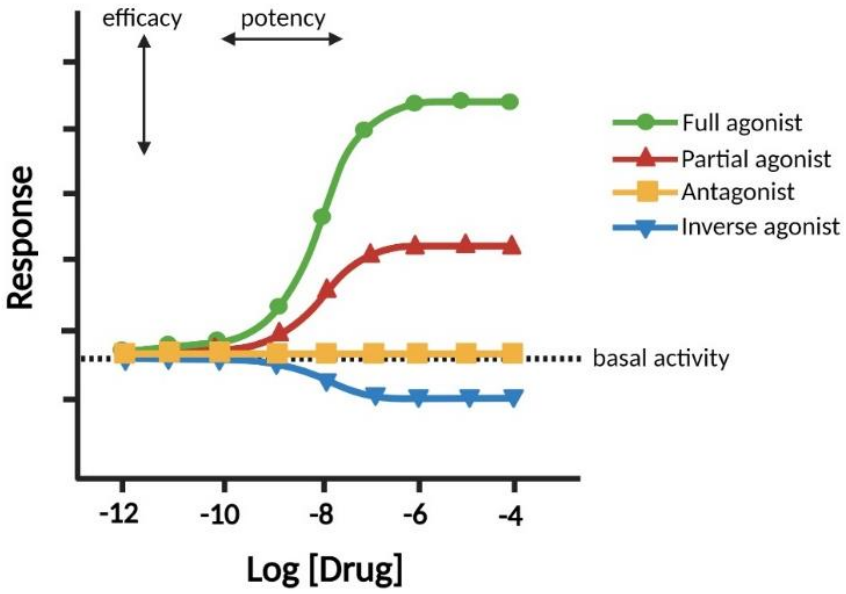

Figure 1.2 Overview of pharmacology concepts.

A graphical illustration of classic pharmacology where drug potency is graphed on the x-axis (drug concentration), and response (a measure of efficacy) on the y-axis. A full agonist increases receptor response above basal activity to a maximum possible response. A partial agonist increases receptor response less than a full agonist. By itself, a neutral antagonist does not increase or decrease response of the receptor; however, in the presence of other compounds it but can blunt responses. An inverse agonist reduces basal response of the receptor. Drug potency is typically measured as the concentration needed to inhibit or elicit a 50% maximal response (IC_{50}/EC_{50}). This figure was created using BioRender.com.

1.2 Opioid Receptors are one of the most-studied families of GPCRs

1.2.1 Discovery of opioid receptors

One of the most widely known compounds to interact with a GPCR is morphine, an opioid used for centuries to treat pain. Morphine was first isolated by chemist Friedrich Wilhelm Serturner in 1805 from opium poppies (Schmitz, 1985), who, based on morphine's side effects, named it after the god of dreams, Morpheus (Scott, 1969). Elucidating the structure of morphine led to the development of heroin, a synthetic opioid, which was more potent than morphine and likewise was unfortunately more effective at causing the development of addictive behaviors. In the early 20th century, growing concern over increased opiate use and addiction developed worldwide, and so, though initially hailed as a cure-all for man's ills, acclamation for opioid use was upended. This culminated in the Harrison Narcotics Act of 1914 that instituted regulations on production,

distribution, and import of opium compounds and derivatives (Das, 1993). Further regulations were imposed in 1971 in President Nixon's "war on heroin" which made additional funding available for drug abuse research centers (Snyder and Pasternak, 2003).

This funding supported an exciting time in opioid research. While the presence of discrete receptors for opioids was suggested earlier, the existence of opioid receptors was proven in 1973 by three separate research groups using radioligand binding experiments on brain homogenates (Pert and Snyder, 1973; Simon et al., 1973; Terenius, 1973). Three types of opioid receptors were identified, termed μ-, δ-, and κ- opioid receptors (μOR, δOR, and κOR, respectively) and were classified based on differences in their radioligand binding profiles. Shortly after, endogenous opioid peptides cleaved from precursor proteins were discovered and termed enkephalins, endorphins, and dynorphins (Hughes et al., 1975; Nakanishi et al., 1979; Kakidani et al., 1982; Day et al., 1993; Zadina et al., 1999). The enkephalins preferentially bind to δORs but also have affinity for μORs (Kosterlitz, 1985). In contrast, dynorphins have modest selectivity for κORs, and endomorphins generally have preferential affinity for μORs (Chavkin et al., 1982; Raynor et al., 1994).

In the 1980s the genes encoding the opioid receptors were identified, and in the 1990s these genes were cloned and termed as the Oprm1, Oprd1, and Oprk1 genes (corresponding to μOR, δOR, and κOR, respectively) (Evans et al., 1992; Kieffer et al., 1992; Chen et al., 1993; Minami et al., 1993; Thompson et al., 1993; Wang et al., 1993).The three opioid receptors share a high degree of sequence homology, approximately 60%, with the most homology occurring within the transmembrane helices, intracellular domains, and opioid binding pocket (Minami and Satoh, 1995; Décaillot et al., 2003), and the least occurring in extracellular domains (Kane et al., 2006). μOR, δOR, and κOR are considered the classical members of the opioid receptor family and are all sensitive to the antagonistic effects of naloxone (McDonald and Lambert, 2015). A fourth member of the opioid receptor family, the nociceptin opioid receptor (NOR; also referred to the nociceptin opioid-like receptor), was discovered in 1994 and shares sequence homology with μOR, δOR, and κOR (Mollereau et al., 1994). However, NOR is not considered a "classical" opioid receptor because is not sensitive to naloxone (Lambert, 2008). Moving forward, this dissertation will focus only on the effects and clinical relevance of the classical opioid receptors μOR, δOR, and κOR.

1.2.2 Opioid receptor expression & related effects

As indicated by their discovery in brain homogenates, opioid receptors are primarily expressed in the central nervous system (CNS), but also have some enteric expression (Le Merrer et al., 2009). The enteric expression of opioid receptors is what underlies the gastrointestinal side effects related to opioid use such as constipation (Mori et al., 2013), but the focus here will be on key areas of receptor expression in the brain. Briefly, ORs are predominately expressed in brain regions involved in pain-modulating pathways including the locus coeruleus, medulla, and periaqueductal grey (Le Merrer et al., 2009). Expression is also observed in cortical, midbrain, and limbic structures (Le Merrer et al., 2009). Although ORs are expressed both pre- and post-synaptically in neurons, their most well-defined mechanism of action in the context of analgesia involves presynaptic inhibition of neuron firing and neurotransmitter release, which mitigates pain transmission in the spinal cord (Ossipov et al., 2010). However, OR expression in other brain regions such as the ventral tegmental area, nucleus accumbens, striatum, and habenula mediate undesirable opioid side effects such as reward and addiction (Al-Hasani and Bruchas, 2011; Valentino and Volkow, 2018).

The opioid receptors are also expressed in brain regions that are associated with regulation of mood and affect. Affect, broadly defined for the purposes of this dissertation, is the experience of any feeling or emotion (Barrett and Bliss-Moreau, 2009). In regards to specific expression, the δOR is highly expressed in the hippocampus, prefrontal cortex, and amygdala, all which contribute to circuitry regulating emotional response (Chu Sin Chung and Kieffer, 2013). The μOR and κOR have similar expression throughout the brain but their high expression in the nucleus accumbens underlies their opposing roles in modulation of hedonic homeostasis, or pleasurable experiences (Spanagel et al., 1992; Le Merrer et al., 2009). The μOR promotes euphoria by promoting dopamine release in the nucleus accumbens whereas the κOR induces dysphoria through inhibiting dopamine release in this region (Spanagel et al., 1992). The roles of each of the opioid receptors in the modulation of mood and hedonic homeostasis is summarized in **Figure 1.3**.

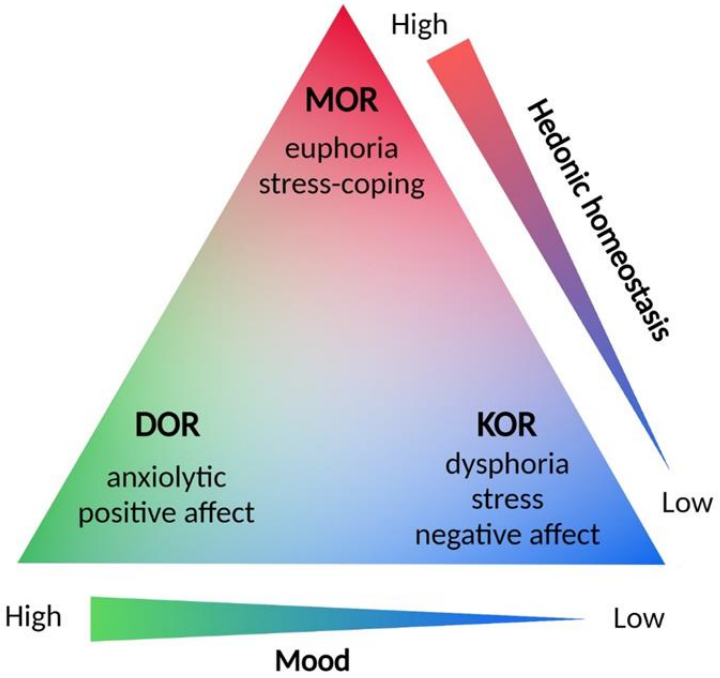

Figure 1.3 Opioid regulation of mood and hedonic homeostasis

The opioid receptors modulate opposite responses in mood and hedonic measures, with the κOR on the "low" ends of both continuums, promoting dysphoric effects, stress, and negative affect. On the "high" ends of spectrums, the δOR promotes positive affect and is anxiolytic whereas the μOR can produce euphoria and is promotes stress coping. These effects have been well documented through pharmacological studies and genetic models. This figure was adapted from (Valentino and Volkow, 2018) and created using Biorender.com.

1.2.3 Significance in studying opioid receptor signaling

Opioid receptors are primarily coupled to Gαi proteins, a member of the Gαi/o subfamily that is notably sensitive to pertussis toxin (Minneman and Iversen, 1976; Standifer and Pasternak, 1997). As mentioned previously, Gαi proteins inhibit the actions of adenylyl cyclase, thereby decreasing levels of cAMP in the cell. The reduction in available cAMP decreases the activity of cAMP-dependent kinases such as PKA, which is one mechanism by which opioids can decrease neurotransmitter release (Greengard et al., 1991). In addition to this, the Gβ-Gγ dimer can interact and activate G-protein gated inwardly rectifying potassium channels (GIRKs), hyperpolarizing the cell (Williams et al., 1982; North and Williams, 1985; Torrecilla et al., 2002). Furthermore, the Gβ-Gγ dimer can also bind directly to calcium channels, providing additional contribution to cell hyperpolarization (Mudge et al., 1979; Rusin et al., 1997). Through these coordinated intracellular events, pain-modulating neurons expressing activated opioid receptors become less excitable, and

the propagation of action potentials is reduced (Pepper and Henderson, 1980; Vaughan and Christie, 1997). This decrease in neuron excitability translates to an inhibition of pain transmission, and thus each member of the opioid receptor family can produce analgesic responses although with varying degrees of efficacy and different sites of action (Schröder et al., 2014; McDonald and Lambert, 2015).

Once opioid receptors are activated and the associated Gαi protein is displaced, receptor phosphorylation can occur, primarily by GRK2 and GRK3 (Lemel et al., 2020). This leads to recruitment of β-arrestin 1 and/or 2, both highly expressed in the brain (Attramadal et al., 1992; Gurevich et al., 2002), which can then lead to receptor desensitization, internalization, and unique cellular responses. When internalized, the μOR is generally redistributed back to the cell membrane, whereas δORs are largely targeted towards degradation pathways (Henry et al., 2011; Nagi and Piñeyro, 2011; Pradhan et al., 2012). It is believed that receptor phosphorylation plays a role in receptor desensitization, or reduced responsiveness to a ligand, and that β-arrestins may mediate receptor resensitization (Cahill et al., 2016). In addition, phosphorylated β-arrestin-bound opioid receptors can induce alternate downstream signaling cascades such as the mitogen-activated protein kinase (MAPK) cascade, which consists of extracellular signal regulated kinase 1 and 2 (ERK1/2), p38, and c-Jun N-terminal kinase 1-3 (JNK1-3) (Bruchas et al., 2006; Macey et al., 2006; Eisinger and Ammer, 2008; Al-Hasani and Bruchas, 2011). This can regulate several cellular processes such as cell differentiation, cell proliferation, ion channel regulation, protein scaffolding, and neurotransporter regulation (Raman et al., 2007).

The therapeutic relevance of opioid receptors, described in more detail below, coupled with their well-characterized research methods makes them excellent targets to study pharmacology and drug activity. Additionally, due to drug discovery efforts there exists a multitude of ligands for each of the opioid receptors with differing potencies, efficacies, and selectivities (Eguchi, 2004). Accordingly, subtle differences in structure between compounds acting as agonists and antagonists have been studied extensively with opiates (Snyder and Pasternak, 2003). Furthermore, since safer analgesics have been sought for decades, there exists many behavioral models and paradigms designed to evaluate therapeutic efficacy and side effects. The opioid receptors therefore have well-defined behavioral correlates of receptor activation such as antinociception (analgesia in animals), tolerance, reward, locomotion, and respiratory depression that have been characterized more than other classes of receptors or drugs (Snyder and Pasternak, 2003). In review,

the therapeutic relevance, behavioral correlates of receptor activation, and ligand diversity of opioid receptors thus makes them ideal to study— not only for the development of better pharmacological therapies, but also for the insights they can provide in receptor pharmacology.

1.2.4 Clinical applications and limitations in targeting opioid receptors

Congruent with their expression in the brain and in gut, opioids are currently being investigated as treatments for a host of central diseases and conditions as well as those that are enteric. To direct the topic discussed here to a focus relevant to this dissertation, only centrally mediated diseases and conditions will be discussed. To refine further, this section will describe the primary clinical relevance and current and past efforts of targeting each classical opioid receptor, and limitations that exist therein. In the absence of approved clinical use, relevant ongoing clinical trial investigations are discussed.

Mu opioid receptor

Although all opioid receptor family members can elicit analgesic responses, the clinical gold standard for acute pain treatment are agonists for the μOR such as morphine, oxycodone, and fentanyl (Al-Hasani and Bruchas, 2011). Several μOR agonists have been approved for use in the U.S.; due to their similar mechanism of action, not all of these agonists will be discussed in the text. Several side effects accompany opioid use, and briefly, the most concerning central effects of short-duration μOR agonism are euphoria, sedation, nausea, and respiratory depression (Al-Hasani and Bruchas, 2011). Because of the efficacy of μOR agonists in providing analgesia, however, these side effects are usually tolerated during short-term administration, or mitigated with additional pharmaceutical intervention such as anti-nausea medication (Benyamin et al., 2008). While agonism of the μOR is a useful therapy in brief pain management, this approach is not as useful for the treatment of long-term, chronic pain conditions such as palliative cancer care, lower back pain, and arthritis due to side effects that develop with extended use (Ruiz-Garcia and Lopez-Briz, 2008; Witkin et al., 2017). Long term use of μOR agonists is accompanied by side effects such as tolerance, addiction, and hyperalgesia, with tolerance to μOR agonists driving dose escalation (Volkow et al., 2018). While tolerance to most opioid side effects can develop with chronic use, tolerance does not develop at the same rate or to the same degree across responses

(Volkow et al., 2018). Importantly, analgesic tolerance tends to develop more quickly than tolerance to respiratory depression (Ling et al., 1989; Hill et al., 2016), which elevates the risk of opioid overdose with dose escalation (Volkow et al., 2018). To reduce the tolerance side effects related to long-term opioid use, opioid rotation can sometimes be helpful for the patient (Benyamin et al., 2008).

Tolerance and risk of addiction are some of the biggest challenges in opioid treatment, and these effects, along with opioid overprescribing, ultimately led to the ongoing national opioid crisis (Makary et al., 2017), where opioid overdoses (prescription or illicit) claim the lives of over 100 U.S. citizens per day (Hedegaard et al., 2017). Additionally, 1.4 million people in the U.S. were estimated to have a substance use disorder associated with prescription opioids in 2019 (Substance Abuse Center for Behavioral Health Statistics and Quality, 2020). Despite new prescribing guidelines in 2016 and an overall decrease in opioid prescriptions (Dowell et al., 2016; Guy, 2017; Pezalla et al., 2017; Bohnert et al., 2018), drug overdoses have continued to increase in the U.S. and are primarily driven by opioid overdoses (National Institute on Drug Abuse, 2021). The unique social and mental health challenges of the COVID-19 pandemic further intensified drug-related overdoses, with nearly 100,000 drug overdose deaths estimated in 2020, two-thirds of which were attributed to opioids (Centers for Disease Control, 2020, 2021). Pan-opioid receptor antagonists such as naloxone and naltrexone can be used to treat opioid overdose, with naloxone primarily used in emergency situations and naltrexone primarily used as a preventative to opioid overdose (Blanco and Volkow, 2019). While these compounds antagonize all of the opioid receptors, it's their antagonist actions at μOR that drive the clinical effect against potent μOR agonists. Naltrexone can also be used to treat opioid use disorder, defined as a pattern of problematic opioid use that interferes with daily life, by inhibiting the actions of misused opioids and potential overdose (Blanco and Volkow, 2019). In a mechanism of reward devaluation, naltrexone can also be used to treat alcohol use disorder (Kranzler and Soyka, 2018), described in more detail in section 1.4.2. One side effect of opioid antagonist treatment is antagonist-precipitated withdrawal; however, these symptoms can be managed in a healthcare setting under accelerated withdrawal protocols (Theriot et al., 2021; Volkow and Blanco, 2021).

While treating pain is the primary clinical use of μOR agonists, μOR agonists such as methadone and buprenorphine are also used to treat opioid use disorder. While it may seem paradoxical to treat abuse of opioid agonists with opioid agonists, buprenorphine and methadone

have distinct pharmacological profiles that make them useful in treating opioid use disorder as a method of harm reduction. Buprenorphine is a partial μOR agonist, partial δOR agonist, and κOR antagonist that activates μORs less efficaciously than a full agonist such as fentanyl while retaining high affinity and potency for the μOR (Sittl et al., 2005; Mercadante et al., 2009; Bidlack et al., 2018; Browne and Lucki, 2019; Gillis et al., 2020). Methadone is a full μOR agonist with a long elimination time, allowing the opioid to stay in the system longer and for single daily administration to be possible (Ferrari et al., 2004). In addition, methadone has reduced reward abuse liability compared to other full agonists such as morphine due to its slow onset and offset of action, as well as its interaction with galanin-μOR receptor heteromers that lessen the ability of μORs to stimulate reward pathways (Kreek et al., 2010; Cai et al., 2019). Because of these pharmacological profiles, buprenorphine and methadone can help to reduce opioid cravings without causing euphoria, while also lessening withdrawal side effects. Though buprenorphine has reduced abuse liability in comparison to other full μOR agonists (Davis, 2012), it still carries abuse liability with extended administration and also carries legal restrictions in prescribing (Cicero et al., 2014; Manhapra et al., 2016, 2017; Tsui et al., 2018). Although methadone also carries legal restrictions in prescribing, methadone is the most widely used pharmacological therapy for opioid maintenance and has notably been used successfully for over 40 years in the treatment of opioid use disorder (Mattick et al., 2009).

Delta opioid receptor

Currently, there are no FDA-approved pharmacological therapies that selectively target the δOR, but compounds that mediate δOR signaling have been shown to confer benefits in several neurological conditions. In line with δOR expression in brain regions that regulate emotional tone, δOR agonists have been extensively studied for their ability to produce anti-depressant and anxiolytic effects (Broom et al., 2002; Saitoh et al., 2004; Perrine et al., 2006; Pradhan et al., 2011). In the last decade, δOR agonists AZD7268 and AZD2327 have been tested in Phase II clinical trials for treatment of Major Depressive Disorder (MDD) and anxious major depressive disorder (AMDD), respectively (Astra Zeneca Pharmaceuticals, 2012; Richards et al., 2016) (ClinicalTrials.gov, NCT01020799; NCT00759395). While both clinical trials were discontinued as neither study met their primary endpoints, secondary analysis of AZD2327 showed some benefit in the treatment of anxiety, supporting the utility of targeting the δOR for mood disorders.

While μOR-based therapies are highly effective in treating acute pain states, δOR agonists are comparatively ineffective in these scenarios, but in contrast offer an alternative in the treatment of chronic pain states (Hurley and Hammond, 2000; Cahill et al., 2003; Gallantine and Meert, 2005; Nadal et al., 2006; Gavériaux-Ruff et al., 2008; Pradhan et al., 2009, 2010). Depression and anxiety have a high co-morbidity in chronic pain conditions (Yalcin and Barrot, 2014), and modulation of emotion by δOR agonists may underlie their utility in treating chronic pain in mice. However, in clinical trials testing the analgesic efficacy of δOR agonists in osteoarthritic pain and portherpetic neuralgia, two chronic pain conditions, neither tested compound (ADL5859 and ADL5747) met primary endpoints for study continuation (ClinicalTrials.gov, NCT00979953, NCT01058642).

While these early studies do not paint a conclusive picture for δOR as a target for the treatment of peripheral chronic pain, there is continued interest in targeting δOR for central chronic pain conditions such as migraine. μOR opioids are sometimes used to treat migraine (Bigal and Lipton, 2009), but their chronic use can paradoxically increase pain by inducing hyperalgesia (Hayhurst and Durieux, 2016). This reaction is clearly observed in headache patients and can result in worsened headache symptoms (Bigal and Lipton, 2009; Buse et al., 2012). In contrast to μOR's pro-migraine effects, δOR agonists mitigate migraine-like behaviors in rodent models and produce limited opioid-induced hyperalgesia with chronic treatment (Charles and Pradhan, 2016; Moye et al., 2019). Recently, a phase 1 clinical trial was recently performed to assess the safety of δOR agonist TRV250 in acute migraine (ClinicalTrials.gov, NCT04201080) (Fossler et al., 2020). Findings from this study indicate that TRV250 shows tolerability, safety, and a beneficial pharmacokinetic profile in healthy volunteers. This profile supports further study of TRV250 in clinical trials of efficacy, and further highlights the δOR as a targetable option for certain pain conditions. Additional clinical data on TRV250 and other δOR agonists will continue to shed light on the validity of this receptor as a target in a variety of pain disorders.

It is important to note that all the aforementioned δOR agonists tested in clinical trials displayed minimal to no adverse events and were generally well-tolerated. However, one limiting factor in the development of δOR agonists is the ability of some δOR agonists like SNC80 and (+)BW373U86 to produce convulsions and sporadic locomotor hyperactivity (O'Neill et al., 1997; Hong et al., 1998; Jutkiewicz et al., 2004, 2006). These seizure-like side effects have been found to be specific to δOR activation (Broom et al., 2002), with δOR-mediated GABAergic signaling in the hippocampus primarily implicated (Haffmans and Dzoljic, 1983; De Sarro et al., 1992; Chu

Sin Chung et al., 2015), but these effects are importantly ligand-specific. While it is currently unclear what properties of ligands such as SNC80 contribute to seizure side effects, some studies have suggested that β-arrestin recruitment plays a role (Dripps et al., 2018; Vicente-Sanchez et al., 2018), although these findings do not fully define a mechanism and instead indicate that different β-arrestin isoforms may mediate some of these effects. Further investigations into differential downstream δOR signaling mechanisms may reveal a way to uncouple this consequence from the beneficial effects of δOR agonism. In contrast to μOR agonism, δOR agonism is associated with less respiratory depressant and gastrointestinal effects (May et al., 1989; Gallantine and Meert, 2005). In addition, although δOR agonism can lead to physical dependence with repeated administration, δOR agonism is correlated with reduced reward liability in comparison to μOR agonism (Negus et al., 1998; Brandt et al., 2001; Stevenson et al., 2005; Do Carmo et al., 2009).

Kappa opioid receptor

Unlike the μOR and δOR, agonism of the κOR system is strongly correlated with dysphoria, stress, and negative affect in mice and humans (Pfeiffer et al., 1986; Lutz and Kieffer, 2013). Negative affect is generally defined as a negative emotional or affective state and can sometimes be described as an aversive or depressive-like mood. The ability of κOR agonists to promote dysphoria and negative affect is a clinically limiting side effect of their development. However, not all κOR agonists cause these reactions; notable examples are nalfurafine and difelikefalin, two clinically used κOR agonists described below. Thus, it is not fully defined what downstream mechanisms of κOR agonism lead to dysphoria, although some preclinical studies implicate arrestin signaling, described in section 1.3.2 in more detail (Bruchas et al., 2006, 2007b; Land et al., 2009).

Because κOR agonism is associated with negative affect, interest in κOR antagonists expanded as a treatment option for stress and mood disorders such as depression and anxiety. Early κOR antagonists such as JDTic, GNTI, and nor-BNI displayed atypical pharmacokinetic properties such as delayed drug onset and lengthy duration of actions that prevented their clinical translation (Munro et al., 2012; Urbano et al., 2014; Banks, 2020). However, several κOR antagonists have been discovered or developed that possess relatively rapid onsets and shorter durations of action. As such, the potent and selective KOR antagonist aticaprant (formerly known as JNJ-67953964, CERC501, LY-2456302) has been tested in clinical trials for the therapeutic efficacy in treatment

of patients with mood and anxiety spectrum disorders (ClinicalTrials.gov, NCT02218736). Following daily administration after 8 weeks, gradual decreases in anhedonic symptoms (inability to experience pleasure) were reported and additional analysis of trial data strongly suggests that antagonism of the κOR is a mechanism that can mitigate anhedonia in those with mood and anxiety disorders (Krystal et al., 2020; Pizzagalli et al., 2020). Similarly, the clinical benefits of κOR antagonism in psychiatric disorders have been investigated in clinical trials with a combination treatment of buprenorphine and samidorphan, both F.D.A. approved drugs. As mentioned above, buprenorphine is a partial μOR agonist, κOR antagonist, and partial δOR agonist, and samidorphan is a μOR antagonist. In pharmacological characterization of this combination treatment, it has been demonstrated that samidorphan blocks the partial agonism of buprenorphine at μOR and δOR but does not affect buprenorphine's κOR activity (Bidlack et al., 2018). As such, this combination treatment results in net antagonism of the κOR. In clinical trials, dual treatment with buprenorphine and samidorphan has shown therapeutic benefit in patients with treatment resistant depression, further supporting κOR antagonism as a mechanism to treat mood disorders (Ehrich et al., 2015).

In contrast to agonism of the μOR which produces itch, also known as pruritis, agonists of the κOR inhibit itch (Ballantyne et al., 1988; Tseng and Hoon, 2020). κORs inhibit the action of sensory neurons that innervate the skin and modulate itch, but the precise mechanistic circuit is not well-defined (Tseng and Hoon, 2020). Recently, however, the peripherally-restricted κOR agonist difelikefalin (Korsuva™) was approved by the F.D.A. for treatment of uremic pruritus (Deeks, 2021). Though difelikefalin is the first selective κOR agonist approved for use in humans in the U.S., another well-known κOR agonist, nalfurafine hydrochloride (Remitch®), has been used for over a decade in Japan for similar treatment of pruritus, underscoring the safety and utility of κOR agonists in clinical therapeutics (Kumagai et al., 2010).

Furthermore, the κOR has generated significant interest as a target for pain due to its ability to promote antinociception without causing respiratory depressant and gastrointestinal side effects common with μOR-targeting treatments (Porreca et al., 1983, 1984; Unterwald et al., 1987; Shippenberg et al., 1988; Di Chiara, 1998; Field et al., 1999; Kivell and Prisinzano, 2010). To avoid the dysphoric side effects caused with central activation of κORs, peripherally restricted κOR agonists have been developed for the treatment of pain. As such, peripherally-restricted κOR agonist difelikefalin has been evaluated in phase II efficacy clinical trials to determine if it produces clinically relevant pain reduction following hysterectomy and bunionectomy

(ClinicalTrials.gov, NCT01361568; NCT02944448). In both of these studies, primary endpoints were achieved, indicating that targeting peripheral κORs is an effective strategy to treat pain with minimal adverse effects.

1.3 Applications of biased signaling at opioid receptors

1.3.1 Discovery of signaling bias at opioid receptors

Classical receptor theory suggests GPCRs exist in equilibrium between two states, inactive (R) and active (R*), and that upon binding, all agonists promote identical receptor regulation and downstream signaling cascades (Kenakin, 2004). In the past 25 years, however, this theory has been challenged by many studies and the current understanding is that receptors exist in many distinct states, following the principles of thermodynamics (Alhadeff et al., 2018), and that different agonists can engage selective receptor conformations to initiate distinctive signaling responses (Kenakin, 2011; Reiter et al., 2012). This latter concept has gone by many names, but is most commonly referred to as functional selectivity, or biased signaling (Galandrin et al., 2007; Rajagopal et al., 2010; Vaidehi and Kenakin, 2010).

Functional selectivity has been observed in many families of receptors, including dopamine receptors, adrenergic receptors, serotonin receptors, but has gathered considerable interest in the opioid receptor field as a possible "holy grail" that would allow development of opioid analgesics with reduced side effect profiles. Some of the first demonstrations of functional differences between opioid agonists were in experiments looking at ligand ability to induce endocytosis of epitope-labeled receptors as well as regulate adenylate cyclase activity and GIRK channels (Keith et al., 1996, 1998; Sternini et al., 1996; Whistler et al., 1999). For instance, the selective μOR agonists DAMGO and methadone strongly induced μOR endocytosis whereas a lessened response was seen with morphine (Keith et al., 1996; Whistler et al., 1999). When observing agonist ability to regulate GIRK channel activity, however, methadone and morphine display much more similar effects (Whistler et al., 1999; Alvarez et al., 2002). These findings are not in agreement with a two-state receptor model, and instead suggest that multiple active conformations exist for the μOR, similar to the assumptions made with earlier speculations of protean agonists (Kenakin, 2001).

The idea of biased signaling as an approach for safer μOR analgesics gained traction after findings from Bohn et al. demonstrated morphine produced an enhanced antinociceptive effect in

mice devoid of β-arrestin2 (from here on referred to as βarr2 knockout (KO) mice) compared to wildtype mice (Bohn et al., 1999). Subsequent studies from the same group examined the role of β-arrestin2 in the development of morphine's side effects and found that βarr2 KO mice did not develop tolerance to morphine compared to wildtype mice, but did demonstrate morphine dependence as measured in drug reward paradigms (Bohn et al., 2000). These results were further supported with findings in mice with knock-down of β-arrestin2 via siRNA and antigene RNA that similarly displayed potent morphine antinociception without tolerance (Li et al., 2009; Yang et al., 2011). Similarly, βarr2 KO mice also displayed reduced gastrointestinal and respiratory depression side effects, both which are additional significant clinical challenges with morphine administration (Raehal et al., 2005). From these findings, β-arrestin2 was collectively interpreted as an agent of desensitization following morphine administration, contributing to tolerance, while also having a causative role in signaling events associated with negative gastrointestinal and respiratory effects. As such, efforts in the field of opioid research moved towards the development of ligands that avoided recruiting β-arrestin2 and were so-called "G-protein biased" opioids (**Figure 1.4**). In this research, different methods of bias quantification are used, but most common is the calculation of a "bias factor." This parameter is calculated as the ratio between some measure of G-protein signaling to a measure of β-arrestin recruitment in relation to a unbiased reference compound (Kenakin et al., 2012; van der Westhuizen et al., 2014).

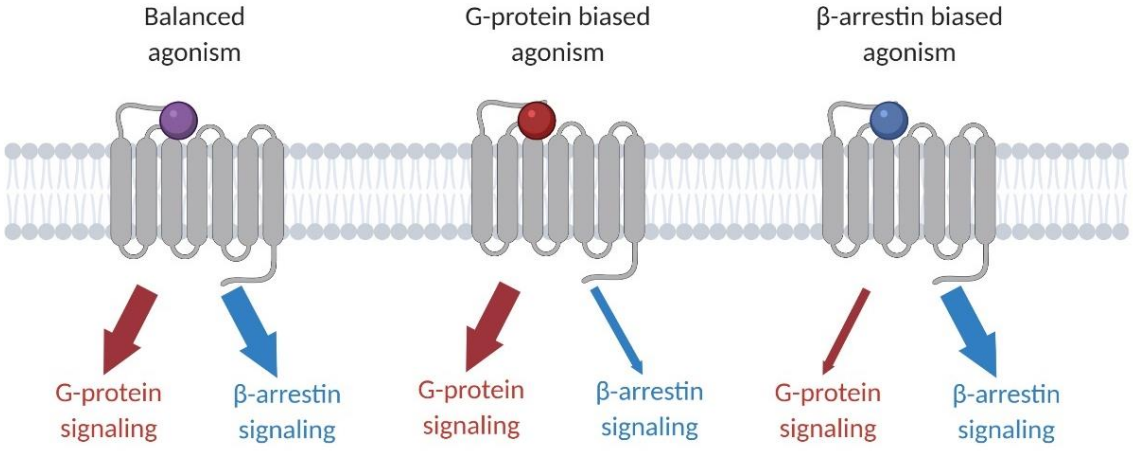

Figure 1.4 Schematic of general biased signaling concept for opioid receptors

Ligands displaying balanced agonism at the opioid receptors promote G-protein signaling and β-arrestin signaling mechanisms, whereas biased mechanisms favor one of these pathways. The original hypothesis underscoring the significance of these discrepant responses was data suggesting that avoiding β-arrestin recruitment pathways would reduce side effects associated with opioid use such as respiratory depression and tolerance. Figure created using Biorender.com.

While μOR was the initial focus of biased agonism research, interest in biased signaling expanded to δOR and κOR. Aiding the efforts of biased drug design for these receptors were crystal structures of μOR, δOR, and κOR bound to antagonists in the inactive state that provided information about the spatial organization of the binding pockets that help regulate functional selectivity (Granier et al., 2012; Manglik et al., 2012; Wu et al., 2012). These structures allowed for compound libraries to be computationally docked, screened, and examined for novel scaffolds and receptor interactions. It was with this method that μOR agonist PZM21 was developed following a library screen of 3 million molecules (Manglik et al., 2016). In this computational study, hit compounds were identified after they were predicted to have selectivity for μOR and were identified as having structural novelty in comparison to traditional opioids such as morphine. From one of the hits, PZM21 was optimized to increase potency and efficacy before further testing in cells and animals. When assessing its pharmacology at μOR, PZM21 displayed potency in activating G-protein signaling but induced minimal β-arrestin2 recruitment and possessed antinociceptive properties but with reduced respiratory and reinforcing effects compared to morphine. While this computational study was docked against the structure of inactive μOR, more recent studies have revealed the structures of the less stable, active conformations of μOR, δOR, and κOR, which will further aid in the understanding of opioid receptor structural dynamics and computationally directed high-throughput drug design (Huang et al., 2015; Che et al., 2018; Claff et al., 2019; Kapoor et al., 2020; Mafi et al., 2020b). Furthermore, there have been a number of structural and computational studies investigating differences in receptor conformation when bound to non-biased versus biased compounds (Cong et al., 2021; Kelly et al., 2021; Piekielna-Ciesielska et al., 2021), specific receptor binding sub-pockets that are engaged with biased agonism (Marmolejo-Valencia et al., 2021; Uprety et al., 2021), and differences in β-arrestin recruitment between biased and non-biased agonists (Mafi et al., 2020a). These studies bring insight to the mechanisms of biased agonism at the receptor level and will be useful in *in silica* screens for biased agonists.

1.3.2 Clinical relevance of biased agonists at the opioid receptors

As mentioned previously, developing analgesics with lessened side effects is a major objective in developing G-protein biased agonists for the μOR. While many G-protein biased μOR agonists have been discovered or developed preclinically, the most clinically successful outcome

of these efforts is TRV130, or oliceridine, which was developed by pharmaceutical company Trevena (DeWire et al., 2013). The compound was the result of high-throughput screening efforts of Trevena's chemical libraries, and further compound optimization with respect to ligand bias, selectivity, and potency. After displaying potent antinociception and a reduced side effect profile in rodents, oliceridine advanced through several phases of clinical trials where it demonstrated rapid and potent analgesia for moderate and severe pain states (Soergel et al., 2014b; Viscusi et al., 2016; Singla et al., 2017). The safety and tolerability profile of oliceridine regarding respiratory depression and gastrointestinal side effects were also compared to morphine in several Phase III studies, which had incongruous results (Bergese et al., 2019; Singla et al., 2019; Viscusi et al., 2019; Dahan et al., 2020). However, despite a lack of consensus on whether treatment with oliceridine conferred clear improvements in safety compared to morphine, oliceridine was approved by the FDA in 2020 under the trade name Olinvyk™ for short-term intravenous use in controlled settings such as hospitals (Food and Drug Administration, 2020). Additional Phase IV trials, also known as post-approval studies, will continue to shed more light on the analgesic efficacy and safety of oliceridine in clinical practice.

Described above, nalfurafine is a selective κOR agonist approved for treatment of pruritis in Japan, and its side effect profile is notably devoid of any negative dysphoric or hallucinogenic effects (Kumagai et al., 2010). Research on nalfurafine's pharmacology using downstream kinase phosphorylation patterns as a measure of G-protein activity and β-arrestin signaling suggested that nalfurafine acted as a G-protein biased agonist at κOR (Kenakin and Christopoulos, 2013; van der Westhuizen et al., 2014; Schattauer et al., 2017). These findings bolstered the idea that G-protein biased κOR agonists provided a pathway to develop safer κOR agonists for clinical development (Chavkin, 2011). However, kinase phosphorylation does not provide reliable endpoints for bias calculation (Lovell et al., 2015), and more recent research on nalfurafine's pharmacology indicates that it potently and efficaciously recruits β-arrestin2 (Mores et al., 2019; Cao et al., 2020). Still, some research maintains that nalfurafine does have a slight degree of G-protein bias, and that this bias may be more evident and relevant in humans than in rodents (Schattauer et al., 2017; Cao et al., 2020). Thus, it is not yet clear what role biased κOR agonists have in therapeutics, although some research has indicated that there is an association between β-arrestin2 recruitment at the κOR and clinically limiting side effects such as dysphoria. In studies investigating the mechanisms responsible for aversion by selective κOR agonist U50,488, it was found that p38 activation was

required (Bruchas et al., 2007b), and that this activation was dependent on both GRK3 phosphorylation of the receptor as well as arrestin recruitment (Bruchas et al., 2006). This implicates the β-arrestin2 pathway in κOR-mediated aversion, but as reviewed in Bruchas & Chavkin, p38 activation is one of several pathways downstream of β-arrestin2 recruitment at the κOR (Bruchas and Chavkin, 2010). Thus, β-arrestin 2 recruitment itself may not be the key mediator responsible for κOR-induced aversion, but instead the first step in a specific signal cascade that leads to this effect; this is supported by nalfurafine's lack of dysphoric effects despite its potent and efficacious β-arrestin2 recruitment. To support further clinical development of κOR drugs, additional studies are needed to parse out these downstream signaling cascades in relation to κOR-mediated side effects.

Unlike μOR and κOR, no δOR-selective drugs are currently used in the clinic, although several are being investigated in clinical trials. One G-protein biased δOR ligand, TRV250, has recently been tested in a phase I clinical trial for safety and has demonstrated no adverse side effects (Fossler et al., 2020). This compound was designed by Trevena for the treatment of migraine on the basis that it's G-protein biased pharmacology would purportedly minimize seizure side effects (Dripps et al., 2018; Vicente-Sanchez et al., 2018). However, TRV250 has demonstrated partial β-arrestin2 recruitment with about 30% efficacy (Crombie et al., 2015), a similar level of β-arrestin2 efficacy seen with TAN67 which produces seizure-like behavior at high doses (Nielsen et al., 2012a), which indicates TRV250 may produce similar effects with increased dosage. Still, it is not yet clear whether avoiding β-arrestin recruitment to avoid seizure side effects is applicable for every compound (i.e. some δOR agonists recruit β-arrestin and do not cause seizure side effects). For example, δOR agonist ADL5859 displays β-arrestin2 recruitment with greater than 100% efficacy relative to control leucine-enkephalin (Ko et al., 2021), yet ADL5859 was generally well tolerated in clinical trials with no serious adverse effects reported (ClinicalTrials.gov, NCT00603265, NCT00626275, NCT00979953, NCT00993863). Therefore, additional research is needed to elucidate the mechanisms underlying δOR-mediated seizures. In conclusion, G-protein biased δOR agonists are being designed for the treatment of many conditions, especially psychiatric disorders and chronic pain (Gotoh et al., 2017, 127; Conibear et al., 2020), and one area of interest in this dissertation research is the application of such compounds in alcohol abuse, described in more detail in section 1.4.2.

1.3.3 Controversy surrounding concept of biased signaling for safer μOR therapeutics

While oliceridine was approved by the FDA for intravenous use in acute pain conditions, it notably failed to convincingly lessen gastrointestinal and respiratory depression side effects when compared to morphine in clinical trials, sowing doubt in whether G-protein biased μOR agonists are safer analgesics than traditional opioids. Further undermining the bias hypothesis is recent research findings from 3 independent research groups in Germany, the United Kingdom, and Australia re-evaluating morphine's side effects in βarr2 KO mice (Kliewer et al., 2020). Each lab group independently bred βarr2 KO and wildtype mice and demonstrated that morphine produced nearly indistinguishable respiratory depression effects in both genotypes. Similar results were also found with fentanyl, indicating the effect was not drug specific. Furthermore, the groups demonstrated that morphine and fentanyl both induced similar gastrointestinal effects in both βarr2 KO and wildtype mice, indicating that eliminating β-arrestin2 recruitment does not confer benefits for morphine's therapeutic window. While the side effect profile of morphine remained unchanged between genotypes, the groups found that morphine antinociception is more potent in βarr2 KO mice compared to wildtype, which is in line with the original findings from the Bohn lab (Bohn et al., 1999; Kliewer et al., 2020). An explanation for these discrepant results in βarr2 KO mice between research groups is not fully defined, but it has recently been shown that the mouse genetic background used in some of the original βarr2 KO studies is a strain that is less sensitive to morphine-induced respiratory depression (He et al., 2021).

A recent study shed light on the relationship between β-arrestin recruitment and morphine's analgesic and negative side effects (Kliewer et al., 2019). As described in section 1.1.2 and 1.2.3, β-arrestins are recruited to the C-terminal tail of an opioid receptor when serine or threonine residues in this region become phosphorylated. In this study, β-arrestin recruitment was prevented through the generation of several mutant mouse strains with a genetic knock-in of increasingly non-phosphorylatable μOR due to threonine- and serine-to-alanine mutations. As a result, the mutant mouse lines expressed μORs that were G-protein biased. In regards to morphine's analgesic effects, the mice with G-protein biased receptors had similar phenotypes to βarr2 KO mice: enhanced analgesia and a reduction in developed tolerance with repeated exposure. However, the mice with the G-protein biased receptors also displayed respiratory depression and gastrointestinal effects in response to morphine treatment. These data suggested that β-arrestin2 recruitment at the μOR is a regulator of opioid analgesia and resulting tolerance, but not of respiratory depressant

and gastrointestinal side effects. Moreover, when assessing the effective doses for analgesia and the effective doses for side effects in the increasingly G-protein biased μOR knock-in mice, a significant correlation was found. This suggests that increasingly G-protein biased agonism of the μOR (or decreasing ability to recruit β-arrestins) promotes enhanced antinociception but also a proportional increase in side effects.

However, the results from the previous study indicating β-arrestin2 recruitment is associated with the development of tolerance (demonstrated by a lack of tolerance seen in mice with non-phosphorylatable μOR receptors) is at odds with data from the Whistler and von Zastrow labs suggesting β-arrestin2 recruitment is beneficial in preventing tolerance (Whistler and Zastrow, 1998; Whistler et al., 1999; Finn and Whistler, 2001; Kim et al., 2008; Berger and Whistler, 2011). Briefly, knock-in mice were developed, referred to as "recycling μOR" mice, that expressed mutant μORs able to internalize and recycle following treatment with morphine, in contrast to wildtype μORs (Kim et al., 2008). This mutant μOR was developed by replacing the cytoplasmic tail of the μOR with that of the δOR, which has been demonstrated to be a highly favored substrate for GRK phosphorylation (Pei et al., 1995; Kovoor et al., 1997), conferring a gain-of function phenotype wherein morphine agonism can induce receptor phosphorylation, β-arrestin recruitment, and subsequent receptor endocytosis (Whistler et al., 1999). In comparison to wildtype mice, recycling μOR mice displayed reduced tolerance to morphine analgesia, indicating a protective role for β-arrestin recruitment and subsequent internalization (Kim et al., 2008). Importantly, compared to partial agonist morphine, full agonist methadone displayed minimal development of analgesic tolerance in both wildtype and recycling μOR mice (Kim et al., 2008). This suggests that compounds with high internalizing properties such as methadone have reduced tolerance side effects when compared to compounds with low internalizing properties such as morphine. It is hypothesized that internalization and recycling of the μOR helps to re-sensitize the receptor to ligand effects, and as such, μOR agonism by ligands with poor internalizing ability results in desensitized receptors on the cell surface that drive cellular adaptations further promoting tolerance. To reconcile these findings with those in Kliewer et al., it is proposed that the mice with non-phosphorylatable receptors likely exhibit a decrease in desensitization compared to wildtype mice that drives the lessened tolerance phenotype (Kliewer et al., 2019; He et al., 2021).

The findings from Kliewer et al. suggesting that increasingly G-protein biased agonism of the μOR is associated with a proportional increase in side effects is supported by a recent study

from Gillis et al. This study involved a careful reexamination of the pharmacological profiles of PZM21, oliceridine, and other purported G-protein biased μOR agonists, as well as clinically relevant drugs such as buprenorphine, fentanyl, methadone, morphine, and oxycodone (Gillis et al., 2020). One limiting factor in comparing results between different groups aiming to quantify bias, potency and efficacy of compounds is the context in which the assay is performed. For example, the accumulation of cAMP is often used as a measurement for G-protein activation but because cAMP production is downstream of G-protein activation, this readout can lead to signal amplification. In contrast, β-arrestin recruitment assays typically have less signal amplification since the read-out relies on direct interaction of β-arrestin proteins with the GPCR of interest. As a result, when comparing a compound's pharmacology in a highly amplified system of G-protein activation and a low amplification system for β-arrestin recruitment, a compound that has "balanced" signaling may appear as G-protein biased. In order to mitigate effects such as these, Gillis et al. employed rigorous approaches to characterize the pharmacology of the panel of μOR agonists by using multiple assays to survey G-protein activity and β-arrestin recruitment, as well as including multiple controls for conditions which would manipulate the efficiency of receptor signaling, such as overexpressed receptors, GRK proteins, or reporter probes. The results demonstrated that PZM21 and oliceridine are partial rather than full μOR agonists, a finding that was also supported by a previous study demonstrating both compounds were partial agonists in regard to ion channel signaling (Yudin and Rohacs, 2019). Gillis et al. also found that the rank order of maximal effects for the panel of μOR agonists was the same for G-protein activity and for β-arrestin recruitment, suggesting that there was no measurable signaling bias for the compounds, including oliceridine and PZM21.

In the same study, the antinociceptive and respiratory depression effects were evaluated for the panel of μOR agonists. In dose-response hot plate and plethysmography assays, all of the agonists induced potent antinociception as well as decreases in respiration, although the respiratory effects of oliceridine, PZM21, and buprenorphine were less severe than morphine or fentanyl (Gillis et al., 2020). Using this data, the therapeutic window was computed for each compound and compared to the pharmacological data gathered previously in the study. It was found that there was no correlation between bias factor and therapeutic window, but instead a pronounced inverse correlation between ligand efficacy and therapeutic window. In other words, compounds that were partial agonists, such as buprenorphine and oliceridine, had greater therapeutic windows.

Collectively, these data indicate that β-arrestin2 recruitment is not a good predictor of respiratory risk, and that biased signaling is not a good predictor of whether an analgesic has a lessened side effect profile, but rather efficacy.

Soon after the release of the partial efficacy hypothesis by Gillis et al., a responding article from Stahl & Bohn was published, reevaluating the findings of Gillis et al. to include additional parameters in the bias calculations (Stahl and Bohn, 2021). After reanalysis of the data, the authors argue that the findings in Gillis et al. show that signaling bias was observed, notably for buprenorphine, and that while partial efficacy may be a beneficial pharmacological property, biased signaling still serves as an avenue to widen the therapeutic window of μOR opioids. As evidenced by this exchange, the debate on whether biased agonism of the μOR is an effective pharmacological parameter is still ongoing and emphasizes the need for further mechanistic understanding of opioid receptor signaling. Activation of G-proteins versus recruitment of β-arrestins can be considered as the first point of divergence for biased signaling at opioid receptors; a better understanding of the differential activation of downstream cascades and signal transducers may better define the complexity of biased signaling and lead to new pharmacological tools, endpoints, and screens for compound evaluation. It is important to note that thus far the controversy surrounding biased signaling and its application in safer therapeutics has focused on μOR research. As previously mentioned, findings and applications of biased signaling have been reported at the δOR and κOR with respect to improvements over "balanced" opioids, but these studies have not been analyzed with the same depth of scrutiny.

1.4 Natural products as a source of new opioid therapeutics to treat pain and alcohol use disorder

1.4.1 Opioids in the treatment of chronic pain

Background

Pain is the most common symptom reported by patients in primary care visits (Andersson, 1999), and correspondingly chronic pain is one of the prevailing reasons patients seek medical care in the first place (Schappert and Burt, 2006). Pain is defined by the International Association of the Study of Pain as, "an unpleasant sensory and emotional experience associated with actual

or potential tissue damage or described in terms of such damage," and chronic pain is defined as, "pain that persists beyond normal tissue healing time, which is assumed to be three months" (Merskey et al., 1986). In 2016, it was estimated that chronic pain affected over 50 million adults in the U.S. and cost the nation nearly $600 billion in medical costs and losses in worker productivity (Institute of Medicine (US) Committee on Advancing Pain Research, Care, and Education, 2011). On an annual basis, national costs for pain surpassed those of heart disease, cancer, and diabetes (Gaskin and Richard, 2012). Furthermore, chronic pain is also associated with negative affective states such as anxiety and depression, with some reports estimating that anxiety or depression is present in about 60% or 80% of patients, respectively (Fishbain et al., 1986; Poole et al., 2009). This comorbid presentation contributes to lessened quality of life among patients and contributes to poor therapeutic outcomes and the socioeconomic burden of pain (Ferdousi and Finn, 2018).

Pain pathways

The transmission of pain is complex process with the mediation of pain occurring in the ascending pain pathway, and the modulation of pain through the descending pathway (Millan, 1999, 2002; Ossipov et al., 2010). To briefly describe the ascending pathway, upon painful stimuli, sensory receptors in primary afferent neurons will relay the nociceptive signal to the spinal cord dorsal horn where the signal will be transmitted through a series of second order neurons before the information is relayed to brain regions where the sensory and affective pain components are processed. These brain regions include but are not limited to the cortex, hypothalamus, thalamus, amygdala, and parabrachial nucleus. Once the ascending pain pathway is activated, the mediation of nociceptive signals through the ascending pain pathway can be modulated by the descending pathway. In this pathway, neurons from several brain regions, notably the cortex, hypothalamus, and amygdala, project to the periaqueductal gray which then projects to the rostral ventromedial medulla. From there, projections terminate at the dorsal horn of the spinal cord to result in either inhibition of pain transmission under physiological states, or facilitation of pain transmission in pathophysiological states.

Throughout the descending pain pathway, opioid receptors and respective endogenous opioid peptides are extensively expressed (McNally and Akil, 2002; Benarroch, 2012). The ability of the opioid system to inhibit nociceptive signaling through this pathway has been confirmed through

pharmacological investigation. For example, selective injection of morphine into regions of the descending pathway has been shown to produce nociception, a response that can be blocked with opioid antagonist naloxone (Akil et al., 1976; Yaksh et al., 1976; Manning et al., 1994). It is through this endogenous pathway that therapeutic opioids elicit the powerful analgesic effects that has solidified their role as a mainstay in pain management (Corder et al., 2018).

Pain treatments and limitations

While acupuncture, psychotherapy, physical therapy, nerve stimulation, and relaxation are alternatives in the treatment of chronic pain, opioids remain the most widely prescribed pharmacotherapy for the management of pain in the United States (Reuben et al., 2015; Volkow et al., 2018). It is worth noting that chronic pain can often be categorized as neuropathic, arising from damage or compression of neural tissue, or nociceptive, arising from damage to body tissue. In most cases, neuropathic pain is resistant to treatment with opioids while nociceptive pain is not (Alles and Smith, 2018). Here, the focus will be on nociceptive pain and its respective treatment options. As mentioned above, μOR-targeting opioids are a mainstay in pain treatment, but the FDA has approved other, nonopioid analgesics to treat chronic pain including calcium channel blockers, cyclooxygenase inhibitors, and monoamine reuptake inhibitors. However, all of these treatments have clinical limitations including slow onset of action in comparison to opioids, as well as limited efficacy and other side effects.

Opioids are also not without side effects, however, as described in section 1.2.4. Briefly, the most common side effects with opioid treatment are nausea, sedation, constipation, hyperalgesia and rashes (Al-Hasani and Bruchas, 2011). With chronic treatment, tolerance to most of these adverse effects can develop, though usually not to constipation, but this can be managed with additional pharmacotherapies or by switching opioids (Benyamin et al., 2008; Volkow et al., 2018). Of course, the addictive properties of opioids are also well known, and have contributed to the national opioid crisis (Hedegaard et al., 2017; Makary et al., 2017; Compton et al., 2019). Still, individuals suffering with chronic pain or recurrent bouts of severe pain remain reliant on long-term opioid use for their pain management and quality of life (Ballas et al., 2018). Additionally, although opioids do carry risk of abuse, it should be noted that only a small fraction of patients using opioids to treat chronic pain fall victim to addiction (Vowles et al., 2015).

Looking ahead, it is evident that new therapies are needed to treat patients suffering with chronic pain. There are two paths forward that combat the opioid epidemic: developing non-opioid analgesics that have superior or equal efficacy in treating pain or improving the current repertoire of opioid therapies. In this dissertation research, I address the latter approach by investigating natural products for new opioids, specifically G-protein biased opioids that may provide scaffolds for future drug design and/or optimization.

1.4.2 Targeting the δOR as an alternative to current Alcohol Use Disorder therapeutics

Background

Besides pain, another costly and prevalent societal and economic concern in the United States is alcohol abuse which affected nearly 15 million people in 2019 (SAMHSA, 2019) and results in an estimated societal cost of $250 billion per year (Sacks et al., 2015). Additionally, harmful alcohol use has increased during the COVID19 pandemic (Pollard et al., 2020; Killgore et al., 2021), coinciding with an increase in alcohol sales in the U.S. (The Nielsen Company, 2020). Frequent abuse of alcohol can lead to an alcohol use disorder (AUD), which is defined as a "problematic pattern of alcohol use accompanied by clinically significant impairment or distress," and can be characterized as mild, moderate, or severe based on 11 diagnostic criteria defined by the fifth edition of the Diagnostic and Statistical Manual of Mental Disorders (American Psychiatric Association, 2013). Psychiatric disorders also frequently co-occur with heavy alcohol use, with depressive disorders being the most common (Grant et al., 2004; McHugh and Weiss, 2019). In one study, 77% of alcohol dependent individuals reported suffering from a moderate to severe psychiatric and/or somatic disorder (Odlaug et al., 2016). Co-occurrence of a psychiatric disorder with AUD is correlated with worsened prognosis and greater severity than either disorder individually, and also puts an individual at a heightened suicidal risk (Greenfield et al., 1998; Hasin et al., 2002; Conner et al., 2014).

Alcohol's CNS effects

Contributing to these mental health concerns are the neuroadaptations that occur with chronic alcohol use. Alcohol exerts complex and numerous pharmacological effects in the brain through interaction with several neurotransmitters. Alcohol's rewarding effects are due to

modulation of neurotransmitters such as dopamine, serotonin, endogenous opioid peptides, GABA, as well as endocannabinoids. In particular, upon alcohol consumption an increase in dopamine release occurs in the mesolimbic reward system, which has projections to brain areas that regulate cognitive control and motivation such at the prefrontal and orbitofrontal cortices (Noronha et al., 2014). The aforementioned increase in dopamine transmission within the mesolimbic pathway is modulated by endogenous opioid receptor signaling in the brain, which is activated by endogenous opioids released upon alcohol consumption (Herz, 1997; Gianoulakis, 2001). Through this mechanism, the opioid system in the brain plays a key role in mediating alcohol's rewarding and addictive effects.

Furthermore, with chronic, long-term exposure to alcohol, adaptive changes in the brain occur with many neurotransmitters, namely GABA and glutamate (Witkiewitz et al., 2019). GABA is one of the most common inhibitory neurotransmitters in the brain while glutamate is a major excitatory neurotransmitter. Acute alcohol consumption has a net inhibitory effect in the brain (leading to drowsiness), but with chronic alcohol use the brain adapts to this net inhibitory effect by upregulating glutamate transmission and downregulating GABA transmission (De Witte et al., 2005). Discontinuing alcohol consumption after chronic use therefore results in alcohol withdrawal symptoms of nervous system hyperactivity and dysregulation that can be so severe it is fatal if not properly managed (Koob, 2003; Schuckit, 2014; Koob and Volkow, 2016).

Current AUD treatments

There are only three F.D.A. approved treatments for AUD in the U.S., and they either target the hyperactivity that occurs with discontinuing alcohol use or by interfering with alcohol-related reward. In 1949, disulfiram was the first treatment approved to treat AUD in the U.S., although it was first proposed as an alcohol abuse remedy in 1784 (Rush, 1784). In the metabolism of alcohol in the body, alcohol is first metabolized to acetaldehyde before being converted to acetate. Disulfiram inhibits the enzyme aldehyde dehydrogenase which is involved in the conversion of acetaldehyde to acetate, and overall leads to an accumulation of acetaldehyde in the body. This excess acetaldehyde causes numerous unpleasant symptoms such as headache, tachycardia, nausea, and vomiting that pairs alcohol consumption with an adverse reaction. Therefore, alcohol consumption becomes unpleasant and is associated with a potential threat of malaise, which encourages the user to avoid alcohol use. Due to its sometimes-severe side effects and

neurotoxicity associated with excess acetaldehyde, disulfiram is not advised to help patients reduce alcohol consumption, but instead is more useful to maintain abstinence from alcohol (Chick, 1999; Skinner et al., 2014).

Naltrexone was the second drug to receive approval for AUD treatment in 1994, and later in 2006 an injectable extended-release formulation was developed with the aim of improving medication adherence. As mentioned previously, naltrexone is a pan-opioid antagonist and acts by reducing opioidergic activity in the mesolimbic pathway, thereby curbing dopamine-induced alcohol craving and reward (Benjamin et al., 1993; Gonzales and Weiss, 1998; Kranzler and Soyka, 2018). Naltrexone has been found to be most effective in reducing heavy alcohol consumption (Maisel et al., 2013; Jonas et al., 2014; Kranzler and Soyka, 2018), but there is less evidence supporting its ability to promote abstinence (Maisel et al., 2013). Common side effects are tiredness, nausea and dizziness, but generally naltrexone is well-tolerated (Rösner et al., 2010b).

Lastly, acamprosate was approved to treat AUD in the U.S. in 2004. The mechanism of acamprosate is not fully understood, but it is thought to modulate the maladaptive hyperactive glutamate system that occurs with chronic alcohol use and may help reduce alcohol withdrawal symptoms (De Witte et al., 2005; Rösner et al., 2010a; Witkiewitz et al., 2012). As such, evidence shows that acamprosate is more helpful in aiding abstinent AUD patients than in helping patients reduce levels of alcohol consumption, similar to disulfiram (Maisel et al., 2013). Overall, acamprosate is fairly well-tolerated and is not associated with severely limiting side effects (Rösner et al., 2010a). Though not reviewed in detail here, psychosocial intervention such as cognitive behavioral therapy and motivational enhancement has also shown promise in treating AUDs, especially when supplementing pharmacological therapies (Petry et al., 2014).

Despite the large number of U.S. adults diagnosed with an alcohol use disorder, pharmacological treatment is prescribed to less than 9% of 15 million patients (SAMHSA, 2015; Kranzler and Soyka, 2018), and even then, treatment is not successful for all patients (Franck and Jayaram-Lindström, 2013). Furthermore, existing FDA-approved treatments for AUD, acamprosate, disulfiram, and naltrexone (once-a-day pill or extended release injection), have all exhibited inconsistent outcomes in clinical trials (Litten et al., 2012; Franck and Jayaram-Lindström, 2013; Swift and Aston, 2015). Given that no new treatments for AUD have been approved over the last 15 years, coupled with limitations of current pharmacotherapies, there is a pressing need for new AUD treatments with novel targets and increased efficacy.

Targeting δOR for AUD

Because alcohol modulates endogenous opioid signaling and chronic alcohol use can lead to longstanding adaptive changes within the mesolimbic opioid system (Herz, 1997; Koob, 2003; Le Merrer et al., 2009), opioid receptors provide a promising target to treat alcohol related effects (Walker et al., 2012). This approach is further validated by the ability of naltrexone to reduce heavy drinking in some AUD patients (Maisel et al., 2013). Instead of antagonizing the opioid receptor system to decrease alcohol-associated reward, here I discuss specifically agonizing the δOR in a G-protein biased manner as a mechanism to reduce alcohol consumption, which has been demonstrated to be an effective target in reducing alcohol consumption behaviors in mice (van Rijn and Whistler, 2009; van Rijn et al., 2010, 2012a; Chiang et al., 2016; Robins et al., 2018b).

The role of δORs in modulating alcohol behaviors is exceedingly complex. It is known that δOR pharmacology is impacted following acute or chronic alcohol exposure at several interrelated levels such as changes in endogenous opioids concentrations, changes in receptor expression, and changes to specific brain regions that affect ligand affinity and/or potency (Alongkronrusmee et al., 2018). Furthermore, multiple studies have observed elevation in functional δOR expression following alcohol exposure, supporting it's targetability for alcohol abuse treatments (Margolis et al., 2008; Bie et al., 2009; van Rijn et al., 2012b). Selective δOR antagonists naltriben and naltrindole have been shown to cause inconsistent effects in the modulation of alcohol consumption in different rodent models, with naltriben demonstrating an ability to decrease alcohol consumption in mice and rats, whereas naltrindole does not decrease alcohol consumption in mice but does in rats (Krishnan-Sarin et al., 1995a, 1995b; van Rijn and Whistler, 2009). These effects may be explained by the presence of δOR subtypes, further complicating the interpretation of δOR-mediated effects on alcohol consumption (van Rijn and Whistler, 2009). Similarly, δOR agonists TAN-67 and SNC80 modulate opposing effects on alcohol consumption in mice, with TAN-67 effectively decreasing consumption and SNC80 increasing consumption (van Rijn et al., 2010). A subsequent study with a panel of δOR agonists revealed a strong correlation between the ability of a δOR agonist to recruit β-arrestin2 and its ability to promote ethanol consumption in mice (Chiang et al., 2016). The previous TAN-67 and SNC80 ethanol consumption data gathered in van Rijn et al. coincided with this correlation; TAN-67 displayed low efficacy in recruiting β-arrestin2 recruitment while SNC80 had high efficacy (van Rijn et al., 2010; Chiang et al., 2016). This led to the conclusion that G-protein biased δOR agonists (that avoid β-arrestin2 recruitment)

provide a pathway for the development of new alcohol abuse therapeutics. It is important to note that the δOR-mediated effects on alcohol consumption are rapid (within 4 hours following administration), suggesting that downstream signaling mechanisms directed towards gene expression are not immediately involved. Instead, it is likely that changes in δOR modulation of calcium and or potassium channels, or neurotransmitter release such as GABA are mediating these effects (Margolis et al., 2008, 2017). Further interpretation of the mechanism of action for the G-protein biased δOR agonists explored in this dissertation is provided in section 5.1.1. In addition to reducing alcohol consumption levels, δOR agonists may also offer an advantage over current AUD treatments in reducing alcohol relapse, supporting their potential application in abstinence pharmacotherapy as well (Kotlińska and Langwiński, 1986; Sinha and Li, 2007; Heilig et al., 2010; van Rijn et al., 2013).

To better understand the complex role of δORs in alcohol modulation, additional investigations into biased agonism at this receptor are necessary. Because there is a paucity of G-protein biased agonists that target the δOR compared to the other opioid receptors (Faouzi et al., 2020), here I investigate natural products as a source for new biased opioid therapeutics for the δOR.

1.4.3 Drive to discover unique pharmacology at the opioid receptors

Historically, natural products from plants, fungi, bacteria and animals have played an important role in the discovery of new drugs (Harvey et al., 2015; Newman and Cragg, 2020). Since the discovery of morphine in 1805 by Serturner, many drugs have been discovered from natural products that contributed greatly to the emerging field of pharmacology. For instance, nomenclature for acetylcholine receptors is based on prototypical agonists nicotine and muscarine which are from the plants Nicotiana tabacum and Amanita muscaria (Muratspahić et al., 2019). Many drugs from natural products, such as paclitaxel, penicillin, lovastatin, doxorubicin and quinine have also had considerable impact in medicine. Because of the chemical and structural diversity of natural products, they continue to be one of the best options for discovering novel compounds and scaffolds, with derivatization efforts leading to the development of synthetic drugs such as aspirin, chloroquine, pentazocine, and atorvastatin (atorvastatin, also known as Lipitor, is notably the best-selling drug of the past 25 years with sales nearing $100 billion) (Clark, 1996; Newman and Cragg, 2020). In fact, it has been found that 34% of new FDA-approved drugs

between 1981 and 2014 were derived from natural products or their derivatives (Newman and Cragg, 2016). While the number of natural products research groups as well as government funding for natural products research has decreased over time, the "influence of natural products structures" has not been lessened, and natural products remain a rich resource for novel drug agents and templates that will continue to yield opportunities as new technological methods develop (Newman and Cragg, 2020; Atanasov et al., 2021).

Morphine and codeine, isoquinoline alkaloids found in Papaver somniferum, are the best-known natural products that interact at the μOR (Phillipson et al., 1985). Opioids are found in many other plants, however, and of different structural classes (Lovell et al., 2009). For instance, salvinorum A is a diterpenoid found in Salvia divinorum, or seer's sage, a plant well-known for its hallucinogenic effects (Ortega et al., 1982; Valdés et al., 1987). Salvinorum A was found to elicit its psychotropic effects through selective and potent agonism of the κOR, and is notably the first non-alkaloid compound to interact at this receptor (Roth et al., 2002). Similarly, highly selective peptides for the δOR known as deltorphins have been isolated from the skin of Phyllomedusa bicolor, a type of frog (Erspamer et al., 1989), and have been shown to produce δOR-mediated antinociceptive effects in mice (Jiang et al., 1990). In fact, peptides have recently been identified as a growing class for natural products discovery (Muratspahić et al., 2019). There have been numerous other opioids of different structural classes found from natural sources and are well reviewed in Lovell et al., but more recently several biased opioids have been identified in natural products (Lovell et al., 2009). Indole alkaloids from a plant known as kratom, or Mitragyna speciosa, were the first opioids from a natural product reported to target the opioid receptors in a biased manner (Kruegel et al., 2016). Shortly after, several other biased opioids were discovered from natural products such as collybolide isolated from mushroom Collybia maculata (Gupta et al., 2016), rubiscolin peptides from plant protein RuBisCO (Cassell et al., 2019), and tetrapeptides from Australian fungus (Dekan et al., 2019), to name a few. The drug scaffolds of these biased compounds, especially those of kratom, have also been used in derivatization efforts to enhance compounds potency and/or selectivity (Kruegel et al., 2016; Chakraborty et al., 2021b; Wilson et al., 2021). The findings presented in this dissertation builds on this body of research through investigation of the biased mechanisms of kratom and kratom derivatives in alcohol consumption, and examines the pharmacology of additional indole alkaloids from a plant known as akuamma and their utility in promoting antinociception.

CHAPTER 2. G PROTEIN-BIASED KRATOM-ALKALOIDS AND SYNTHETIC CARFENTANIL-AMIDE OPIOIDS AS POTENTIAL TREATMENTS FOR ALCOHOL USE DISORDER

This chapter was previously published in the British Journal of Pharmacology with the following DOI: 10.1111/bph.14913 and citation:
Gutridge, A.M., Robins, M.T., Cassell, R.J., Uprety, R., Mores, K.L., Ko, M.J., Pasternak, G.W., Majumdar, S. and van Rijn, R.M., 2020. G protein-biased kratom-alkaloids and synthetic carfentanil-amide opioids as potential treatments for alcohol use disorder. *British journal of pharmacology*, 177(7), pp.1497-1513.
Supplemental data including extensive statistical analyses and chemical characterization is freely available at the following location:
https://bpspubs.onlinelibrary.wiley.com/doi/10.1111/bph.14913
Additionally, findings in this chapter were also previously published as part Meridith T. Robins' dissertation at Purdue University.

2.1 Introduction

Interest in and use of the psychoactive plant *Mitragyna speciosa* (kratom) has risen dramatically across North America and Europe over the last five years (Singh et al., 2016), (**Figure 2.1A-B**). Historically, kratom has been used in its indigenous Southeast Asian regions to relieve pain, diarrhea, and cough, or to provide stimulation (Prozialeck et al., 2012). The currently inflated interest in kratom in the United States coincides with changes in opioid prescribing guidelines by the Center for Disease Control and Prevention in 2016 (Renthal, 2016) and the rise in heroin adulterated with fentanyl-like opioids, leading to a spike in fatal and non-fatal overdoses (Dowell et al., 2017; Gostin et al., 2017). Kratom contains greater than forty alkaloids with varying affinity and activity at opioid receptors (Takayama, 2004; Adkins et al., 2011; Hassan et al., 2013; Kruegel et al., 2016; Brown et al., 2017) and is commonly used for the self-medication of opioid dependence and withdrawal, the management of chronic pain and mood disorders, or as substitute for heroin or prescription opioids (Singh et al., 2016; Grundmann, 2017; Smith and Lawson, 2017). Despite these perceived benefits, increasing rates of kratom use have led to concomitant increases in reports of adverse effects following consumption, although to date no fatal overdoses have been attributed to kratom use alone (Cinosi et al., 2015; Kruegel and Grundmann, 2018). While the Drug Enforcement Administration recently decided to withhold its decision on classifying kratom as a Schedule I drug (Griffin and Webb, 2018; Grundmann et al., 2018), reservations about the

safety of kratom remain, leading to increased scrutiny of its current legal status in the United States (Prozialeck, 2016; Henningfield et al., 2018).

The ability of kratom alkaloids to stimulate the μ-opioid receptor (μOR) is a major factor in their activity (Boyer et al., 2007; Hassan et al., 2013; Angkurawaranon et al., 2018). Particularly, 7-hydroxymitragynine, with (K_i) affinities for μOR, δ and κ opioid receptors (δOR and κOR) of 37±4 nM, 91±8 nM, and 132±7 nM respectively (Váradi et al., 2016), has been of particular interest because of prior reports indicating 4-5x more potent antinociceptive activity than morphine in rodents while also producing less constipation (Takayama et al., 2002; Matsumoto et al., 2004, 2006; Váradi et al., 2016). The potential reduced side effect profile of kratom alkaloids has been associated with their negligible μOR-mediated β-arrestin 2 recruitment (Kruegel et al., 2016; Váradi et al., 2016), characterizing them as so-called G protein-biased agonists (Whalen et al., 2011; Schmid et al., 2017; Majumdar and Devi, 2018).

Only a small number of pharmacologic treatment options are approved for the treatment of alcohol use disorder, all of which are limited by inconsistent and/or poor efficacy. This lack of effective therapies may explain why kratom use has also been reportedly used in the self-medication of symptoms associated with alcohol withdrawal (McWhirter and Morris, 2010; Havemann-Reinecke, 2011; Singh et al., 2014; Suhaimi et al., 2016). Previous research has shown that G protein-biased δOP agonists decrease voluntary alcohol intake in C57Bl/6 male mice, while δOR agonists that strongly recruit β-arrestin 2 increase voluntary alcohol intake (Nielsen et al., 2012b; Chiang et al., 2016; Robins et al., 2018a). From these findings, we hypothesized that the reported utility of kratom in reducing alcohol intake stems from kratom's constituent alkaloids displaying G protein bias at δOR. To address our hypothesis, we characterized the μOR, δOR, and κOR pharmacology of two separate kratom extracts, four isolated major kratom alkaloids (mitragynine, speciogynine, paynantheine and 7-hydroxymitragynine, **Figure 2.1C**), as well as three synthetic opioids N-cycloheptyl-1-phenethyl-4-(N-phenylpropionamido)piperidine-4-carboxamide, N-cyclopropyl-1-phenethyl-4-(N-phenylpropionamido)piperidine-4-carboxamide, N-(tert-butyl)-1-phenethyl-4-(N-phenylpropionamido)piperidine-4-carboxamide (MP102, MP103, MP105, respectively) that have G protein-biased pharmacology similar to the kratom alkaloids. These extracts and drugs were also assessed for their ability to modulate alcohol intake, affect general locomotive behavior, and for their rewarding properties.

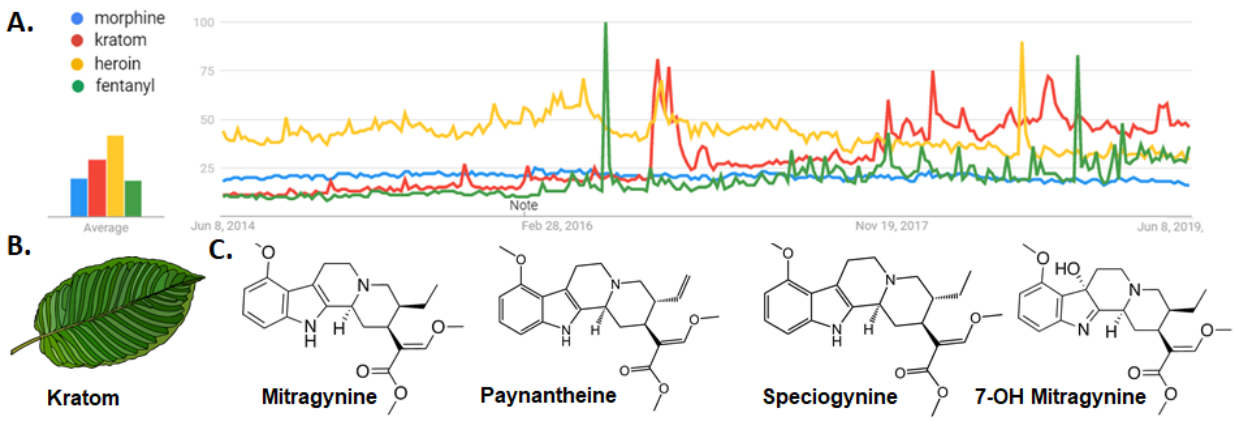

Figure 2.1 Interest in kratom has steadily increased over the last five year period.

Five-year Google trends analysis from June 2014 - June 2019 (performed June 8th, 2019) comparing morphine (blue), kratom (red), heroin (yellow) and fentanyl (green). Note that Google searches for kratom outnumbered those for heroin starting November 2017. The spike in heroin searches coincide with the overdose of Demi Lovato. The first spike in fentanyl searches coincide with the death of Prince and the second spike with FDA approval of Dsuvia™ (sufentanil). The initial increase in kratom searches in the fall of 2016 coincided with the DEA's decision to defer their scheduling kratom (**A**). Animated depiction of a kratom leaf (**B**). Chemical structures of characterized kratom alkaloids (**C**). Results shown in in this figure were also previously published as part Meridith T. Robins' dissertation at Purdue University.

2.2 Methods

2.2.1 Materials

Speciogynine, paynantheine, 7-hydroxymitragynine, and mitragynine were isolated (purity; >95%) by column chromatography and provided by Dr. Majumdar. MP102, MP103, and MP105 were synthetically derived (purity; >97%) and provided by Dr. Majumdar. Morphine sulfate pentahydrate, leu-enkephalin, forskolin, hydrochloric acid, sodium sulfate, dichloromethane, ammonia, hexanes, and ethyl alcohol (200 proof) were purchased from Sigma-Aldrich (St. Louis, MO USA). Naltrindole hydrochloride, (2S)-2-[[2-[[(2R)-2-[[(2S)-2-Amino-3-(4-hydroxyphenyl)propanoyl]amino]propanoyl]amino]acetyl]-methylamino]-N-(2-hydroxyethyl)-3-phenylpropanamide (DAMGO), and 2-(3,4-dichlorophenyl)-N-methyl-N-[(1R,2R)-2-pyrrolidin-1-ylcyclohexyl]acetamide (U50,488) were purchased from Tocris Bioscience (Bio-techne Corporation, Minneapolis, MN, USA). (3-Methoxythiophen-2-yl)methyl]((2-[(9R)-9-(pyridin-2-yl)-6-oxaspiro-[4.5]decan-9-yl]ethyl))amine (TRV130) was purchased from AdooQ Bioscience

(Irvine, CA, USA). For animal drinking assays, pure ethyl alcohol was diluted to 10% or 20% alcohol in reverse osmosis water.

2.2.2 Kratom Extract #1

An alkaloid extract was obtained from Maeng Da Micro Powder (MoonKratom, Austin, TX USA) as described previously by Orio et al. (Orio et al., 2012). In brief, as shown in Figure S1A of the online supplement, extraction was performed by treating kratom powder in 95% ethanol at 50 °C for four hours followed by removal of the remaining organic material by vacuum filtration. Solvent was then removed under reduced pressure and the crude extract re-suspended in dilute aqueous hydrochloric acid (pH=3) and washed with hexane. The aqueous solution was then basified (pH=9) with 0.1 M aqueous ammonia and the freebase alkaloid fraction extracted with dichloromethane. The alkaloid containing fraction was dried over anhydrous sodium sulfate and filtered, followed by removal of solvent under reduced pressure and further drying under high vacuum to obtain our kratom alkaloid extract as a crystalline, light brown solid. Extract composition was assessed on a 6550-quadropole time-of-flight (Aligent, Santa Clara, CA, USA) (scan 105-100 amu) using a Zorbax Extend-C18 column (Aligent) held at 30°C and a 0.3 mL/minute flow rate.

2.2.3 Kratom extract #2

Mitragynine was extracted from the powdered leaves by following our previously reported methods (Váradi et al., 2016)(Figure S1B of the online supplement). “Red Indonesian Micro Powder” was purchased from MoonKratom. The kratom powder (500 g) was heated to 75°C to reflux in methanol 700 mL for 40 min. The suspension was filtered and the methanolic extraction process was repeated (3 x 500 mL). The solvent of combined methanolic extract was removed under reduced pressure and the content was dried using high vacuum. The dry residue was resuspended in 20% acetic acid solution (1 L) (pH=4) and washed with petroleum ether (4 x 500 mL). The aqueous layer was then cooled on ice bath and basified (pH ~9) slowly with aqueous sodium hydroxide solution (3.5M. ~1L). Alkaloids were extracted in dichloromethane (4 x 400 mL) from the aqueous layer. The combined dichloromethane fractions were washed with brine (300 mL) and dried over anhydrous sodium sulfate and filtered. The solvent was removed under

reduced pressure, and the residue was dried under high vacuum to obtain kratom extract. The kratom extract was subjected to column chromatography (gradient: 0-40% ethylacetate in hexanes) to isolate mitragynine (Yield; 4.9 g), and smaller quantities of paynantheine (0.58 g) and speciogynine (0.35 g).

For cellular assays, kratom extracts were dissolved to a concentration of 10 mM in 100% DMSO. The calculated concentration was estimated by assigning the kratom extract an estimated molecular mass of 400 g/mol, which is the average size of kratom alkaloids.

2.2.4 Cell culture and biased signaling assays

cAMP inhibition and β-arrestin 2 recruitment assays were performed as previously described (Chiang et al., 2016). In brief, for cAMP inhibition assays, HEK 293 (Life Technologies, Grand Island, NY, USA) cells were transiently transfected in a 1:3 ratio with FLAG-mouse δOR, HA-mouse μOR or FLAG-mouse κOR and pGloSensor22F-cAMP plasmids (Promega, Madison, WI, USA) using Xtremegene9 (Sigma). Two days post-transfection, cells (20,000 cells/well, 7.5 μl) were seeded in low-volume Greiner 384-well plates (#82051-458, VWR, Batavia, IL, USA) and incubated with GloSensor reagent (Promega, 7.5 μl, 2% final concentration) for 90 minutes at room temperature. Cells were stimulated with 5 μl drug solution for 20 minutes at room temperature prior to stimulation with 5 μl forskolin (final concentration 30 μM) for an additional 15 minutes at room temperature. For β-arrestin recruitment assays, CHO-human μOR PathHunter β-arrestin 2 cells and CHO-human δOR PathHunter β-arrestin 2 cells or U-2 osteosarcoma (U2OS)-human κOR PathHunter β-arrestin 2 cells (DiscoverX, Fremont, CA, USA) were plated (2,500 cells/well, 10 μl) one day prior to stimulation with 2.5 μl drug solution for 90 minutes at 37°C/5%CO_2, after which cells were incubated with 6 μl cell PathHunter assay buffer (DiscoverX) for 60 minutes at room temperature as per the manufacturer's protocol. Luminescence for each of these assays was measured using a FlexStation3 plate reader (Molecular Devices, Sunnyvale, CA, USA).

2.2.5 Calculation of bias factor

In order to determine ligand bias, we followed the operational model equation in Prism 8 to calculate Log R (τ/KA) (Table S1 of the online supplement), ΔLogR and ΔΔLogR as previously

described (van der Westhuizen et al., 2014). Subsequently bias factors ($10^{\Delta\Delta LogR}$) were calculated using DAMGO, leu-enkephalin and U50,488 as reference compounds for μOR, δOR and κOR, respectively. All three reference compounds were more potent in the cAMP (G protein) assay than in the β-arrestin 2 recruitment assay, and thus were not unbiased but G protein-biased to begin with. A bias factor >1 meant that the agonist was more G protein-biased than the reference compound; a bias factor <1 meant that the agonist was less G protein-biased than the reference compound. Bias factors for compounds with <30% efficacy for β-arrestin 2 recruitment could not reliably be calculated and are listed as undeterminable (**Table 2.1**), which indicates that these agonists can be considered to be efficacy-dominant for G protein signaling (Kenakin, 2015).

2.2.6 Animals

The animal protocol (#1305000864) describing the care and use of experimental animals was approved by the Purdue University Institutional Animal Care and Use Committee (https://www.purdue.edu/research/regulatory-affairs/animal-research/staff.php). Animal studies were carried out in accordance with the ARRIVE guidelines (Kilkenny et al., 2010a) and recommendations made by the *British Journal of Pharmacology* as well as recommendations of the National Institutes of Health Guide for the Care and Use of Laboratory Animals. For our experiments we used adult male (19-24 g) and female (17-21 g) wild-type C57/BL6 mice (8-10 week old) purchased from (Envigo, Indianapolis, IN, USA). This is a strain known to readily consume alcohol (Belknap et al., 1993). We also used male δOR knockout C57BL/6 mice of similar age in a subset of experiments. δOR knockout mice were produced by removal of exon 2 as previously described (van Rijn and Whistler, 2009) and outbred to a C57BL/6 background (>10 generations). Roughly every 3 years, the strain is backcrossed to commercially obtained C57BL/6 mice (Envigo) to mitigate the effects of genetic drift.

We provided food and water *ad libitum* unless specified otherwise for the binge ethanol experiments. With the exception of the ethanol experiments where mice were individually housed in double grommet cages, animals were group housed in plexiglass cages in ventilated racks at ambient temperature of (21°C) in a room maintained on a reversed 12L:12D cycle (lights off at 10.00, lights on at 22.00) in Purdue University's animal facility, which is accredited by the Association for Assessment and Accreditation of Laboratory Animal Care. Mice were used only in a single behavioral paradigm with the exception of the two-bottle choice model of moderate 10%

alcohol consumption (Section 2.6) in which mice received increasing doses of the test drug over multiple weeks.

2.2.7 Two-bottle choice model of moderate 10% alcohol consumption

Mice were trained to voluntarily consume alcohol in a limited access (four hours/day), 2-bottle choice (water vs. 10% ethanol), drinking-in-the-dark (DID) protocol during their active phase (three hours after the start of the dark cycle) until the alcohol intake was stable as previously described (van Rijn and Whistler, 2009). During the first three weeks of limited alcohol access, h the mice increased their alcohol intake prior to reaching steady state consumption. After the completion of the third week of voluntary alcohol intake, injections were administered every Friday thirty minutes prior to the four-hour drinking session. Drug effect on alcohol and water intake was measured as a change in Friday total drinking minus average alcohol intake between Tuesday-Thursday (g/kg). Raw data for alcohol intake, water intake, alcohol preference and associated statistical analysis are provided in the supplemental material (Figure S2-4, Table S2 of the online supplement).

2.2.8 Intermittent, limited-access of 20% alcohol binge consumption model

To measure the effects of drug administration on binge-like alcohol consumption, we followed a DID binge protocol (Rhodes et al., 2005; Robins et al., 2018a). In this one-week protocol, the water bottle for each cage was replaced with a bottle containing 20% ethanol for two hours on Monday-Thursday (i.e. no 2-bottle choice). Using consumption data from these four days, the average ethanol consumption of the mice was ranked and the mice were sorted into groups of comparable/equal drinking (with each group to be administered either vehicle or a drug). On the Friday of the binge protocol, mice received IP injections of either vehicle or drug thirty minutes prior to a four hour "binge" drinking period with access to 20% ethanol. To determine drug effect on alcohol intake, the amount of ethanol consumed during the binge period was compared between vehicle and drug-treated groups.

For all ethanol consumption experiments, bottle weights were measured directly before and after the ethanol access periods to the second decimal point to determine fluid intake and weights

of bottles were corrected for any spillage. In addition, the location of alcohol bottles in each paradigm was alternated daily (right vs. left grommet) to prevent habit formation.

2.2.9 General locomotor activity assessment

Square locomotor boxes from Med Associates (L 27.3 cm x W 27.3 cm x H 20.3 cm, St. Albans VT, USA) were used to monitor locomotor activity. For all locomotor studies, animals were moved to the testing room for 60 minutes prior to testing for habituation. A 90-minute baseline habituation session to the boxes was conducted prior to drug administration to reduce novelty locomotor differences. The following day, mice were again habituated to the room for 60 minutes. Then mice were injected with drug or vehicle and locomotor activity was monitored immediately for a total of 90 minutes. All testing was conducted during the dark/active phase.

2.2.10 Acute thermal antinociception

To measure antinociception we utilized a tail-flick assay as previously described (van Rijn et al., 2012b). In short, 8 week-old male C57BL/6 wild-type mice (n=10) were habituated to handling. The following day a baseline tail-flick response was recorded using a radiant-heat tail-flick apparatus (Columbus Instruments, Columbus, OH, USA). The light intensity was set to '9' to produce an average baseline response of 2-3 seconds. We utilized a maximal cutoff of 3x baseline to reduce the risk of damaging the mice tails. For each test, two tail-flick responses were recorded and the average was used for further analysis. Immediately after the baseline recording, mice were injected s.c. with saline and 30 minutes later a new tail-flick response was measured. After the saline injection, mice were injected with 1 mg/kg TRV130 (s.c.) and a third tail-flick response was recorded 30 minutes post TRV130 injection. The experiment was repeated in the same cohort of mice on the following two days but using 3 mg/kg and 10 mg/kg TRV130 instead. We only tested 8 mice with 10 mg/kg TRV130 and injected the remaining 2 mice with 10 mg/kg morphine as internal control (both mice displayed 100% antinociception, data not shown). Antinociception was calculated as maximal possible effect (%MPE) = $(Response_{drug} - Response_{baseline})/(Response_{cutoff} - Response_{baseline})*100$.

2.2.11 "Brief" conditioned place preference (CPP)

Mice were conditioned to drugs or vehicle as described previously (Váradi et al., 2015a) with two modifications: 1) conditioning sessions lasted 40 minutes rather than 30 minutes and 2) a two-chamber apparatus rather than a three-chamber set up was utilized. One chamber contained a wire mesh floor and horizontal black/white striped wallpaper, whereas the second chamber contained a metal rod floor and vertical black/white striped wallpaper. To determine initial compartment bias, a vehicle injection was administered intraperitoneally immediately prior to the pre-conditioning session to create an unbiased, counterbalanced approach for drug-pairing (half of the animals received drug on the pre-test preferred side, while half received drug on the pre-test non-preferred side). Animals exhibiting >70% preference for one of the two chambers were removed from further testing. Over the following two days, two conditioning sessions per day were performed four hours apart (morning and afternoon, vehicle or drug semi-random) for a total of four conditioning sessions (two to vehicle on the non-drug-paired side and two to drug on the drug-paired side). On the post-conditioning testing day, a vehicle injection was administered directly before placing the animals in the testing apparatus to determine post-conditioning preference. For all sessions, animals were habituated to the testing room 60 minutes before sessions and all behavior was conducted during the dark/active phase.

2.2.12 "Extended" CPP

The differences between the "brief" and "extended" CPP were as follows 1) conditioning sessions were 30 minutes instead of 40 minutes, 2) mice only received one conditioning session per day (none on the weekend), and 3) mice received four rather than two vehicle and drug exposures. In the initial habituation session, a vehicle intraperitoneal injection was administered prior to the session to assess initial bias towards either chamber. An unbiased, counterbalanced approach was then used to assign the drug-paired side for each animal (half of the animals received drug on the pre-test preferred side, while half received drug on the pre-test non-preferred side). Animals exhibiting >70% preference for one of the two chambers were removed from further testing. Over the course of two weeks, mice were conditioned on eight days, but with only one conditioning session per day (four to vehicle on the non-drug-paired side, four to drug on the drug-paired side). On the post-conditioning testing day, a vehicle injection was administered directly

before placing the animals in the testing apparatus where animals were allowed to explore both chambers to determine post-conditioning preference. For all sessions, animals were habituated to the testing room 60 minutes before sessions and all behavior was conducted during the dark/active phase.

2.2.13 Data and Statistical analysis

Data and statistical analysis comply with the recommendations on experimental design and analysis in pharmacology (Curtis et al., 2018). All data are presented as means ± standard error of the mean, and analysis was performed using GraphPad Prism 8 software (GraphPad Software, La Jolla, CA). For *in vitro* assays, nonlinear regression was conducted to determine pIC_{50} (cAMP) or pEC_{50} (β-arrestin 2 recruitment). Technical replicates were used to ensure the reliability of single values, specifically each data point for binding and arrestin recruitment was run in duplicate, and for the cAMP assay in triplicate. The averages of each independent run were considered a single experiment and combined to provide a composite curve in favor of providing a 'representative' curve. In each experimental run, a positive control/standard was utilized to allow the data to be normalized, thereby providing the opportunity to calculate the log bias value which relies on the presence of the standard. For the data analysis of the behavioral experiments, we first we established that data set did not contain an outlier using the Grubbs' test. If the test revealed an outlier, this value was removed, but removal was limited to one data point per set. We then verified if the data values came from a Gaussian distribution using the D'Augostino and Pearson omnibus normality test. If the data followed a Gaussian distribution we carried out a parametric test, otherwise we opted for the non-parametric test. To determine statistical differences in the means between two values, we performed a t-test if the two datasets passed the normality test, but with a Welch's correction if the datasets did not have the same standard deviation. For those datasets, where one or both datasets did not pass the normality test, we performed a Mann-Whitney *U*-test. Significant changes in average alcohol intake were determined by one-way, repeated measures analysis of variance (ANOVA) with Tukey's multiple comparisons (MC) test. For CPP, two-way, repeated measures ANOVA with Bonferroni MC was used to determine significant differences in time spent on the drug-paired side pre- versus post-conditioning. One-way ANOVA with Bonferroni MC determined significance for locomotor studies. For the repeated measures tests, whenever we could not assume sphericity, a Geisser-Greenhouse correction was carried out by

Prism. *P* values <.05 were considered as statistically significant (Table S3 in the online supplement). Whenever possible, the experimenter was blind to the drug and/or dose tested; however, we always started with the lowest drug dose if multiple doses were to be tested. Animals were assigned to groups such that the baseline responding was equal across groups. The treatment that each group received was then randomized . Group size were equal by design, and based on a power analysis calculated using the observed deviation in our prior published work. On occasion mice were excluded prior to drug treatment because of a failure to consume alcohol during the initial alcohol voluntary consumption phase; however, on some occasions we started with a larger group size to account for potential non-responders. We did not explicitly design our experiments to test for sex differences; with the exception of the study of kratom impact on binge alcohol use, male and female groups were of unequal size. To account for the unequal sample size, we utilized the Sidak's post-hoc test.

2.3 Results

2.3.1 Different strains of kratom differ slightly in alkaloid composition.

The Maeng Da kratom extract #1 consisted of mitragynine (44.9%), paynantheine (14.1%), speciogynine (8.9%), and 7-hydroxymitragynine (2.9%) as major alkaloids. In contrast, Red Indonesian Micro powder kratom extract #2 was notably devoid of 7-hydroxymitragynine and consisted of mitragynine (49%), paynantheine (9%), and, speciogynine (3.5%). The alkaloid compositions of the kratom extracts were in line with those previously reported (Hassan et al., 2013).

2.3.2 Mice injected with kratom extract decrease moderate and binge alcohol intake.

To corroborate the self-prescribed use of kratom for alcohol use disorder, male C57BL/6 mice (n=9) were injected (i.p.) with kratom extract #1, resulting in a dose-dependent decrease in their volitional alcohol intake (**Figure 2.2 A**), with the dose of 30 mg/kg kratom extract #1 displaying a significant decrease compared with vehicle (0.9% saline) or 10 mg/kg. We obtained a significant similar result in male mice (n=10) when injected with kratom extract #2 (Figure S5 of the online supplement). It should be noted that while kratom extract #2 did not contain 7-hydroxymitragynine, mitragynine can be metabolized into 7-hydroxymitragynine (Kruegel et al.,

2019) and thus extract #1 and #2 may not differ much i*n vivo*. We found that 30 mg/kg kratom extract #1 significantly reduced alcohol intake in male C57BL/5 mice (n=8) in a model of 20% alcohol binge use (**Figure 2.2 B**). We assessed if mice receiving 30 mg/kg of kratom extract #1 displayed altered locomotor activity compared with vehicle-treated male mice (vehicle, n=14; kratom, n=12). Over a 90-minute timespan, mice receiving kratom extract #1 had a slight but significant decrease in their total locomotor activity compared with vehicle-treated mice (**Figure 2.2 C**). The difference was driven by a rapid but short decrease in locomotor activity in the first 30 minutes following injection (**Figure 2.2 D**). As for the male mice, we also observed that kratom extract #1 dose dependently decreased alcohol intake in female mice (**Figure 2.2E**, n=12) and 30 mg/kg kratom extract #1 similarly decreased binge alcohol intake in female mice (**Figure 2.2F**, n=8). The dose of 30 mg/kg kratom extract #1 decreased locomotor activity in female mice (**Figure 2.2G**, n=8). As for the males a sharp decrease in locomotor activity was observed during the first 10-40 minutes post-injection (**Figure 2.2H**). Sex differences exist for basal alcohol intake by C57BL/6 mice (Nocjar et al., 1999; Robins et al., 2018a) and were apparent for moderate alcohol intake 3.0 mg/kg vs 5.0 mg/kg, but not significant for binge alcohol intake 6.6 mg/kg vs 7.5 mg/kg. There was a sex-drug interaction for the locomotor effects of kratom, but not for modulation of moderate alcohol intake or binge alcohol intake.

2.3.3 Kratom alkaloid extracts exhibit G protein bias.

Both kratom extracts inhibited forskolin-stimulated cAMP production in HEK293 cells transiently transfected with mouse μOR, δOR or κOR, although with decreased potency and efficacy compared with the reference ligands DAMGO, leu-enkephalin and U50,488, respectively (**Figure 2.3A-C**). In general, the kratom extracts were less potent than morphine, with the exception of kratom extract #2 at κOR. The reference opioids all efficaciously recruited β-arrestin 2 while morphine weakly recruited β-arrestin 2 at μOR. The kratom extracts did not lead to detectable β-arrestin 2 recruitment at μOR or δOR, with very weak recruitment at κOR, similar to that of morphine at κOP (**Table 2.1** and **Figure 2.3D-F**).

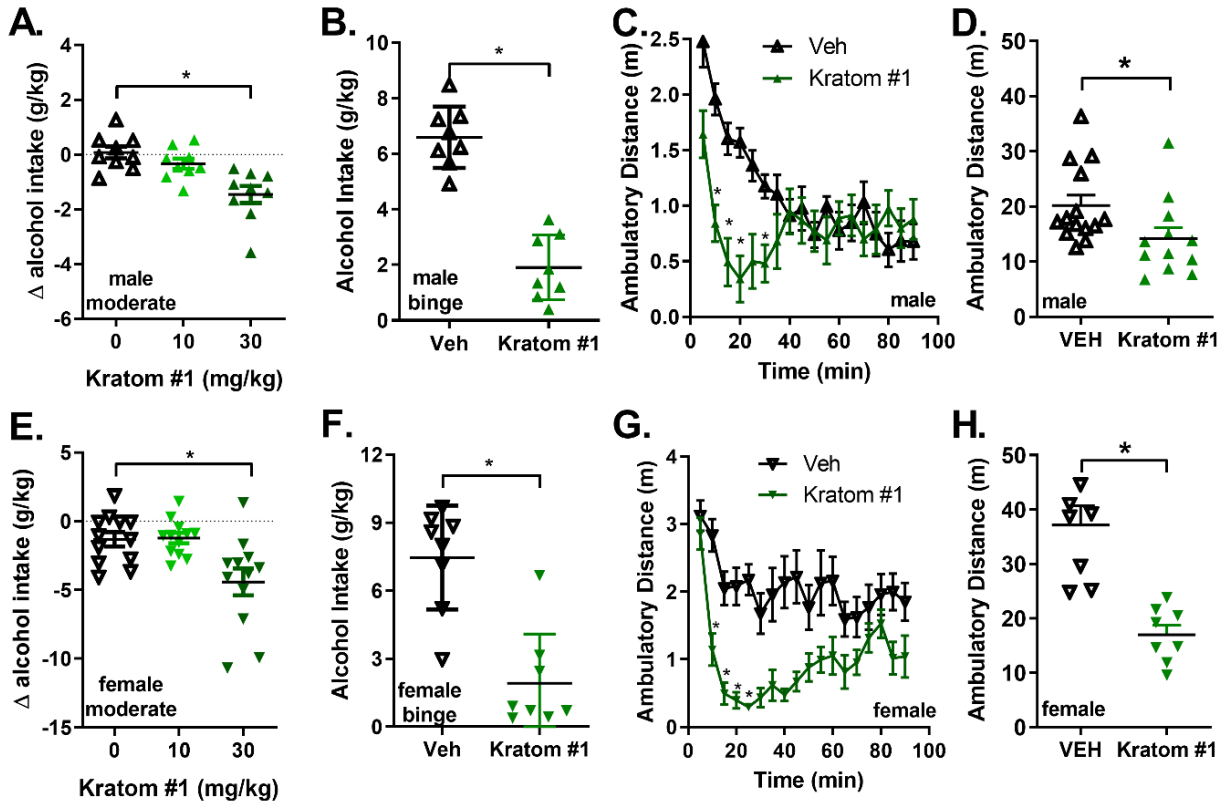

Figure 2.2 Kratom reduces alcohol intake and locomotor activity in male and female mice.

Systemic (i.p.) injection of kratom extract #1 dose-dependently reduced 10% alcohol intake in male mice (**A**). Systemic administration of 30 mg/kg kratom extract #1 decreased 20% alcohol intake in male mice (**B**). Time course of male locomotor activity following kratom extract #1 injection (30 mg/kg, i.p.) (**C**). Systemic administration of 30 mg/kg kratom extract #1 reduced general locomotor activity of male mice (**D**). Systemic (i.p.) injection of kratom extract #1 dose-dependently reduced 10% alcohol intake in female mice (**E**). Systemic administration of 30 mg/kg kratom extract #1 decreased 20% alcohol intake in female mice (**F**). Time course of female locomotor activity following kratom extract #1 injection (30 mg/kg, i.p.) (**G**). Systemic administration of 30 mg/kg kratom extract #1 reduced general locomotor activity of female mice (H). Results shown in in this figure were also previously published as part Meridith T. Robins' dissertation at Purdue University.

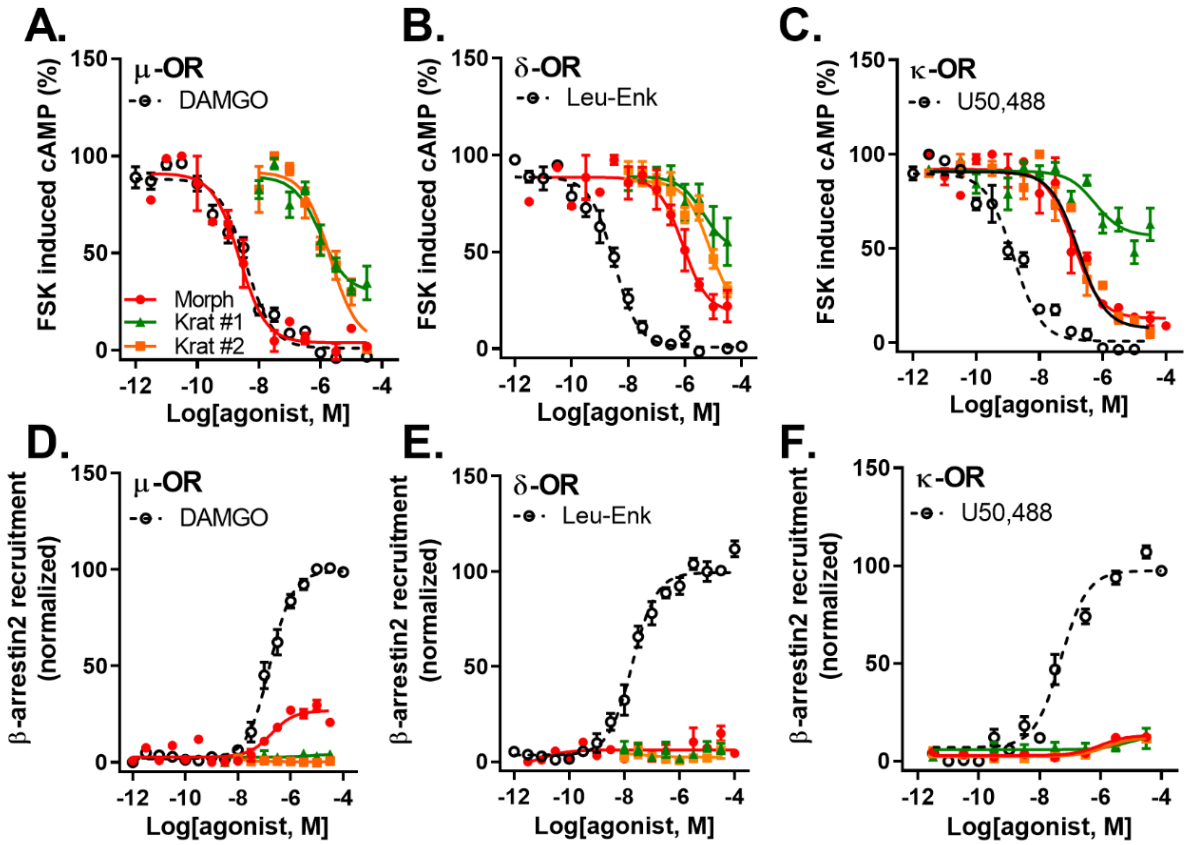

Figure 2.3 Kratom extracts display G protein bias at μOR, δOR or κOR.

Comparison of morphine with kratom extract #1 and #2 for the ability to reduce forskolin (FSK)-induced cAMP production in HEK293 cells expressing μOR (**A**), δOR (**B**) or κOR (**C**), normalized to the relevant positive controls (dotted lines, open circles) DAMGO (μOR), leu-enkephalin (δOR) and U50,488 (κOR). Comparison of morphine (red filled circles) with kratom extract #1 (green triangles) and extract #2 (orange squares) for the ability to recruit β-arrestin 2 in CHO-μOR (**D**), CHO-δOR (**E**) or U2OS-κOR (**F**) PathHunter cells normalized to the relevant positive controls (dotted lines). Results shown in in this figure were also previously published as part Meridith T. Robins' dissertation at Purdue University.

2.3.4 Kratom alkaloids display G protein bias at all three opioid receptors *in vitro*.

We next assessed if the individual kratom alkaloids mitragynine, paynantheine, speciogynine, and 7-hydroxymitragynine (**Figure 2.1C**) are G protein-biased at all three opioid receptors by measuring cAMP inhibition and β-arrestin 2 recruitment at μOR, δOR and κORs. All four alkaloids inhibited cAMP production, with 7-hydroxymitragynine being the most potent at all three opioid receptors (**Figure 2.4A-C**). In line with the limited β-arrestin 2 recruitment observed for the kratom extracts, the individual alkaloids did not recruit β-arrestin 2 to a measurable extent (**Table 2.1** and **Figure 2.4D-F**).

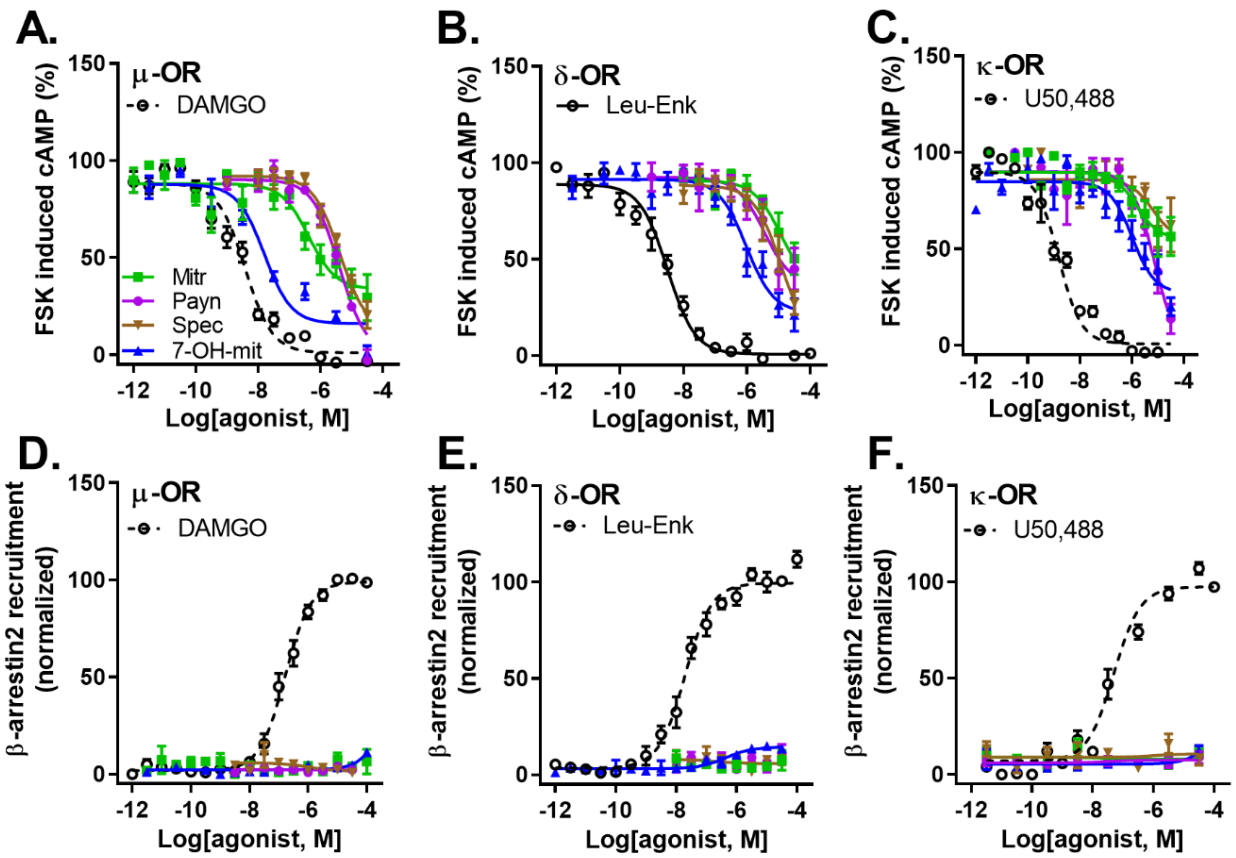

Figure 2.4 Kratom alkaloids display G protein bias at μOR, δOR or κOR.

Mitragynine (green ■), 7-OH-mitragynine (blue ▲), paynantheine (purple ●) and speciogynine (brown▼) reduce forskolin (FSK)-induced cAMP production in HEK293 cells expressing μOR (A), δOR (B) or κOR (C), normalized to the relevant positive controls (dotted lines) DAMGO (μOR), leu-enkephalin (δOR) and U50,488 (κOR). Mitragynine (green ■), 7-OH-mitragynine (blue ▲), paynantheine (purple ●) and speciogynine (brown▼) do not recruit β-arrestin 2 in CHO-μOR (D), CHO-δOR (E) or U2OS-κOR (F) PathHunter cells normalized to the relevant positive controls (dotted lines, open circles). Results shown in in this figure were also previously published as part Meridith T. Robins' dissertation at Purdue University.

2.3.5 Kratom alkaloids decrease alcohol intake, but differentially affect general locomotion.

We next investigated whether the individual kratom alkaloids would modulate alcohol intake. We chose to use male mice, as their locomotor activity was impacted less by kratom than female mice. Alcohol intake in male C57BL/7 mice was significantly decreased upon administration of 30 mg/kg and 100 mg/kg mitragynine compared with average change in alcohol intake after vehicle (0.9% saline) injection (**Figure 2.5A**). Paynantheine dose-dependently decreased voluntary alcohol intake at both 10 mg/kg and 30 mg/kg (**Figure 2.5B**), while speciogynine decreased alcohol intake only at the 30 mg/kg dose (**Figure 2.5C**). For 7-hydroxymitragynine, the most potent of the alkaloids, a decrease in alcohol intake was observed at both 3 and 10 mg/kg with a dose-dependent efficacy (**Figure 2.5D**). In female mice, administration of 3 mg/kg 7-hydroxymitragynine also significantly decreased alcohol intake in the same 10% voluntary ethanol consumption protocol (**Figure 2.5E**). Given that the kratom extract altered general locomotion, we also assessed whether the individual alkaloids had similar effects on locomotor activity of mice when given at the lowest effective dose. The kratom alkaloids produced variable locomotor effects in the male mice. Both 30 mg/kg mitragynine (n=8) and 3 mg/kg 7-hydroxymitragynine (n=8) increased locomotor activity, although only the increase induced by 7-hydroxymitragynine was significant compared with vehicle. In contrast, 10 mg/kg paynantheine (n=8) did not significantly alter locomotion whereas 30 mg/kg speciogynine (n=8) significantly decreased locomotion compared with vehicle (0.9% saline, n=10) control (**Figure 2.5F**). The 3 mg/kg dose of 7-hydroxymitragynine also increased locomotor activity in female mice (**Figure 2.5F**).

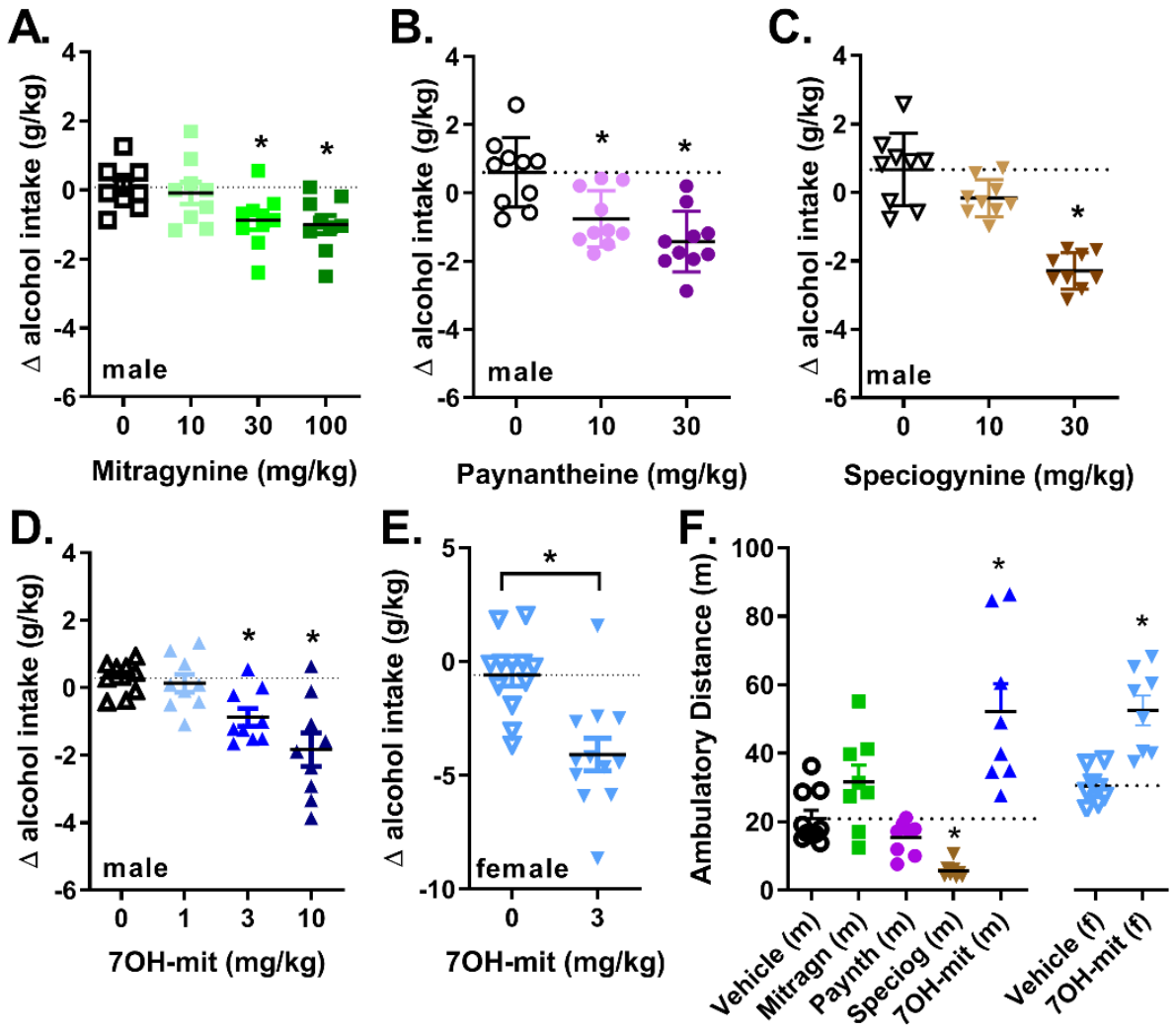

Figure 2.5 Kratom alkaloids reduce alcohol intake but differentially affect locomotor activity.

Systemic (i.p.) injection of mitragynine (**A**), paynantheine (**B**), speciogynine (**C**) and 7-hydroxymitragynine (7-OH-mit, **D**) modified 2-bottle choice drinking behavior in male C57BL/6 mice. Systemic injection of 7-hydroxymitragynine (3 mg/kg, i.p.), reduced 10% alcohol intake in female mice (**E**). 7-hydroxymitragynine (3 mg/kg, i.p.) increased locomotor activity of male and female mice, whereas speciogynine (30 mg/kg, i.p.) decreased locomotor activity in male mice (**F**). Results shown in in this figure were also previously published as part Meridith T. Robins' dissertation at Purdue University.

2.3.6 Selective G protein activation of μOR is insufficient to reduce alcohol intake.

We next sought to determine whether the changes in alcohol intake by kratom and kratom alkaloids were μOR mediated. We were limited in our approach as removal of functional μORs through antagonism or knockout cause animals to self-administer less alcohol (Middaugh and Bandy, 2000; Roberts et al., 2000). As an alternative approach, to determine if G protein-biased μOR signaling underlies the observed alcohol phenotype of kratom, we investigated whether TRV130 (oliceridine), a known μOR G protein-biased agonist (DeWire et al., 2013), could reduce alcohol intake. We first confirmed that TRV130 is a G protein-biased and μOR-selective agonist (**Figure 2.6A-B**, **Table 2.1**, and Figure S8 in the online supplement). Yet, at doses (1 and 3 mg/kg i.p.) known to produce μOR-mediated analgesia (DeWire et al., 2013) (Fig.S9 in the online supplement), TRV130 failed to decrease 10% alcohol intake in wild-type male mice (**Figure 2.6C**) compared to vehicle (saline 0.9%).

2.3.7 7-hydroxymitragynine's effect on alcohol intake, but not on locomotion, requires δORs.

We next examined the contribution of δORs to these observed behaviors, particularly because G protein-biased δOR agonists can reduce moderate alcohol intake in mice (Chiang et al., 2016; Robins et al., 2018b). Because 7-hydroxymitragynine has affinity and potency at δORs, we assessed this alkaloids response in δOR knockout male mice. We did not observe changes in 10% alcohol intake at 3 mg/kg or 10 mg/kg 7-hydroxymitragynine compared to vehicle (0.9% saline) in δOR knockout mice (**Figure 2.6D**). In a different cohort of δOR knockout mice, 3 mg/kg 7-hydroxymitragynine (n=6) significantly increased locomotor activity compared with controls (n=12) (**Figure 2.6E**), with a peak in activity immediately after injection (**Figure 2.6F**). The lack of impact of 7-hydroxymitragynine on alcohol intake in δOR knockout mice, despite increased locomotor activity, suggests that hyperlocomotion alone did not contribute to the observed decrease in alcohol intake at 3 mg/kg 7-hydroxymitragynine in wild-type mice (**Figure 2.5D**). There was no sex-drug interaction for the locomotor effects of 7-hydroxymitragynine, but there was an interaction for modulation of moderate alcohol intake.

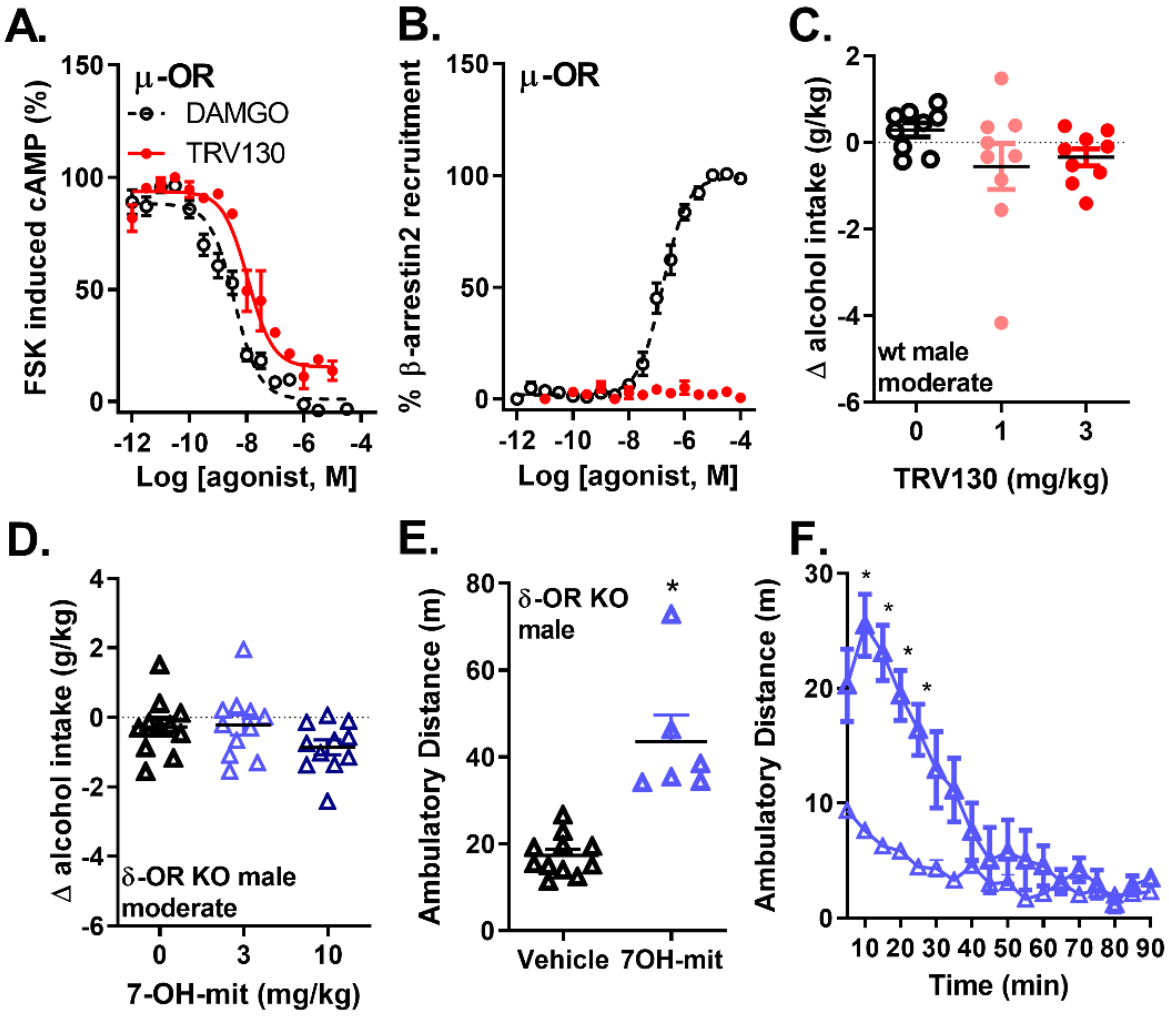

Figure 2.6 Kratom alkaloids reduce alcohol intake in mice through a δOR-dependent mechanism.

The G protein-biased μOR agonist TRV130 (red ●) potently reduced forskolin (FSK)-induced cAMP production in HEK293 cells expressing μOR (**A,** Data is normalized to the positive control DAMGO, dotted line). TRV130 (red ●) did not recruit β-arrestin 2 in CHO-μOR (**B,** Data is normalized to the positive control DAMGO, dotted line). Systemic (i.p.) injection of TRV130 did not decrease 10% alcohol intake in male wild-type (WT) mice (**C**). Systemic (i.p.) injection of 7-hydroxymitragynine did not decrease 10% alcohol intake in male δOR knockout (KO) male mice (**D**). Systemic injection of 7-hydroxymitragynine (3 mg/kg, i.p.) increased locomotor activity of δOR knockout (KO) male mice (**E**). Time course of male locomotor activity following 3 mg/kg, 7-hydroxymitragynine i.p. injection (**F**). Results shown in in this figure were also previously published as part Meridith T. Robins' dissertation at Purdue University.

2.3.8 Kratom and 7-hydroxymitragynine require more conditioning sessions to establish CPP than morphine.

Opioids that activate μORs, even those that are G protein-biased such as TRV130 (Altarifi et al., 2017; Austin Zamarripa et al., 2018), are rewarding (Fields and Margolis, 2015). We next assessed whether male mice will develop place preference to kratom or 7-hydroxymitragynine using morphine as the positive control. In our brief CPP paradigm (2 conditioning sessions), only 6 mg/kg morphine (n=6) produced significant place preference (as determined by increased time spent on the drug-paired side after conditioning) (**Figure 2.7A**). Surprisingly, 30 mg/kg kratom extract #1 (n=8), and 3 (n=7) and 10 mg/kg (n=8) 7-hydroxymitragynine did not produce statistically significant increases in the amount of time spent on the drug-paired side in the short CPP paradigm (**Figure 2.7A**). CPP magnitude can be enhanced for many substances of abuse by increasing the drug exposures (Lett, 1989). When extending the number of conditioning sessions from two to four, place preference was established for 30 mg/kg kratom extract #1 (n=12), 3 mg/kg 7-hydroxymitragynine (n=8), and 6 mg/kg morphine (n=12) (**Figure 2.7B**).

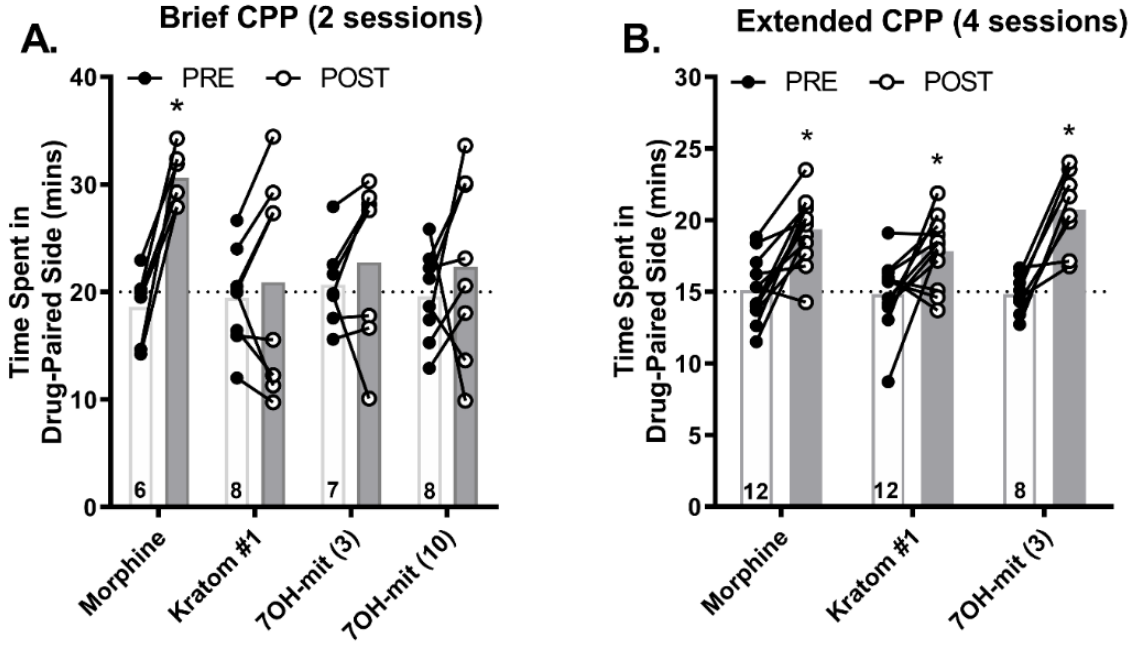

Figure 2.7 Mice will develop conditioned place preference for kratom and 7-hydroxymitragynine but require more conditioning sessions than morphine.

Male C56BL/6 wild-type mice were conditioned to vehicle and 6 mg/kg morphine, 30 mg/kg kratom #1, 3 or 10 mg/kg 7-hydroxymitragynine (7-OH-mit) for two days (Brief CPP). Pre- and post-conditioning exploration of the drug-paired chamber was recorded over 40 minutes (**A**). Male C56BL/6 wild-type mice were alternately conditioned for four times to vehicle and four times to 6 mg/kg morphine, 30 mg/kg kratom #1, or 3 mg/kg 7-hydroxymitragynine over the course of two weeks (Extended CPP). Pre- and post-conditioning exploration of the drug-paired chamber was recorded over 30 minutes (**B**). Results shown in in this figure were also previously published as part Meridith T. Robins' dissertation at Purdue University.

2.3.9 Synthetic G protein-biased opioids reduce alcohol intake with relatively limited rewarding effects.

Given that kratom and 7-hydroxymitragynine still produced CPP, we next assessed whether an alternative drug that displayed selectivity for δOR over μOR would be more beneficial in reducing alcohol intake and produce fewer adverse side effects. We characterized a series of carfentanil-amides (MP102, MP103 and MP105, **Figure 2.8**) previously shown to bind and activate both μOR and δOR (Varadi et al., 2015b). We found that the three carfentanil-amide opioids dose-dependently inhibited cAMP production at μOR, δOR and κOR (**Figure 2.9A-C, Table 2.1**). In agreement with the previously reported characterization (Váradi et al., 2015b), MP102 was more potent at δOR than at μOR (**Table 2.1**). Similar to the kratom alkaloids, the carfentanil-amide opioids did not strongly recruit β-arrestin 2 at μOR, δOR or κOR; MP102 displayed equally low β-arrestin 2 recruitment efficacy at μOR and δOR; however, MP103 and MP105 were more efficacious at μOR than at δOR (**Figure 2.9D-F**, **Table 2.1**). *In vivo*, we found that MP102 and MP103 dose-dependently reduced alcohol intake in male wild-type mice (**Figure 2.9G and H**) with effective doses of 10 and 30 mg/kg for MP102 and a dose of 3 mg/kg for MP103. A dose of 1 mg/kg MP105 did not significantly decrease alcohol intake; however, at this dose mice displayed abnormal head twitching behavior, therefore we refrained from testing any higher doses (**Figure 2.9I**). Similar to 7-hydroxymitragynine, the ability of MP102 to reduce alcohol intake was dependent on the presence of δOR, as neither 10 or 30 mg/kg MP102 was able to significantly reduce alcohol intake in δOR knockout mice (**Figure 2.9J**). The effective dose of 10 mg/kg MP102 (n=8) did not alter the locomotor activity of male wild-type mice (**Figure 2.9K**). In the extended CPP paradigm, we observed that mice injected with 10 mg/kg MP102 spent significantly more time in the drug-paired side, an effect which persisted in δOR knockout mice (**Figure 2.9L**).

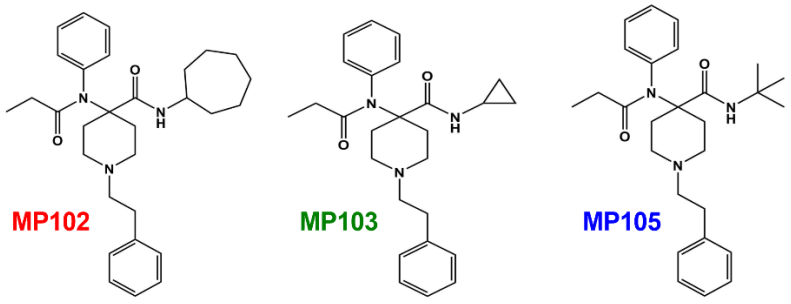

Figure 2.8 Chemical structures of MP102, MP103 and MP105.

Figure 2.9 Synthetic G protein-biased opioids reduce alcohol intake in mice.

MP102 (red ●), MP103 (green ▲) and MP105 (blue ■) reduced forskolin (FSK)-induced cAMP production in HEK293 cells expressing μOR (**A**), δOR (**B**) or κOR (**C**), normalized to the relevant positive controls (dotted lines) DAMGO (μOR), leu-enkephalin (δOR) and U50,488 (κOR). MP102 (red ●), only weakly recruited β-arrestin 2 compared to MP103 (green ▲) and MP105 (blue ■) in CHO-μOR (**D**), CHO-δOR (**E**) or U2OS-κOR (**G**) PathHunter cells normalized to the relevant positive controls (dotted lines). Systemic (i.p.) injection of MP102 (**F**) and MP103 (**H**) dose-dependently decreased alcohol intake in male mice. Systemic injection of MP105 (1 mg/kg, i.p.) did not significantly decrease 10% alcohol intake (**I**). Systemic (i.p.) injection of MP102 did not reduce 10% alcohol intake in δOR knockout (KO) male mice (**J**). MP102 (10 mg/kg, i.p.) did not alter locomotor activity of male mice (**K**) but mice showed conditioned place preference to 10 mg/kg MP102 (**L**). See the results section and online supplement for statistical analysis. Results shown in in this figure were also previously published as part Meridith T. Robins' dissertation at Purdue University.

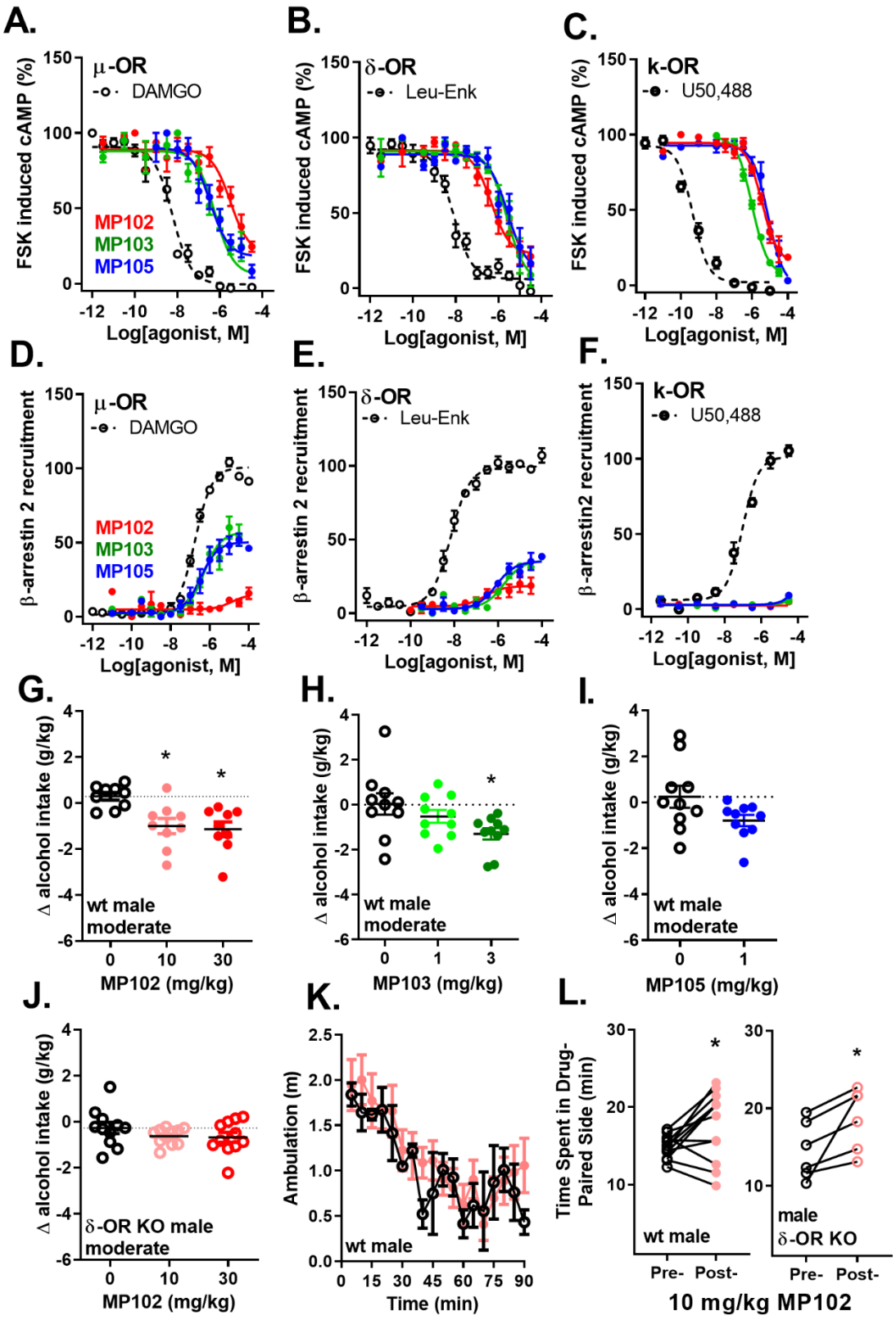
A.
μ-OR
DAMGO
MP102
MP103
MP105
FSK induced cAMP (%)
Log[agonist, M]
B.
δ-OR
Leu-Enk
C.
k-OR
U50,488
D.
β-arrestin 2 recruitment
E.
F.
β-arrestin2 recruitment
G.
Δ alcohol intake (g/kg)
wt male
moderate
MP102 (mg/kg)
H.
MP103 (mg/kg)
I.
MP105 (mg/kg)
J.
δ-OR KO male
moderate
K.
Ambulation (m)
wt male
Time (min)
L.
Time Spent in Drug-Paired Side (min)
Pre-
Post-
male
δ-OR KO
10 mg/kg MP102

Table 2.1 Pharmacological characterization of kratom alkaloids and synthetic G protein-biased opioids at the μ, δ and κ opioid receptor.

cAMP inhibition potencies (pIC_{50}, drug concentration at 50% maximal efficacy) and efficacies (α, % inhibition at maximal efficacy normalized to DAMGO [μOR], leu-enkephalin [δOR] or U50,488 [κOR]) for OR agonists to inhibit cAMP production are indicated ±SEM. β-arrestin 2 recruitment potencies (pEC_{50}) and efficacies (α, normalized to DAMGO, leu-enkephalin or U50,488) of OR agonists to recruit β-arrestin 2 are indicated ±SEM. The number of repetitions is indicated in parentheses. ND = not detectable. UD = undeterminable. Results shown in in this table were also previously published as part Meridith T. Robins' dissertation at Purdue University.

Compounds	**cAMP**		**β-arrestin 2**		
μOR	**pIC_{50}**	**α**	**pEC_{50}**	**α**	**Bias factor**
DAMGO	8.4±0.1 (23)	100	6.7±0.1 (22)	100	1
Kratom #1	6.0±0.2 (7)	71±7	ND (3)	ND	UD
Kratom #2	5.7±0.3 (3)	100±7	ND (3)	ND	UD
Morphine	8.5±0.2 (3)	95±4	6.8±0.1 (3)	26±2	UD
Mitragynine	6.3±0.2 (8)	75±6	ND (3)	ND	UD
7-OH-mitragynine	7.8±0.1 (5)	84±3	ND (3)	ND	UD
Speciogynine	5.5±0.1 (5)	87±6	ND (3)	ND	UD
Paynantheine	5.4±0.1 (5)	100±0	ND (3)	ND	UD
TRV130	7.9±0.2 (7)	86±3	ND (4)	ND	UD
MP102	5.4±0.2 (6)	88±4	5.2±0. 1(4)	16±5	UD
MP103	6.5±0.2 (5)	90±4	6.3±0.2 (7)	63±7	0.03
MP105	6.7±0.4 (5)	87±6	6.6±0.2(6)	54±5	0.02
δOR	**pIC_{50}**	**α**	**pEC_{50}**	**α**	**Bias factor**
Leu-enkephalin	8.5±0.1 (34)	100	8.0±0.1 (29)	100	1
Kratom #1	4.4±0.3 (6)	30±20	ND (4)	ND	UD
Kratom #2	5.8±0.5 (4)	72±13	ND (3)	ND	UD
Morphine	6.1±0.2 (5)	82±8	ND (3)	ND	UD
Mitragynine	4.8±0.2 (5)	88±8	ND (3)	ND	UD
7-OH-mitragynine	5.7±0.2 (8)	80±8	6.4±0.3 (3)	14±1	UD
Speciogynine	5.0±0.3 (5)	94±4	ND (3)	ND	UD
Paynantheine	5.6±0.2 (4)	64±13	ND (3)	ND	UD
TRV130	5.6±0.4 (5)	48±12	ND (4)	ND	UD
MP102	6.4±0.1 (4)	77±7	6.7±0.4 (5)	20±6	UD
MP103	5.5±0.2 (4)	100±1	5.8±0.1 (3)	35±2	3.8
MP105	5.4±0.3 (4)	94±5	6.2±0.1 (3)	35±4	1.4
κOR	**pIC_{50}**	**α**	**pEC_{50}**	**α**	**Bias factor**
U50,488	8.9±0.1 (18)	100	7.3±0.2 (10)	100	1
Kratom #1	6.8±0.4 (8)	41±8	ND (6)	ND	UD
Kratom #2	7.0±0.2 (4)	93±2	6.0±0.2 (5)	12±2	UD
Morphine	7.3±0.2 (5)	89±2	5.8±0.2 (3)	16±2	UD
Mitragynine	5.4±0.4 (5)	67±12	ND (4)	ND	UD
7-OH-mitragynine	6.2±0.3 (9)	77±5	ND (4)	ND	UD
Speciogynine	4.7±0.3 (5)	70±20	ND (4)	ND	UD
Paynantheine	5.3±0.2 (4)	95±5	ND (6)	ND	UD
TRV130	4.9±0.1 (3)	74±6	ND (3)	ND	UD
MP102	5.4±0.1 (5)	85±8	ND (3)	ND	UD
MP103	6.0±0.1 (3)	93±3	ND (3)	ND	UD
MP105	5.2±0.2 (5)	96±3	ND (3)	ND	UD

2.4 Discussion

Prior research regarding kratom and its alkaloids has emphasized the antinociceptive properties of 7-hydroxymitragynine and kratom-derived alkaloid synthetic derivatives, such as mitragynine pseudoindoxyls (Takayama et al., 2002; Matsumoto et al., 2006, 2008; Váradi et al., 2016) because these alkaloids appear to be G protein-biased at the μOR, a characteristic potentially crucial for novel analgesic drug development. For example, recently developed G protein-biased μOR agonists TRV130/oliceridine and PZM21 supposedly increased the therapeutic window of μOR analgesics (DeWire et al., 2013; Soergel et al., 2014a; Manglik et al., 2016; Viscusi et al., 2016; Singla et al., 2017), although recent reports have raised doubts on the robustness of these findings (Austin Zamarripa et al., 2018; Hill et al., 2018). In these studies, and in agreement with our findings, limited β-arrestin 2 recruitment was observed at the μOR for both mitragynine and 7-hydroxymitragynine compared with G protein activity (Kruegel et al., 2016; Váradi et al., 2016). By comparing G protein-mediated cAMP inhibition with β-arrestin 2 recruitment, our current results suggested that this functional selectivity of kratom alkaloids also holds true at the δOR and κOR. It is noteworthy that in our hands, 7-hydroxymitragynine acted as a partial agonist at the δOR rather than as an antagonist as previously reported (Kruegel et al., 2016; Váradi et al., 2016). This discrepancy is possibly due to the use of different cellular assays to measure G protein activation: specifically, GTPγS and BRET assays versus inhibition of adenylyl cyclase mediated cAMP production (as used in this study). The cAMP assay may amplify signals such that a partial agonist in the GTPγS assay displays full agonism, or a compound with no detectable activity in the GTPγS assay may display partial agonism in the cAMP assay. Supporting our *in vitro* finding of δOR agonism for 7-hydroxymitragynine, 7-hydroxymitragynine-induced inhibition of cAMP production in cells expressing the δOR was attenuated using the δOR selective antagonist naltrindole (Figure S10 in the online supplement).

Across our assays, the calculated bias factor of 0.44 for 7-hydroxymitragynine at the δOR - suggestive bias towards β-arrestin 2 - although this calculated factor was driven by a higher apparent potency for β-arrestin 2 recruitment when compared with cAMP inhibition potency and depended less on the observable weak efficacy of β-arrestin 2 recruitment (**Table 2.1**). However, we have previously shown that β-arrestin 2 recruitment efficacy (between 36-142%) strongly correlated with modulation of alcohol intake by δOR selective agonists (Chiang et al., 2016). This

correlation holds true for both 7-hydroxymtraginine and MP102, and extends the lower end of the correlation window to 14% β-arrestin 2 recruitment efficacy (**Figure 2.10**).

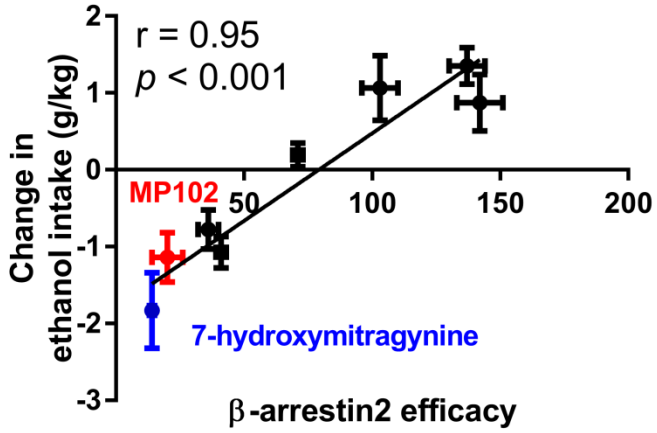

Figure 2.10 Correlation between β-arrestin 2 recruitment efficacy at δOR and modulation of alcohol intake.

Addition of the very weak β-arrestin 2 recruiters MP102 and 7-hydroxymitragynine to the correlation previously established using the δOR selective agonists TAN-67, NIH11082, KNT127, ARM390, SNC80 and SNC162 further strengthens the hypothesis that β-arrestin 2 recruitment efficacy, not necessarily potency, impacts the directional response of a δOR agonist on alcohol intake (Chiang et al., 2016). Results shown in in this figure were also previously published as part Meridith T. Robins' dissertation at Purdue University.

A major concern with opioid agonists, particularly those with strong activity at μOR, is the development of physical and psychological dependence. There is a strong correlation between opioid self-administration and opioid CPP (Tzschentke, 2007; Morgan and Christie, 2011). CPP to morphine is dependent on μOR expression (Matthes et al., 1996) but is enhanced in the absence of β-arrestin 2 (Bohn et al., 2003), which would suggest that a G protein-biased μOR agonists would have rewarding properties. Indeed, rats and mice develop conditioned place preference for G protein-biased mitragynine and 7-hydroxymitragynine (Matsumoto et al., 2008; Sufka et al., 2014). A recent rat self-administration study that found that 7-hydromitragynine, but not mitragynine, could substitute for morphine. Interestingly, this response was blocked by a μOR antagonist as well as by the δOR antagonist naltrindole, although the naltrindole dose was relatively high and may not have been δOR specific (Hemby et al., 2019). Our results were in agreement with the published findings that mice display CPP for kratom and 7-

hydroxymitragyninine; however, we found that two conditioning sessions were insufficient to robustly produce kratom or 7-hydroxymitragynine CPP in mice. In contrast, two conditioning sessions were sufficient to produce morphine CPP (**Figure 2.7**). In fact, even a single dose of morphine produces CPP (Bardo and Neisewander, 1986). However, increasing the number of conditioning sessions to four revealed CPP for 7-hydroxymitragynine and kratom extract #1. Thus, as predicted based on the enhanced morphine CPP in β-arrestin 2 knockout mice (Bohn et al., 2003), kratom and 7-hydroxymitragynine were not strongly rewarding, but did indeed possess rewarding properties.

In the 'brief CPP' assay, we noticed that some mice developed conditioned place aversion to kratom extract #1 and 7-hydroxymitragynine (see **Figure 2.7A**, points with negative slope). It is possible that this aversion was mediated by alkaloid activity at κOR. The aversive, dysphoric effects of κOR agonists have been associated with β-arrestin 2 mediated p38 signaling by κOR (Bruchas et al., 2007b; Land et al., 2009). However, a recent study revealed that κOR agonists still produced conditioned place aversion in β-arrestin 2 knockout mice (White et al., 2015), and a number of studies have found that G protein-biased κOR agonists still induced conditioned place aversion (White et al., 2015; Gupta et al., 2016; Spetea et al., 2017). Thus, it is possible that one mechanism by which kratom produced less pronounced CPP was via action at κOR-associated dysphoria. κORs and their endogenous opioid dynorphins have been associated with the negative affect of alcohol intake and withdrawal (Walker and Koob, 2008). In this study, we did not investigate if κOR-induced aversion by kratom or kratom alkaloids contributed to the mechanism by which these alkaloids reduced alcohol intake. In our study, the potent and μOR selective, G protein-biased agonist TRV130 did not alter alcohol intake in mice at effective analgesic doses (DeWire et al., 2013), suggesting that G protein-biased μOR activity did not drive the decreased alcohol consumption observed for kratom and its alkaloids. Additionally, at the tested doses TRV130 is known to be reinforcing (Altarifi et al., 2017), which would further suggest that mice were not consuming less alcohol when administered kratom because their μOR-reward pathway activation.

Several studies have shown that activation of δORs can modulate alcohol intake (Alongkronrusmee et al., 2018), and thus a synthetic opioid that preferentially activates δOR could minimize the impact of μOR-mediated reward and κOR-mediated aversion on the behavioral effects in the alcohol assays. Indeed, our characterization revealed that MP102 had the desired *in*

vitro pharmacological profile of a G protein-biased, δOR-preferring agonist. In accordance with our hypothesis, MP102 reduced alcohol intake in wild-type (but not δOR knockout mice) and did not significantly alter locomotor activity. In comparison to μOR agonists and in agreement with prior findings, non-peptidic δOR agonists were less rewarding (Negus et al., 1998; Stevenson et al., 2005; Do Carmo et al., 2009; van Rijn et al., 2012a) and while MP102 still produced CPP, this conditioning was less robust than that observed for 7-hydroxymitragynine and appeared not mediated by δOR, as it was still present in δOR knockout mice.

In conclusion, we found that kratom alkaloids do not recruit β-arrestin 2 at the μOR, δOR and κOR and can significantly reduce both moderate and binge alcohol intake in male mice and female mice. This pharmacological profile and effect on alcohol intake in rodents may explain why some find kratom useful to self-medicate for alcohol use disorder. Yet, as we observed that kratom extract and 7-hydroxymitragynine exhibited reinforcing properties, our study also highlights the risks associated with kratom use. Our results indicate that δORs contributed to the efficacy of the kratom alkaloids to reduce alcohol intake, whereas the lack of efficacy for the G protein-biased μOR agonist TRV130 to decrease alcohol intake argued against a major role for the μOR in this behavioral response. The ability of MP102, a synthetic G protein-biased opioid with a preference for δOR, to reduce alcohol intake without affecting general locomotion or inducing (δOR-mediated) CPP provides support for future efforts to produce G protein-selective, δOR-selective opioids for the treatment of alcohol use disorder, some of which could be plant-derived still as well (Cassell et al., 2019).

CHAPTER 3. EVALUATION OF KRATOM OPIOID DERIVATIVES AS POTENTIAL TREATMENT OPTION FOR ALCOHOL USE DISORDER

This chapter was previously published in the Frontiers in Pharmacology Journal of Experimental Pharmacology and Drug Discovery with the following DOI: 10.3389/fphar.2021.764885 and citation:
Gutridge, A.M., Chakraborty, S., Varga, B.R., Rhoda, E.S., French, A.R., Blaine, A.T., Royer, Q.H., Cui, H., Yuan, J., Cassell, R.J., Szabó, M., Majumdar, S., van Rijn, R.M. 2021. Evaluation of kratom opioid derivatives as potential treatment option for alcohol use disorder. *Frontiers in Pharmacology*, p.2943.
Supplemental data including extensive statistical analyses and chemical characterization is freely available at the following location:
https://www.frontiersin.org/articles/10.3389/fphar.2021.764885/full

3.1 Introduction

Mitragyna speciosa, more commonly known as Kratom, is growing increasingly popular in the United States, with nearly 1% of the population age 12 and older using kratom in 2019 (Palamar, 2021). While kratom is most commonly used to self-manage pain or reduce dependence to opioids and opiates (Coe et al., 2019), a recent online survey revealed 18% of kratom users indicate reducing or quitting alcohol consumption is a reason they use kratom (Coe et al., 2019). This indication is in line with reports of individuals claiming that kratom was useful for reducing their alcohol intake (Havemann-Reinecke, 2011; Singh et al., 2014; Suhaimi et al., 2021). We have previously demonstrated that systemic injections of kratom extract and kratom alkaloids (7-hydroxymitragynine, paynantheine, speciogynine, mitragynine) decreases voluntary alcohol drinking in mouse models of moderate and binge alcohol consumption, with the kratom alkaloid 7-hydroxymitragynine being the most efficacious (Gutridge et al., 2020). Kratom alkaloids differ from opium-derived opioids and clinically used synthetic opioids in that upon binding to opioid receptors they activate the $G\alpha_{i/o}$ protein, without promoting β-arrestin recruitment to the receptor (Kruegel et al., 2016; Váradi et al., 2016; Faouzi et al., 2020; Chakraborty and Majumdar, 2021). Several preclinical studies in mice strongly suggest that β-arrestin recruitment at the delta opioid receptor (δOR) is a liability for enhanced alcohol use and should be avoided (Chiang et al., 2016; Robins et al., 2018b; Gutridge et al., 2020). We have previously demonstrated that 7-hydroxymitragynine and other kratom alkaloids poorly recruit β-arrestin2 at mu opioid receptors

(μORs) and δORs, and possess a degree of G-protein bias at this receptor (Gutridge et al., 2020). Moreover, our studies in δOR knockout mice revealed that 7-hydroxymitragynine's modulation of alcohol consumption was due to its activity at the δOR (Gutridge et al., 2020).

However, a possible concern is that 7-hydroxymitragynine and other kratom alkaloids generally have comparable if not higher affinity and potency at the μOR (Takayama et al., 2002; Matsumoto et al., 2004).While this μOR potency may be responsible for the alkaloids' ability to promote antinociception in mice (Matsumoto et al., 2004; Obeng et al., 2020a; Wilson et al., 2020a, 2021) and in humans (Vicknasingam et al., 2020), it appears that because of their μOR potency, kratom alkaloids, especially 7-hydroxymitragynine, are shown or predicted to share some of the same negative side effects associated with traditional opioids such as abuse liability. Accordingly, in rodent preclinical studies, 7-hydroxymitragynine has been shown to have rewarding qualities in models of conditioned place preference and self-administration, which indicates it may have abuse liability (Yue et al., 2018; Hemby et al., 2019; Gutridge et al., 2020). Likewise, withdrawal symptoms following kratom exposure have also been recorded in rodents (Matsumoto et al., 2005; Wilson et al., 2021). Similarly, regular kratom use in humans leads to dependence problems in over 50% of users (Singh et al., 2014), and kratom withdrawal symptoms equally have been widely reported in humans (Singh et al., 2014; Saref et al., 2019; Stanciu et al., 2019; Anand and Hosanagar, 2021). Likely attributed to its potency at the μOR, another side effect of 7-hydroxymitragynine in mice is hyperlocomotion (Becker et al., 2000; Gutridge et al., 2020); this effect mirrors one of kratom's traditional uses as a stimulant (Suwanlert, 1975; Ahmad and Aziz, 2012). Still, relative to traditional opioids such as morphine, the negative side effect profile of kratom and kratom opioids is slightly lessened in regards to reward, respiratory depression, and withdrawal symptoms (Hemby et al., 2019; Wilson et al., 2020a, 2021). This reduction in side effect profile was first attributed to G-protein biased activity of the kratom alkaloids at the μOR (Kruegel et al., 2016; Váradi et al., 2016), but new research suggests that partial agonism at the μOR likely drives these effects (Gillis et al., 2020; Bhowmik et al., 2021; Uprety et al., 2021). Despite the reduced μOR-mediated side effects relative to traditional opioids, kratom use is not without risk, and this is reflected in controversial efforts to place 7-hydroxymitragynine and mitragynine under Schedule I regulation by the Drug Enforcement Agency (DEA, 2016; Griffin and Webb, 2018).

An additional side effect of kratom use is seizure activity (Coonan and Tatum, 2021). In rats, abnormal EEG activity has been reported following chronic exposure to mitragynine, the most abundant alkaloid in kratom (Suhaimi et al., 2021). In humans, several individual case reports have highlighted seizure side effects induced by kratom use or withdrawal (Boyer et al., 2008a; Nelsen et al., 2010; Tatum et al., 2018; Burke et al., 2019; Afzal et al., 2020; Valenti et al., 2021), and retrospective analysis of kratom exposure reports to the National Poison Data System reveals that 6.1% of reports detail seizure side-effects (Eggleston et al., 2019). Currently the mechanism underlying these reported seizure effects of kratom have not been defined.

We hypothesized that compared to 7-hydroxymitragynine, derivatizing kratom analogs with reduced μOR potency relative to δOR potency would reduce restrictive side effects such as abuse liability and hyperlocomotion, leading to an increased therapeutic window. Prior efforts have been made to utilize the unique kratom alkaloid scaffolds to develop improved therapeutic options (Kruegel et al., 2016; Chakraborty et al., 2021a; Wilson et al., 2021). Similarly, here we investigate four novel kratom-derived analogs as well as two naturally occurring kratom alkaloids for their ability to decrease alcohol consumption while monitoring lead compounds for their ability to produce seizure activity, induce reward properties, and affect general locomotion.

3.2 Methods

3.2.1 Materials

Kratom "Red Indonesian Micro Powder" was purchased from Moon Kratom (Austin, TX). Corynoxine and corynoxine B were purchased from BOC Sciences (NY, USA). Leu-enkephalin, forskolin, and morphine sulfate pentahydrate were purchased from Sigma Aldrich (St. Louis, MO, USA). (2S)-2-[[2-[[(2R)-2-[[(2S)-2-Amino-3-(4-hydroxyphenyl)propanoyl] amino] propanoyl] amino]acetyl]-methylamino]-N-(2-hydroxyethyl)-3-phenylpropanamide (DAMGO), 2-(3,4-dichlorophenyl)-N-methyl-N-[(1R,2R)-2-pyrrolidin-1-ylcyclohexyl]acetamide (U50,488), and naloxone hydrochloride were purchased from Tocris Bioscience (Bio-techne Corporation, Minneapolis, MN, USA). [3H]DAMGO (53.7 Ci/mmol, lot#2376538; 51.7 Ci/mmol, lot#2815607), [3H]U69,593 (60 Ci/mmol, lot#2367921 and lot#2644168; 49.2 Ci/mmol, lot#2791786), [3H]DPDPE (49.2 CI/mmol, lot#2573313 and lot#2726659; 48.6 Ci/mmol, lot#2826289) were purchased from Perkin Elmer (Waltham, MA, USA). For *in vivo* experiments,

morphine and naloxone were prepared in a saline vehicle. Kratom derived analogs were dissolved in a 1:1:8 ethanol:cremophor:saline vehicle for all behavioral experiments. For the 2-bottle choice experiment in δOR KO mice, paynantheine was prepared in the same 1:1:8 ethanol:cremophor:saline vehicle. For all other experiments paynantheine and speciociliatine were dissolved in a slightly acidic saline solution that was adjusted to a pH of 6-7 before administration.

3.2.2 Chemistry

General

All chemicals were purchased from Sigma-Aldrich Chemicals and used without further purification. Reactions were carried out in flame-dried reaction flasks under Argon. Reaction mixtures were purified by silica flash chromatography on E. Merck 230−400 mesh silica gel 60 using a Teledyne ISCO CombiFlash Rf instrument with UV detection at 280 and 254 nm. RediSep Rf silica gel normal phase columns were used. The yields reported are isolated yields. NMR spectra were recorded on a Varian 400/500 MHz NMR spectrometer. NMR spectra were processed with MestReNova software. The chemical shifts were reported as δ ppm relative to TMS using residual solvent peak as the reference unless otherwise noted (CDCl3 1H: 7.26, 13C: 77.3). Peak multiplicity is reported as follows: s, singlet; d, doublet; t, triplet; q, quartet; m, multiplet. Coupling constants (J) are expressed in Hz. High resolution mass spectra were obtained on a Bruker Daltonics 10 Tesla Apex Qe Fourier Transform Ion Cyclotron Resonance-Mass Spectrometer by electrospray ionization (ESI). Accurate masses are reported for the molecular ion [M + Na]+.

Isolation of mitragynine from Mitragyna speciosa (kratom)

Mitragynine was extracted from the powdered leaves by following our previously reported methods (Gutridge et al., 2020). Kratom powder (500 g) was heated to reflux in MeOH 700 mL for 40 min. The suspension was filtered and the methanolic extraction process was repeated (3 x 500 mL). The solvent of combined methanolic extract was removed under reduced pressure and the content was dried using high vacuum. The dry residue was resuspended in 20% acetic acid solution (1 L) and washed with petroleum ether (4 x 500 mL). The aqueous layer was then cooled on ice bath and basified (pH ~9) with aqueous NaOH solution (3.5M. ~1L) slowly. Alkaloids were extracted in DCM (4 x 400 mL) from the aqueous layer. The combined DCM layer was washed

with brine 300 mL and dried over anhydrous Na_2SO_4 and filtered. The solvent was removed under reduced pressure, and the residue was dried under high vacuum to obtain kratom extract (9.8 g). Then, this crude kratom extract was subjected to silica gel column chromatography; using 0-15% MeOH in dichloromethane to isolate mitragynine (4.7 g); paynantheine (568 mg), speciogynine (343 mg), and speciociliatine (754 mg) along with some minor alkaloids.

7-hydroxypaynantheine (7OH Pay/7)

Paynantheine (100 mg, 0.25 mmol) was dissolved in acetonitrile (7 mL), then water (2 mL) was added. The resulting suspension was cooled to 0 °C, and PIFA (108 mg, 1.1 equiv) dissolved in acetonitrile (1.1 mL) was added slowly over the course of several minutes. The reaction mixture was stirred at 0 °C for 45 minutes. Then, saturated aqueous $NaHCO_3$ solution was added, and the mixture extracted with EtOAc (3x15 mL). The organic phase was washed with brine (20 mL) and dried over anhydrous Na_2SO_4. The solvent was removed under reduced pressure. The residue was purified on a silica column using 10-75% EtOAc in hexanes as eluent. The fractions containing the product were evaporated to yield 42 mg (40%) of **9** as a light magenta amorphous powder. ^{1}H δ (400 MHz, ppm): 7.31 (1H, s, 17); 7.29 (1H, t, 3J = 7.7 Hz, 11); 7.19 (1H, t, 3J = 7.7 Hz, 12); 6.74 (1H, d, ^3J = 7.7 Hz, 10); 5.57 (1H, ddd, ^3J = 18.0, 10.3, 7.2 Hz, 19); 4.99 (1H, dd, ^3J = 18.0, ^2J = 1.5 Hz, 18 *trans*); 4.94 (1H, dd, ^3J = 10.3, ^2J = 1.5 Hz, 18 *cis*); 3.86 (3H, s, 9-OMe); 3.79 (3H, s, 17-OMe); 3.68 (3H, s, 16-COOMe); 3.46 (1H, s, 7-OH); 3.23 (1H, m, 3); 3.03 (1H, m, 21/1); 3.01 (1H, m, 20); 2.85 (1H, m, 5/2); 2.73 (1H, m, 5/1); 2.72 (1H, m, 15); 2.66 (1H, m, 6/1); 2.39 (1H, m, 14/1); 2.30 (1H, m, 21/2); 2.05 (1H, m, 14/2); 1.70 (1H, m, 6/2);. ^{13}C δ (100 MHz, ppm): 183.5 (2); 168.8 (16-CO); 159.8 (17); 155.9 (9); 154.9 (13); 139.3 (19); 131.0 (11); 126.4 (8); 115.4 (18); 114.3 (12); 111.4 (16); 109.1 (10); 81.0 (7); 61.6 (21); 61.5 (17-OMe); 60.2 (3); 55.5 (9-OMe); 51.2 (16-COOMe); 49.8 (5); 42.8 (20); 38.2 (15); 35.9 (6); 30.4 (14). Relative configuration was determined based on the NOE cross peaks between the following ^{1}H nuclei: 3 – 5/2; 3 – 14/2; 3 – 21/2; 3 – 5/2; 15 – 19; 19 – 21/2 (/1 always indicates the hydrogen pointing towards the reader from the paper; /2 indicate the hydrogen pointing behind the plain of the paper). HRMS (ESI-TOF) m/z: [M+Na]+ Calcd for $C_{23}H_{28}N_2NaO_5$ 435.189043; found. 435.189116

Paynantheine pseudoindoxyl (Pay PI/8)

7-hydroxypaynantheine (**9**, 40 mg, 0.1 mmol) was dissolved in dry toluene (1.5 mL), and $Zn(OTf)_2$ (70 mg, 2 equiv) was added. The reaction mixture was stirred in a sealed tube for 30 minutes at 115 °C. To the cooled mixture were added 2 mL sat. aqueous $NaHCO_3$ solution and water (5 mL) and the organics were extracted with EtOAc (10 mL). The organic layer was rinsed with brine (10 mL) and dried over anhydrous Na_2SO_4. After evaporation of the solvent under reduced pressure, the residue was purified by flash column chromatography on silica (gradient: 40-75% EtOAc in hexanes) to yield 15 mg (38%) of product as a light yellow gum. ^{1}H δ (400 MHz, ppm): 7.32 (1H, t, ^3J = 8.2 Hz, 11); 7.18 (1H, s, 16); 6.37 (1H, d, ^3J = 8.2 Hz, 12); 6.13 (1H, d, ^{3}J = 8.2 Hz, 10); 5.49 (1H, ddd, ^3J = 18.2, 10.3, 7.4 Hz, 19); 5.25 (1H, br s, 1); 4.95 (1H, d, ^3J = 18.2, 18 *trans*); 4.9 (1H, d, ^3J = 10.3, 18 *cis*); 3.89 (3H, s, 9-OCH3); 3.73 (3H, s, 17-OCH3); 3.62 (3H, s, 16-$COOCH_3$); 3.23 (1H, m, 5/1); 3.11 (1H, m, 21/1); 2.87 (1H, m, 20); 2.49 (1H, m, 15); 2.39 (1H, m, 5/2); 2.39 (1H, m, 6/2); 2.34 (1H, m, 3); 1.98 (1H, m, 21/2); 1.94 (1H, m, 6/1); 1.79 (1H, br q ^3J = 11.3 Hz, 14/1); 1.26 (1H, br d, ^3J = 11.3 Hz, 14/2). ^{13}C δ (100 MHz, ppm): 199.8 (7); 168.2 (16-C=O); 162.1 (13); 159.7 (17); 158.7 (9); 139.5 (19); 139 (11); 115.6 (18); 111.9 (16); 109.5 (8); 104 (12); 99.2 (10); 74.7 (2); 72.4 (3); 61.5 (17-O-CH_3); 58.8 (21); 55.8 (9-OCH_3); 53.2 (5); 51.1 (COO-CH_3); 42.3 (20); 36.9 (15); 35.3 (6); 28.3 (14). Relative configuration was determined based on the NOE cross peaks between the following ^{1}H nuclei: 1 – 6/1; 3 – 14/2; 1 – 14/1; 14/1 – 20; 15 – 19; 19 – 21/2. HRMS (ESI-TOF) m/z: [M+Na]+ Calcd for $C_{23}H_{28}N_2NaO_5$ 435.189043; found. 435.189219

7-hydroxyspeciogynine (7OH Spg/9)

Speciogynine (200 mg, 0.5 mmol) was dissolved in acetonitrile (15 mL), then water (5 mL) was added. The resulting suspension was cooled to 0 °C, and PIFA (216 mg, 1.1 equiv) dissolved in acetonitrile (2.2 mL) was added slowly over the course of several minutes. The reaction mixture was stirred at 0 °C for one hour. Then, saturated aqueous $NaHCO_3$ solution was added, and the mixture extracted with EtOAc (3x40 mL). The organic phase was washed with brine (30 mL) and dried over anhydrous Na_2SO_4. The solvent was removed under reduced pressure. The residue was redissolved in DCM and was purified using silica column chromatography 10-75% EtOAc in hexanes. The fractions containing the product were evaporated to yield 107 mg (57%) of **9** as a light brown amorphous powder. ^{1}H NMR (400 MHz, Chloroform-d) δ 7.36 – 7.29 (m, 1H), 7.26 (dd, J = 8.8, 7.2 Hz, 1H), 7.17 (d, J = 7.7 Hz, 1H), 6.71 (d, J = 8.3 Hz, 1H), 3.84 (s, 3H), 3.75 (s,

3H), 3.66 (s, 3H), 3.21 – 3.08 (m, 2H), 2.82 (t, J = 12.3 Hz, 1H), 2.77 – 2.69 (m, 1H), 2.64 (d, J = 14.4 Hz, 1H), 2.54 (t, J = 11.2 Hz, 1H), 2.30 (d, J = 11.9 Hz, 1H), 2.17 (t, J = 10.5 Hz, 1H), 2.06 (t, J = 11.2 Hz, 2H), 1.80 (s, 1H), 1.69 (td, J = 13.5, 4.5 Hz, 1H), 1.40 (s, 1H), 1.02 (d, J = 17.1 Hz, 1H), 0.82 (t, J = 7.4 Hz, 3H). ^{13}C NMR (100 MHz, Chloroform-d) δ 183.9, 169.61, 160.10, 156.07, 155.15, 131.15, 126.52, 114.42, 111.44, 109.18, 81.16, 61.98, 61.49, 61.52, 55.66, 51.64, 50.21, 39.54, 38.87, 36.13, 24.49, 11.56, 11.29. HRMS (ESI-TOF) m/z: [M+Na]+ Calcd for $C_{23}H_{30}N_2NaO_5$ 437.204693; found. 437.204951.

Speciogynine pseudoindoxyl (Spg PI/10)

7-hydroxyspeciogynine (**9**, 200 mg, 0.48 mmol) was dissolved in dry toluene (6 mL), and $Zn(OTf)_2$ (350 mg, 2 equivalent) was added. The reaction was stirred in a sealed tube for 2 h at 100 °C. To the cooled mixture were added 10 mL sat. aqueous $NaHCO_3$ solution and water (20 mL). Extracted with EtOAc (30 mL). The organic layer was rinsed with brine (20 mL) and dried over anhydrous Na_2SO_4. After evaporation of the solvent under reduced pressure, the residue was redissolved in DCM and purified by flash column chromatography (gradient: 40-75% EtOAc in hexanes) to yield 78 mg (39%) of 10 as a light yellow amorphous powder. ^{1}H NMR (500 MHz, Chloroform-d) 7.31 (1H, t, ^3J = 8.2 Hz, 11), 7.23 (1H, s, 17), 6.36 (1H, d, ^3J = 8.2 Hz, 12), 6.12 (1H, d, ^3J = 8.2 Hz, 10), 5.34 (1H, br s, 1), 3.89 (3H, s, 9-OMe), 3.72 (3H, s, 17-OMe), 3.62 (3H, s, 16-COOMe), 3.25 – 3.23 (1H, m, 21/1), 3.22 – 3.21 (1H, m, 5/1), 2.37 – 2.35 (2H, m, 5/2; 6/2), 2.33 – 2.31 (1H, m, 15), 2.29 – 2.28 (1H, m, 3), 2.08 – 2.04 (1H, m, 20), 1.94 – 1.90 (1H, m, 6/1), 1.81 – 1.77 (1H, m, 14/1), 1.75 – 1.73 (1H, m, 21/2), 1.34 –1.30 (1H, br m, 19/1), 1.18–1.15 (1H, m, 14/2), 0.95–0.92 (1H, br m, 19/2), 0.79 (3H, br, 18). ^{13}C NMR (100 MHz, Chloroform-d) 200.18 (7), 168.02 (16-CO), 162.25 (13), 160.27 (17), 158.83, (9), 139.17 (11), 112.22 (16), 109.5 (8), 104.26 (12), 99.17 (10), 74.94 (2), 72.94 (3), 61.51 (17-OMe), 58.42 (21), 55.99 (9-OMe), 53.57 (5), 51.07 (16-COOMe), 38.15 (20), 37.50 (15), 35.48 (6), 28.95 (4), 24.46 (9), 11.35 (18). Relative configuration was determined based on the NOE cross peaks between the following ^{1}H nuclei: 1 – 6/1; 1 – 14/1; 15 – 19; 19 – 21/2. (/1 always indicates the hydrogen pointing towards the reader from the paper; /2 indicate the hydrogen pointing behind the plain of the paper). HRMS (ESI-TOF) m/z: [M+Na]+ Calcd for $C_{23}H_{30}N_2NaO_5$ 437.204693; found. 437.204760.

3.2.3 Cellular Assays and Associated Statistical Analysis

Membrane Isolation and Competitive Radioligand Binding Assay

Membrane isolation and subsequent binding assays were completed as described previously using membranes stably expressing the μOR, δOR, or κOR were isolated from CHO (μOR, δOR) or U2OS cells (κOR) (DiscoverX) and using OR specific radiolabels [^{3}H]DAMGO, [^{3}H]DPDPE and [^{3}H]U69,593 (Cassell et al., 2019; Creed et al., 2021).

GloSensor cAMP Inhibition Assay

cAMP inhibition assays were performed in HEK cells transiently transfected with pGloSensor22F and either expressing FLAG-mouse δOR, HA-mouse μOR, or FLAG-mouse κOR as previously described (Chiang et al., 2016).

PathHunter β-arrestin2 Recruitment Assay

β-arrestin recruitment assays were performed in PathHunter cells stably expressing the μOR, δOR, or κOR and β-arrestin2 as previously described (Chiang et al., 2016).

Statistical analysis

Data and statistical analysis comply with the recommendations on experimental design and analysis in pharmacology (Curtis et al., 2018). Data analysis was completed using GraphPad 9 (GraphPad Prism software, La Jolla, CA) and is presented as means ± SEM. For findings from cellular assays, composite figures are shown consisting of an averaged curve from a minimum of three independent assays that were normalized to a positive control; best fit values in Table 3.1 were generated by GraphPad Prism from composite figures.

3.2.4 Animals

General

The animal protocols (#1305000864 and #1605001408) describing the care and use of experimental animals was approved by the Purdue University Institutional Animal Care and Use

Committee (https://www.purdue.edu/research/regulatory-affairs/animal-research/staff.php). Animal studies were carried out in accordance with the ARRIVE guidelines (Kilkenny et al., 2010b) and recommendations made by the National Institutes of Health Guide for the Care and Use of Laboratory Animals. Wildtype C57Bl/6N mice (107 male, 10 female; 6-7-weeks old) were purchased from Envigo (Indianapolis, IN) and were acclimated to the facility and to handling and injections for 1 week prior to any experimental procedures. δOR KO mice (27 male, 8-12 weeks old) with a C57Bl/6N background (re-derived in early 2021) were bred in house and were similarly conditioned to handling and injections prior to experimentation. All mice were housed on a reverse 12-hour light (21:30-9:30)/12-hour dark cycle under controlled temperature (21-23 °C) with ad libitum food access. The only exception to this is mice used in the rotarod assay; these mice were housed in 12-hour light (6:00-18:00)/12-hour dark cycle. All experiments were conducted between 10:30-15:00, and all mice were habituated to the test room at least 30 minutes prior to experimentation. Rotarod, nociception, and seizure experiments were conducted in well-lit rooms whereas conditioned place preference, 2-bottle choice, and locomotor experiments were conducted in the dark.

Experimental Groups

For the locomotor assays with 7-hydroxymitragynine, a group of 10 male mice was used. For the paynantheine agonist nociception assays, 10 male mice were treated on different days with 10 and 30 $mg \cdot kg^{-1}$ (i.p) paynantheine. For the paynantheine antagonist nociception assays, a separate group of 10 mice were exposed to 6 $mg \cdot kg^{-1}$ morphine (s.c.) by itself, then again after treatment with 10 and 30 $mg \cdot kg^{-1}$ paynantheine (i.p.). For agonist and antagonist antinociception assays with 7-hydroxyspeciogynine, a total of 11 wildtype male mice were used; all received 7-hydroxyspeciogynine for the agonist mode, and then for antagonist mode n=6 received morphine plus 7-hydroxyspeciogynine and n=5 received vehicle plus 7-hydroxyspeciogynine. For specifics on drug administration timing in the nociception assays see the tail flick thermal nociception methods section. For the 2-bottle choice alcohol consumption experiments with WT male and female mice, separate groups of wildtype mice were used to test increasing doses of each analog (n=8 males for 7-hydroxypaynantheine, n=12 males and n=10 females for 7-hydroxyspeciogynine). For the 2-bottle choice experiments with δOR KO mice, a group of mice (n=9) was repeated tested once per week, with different drug treatments (consistent baseline ethanol consumption across the

drug treatments is shown in Supplemental Figure 7 in the online supplement). A second, separate group of 10 male δOR KO mice were used to examine speciociliatine in the 2-bottle choice paradigm. Following a 3-week period of alcohol withdrawal, five of the δOR KO mice from the first 2-bottle choice group were used to examine seizure activity of paynantheine (30 $mg \cdot kg^{-1}$, i.p.). Similarly, 5 wildtype mice from the naloxone-block locomotor experiment were reused to assess seizure activity of 30 $mg \cdot kg^{-1}$ paynantheine (i.p.) following a week of drug washout. In the rotarod assay, n=8 wildtype male and n=8 δOR KO male mice were used to assess motor incoordination effects following treatment with speciociliatine. Note that one δOR KO mouse died after experiencing severe, level 5-6 seizures following i.p. administration of 30 mg/kg speciociliatine in the rotarod assay, leading to an overall n=7 instead of n=8 for this genotype. For the CPP paradigms, independent groups of wildtype male mice were used to examine paynantheine by itself (n=16 total), paynantheine with morphine (n=14 total), and 7-hydroxyspeciogynine (n=8).

3.2.5 Behavioral Assays and Associated Statistical Analysis

Locomotor Evaluation

To assess drug-induced effects on ambulation for 7-hydroxymitragynine, locomotor activity was assessed in a 2-day protocol as previously described (Gutridge et al., 2020). To assess drug-induced effects on ambulation for paynantheine and 7-hydroxyspeciogynine, locomotor information was extracted from the data generated in the CPP experiments. Distance traveled during each drug and vehicle conditioning session was pulled from the 30- or 40-minute conditioning session (extended or brief CPP paradigm, respectively) and all sessions per treatment were averaged for analysis. A summary of all statistical analyses for the locomotor data can be found in Supplemental Table 2 in the online supplement. In brief, for 7-hydroxymitragynine locomotor data in Figure 1, an unpaired, two-tailed t-test was used. For paynantheine locomotor data in Figure 2G, statistical significance of drug treatment versus vehicle was obtained by a one-way ANOVA with Dunnett's multiple comparisons to VEH + VEH. For paynantheine + morphine locomotor data in Figure 2G, statistical significance of paynantheine + morphine versus morphine alone was obtained via a one-way ANOVA with Dunnett's multiple comparisons to morphine (MOR). For 7-hydroxyspeciogynine locomotor data in Figure 7B, a two-tailed, paired t-test was

used; one mouse was removed from this analysis after being identified as an outlier with the Grubb's test.

Brief and Extended Conditioned Place Preference Paradigms

Mice were conditioned to drugs and vehicle as described previously in two-chamber conditioned place preference (CPP) boxes in a counterbalanced, unbiased approach for either two drug conditioning sessions over two days (brief) or four drug conditioning sessions over eight days (extended) (Váradi et al., 2015a; Gutridge et al., 2020). For brief and extended conditioned place preference experiments, separate groups of mice were used for each drug dose. A summary of all statistical analyses for the CPP data can be found in Supplemental Table 4 in the online supplement. In brief, all CPP data was analyzed with two-tailed, paired t-tests comparing time spent on the drug-paired side pre- and post-conditioning.

Seizure Assay

To assess drug-induced seizurogenic activity, mice were placed in a clear plastic cylinder (25 cm diameter, 35 cm height) immediately following drug injection and their activity was recorded in a well-lit, quiet room using iSpy camera software (iSpyConnect.com). A recording time of 90 minutes was chosen for the tested compounds based on previous observations of seizures time lengths in experiments with 30 $mg \cdot kg^{-1}$ paynantheine. If animals were not presenting with seizure activity after 30 minutes, the recording time was shortened accordingly. Seizure severity was scored based on the modified racine scale (half-scores allowed) in bins of 3-5 minutes. Onset to first seizure symptom, onset to highest racine score, and highest racine score were also assessed. A summary of all statistical analyses for the seizure data can be found in Supplemental Table 3 in the online supplement. In brief, seizure-like behavior between wildtype and δOR KO mice was compared with a two-tailed, unpaired t-test with Welch's correction on area-under the curve data generated from graphing the highest racine score per time bin over 90 minutes for each mouse.

Tail Flick Thermal Nociception Assay

Antinociception via the tail flick assay was measured as previously described (van Rijn et al., 2012b). Mice were first habituated to the handling restraint used during the experimentation. On subsequent test days, a radiant heat tail-flick instrument (Columbus Instruments, Columbus, OH, USA) was used to collect duplicate measurements by testing two different regions on the mouse's tail. The beam intensity was adjusted between each group of mice to elicit reproducible responses between 2-3 seconds (beam intensity of 7-9). At a minimum, mice were given 2 days between experiments to recover from thermal stimuli. For each test day, a baseline tail flick response was collected for each mouse and was used to calculate the testing cut-off time (cutoff time = three times the baseline response time). To test antinociception by drug agonism, a vehicle injection was next administered (i.p. or s.c.) and tail-flick responses were collected after 30 minutes. The drug was then administered (i.p. or s.c.) and tail flick responses were collected after 30 minutes. To test drug antagonism of morphine antinociception, a response to vehicle injections were similarly collected prior to drug administration with a first vehicle injection (i.p. or s.c.) at 0 minutes, followed by a second vehicle injection (s.c.) at 10 minutes before collecting tail flick responses at 30 minutes (twenty minutes after the second vehicle injection. The test compound was then administered (i.p. or s.c.), followed by 6 $mg \cdot kg^{-1}$ morphine (s.c.) 10 minutes later. Tail-flick responses were collected 20 minutes following morphine administration. Data is represented as percent maximal possible effect (%MPE) and is calculated as %MPE = (treatment response time – baseline response time)/(cutoff time – baseline response time) * 100. Data is normalized to vehicle treatment: drug treatment %MPE – saline treatment %MPE. A summary of all statistical analyses for the antinociceptive data can be found in Supplemental Table 5 in the online supplement. In brief, for agonist antinociception assays, significance was calculated via a two-tailed, paired t-test to compare vehicle and drug treatment. For antagonist antinociception assays with three treatment groups in the same group of mice (Figure 3.2D), data was analyzed via repeated measures (RM) one-way ANOVA with Dunnett's multiple comparisons to the morphine-only treatment group. For antagonist antinociception assays with two treatment groups in two different groups of mice (Figure 3.8D), an unpaired t-test with Welch's correction was used to assess significance between the morphine-only group and the morphine plus "antagonist" group.

Two-Bottle Choice Alcohol Paradigm

Mice were subject to a drinking in the dark (DID), limited access (four hours per day), 2-bottle choice (10% ethanol versus water) paradigm in which they were trained to consume alcohol voluntarily as previously described (Rhodes et al., 2005; van Rijn and Whistler, 2009). Mice reached stable alcohol consumption within three weeks of training, and after the third week, drug injections were administered prior to the daily drinking session on Friday. Drug effect on alcohol consumption was measured as the change in Friday's alcohol intake minus the average alcohol intake from the preceding Tuesday-Thursday of that week ($g \cdot kg^{-1}$). A summary of all statistical analyses for the drinking data can be found in Supplemental Tables 6-9 in the online supplement. In brief, results from 2-bottle choice alcohol consumption paradigms were assessed for statistical significance using RM two-way ANOVA for main effects of drug dose, treatment day, and drug dose x treatment day; Sidak's multiple comparisons (MC) between alcohol consumption baseline (Tuesday-Thursday average) vs treatment day consumption (Friday) were then used as the post-hoc test for each drug dose tested. The same RM two-way ANOVA and Sidak's MC post-hoc analyses were used for water consumption and ethanol preference data. For the change in alcohol consumption, change in water consumption, and change in ethanol preference data for 7-hydroxyspeciogynine where male and female data was analyzed together, a mixed-effects model was used (due to missing values) with the Geisser-Greenhouse correction for main effects, followed by Dunnett's MC between alcohol consumption baseline vs treatment day consumption. Sex differences between baseline data were evaluated using RM two-way ANOVA for main effects of sex, treatment baseline, and sex x treatment baseline; Sidak's multiple comparisons (MC) between male and female mice were then used as the post-hoc test for each treatment week tested.

Accelerating Rotarod Test

Mice were trained to walk on a rotarod apparatus (IITC, USA) with 1.25" diameter drums on two days prior to drug testing. The rotarod started at 3 rpm and increased to 30 rpm over 300 seconds. A trial for a mouse ended when it fell and tripped the sensor, when it rode the rotarod for two consecutive revolutions. or after 300 seconds (the maximum trial time)(White et al., 2015). Mice received at least three minutes of rest between trials. On test day, baseline performance was assessed as the average latency to fall in three trials per mouse. Mice were then injected with 30

mg·kg^{-1} speciociliatine (i.p.) and immediately tested for performance on the apparatus (this first data point represented as latency to fall at 5 minutes), and then tested again at 15, 30, 60, and 120 minutes post-injection. Each mouse's performance was normalized to its own baseline and reported as a percentage. A summary of all statistical analyses for the rotarod data can be found in Supplemental Table 2 in the online supplement. In brief data for each tested time point was calculated as a percentage of the baseline, and thus statistical significance was calculated in a two-tailed, one sample t-test versus a hypothetical mean of 100 (baseline was 100%). Rotarod results between WT and δOR KO genotypes was compared with a mixed-effects model with fixed effects for timepoint, genotype, and timepoint x genotype.

3.2.6 Nomenclature of Targets and Ligands

Key protein targets and ligands in this article are hyperlinked to corresponding entries in http://www.guidetopharmacology.org, the common portal for data from the IUPHAR/BPS Guide to PHARMACOLOGY(Harding et al., 2018), and are permanently archived in the Concise Guide to PHARMACOLOGY 2019/20 (Alexander et al., 2019).

3.3 Results

3.3.1 Hyperlocomotion induced by the kratom alkaloid 7-hydroxymitragynine is naloxone-reversible.

The kratom alkaloid 7-hydroxymitragynine was the most potent amongst kratom alkaloids in decreasing alcohol intake (Gutridge et al., 2020), however it produces significant adverse effects such as conditioned place preference and hyperlocomotion. This hyperlocomotion induced by 7-hydroxymitragynine was blocked by a low, 1 mg·kg^{-1} dose of naloxone (unpaired, two-tailed t-test, t=5.441, df=8, p=0.0006) (**Fig. 3.1**).

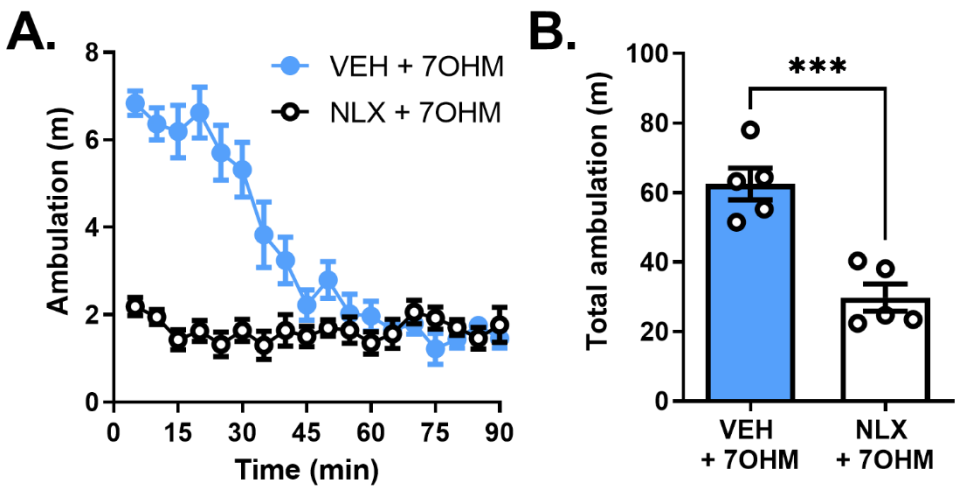

Figure 3.1 Blocking μOR attenuates 7-hydroxymitragynine-induced hyperlocomotion.

(A) 90-minute ambulation time course of wildtype, C57Bl/6 male mice (n= 5 per group) treated with 7-hydroxymitragynine (3 mg·kg^{-1}, i.p.) after pre-treatment with vehicle (s.c.) or naloxone (1 mg·kg^{-1}, s.c.) injection (10 minutes prior to 7-hydroxymitragynine injection). **(B)** Total ambulation (area under the curve) for the same data set. ***p<0.001 (for details see Supplementary Table 2 in the online supplement).

3.3.2 Paynantheine functionally antagonizes morphine effects in vivo.

Paynantheine is a naturally occurring G-protein-biased kratom alkaloid with micromolar potency and affinity at the μOR and δOR that dose-dependently decreases alcohol intake in male mice at 10 and 30 mg·kg^{-1}, but unlike 7-hydroxymitragynine does not produce hyperlocomotion at its effective dose (Gutridge et al., 2020). In contrast to 7-hydroxymitragynine, paynantheine produces modest conditioned place aversion (CPA) in a brief CPP paradigm (paired, two-tailed t-test, t=2.606, df=7, p=0.0351) (**Fig. 3.2A**). However, when using an extended CPP paradigm paynantheine did not produce CPP nor CPA (paired, two-tailed t-test, t=2.227, df=7, p=0.0612) (**Fig. 3.2B**). Additionally, we observed Racine level 1-2 convulsive behaviors in wildtype and δOR KO mice injected with a 30 mg·kg^{-1} dose (**Fig. 3.2C**) with no difference between groups (Welch's t-test, t=0.9205, df=6.738, p=0.3891). In the GloSensor assay of cAMP inhibition, paynantheine displayed partial to full agonism at the ORs (Gutridge et al., 2020) (Supp. Table 1 in the online supplement); however, paynantheine has also been reported as weak antagonist in a BRET-based G-protein assay at human ORs (Kruegel et al., 2016). To obtain a better understanding of paynantheine's pharmacology in vivo, we assessed if paynantheine was antinociceptive in thermal

nociception paradigms. Though the 30 mg·kg^{-1} dose of paynantheine produced a statistically significant difference in %MPE versus vehicle (paired, two-tailed t-test, t=2.925, df=9, p=0.0169), neither the 10 nor 30 mg·kg^{-1} dose displayed meaningful antinociceptive effects (**Fig. 3.2D**, first two columns). Instead, paynantheine dose-dependently blocked antinociception produced by 6 mg·kg^{-1} morphine (RM 1-way ANOVA, overall effect: F(1.943,17.49)=12.38, p=0.0005, with Dunnett's MC to 6 mg·kg^{-1} morphine: p=0.6330 for 10 mg·kg^{-1} dose, p=0.0019 for 30 mg·kg^{-1} dose) (**Fig. 3.2D**, last three columns). Because paynantheine blocked morphine action in a nociception assay and by itself did not produce CPP, we next sought to determine if it could block morphine CPP. However, neither pre-treatment with 10 nor 30 mg·kg^{-1} paynantheine abolished 6 mg·kg^{-1} morphine CPP (paired, two-tailed t-tests, t=3.214, df=7, p =0.0148 for the 10 mg·kg^{-1} dose, t=6.609, df=5, p=0.0012 for the 30 mg·kg^{-1} dose) (**Fig. 3.2E**). However, when assessing locomotor data from the CPP experiments in Figure 2A and 2E, we did observe that paynantheine dose-dependently attenuated hyperlocomotion induced by 6 mg·kg^{-1} morphine (1-way ANOVA, overall effect: F(2,15)=39.25, p<0.0001, with Dunnett's MC to 6 mg·kg^{-1} morphine: p=0.0004 for 10 mg·kg^{-1} dose, p<0.0001 for 30 mg·kg^{-1} dose) (**Fig. 3.2F-G**).

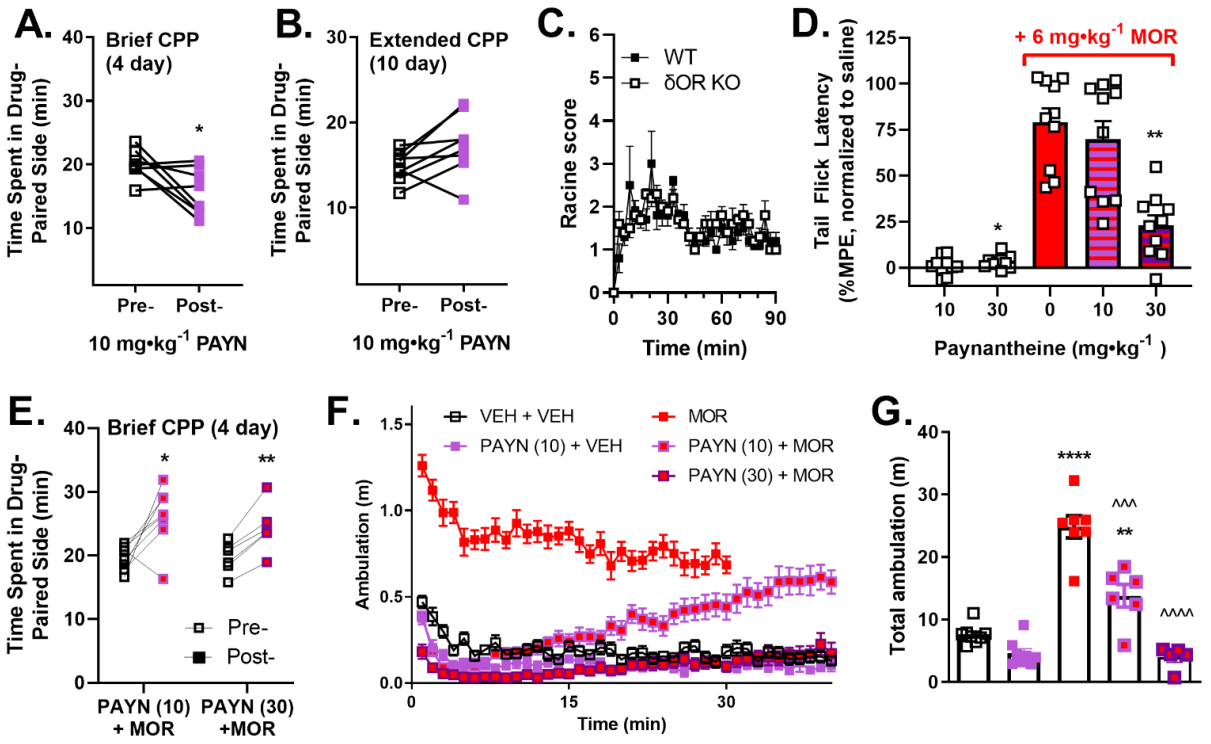

Figure 3.2 Antagonistic action of paynantheine in vivo.

The agonistic and antagonistic actions of kratom alkaloid paynantheine were further investigated in C57Bl/6 mice. Paynantheine (10 mg·kg^{-1}, i.p.) was evaluated in a **(A)** 4-day and **(B)** 10-day model of conditioned place preference (2 versus 4 drug conditioning sessions, respectively, n=8 each). **(C)** Seizure activity induced by paynantheine (30 mg·kg^{-1}, i.p.) was evaluated in male δOR KO and WT mice (n=5 per group). **(D)** Paynantheine (10 and 30 mg·kg^{-1}, i.p.) was tested for agonist and antagonistic properties in male mice (n=10 per dose) via the tail flick thermal nociception assay. For the antagonist assays, morphine (6 mg·kg^{-1}, s.c.) was administered 10 minutes following a dose of paynantheine (10 or 30 mg·kg^{-1}, i.p.). Nociception data is expressed as maximum possible effect (%MPE) normalized to a saline baseline (treatment – saline baseline). **(E)** Paynantheine (10 and 30 mg·kg^{-1}, i.p.) was evaluated for agonist and antagonist activity in an acute model of conditioned place preference by administering 10 minutes prior to morphine (6 mg·kg^{-1}) or vehicle (n=8 for 10 mg·kg^{-1} doses, n=6 for 30 mg·kg^{-1} dose). Locomotor data was extracted from the conditioning sessions of the CPP experiments in **(A** and **E)** and is shown as **(F)** ambulation over time and **(G)** total ambulation (total area under curve). For comparison in **(F-G)**, locomotor data for morphine (6 mg·kg^{-1} morphine) was extracted from a previous CPP experiment with 30-minute conditioning sessions. The vehicle locomotor data was extracted from the non-drug paired side conditioning session for 10 mg·kg^{-1} paynantheine + vehicle group. For locomotor data in (G), statistical significance of drug treatment versus vehicle (VEH + VEH) is shown with stars; statistical significance between paynantheine + morphine treatments and morphine-only treatment (MOR) is shown with carets. * $p<0.05$, ** $p<0.01$, ^^^$p<0.001$, **** or ^^^^ $p<0.0001$ (for details see Supplemental Tables 2-5 in the online supplement.)

3.3.3 Kratom analogs are OR partial agonists with minimal β-arrestin2 recruitment.

In order to produce better lead candidates to treat alcohol use disorder that lack adverse locomotor and rewarding effects, we next aimed to discover kratom alkaloids or alkaloid derivatives with increased δOR affinity and potency, but with limited μOR potency. To this end, we extracted paynantheine (2), speciogynine (3), and speciociliatine (4) from dry kratom powder using a modified protocol reported by Varadi et al. 2016. Paynantheine (2) was converted to 7-hydroxypaynantheine (7), **Fig. 3.3B**) using PIFA in acetonitrile and water. This 7-hydroxypaynantheine was next transformed to paynantheine pseudoindoxyl (8) using $Zn(OTf)_2$ in refluxing toluene. We adopted the same strategy to synthesize 7-hydroxyspeciogynine (9) and speciogynine pseudoindoxyl (10) as shown in **Figure 3.3C**.

Affinity wise, we noted that the paynantheine analogs, especially the 7-hydroxyl analog, showed weak μOR affinity, whereas 7-hydroxyspeciogynine displayed the strongest μOR affinity (**Table 3.1**, **Figure 3.4A**). At the δOR, 7-hydroxyspeciogynine displayed improved binding relative to speciogynine which was on par with affinities for the two pseudoindoxyl analogs. 7-hydroxypaynantheine was a magnitude weaker in binding the δOR than 7-hydroxyspeciogynine; this same trend was apparent at the κOR (**Table 3.1**, **Figure 3.4A-C**).

In terms of cAMP inhibition, we noted clear signs of partial agonism for the analogs at the μOR, with paynantheine pseudoindoxyl, 7-hydroxypaynantheine and 7-hydroxyspeciogynine displaying the lowest potency at the μOR (**Fig. 3.4A**, **Table 3.1**). 7-hydroxyspeciogynine was the strongest activator at the δOR (**Fig. 3.4E**), whereas speciociliatine exhibited the strongest κOR potency out of the tested alkaloids (**Table 3.1**, **Figure 3.4F**). Notably, while speciociliatine displayed binding at the δOR, it showed minimal activity at this receptor in regards to cAMP inhibition, suggestive of it acting as antagonist at the δOR (**Table 3.1**, **Figure 3.4B,E**). At the κOR, we did not detect cAMP inhibition for 7-hydroxypaynantheine at the tested dose range (**Table 3.1**, **Figure 3.4F**). We did not detect any β-arrestin2 recruitment for speciociliatine and the pseudoindoxyl and 7-hydroxyl analogs within the tested dose range (**Table 3.1**, **Figure 3.4G-I**), which is line with the reported G-biased nature of the kratom alkaloids (Kruegel et al., 2016; Váradi et al., 2016; Gutridge et al., 2020).

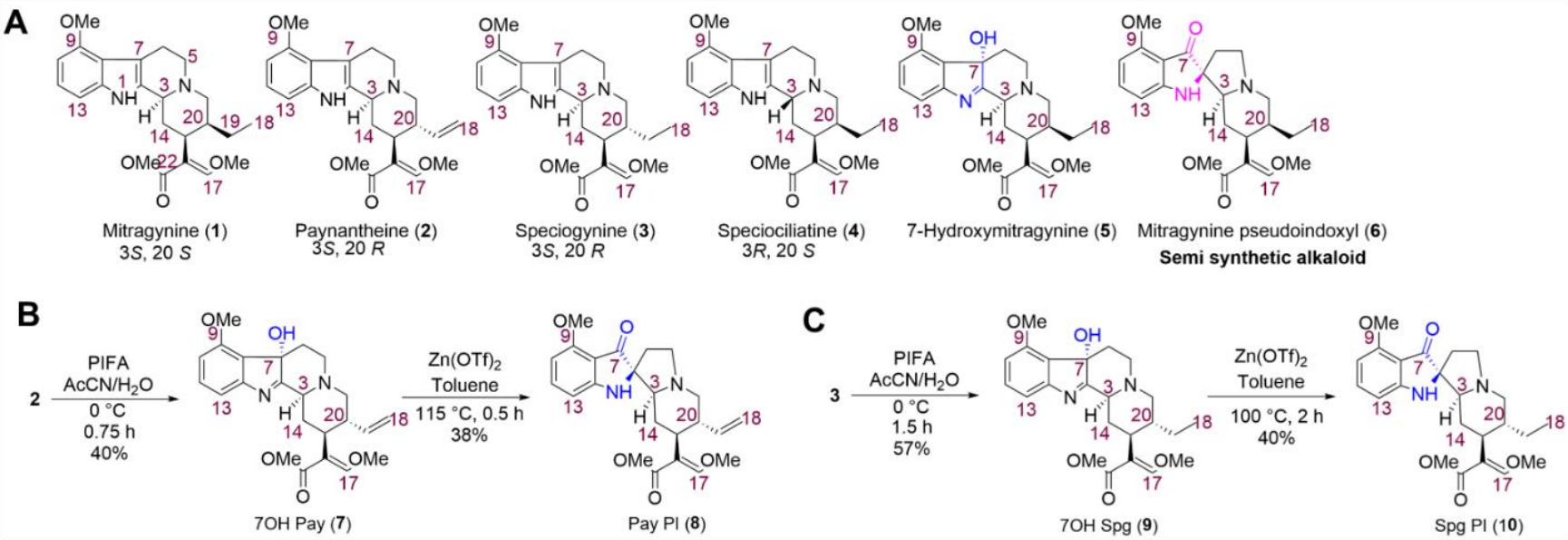

Figure 3.3 Synthesis and characterization of kratom alkaloid analogs**.**

Structures of naturally occurring kratom alkaloids paynantheine and speciogynine were used as scaffolds for analog synthesis. Analogs with pseudo-indoxyl (PI) rearrangements or hydroxyl group additions were made for both compounds, and a naturally occurring minor kratom alkaloid and speciogynine isomer, speciociliatine, was also synthesized for testing. **(A)** Chemical structures of selected indole based kratom alkaloids; **(B)** Synthesis of 7-hydroxypaynantheine (7) and paynantheine pseudoindoxyl (8); **(C)** Synthesis of 7-hydroxyspeciogynine (9) and speciogynine pseudoindoxyl (10).

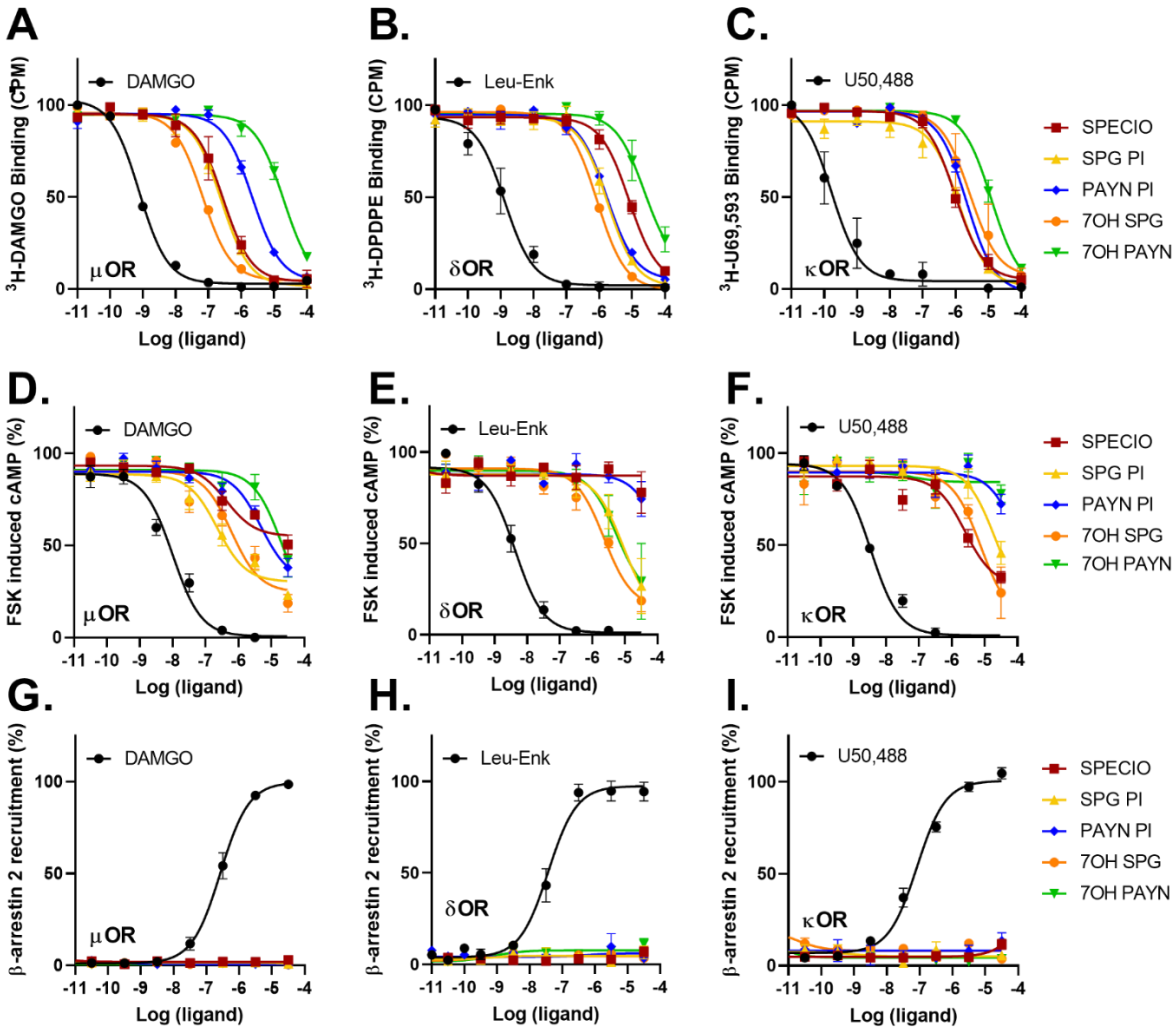

Figure 3.4 Pharmacological characterization of kratom analogs at opioid receptors.

Kratom alkaloid derivatives speciociliatine (SPECIO), speciogynine pseudo indoxyl (SPG PI), paynantheine pseudo indoxyl (PAYN PI), 7-hydroxy speciogynine (7OH SPG), and 7-hydroxy paynantheine (7OH PAYN) were characterized for binding affinity using [^{3}H]DAMGO, [^{3}H]DPDPE, [^{3}H]U69,593 (**A, B, C**), inhibition of forskolin-induced cAMP in a Glo-sensor assay in transfected HEK-293 cells (**D, E, F)** and the ability of the alkaloids to recruit β-arrestin 2 in a PathHunter assay. (**G, H, I**) at μOR (**A, D, G**), δOR (**B, E, H**), and κOR (**C, F, I**). All curves are representative of the averaged values from a minimum of 3 independent assays.

Table 3.1 Pharmacological characterization of kratom derivatives at the μ, δ and κ opioid receptors.

Affinity (pKi, drug concentration at which 50% of receptors is occupied). cAMP inhibition potencies ($pIC_{50,}$ drug concentration at 50% maximal efficacy) and efficacies (α, % inhibition at maximal efficacy normalized to DAMGO [μOR], leu-enkephalin [δOR] or U50,488 [κOR]) for OR agonists to inhibit cAMP production are indicated ± SEM. β-arrestin 2 recruitment potencies (pEC_{50}) and efficacies (α, normalized to DAMGO, leu-enkephalin or U50,488) of OR agonists to recruit β-arrestin 2 are indicated ±SEM. The number of repetitions for each drug is indicated in parentheses. ND = not detectable. Data for 7-hydroxymitragynine (7OH MIT) in the GloSensor cAMP assay and PathHunter β-arrestin2 recruitment assay was generated in a previous publication (Gutridge et al. 2020) and is shown in Supplemental Table 1 for easy comparison to the kratom derivatives.

Table 3.1. Pharmacological characterization of kratom derivatives at opioid receptors							
Compounds	**Binding**		**cAMP**			**β-arrestin 2**	
μOR	**pK_i**	**K_i (μM)**	**pIC_{50}**	**IC_{50} (μM)**	**α**	**pEC_{50}**	**α**
DAMGO	9.6 ± 0.1 (1)	0.00024	8.0 ± 0.1 (6)	0.0099	100	6.6 ± 0.1 (6)	100
7OH MIT	7.7 ± 0.1 (6)	0.019	7.8 ± 0.1 (5)	0.016	84 ± 3	ND (3)	ND
SPECIO	7.1 ± 0.1 (3)	0.086	6.4 ± 0.2 (5)	0.43	38 ± 3	ND (4)	ND
SPG PI	7.1 ± 0.1 (3)	0.077	6.6 ± 0.2 (5)	0.23	58 ± 4	ND (4)	ND
7OH SPG	7.7 ± 0.1 (3)	0.021	6.2 ± 0.2 (6)	0.61	66 ± 6	ND (4)	ND
7OH PAYN	5.2 ± 0.1 (3)	6.15	4.7 ± 0.5 (5)	21.8	80 ± 40	ND (3)	ND
PAYN PI	6.2 ± 0.1 (3)	0.68	5.3 ± 0.2 (4)	4.82	60 ± 6	ND (3)	ND
δOR	**pK_i**	**K_i (μM)**	**pIC_{50}**	**IC_{50} (μM)**	**α**	**pEC_{50}**	**α**
Leu-Enk	9.2 ± 0.1 (3)	0.00070	8.4 ± 0.1 (9)	0.0042	100	7.4 ± 0.1 (7)	100
7OH MIT	6.7 ± 0.1 (4)	0.19	5.7 ± 0.2 (8)	0.96	80 ± 8	6.4 ± 0.3 (6)	14 ± 1
SPECIO	5.4 ± 0.1 (3)	4.34	ND (3)	ND	ND	ND (5)	ND
SPG PI	6.0 ± 0.1 (3)	0.94	5.1 ± 0.3 (4)	8.53	80 ± 20	ND (4)	ND
7OH SPG	6.3 ± 0.1 (3)	0.46	5.6 ± 0.1 (6)	2.27	76 ± 6	ND (4)	ND
7OH PAYN	4.9 ± 0.2 (4)	12.7	5.2 ± 0.3 (5)	5.74	70 ± 20	ND (3)	ND
PAYN PI	6.0 ± 0.1 (3)	0.92	ND (5)	ND	ND	ND (3)	ND
κOR	**pK_i**	**K_i (μM)**	**pIC_{50}**	**IC_{50} (μM)**	**α**	**pEC_{50}**	**α**
U50,488	10.0 ± 0.2 (2)	0.000099	8.5 ± 0.1 (5)	0.0034	100	7.1 ± 0.1 (6)	100
7OH MIT	6.9 ± 0.1 (4)	0.14	6.2 ± 0.3 (9)	1.04	77 ± 5	ND (4)	ND
SPECIO	6.2 ± 0.1 (4)	0.59	5.6 ± 0.2 (4)	2.50	60 ± 7	ND (5)	ND
SPG PI	6.1 ± 0.1 (3)	0.75	4.7 ± 0.5 (4)	20.6	80 ± 30	ND (3)	ND
7OH SPG	5.8 ± 0.2 (3)	1.63	5.1 ± 0.3 (3)	7.71	80 ± 20	ND (5)	ND
7OH PAYN	5.1 ± 0.1 (3)	7.46	ND (3)	ND	ND	ND (3)	ND
PAYN PI	5.9 ± 0.1 (4)	1.31	ND (3)	ND	ND	ND (3)	ND

3.3.4 Speciociliatine modulation of alcohol intake is compounded by drug-induced locomotor incoordination.

Based on our hypothesis that G-protein-biased δOR agonism drives decreased alcohol intake following kratom alkaloid injection, we did not expect speciociliatine to decrease alcohol intake as it behaves in vitro as a partial agonist for μOR and κOR but antagonist at δOR (**Table 3.1**). However, speciociliatine significantly decreased ethanol consumption, but only at the 30 $mg \cdot kg^{-1}$ dose (RM 2-way ANOVA, dose: $F(3, 30) = 36.48$, $p<0.0001$, time: $F(1, 10) = 50.17$, $p<0.0001$, dose x time: $F(3, 30) = 13.30$, $p<0.0001$, with Sidak's MC (T-R vs F), $p<0.0001$ for the 30 $mg \cdot kg^{-1}$ dose) (**Fig. 3.5A**) and with surprisingly strong efficacy (an average decrease of 2.5 ± 0.3 $g \cdot kg^{-1}$ ethanol or a 90 ± 3 % reduction, Supp. Fig. 4A in the online supplement). However, the 30 $mg \cdot kg^{-1}$ dose demonstrated a similar alcohol modulating effect in δOR KO mice (RM 2-way ANOVA, dose: $F(1, 9) = 25.36$, $p=0.0007$, time: $F(1, 9) = 61.69$, $p<0.0001$, dose x time: $F(1, 9) = 83.26$, $p<0.0001$, with Sidak's MC (T-R vs F), $p<0.0001$ for the 30 $mg \cdot kg^{-1}$ dose) (**Fig. 3.5D**). Treatment with speciociliatine did not change water consumption at any of the tested doses in wildtype or δOR KO mice (**Fig. 3.5B** and **E**, respectively). Taking together the lack of compensatory increase in water consumption and the decrease in ethanol consumption at the 30 $mg \cdot kg^{-1}$ dose, the ethanol preference was thus significantly decreased at this dose in wildtype mice (**Fig. 3.5C**) (RM 2-way ANOVA, dose: $F(3, 30) = 24.20$, $p<0.0001$, time: $F(1, 10) = 17.10$, $p=0.002$, dose x time: $F(3, 30) = 7.521$, $p=0.0007$, with Sidak's MC (T-R vs F), $p<0.0001$ for the 30 $mg \cdot kg^{-1}$ dose) and δOR KO mice (**Fig. 3.5F**) (RM 2-way ANOVA, dose: $F(1, 9) = 32.58$, $p=0.0003$, time: $F(1, 9) = 23.26$, $p=0.0009$, dose x time: $F(1, 9) = 64.72$, $p<0.0001$, with Sidak's MC (T-R vs F), $p<0.0001$ for the 30 $mg \cdot kg^{-1}$ dose). The 30 $mg \cdot kg^{-1}$ dose also significantly reduced the ability of treated wildtype mice to perform in the rotarod assessment (**Fig. 3.5G**). This motor effect had a rapid onset, where time spent on the device significantly decreased at 5 minutes (one sample t-test, $t=3.478$, $df=7$, $p = 0.0103$), with the peak effect occurring between 15 and 30 minutes ($t=5.809$, $df=7$, $p = 0.0007$; $t=5.344$, $df=7$, $p = 0.0011$, respectively), and the mice fully recovering at 120 minutes ($t=1.953$, $df=7$, $p = 0.0918$). The same effect was observed in δOR KO mice (mixed effects model with matching for genotype x timepoint, $F(1.941,11.26)=1.930$, $p=0.1906$

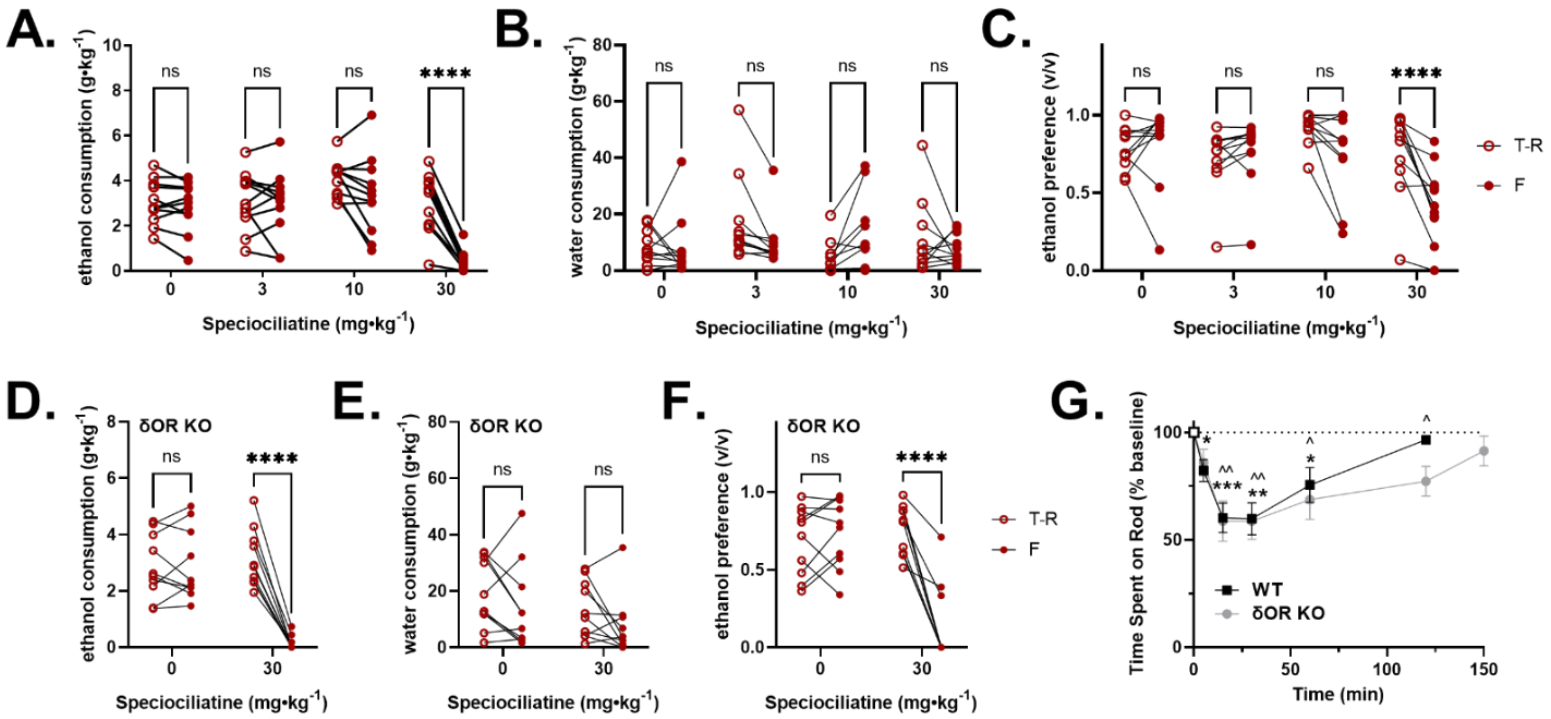

Figure 3.5 Speciociliatine decreases voluntary ethanol consumption and impairs motor coordination in wildtype and δOR knockout mice.

10% ethanol consumption, water consumption and ethanol preference in male C57BL/6 **(A-C**, respectively**)** (n=11) and δOR KO **(D-F**, respectively**)** mice (n = 10) in a voluntary two-bottle choice, limited access, drinking-in-the-dark paradigm, following treatment with speciociliatine (3, 10, and 30 mg·kg^{-1}, i.p.) **(G)** 150 minute-duration rotarod assessment of motor incoordination in WT mice (n=8) and δOR KO mice (n=7), immediately following a 30 mg·kg^{-1} dose of speciociliatine (i.p.); significance for WT mice and δOR KO mice is denoted with stars and carets, respectively. Open circles are the average intake/preference on the preceding three days (baseline), and closed circles are the intake on Fridays following drug exposure. * or ^ p<0.05, ** or ^^ p<0.01, *** p<0.001, **** p<0.0001 (for details see Supplemental Tables 6-8 in the online supplement).

3.3.5 Kratom analogs decrease ethanol consumption in a δOR-dependent mechanism.

Given the weak μOR potency of 7-hydroxyspeciogynine and 7-hydroxypaynantheine but the clear 0.5-1 log-fold difference in potency at the δOR between the two analogs (**Fig. 3.4D, E**), we next assessed the in vivo potency of these two alkaloids in modulating volitional alcohol consumption in mice. In wildtype male mice, 7-hydroxyspeciogynine more potently reduced alcohol intake in a dose-dependent manner at a 3 and 10 mg·kg^{-1} (**Fig. 3.6A**, RM 2-way ANOVA, dose: $F(2, 22) = 6.973$, $p=0.0045$, time: $F(1, 7) = 13.79$, $p=0.0006$, dose x time: $F(2, 22) = 8.675$, $p=0.0017$, with Sidak's MC (T-R vs F), $p=0.0802$ for the 3 mg·kg^{-1} dose, $p<0.0001$ for the 10 mg·kg^{-1} dose). This decrease in ethanol consumption at the 10 mg·kg^{-1} dose was accompanied by a concomitant increase in water consumption during the time course of the voluntary alcohol consumption paradigm (**Fig. 5B**, RM 2-way ANOVA, dose: $F(2, 22) = 8.706$, $p=0.0016$, time: $F(1, 11) = 4.161$, $p=0.0661$, dose x time: $F(2, 22) = 3.489$, $p=0.0483$, with Sidak's MC (T-R vs F), $p=0.0112$), as well as a corresponding decrease in ethanol preference (**Fig. 3.6C**, RM 2-way ANOVA, dose: $F(2, 22) = 9.997$, $p=0.0008$, time: $F(1, 11) = 8.284$, $p=0.0150$, dose x time: $F(2, 22) = 4.140$, $p=0.0298$, with Sidak's MC (T-R vs F), $p=0.0036$). We found that 7-hydroxypaynantheine was able to significantly reduce alcohol intake at a 10 and 30 mg·kg^{-1} dose (**Fig. 3.6D**, RM 2-way ANOVA, dose: $F(2, 14) = 4.200$, $p=0.0373$, time: $F(1, 7) = 13.79$, $p=0.0075$, dose x time: $F(2, 14) = 5.515$, $p=0.0171$, with Sidak's MC (T-R vs F), $p=0.0219$ for the 10 mg·kg^{-1} dose, $p<0.0001$ for the 30 mg·kg^{-1} dose). Similarly, the decrease in ethanol consumption at the 30 mg·kg^{-1} dose of 7-hydroxypaynantheine was accompanied by a concomitant increase in water consumption during the time course of the voluntary alcohol consumption paradigm (**Fig. 3.6E**, RM 2-way ANOVA, dose: $F(2, 14) = 4.129$, $p=0.0389$, time: $F(1, 7) = 4.920$, $p=0.0621$, dose x time: $F(2, 14) = 4.149$, $p=0.0385$, with Sidak's MC (T-R vs F), $p=0.0015$) and a corresponding decrease in ethanol preference (**Fig. 3.6F**, RM 2-way ANOVA, dose: $F(2, 14) = 3.845$, $p=0.0467$, time: $F(1, 7) = 5.193$, $p=0.0567$, dose x time: $F(2, 14) = 3.980$, $p=0.0428$, with Sidak's MC (T-R vs F), $p=0.0036$). In δOR KO mice subject to the same voluntary alcohol consumption paradigm, 10 mg·kg^{-1} 7-hydroxyspeciogynine significantly decreased ethanol consumption (RM 2-way ANOVA, dose: $F(4, 32) = 6.407$, $p=0.0007$, time: $F(1, 8) = 16.46$, $p=0.0036$, dose x time: $F(4, 32) = 1.851$, $p=0.1435$, with Sidak's MC (T-R vs F), $p=0.0269$), but not the 3 mg·kg^{-1}dose of 7-hydroxyspeciogynine or the 30 mg·kg^{-1}dose of 7-hydroxypaynantheine

(**Fig 3.6G**). Water consumption (**Fig. 3.6H**) and ethanol preference (**Fig. 3.6I**) were not significantly changed in the δOR KO mice following treatment with the kratom analogs.

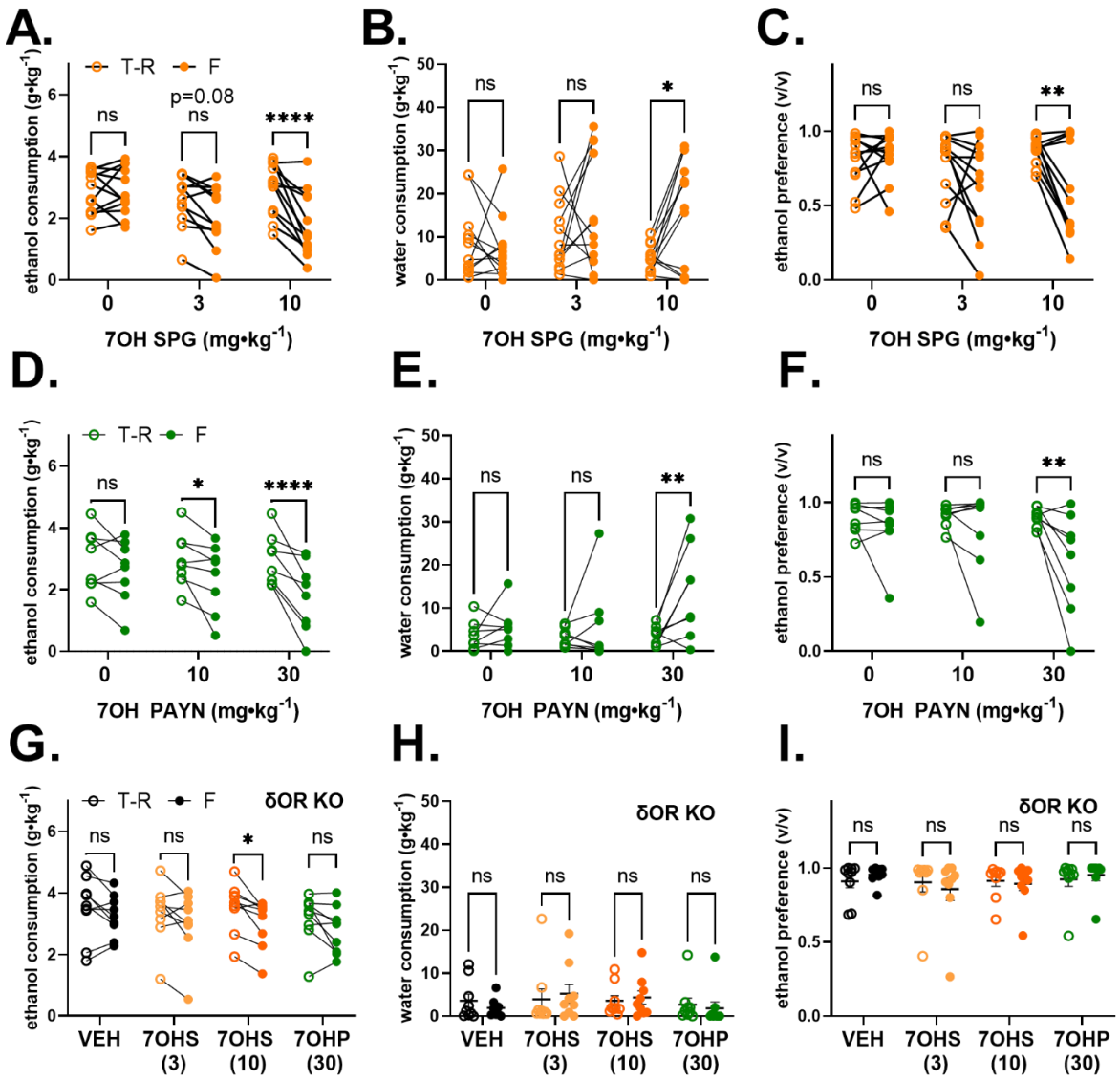

Figure 3.6 Kratom analogs decrease voluntary ethanol consumption in mechanism partially dependent on δOR.

10% ethanol consumption (left column), water consumption (middle column), and ethanol preference (right column) in male C57Bl/6 wild-type mice following treatment with **(A-C)** 7-hydroxyspeciogynine (3 and 10 mg·kg^{-1}, s.c., n=12), **(D-F)** 7-hydroxypaynantheine (10 and/or 30 mg·kg^{-1}, s.c., n=8), and in **(G-I)** male δOR KO mice (n=9) following treatment with effective doses of both analogs in a voluntary two-bottle choice, limited access, drinking-in-the-dark paradigm. Open circles are the average intake/preference on the preceding three days (baseline), and closed circles are the intake on Fridays following drug exposure. * p<0.05, **p<0.01, **** p<0.0001 (for details see Supplemental Tables 6-8 in the online supplement.)

In female mice exposed to the voluntary alcohol consumption paradigm, 7-hydroxyspeciogynine did not significantly modulate ethanol consumption, water consumption, or ethanol preference at the 3 mg·kg^{-1} dose (**Fig. 3.7A-C**, see Supplemental Tables 6-8 in the online supplement for statistical analyses). As previously reported (Rhodes et al., 2005), female mice exhibit a significantly higher baseline of alcohol consumption compared to males (Supplemental Table 9 in the online supplement, RM 2-way ANOVA, sex: $F(1, 20) = 39.05$, $p<0.0001$, time: $F(1, 20) = 6.295$, $p=0.0208$, dose x time: $F(1, 20) = 0.1027$, $p=0.7520$, with Sidak's MC (male vs female), $p<0.0001$ for the vehicle treatment baseline, $p<0.0001$ for the 3 mg·kg^{-1} 7-hydroxyspeciogynine treatment baseline). However, no sex difference was apparent in the Δ ethanol intake (Supplemental Table 9 in the online supplement, RM 2-way ANOVA, sex: $F(1, 20) = 0.1974$, $p=0.6616$, dose: $F(1, 20) = 7.758$, $p=0.0114$, sex x dose: $F(1, 20) = 0.2487$, $p=0.6234$, with Sidak's MC (male vs female), $p=0.9993$ for the Δ ethanol consumption following vehicle treatment, $p=0.7635$ for the Δ ethanol consumption following 3 mg·kg^{-1} 7-hydroxyspeciogynine treatment). Combining the Δ ethanol intake for males and females we found that there was a significant ethanol modulation effect at the 3 mg·kg^{-1} dose when collectively analyzing male and female responses (**Fig. 3.7D**, Mixed effects model (REML) with Geisser-Greenhouse correction, main effect of treatment: $F(1.539, 40.80) = 13.36$, $p=0.0001$, with Dunnett's MC (treatment vs vehicle), $p=0.0165$ for the 3 mg·kg^{-1} dose, $p=0.0064$ for the 10 mg·kg^{-1} dose). After finding similar sex differences in water consumption and ethanol preference but not in the Δ of these parameters (see Supplemental Table 9 in the online supplement for details), pooled male and female responses were similarly analyzed for Δ in response of water consumption and ethanol preference. In the pooled data, a concomitant increase in water consumption was evident at a 10 mg·kg^{-1} dose (**Fig. 3.7E**, Mixed effects model (REML) with Geisser-Greenhouse correction, main effect of treatment: $F(1.733, 27.74) = 5.978$, $p=0.0091$, with Dunnett's MC (treatment vs vehicle), $p=0.1804$ for the 3 mg·kg^{-1} dose, $p=0.0342$ for the 10 mg·kg^{-1} dose). Accordingly, in the pooled data, a significant decrease in ethanol preference was noted at the 10 mg·kg^{-1} dose (**Fig. 3.7F**, Mixed effects model (REML) with Geisser-Greenhouse correction, main effect of treatment: $F(1.645, 43.58) = 7.889$, $p=0.0022$, with Dunnett's MC (treatment vs vehicle), $p=0.1644$ for the 3 mg·kg^{-1} dose, $p=0.0255$ for the 10 mg·kg^{-1} dose).

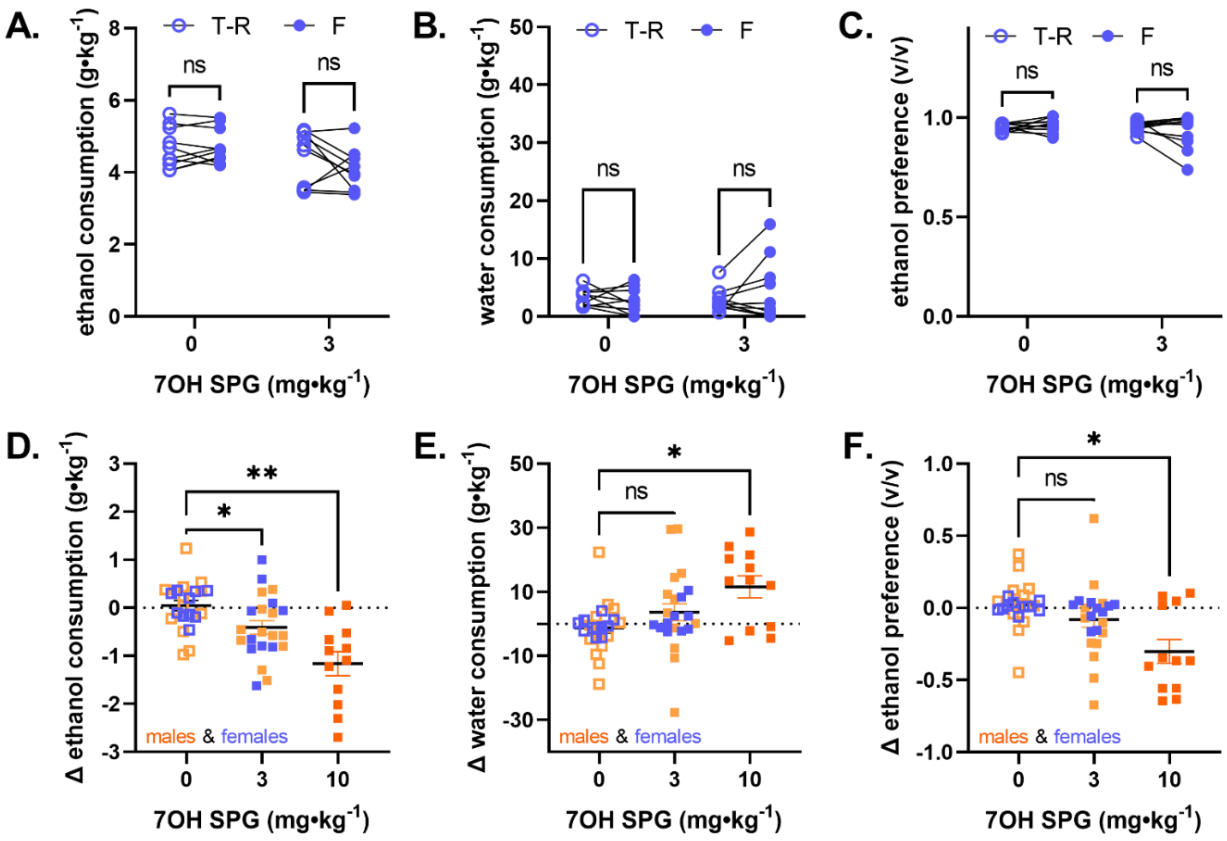

Figure 3.7 Alcohol-modulating effects of 3 mg·kg^{-1} 7-hydroxyspeciogynine are not sex specific.

In WT female mice (n=10), effects of 3 mg·kg^{-1} 7-hydroxyspeciogynine (s.c.) on 10% ethanol consumption **(A)**, water consumption **(B)**, and ethanol preference **(C)** were evaluated in a voluntary two-bottle choice, limited access, drinking-in-the-dark paradigm. Male and female responses to 7-hydroxyspeciogynine (3 and 10 mg·kg^{-1}, s.c.) in the 2-bottle choice paradigm were pooled and are shown as **(D)** change (Δ) in 10% ethanol consumption, **(E)** change (Δ) in water consumption, and **(F)** change (Δ) in ethanol preference. In panels A-C, open circles are the average intake/preference on the preceding three days (baseline), and closed circles are the intake on Fridays following drug exposure. In panel D-F, female and male mice are depicted with blue and orange symbols, respectively. *p<0.05, ** p<0.01 (for details see Supplemental Tables 6-9 in the online supplement.)

3.3.6 7-hydroxyspeciogynine has lessened side effects due to its decreased μOR dependent pharmacology.

From the cellular and behavioral experiments, 7-hydroxyspeciogynine emerged as the most promising kratom-derived analog for reducing alcohol use, with relatively equal in vivo potency as 7-hydroxymitragynine at the δOR, but lower μOR potency (**Table 3.1**). Next, we assessed whether 7-hydroxyspeciogynine exhibited a better side effect profile than 7-hydroxymitragynine due to its limited potency at the μOR. Additionally, to determine if 10 $mg \cdot kg^{-1}$ 7-hydroxyspeciogynine was the maximum tolerated dose (MTD) we assessed the side effect profile for the 10 $mg \cdot kg^{-1}$ dose. We found that mice treated with 10 $mg \cdot kg^{-1}$ 7-hydroxyspeciogynine did not develop conditioned place preference in our 'extended' conditioned place preference protocol, which involves four conditioning sessions each for drug and vehicle (paired, two-tailed t-test, t=1.592, df=7, p=0.1554) (**Figure 3.7A**). The same 10 $mg \cdot kg^{-1}$ dose of 7-hydroxyspeciogynine did not significantly alter ambulation (paired, two-tailed t-test, t=0.7552, df=6, p=0.4787) (**Figure 3.7B**) or induce seizures (**Figure 3.7C**). Akin to 10 $mg \cdot kg^{-1}$ paynantheine, 10 $mg \cdot kg^{-1}$ 7-hydroxyspeciogynine did not produce antinociception (paired, two-tailed t-test, t=0.6193, df=9, p=0.5511) or block morphine analgesia (unpaired t-test with Welch's correction, t=0.2660, df=5.994, p=0.7991) (**Fig. 3.7D**).

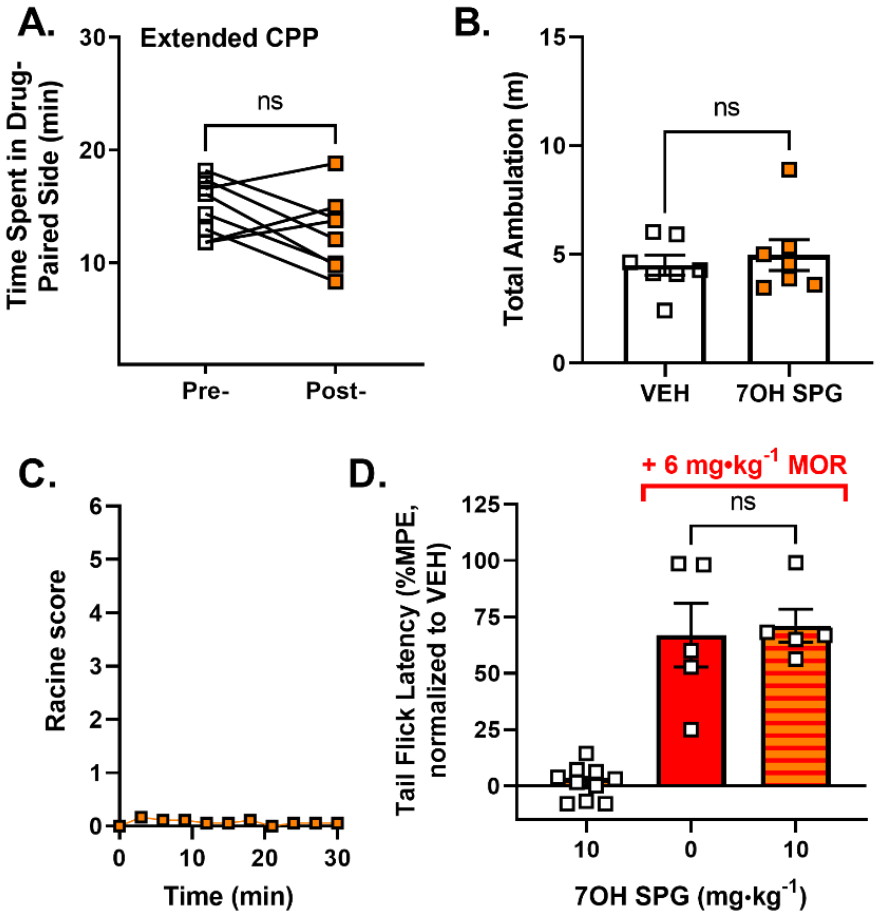

Figure 3.8 Side effect profile of 10 mg·kg^{-1} 7-hydroxyspeciogynine.

(A) In a 10-day conditioned place preference (CPP) paradigm, the rewarding effects of 7-hydroxyspeciogynine (s.c.) were evaluated in male, WT mice (n=8). **(B)** Locomotor data was extracted from the CPP experiment in **(A)** and averaged across all vehicle/drug treatment days (n=7). **(C)** The highest racine score collected every 3 minutes for 30 minutes following administration of 7-hydroxyspeciogynine was evaluated for 30 minutes after drug administration (n=9). **(D)** 7-hydroxyspeciogynine was tested for agonist, analgesic properties in male mice via the tail flick thermal nociception assay (n=10). In the same paradigm, antagonistic effects were evaluated after administering 7-hydroxypeciogynine, followed by morphine (6 mg·kg^{-1}, s.c.) 10 minutes later (n=6) and were compared to vehicle plus morphine administration (n=5). (For statistical details see Supplemental Tables 2-5 in the online supplement.)

3.4 Discussion

Over the past decade, kratom has been reported as a source for naturally occurring, G-protein biased opioidergic alkaloids, and has been investigated for its effects on pain management (Matsumoto et al., 2004; Kruegel et al., 2019; Chakraborty and Majumdar, 2021; Chakraborty et al., 2021b), opioid withdrawal (Wilson et al., 2020a, 2021), and alcohol abuse (Gutridge et al., 2020), as well as its decreased reward profile relative to traditional opioids (Hemby et al., 2019; Wilson et al., 2021). Here, we further probed the effects of kratom alkaloids and synthetic kratom alkaloid derivatives to obtain a better understanding of its in vivo pharmacology and in search of novel treatment options for alcohol use disorder. We report 7-hydroxyspeciogynine as an effective lead compound to reduce alcohol with an MTD of at least 10 $mg \cdot kg^{-1}$.

We previously demonstrated that 7-hydroxymitragynine as well as paynantheine could decrease alcohol consumption (Gutridge et al., 2020). However, we were unable to obtain a MTD for 7-hydroxymitragyinine as it caused both hyperlocomotion and CPP at a 3 $mg \cdot kg^{-1}$ dose which was the minimal effective dose to reduce alcohol intake (Gutridge et al., 2020). It has been well-established that μOR agonism can cause CPP, and that these rewarding effects can be blocked by μOR antagonists (Negus et al., 1993; Piepponen et al., 1997) as well as μOR KO (Matthes et al., 1996). Here we show that 7-hydroxymitragynine-induced hyperlocomotion also appears to be μOR-mediated as it is completely blocked by a dose of naloxone considered to be μOR-selective (Takemori and Portoghese, 1984; Pastor et al., 2005). Since the alcohol-reducing effect of 7-hydroxymitragynine was dependent on δORs (Gutridge et al., 2020), μOR potency may be a liability when exploring kratom alkaloids as treatment option for AUD. Paynantheine has much lower μOR potency while retaining δOR potency and decreases alcohol intake in mice at a 10 $mg \cdot kg^{-1}$ dose without causing hyperlocomotion (Gutridge et al., 2020). In line with the lower μOR potency, we find that 10 $mg \cdot kg^{-1}$ paynantheine does not produce place preference in an extended CPP paradigm. In a brief CPP paradigm, however, the same dose of paynantheine induces conditioned place aversion (CPA). Kratom use can lead to seizures (Coonan and Tatum, 2021) and we noticed that at 30 $mg \cdot kg^{-1}$, paynantheine induced minor seizure activity . It is possible that mice administered a dose of 10 $mg \cdot kg^{-1}$ paynantheine did not feel well despite not showing overt tonic-clonic seizure activity that could contribute to the observed CPA at this dose. δOR agonism can cause seizures (Hong et al., 1998; Broom et al., 2002; Jutkiewicz et al., 2006), however it is reported mostly for δOR agonists that are strong recruiters of β-arrestin, like SNC80 and

BW373U86 (O'Neill et al., 1997; Hong et al., 1998; Jutkiewicz et al., 2005). As such, we were not surprised that the G-protein-biased paynantheine-induced seizures were still present in δOR KO mice, indicating the seizures may be caused by an off-target interaction. Paynantheine can decrease alcohol consumption in wildtype mice (Gutridge et al., 2020), however it also decreases alcohol consumption in δOR KO mice (Supp. Fig 5; RM 2-way ANOVA, dose: $F(4, 32) = 6.407$, $p=0.0007$, time: $F(1, 8) = 16.46$, $p=0.0036$, dose x time: $F(4, 32) = 1.851$, $p=0.1435$, with Sidak's MC (T-R vs F), $p<0.0001$). This analysis provides further evidence that many of paynantheine's in vivo effects are not mediated by δOR.

While antinociception has been reported for 7-hydroxymitragynine, the weaker μOR affinity alkaloid mitragynine reportedly lacks antinociceptive ability, and has been suggested to act as a μOR antagonist (Obeng et al., 2021), although in the cAMP assay, we previously identified mitragynine as a partial agonist (Gutridge et al., 2020), in line with a couple of other reports (Kruegel et al., 2016; Váradi et al., 2016). Paynantheine has weaker potency for the μOR than mitragynine in the cAMP assay, but is more efficacious (Gutridge et al., 2020), which begged the question whether paynantheine possessed antinociceptive activity. However, both the 10 and 30 $mg \cdot kg^{-1}$ doses of paynantheine failed to produce meaningful antinociception in the tail-flick paradigm. In contrast, paynantheine blocks morphine analgesia at a 30 $mg \cdot kg^{-1}$ dose, but not 10 $mg \cdot kg^{-1}$, yet neither dose blocks morphine CPP. Additionally, paynantheine both at 10 and 30 $mg \cdot kg^{-1}$ doses can block morphine hyper-ambulation. Paynantheine, at a 10 $mg \cdot kg^{-1}$ dose only blocks morphine hyper-ambulation within the first 15-20 minutes of the 40-minute conditioning session. Detailed pharmacokinetic data for paynantheine has yet to be reported, but a recent study has shown that following oral administration in rats, a 1.1 $mg \cdot kg^{-1}$ dose of paynantheine had a T_{max} of 10 minutes in plasma, but was undetectable after an hour (Kamble et al., 2021). It similarly appears in our hands that paynantheine is being rapidly metabolized and/or cleared from the brain and plasma, such that it may not block morphine's CPP long enough to inhibit it significantly. This may also explain why the 10 $mg \cdot kg^{-1}$ dose does not block morphine analgesia, which was tested at 20-30 minutes after administration. Furthermore, a day-by-day analysis of the locomotor activity revealed that the 30 $mg \cdot kg^{-1}$ dose of paynantheine does not fully block morphine hyper ambulation within the last 5 minutes of the day 2 conditioning session (Supp. Fig. 1C-D in the online supplement). Because even one exposure to morphine is known to cause place preference in mice (Bardo and Neisewander, 1986), it is possible that mice administered 30 $mg \cdot kg^{-1}$ paynantheine

experienced enough rewarding effects from morphine on day 2 to express CPP. However, since we did not measure CPP for 30 mg·kg^{-1} paynantheine, we cannot rule out that paynantheine is responsible or positively contributed to the observed CPP. Taking together previous findings and the data collected here, we conclude that paynantheine is a weak partial agonist at the μOR and δOR, with functional antagonistic activity at the μOR in the presence of a more potent agonist in vivo. Overall, our conditioned place preference findings indicate that paynantheine has a low risk of reward, but that its use may be limited by its low potency in vivo, and seizure effects that are not δOR-mediated.

We next decided to utilize the G-protein-biased nature of the kratom alkaloid scaffold to discover opioids that have increased δOR potency, but that exhibit relatively low μOR potency. 7-hydroxymitragynine and mitragynine pseudoindoxyl, two previously characterized analogs of mitragynine, had higher δOR as well as μOR affinity and activity in cell lines compared to the indole-based template of mitragynine and showed unique binding poses in computational models (Váradi et al., 2016; Zhou et al., 2021). To extend the structure activity relationship (SAR) to the paynantheine and related speciogynine templates, we synthesized the hydroxylated and spiropseudoindoxyl variants of these natural products. We identified 7-hydroxyspeciogynine and 7-hydroxypaynantheine as having reduced μOR potency but similar δOR potency relative to 7-hydroxymitragynine. In contrast to the mitragynine derived spiropseudoindoxyls, no advantage with respect to potency at the ORs was seen with the pseudoindoxyls derived from paynantheine or speciogynine. Both the novel 7-hydroxyl analogs dose-dependently decreased alcohol consumption, with 7-hydroxyspeciogynine displaying efficacious activity at a dose of 3 mg·kg^{-1} and 7-hydroxypaynantheine at a 10 mg·kg^{-1} dose. We confirmed that the alcohol-modulating effects of these analogs are at least partially acting through a δOR-mediated mechanism as we did not observe statistically significant reductions alcohol consumption in δOR KO mice for the two analogs at their effective doses. Because 7-hydroxyspeciogynine decreases ethanol consumption in δOR KO at a 10 mg·kg^{-1}dose, but not 3 mg·kg^{-1}, this suggests that 7-hydroxyspeciogynine's ethanol modulation is no longer solely mediated by δOR at higher doses.

Additionally, the in vivo potency of these compounds correlates well with their in vitro pharmacology at the δOR where 7-hydroxyspeciogynine is about 0.5-1 log-fold more potent than 7-hydroxypaynantheine (Table 3.1). While 7-hydroxyspeciogynine displays more potent activity at the μOR relative to 7-hydroxypaynantheine in the GloSensor assay (pIC_{50}s of 6.2 ± 0.3 and 4.7

± 0.5, respectively), the activity at this receptor is still less potent than 7-hydroxymitragynine (pIC_{50} = 7.8 ± 0.1). The G-protein-biased μOR activity of 7-hydroxyspeciogynine likely does not contribute to decreased alcohol use because of the lack of effect in δOR KO mice at the 3 $mg \cdot kg^{-1}$ dose and because we have previously shown that selective activation of μOR G-protein signaling using Oliceridine/TRV130 did not decrease alcohol consumption (Gutridge et al., 2020).

Kratom based natural products, including paynantheine and speciociliatine examined here, have been predicted and shown to have activity at adrenergic 2A, 2B, and 2C receptors and serotonin 2A receptors (Boyer et al., 2008b; Ellis et al., 2020a; Foss et al., 2020; Obeng et al., 2020a; León et al., 2021). Since we did not screen the kratom analogs for activity at these or other receptors, it is probable that non-δOR activity contributes to the observed alcohol intake modulation, especially at higher doses. Though there is support for targeting adrenergic and serotonin receptors for treatment of alcohol abuse (Haass-Koffler et al., 2018; DiVito and Leger, 2020; Berquist and Fantegrossi, 2021; Sessa et al., 2021), our data in δOR KO animals shown here and in Gutridge et al. 2020 builds on our hypothesis of an ancillary, if not primary, role of δOR in decreasing alcohol consumption for kratom opioids and derivatives.

Relative to the GTPyS assay, the GloSensor assay of cAMP inhibition uses recombinant overexpressed cell systems and is amplified relative to measuring G-protein activity directly. As such, it is plausible that the partial agonism we detect for the kratom analogs in vitro does not resemble how they act in vivo. For example, at the δOR, mitragynine has partial agonism in the cAMP assay but acts as an antagonist in the GTPγS assay (Váradi et al., 2016; Gutridge et al., 2020). Therefore, it may be suggested that the kratom analogs are acting as functional δOR antagonists in vivo, competing with the fully efficacious activation of δORs by the endogenous Leu-enkephalin. However, our speciociliatine data counters this argument. At the δOR, speciociliatine binds with a pKi of 5.4 ± 0.1 which is in between the binding affinities of 7-hydroxyspeciogynine and 7-hydroxypaynantheine (6.3 ± 0.1 and 4.9 ± 0.2, respectively), yet speciociliatine acts as a δOR antagonist in the cAMP assay. When tested in mice, speciociliatine did cause a significant and sharp decrease in alcohol consumption at a relatively high 30 $mg \cdot kg^{-1}$ dose (Supp. Fig.4A-C in the online supplement, an average decrease of 2.5 ± 0.3 $g \cdot kg^{-1}$ ethanol or a 90 ± 3 % reduction, compared to a decrease of 1.2 ± 0.2 $g \cdot kg^{-1}$ ethanol (40 ± 7 %) for 10 $mg \cdot kg^{-1}$ 7-hydroxyspeciogynine, and 1.1 ± 0.3 $g \cdot kg^{-1}$ ethanol (40 ± 11 %) for 30 $mg \cdot kg^{-1}$ 7-hydroxypaynantheine), which indicates an off-target effect. In support of this explanation, a 30

mg·kg^{-1} dose of speciociliatine similarly decreases ethanol consumption in δOR KO mice and significantly impairs motor incoordination in wildtype and δOR KO mice, which likely contributes to the effects we see in the alcohol consumption paradigm. We did not test the kratom analogs or alkaloids in conjunction with δOR antagonists because the role of δOR antagonists in these behaviors is not well defined. For example, we have previously found that δOR-selective antagonist naltrindole does not decrease alcohol intake at a 10 mg·kg^{-1} dose in this alcohol model whereas another δOR-selective antagonist, naltriben, dose-dependently decreases alcohol consumption at 6 and 10 mg·kg^{-1} doses (van Rijn and Whistler, 2009). Although in rats, both naltrindole and naltriben decrease alcohol intake (Krishnan-Sarin et al., 1995a, 1995b). These discrepant responses may be explained by mediation of distinct δOR subtypes by these specific antagonists (Dietis et al., 2011; van Rijn et al., 2013). Therefore, evaluating alcohol consumption responses in δOR KO mice provides a more straightforward and unambiguous approach for determining broadly δOR-mediated responses for the purposes of the experiments completed here.

At the μOR, it has recently been demonstrated that a reduction in G-protein efficacy is responsible for lessened adverse side effect profiles, rather than a lack of β-arrestin recruitment (Gillis et al., 2020). In the GloSensor cAMP assay, 7-hydroxyspeciogynine and 7-hydroxypaynantheine act as partial agonists at δOR and in vivo they reduce alcohol use. This begs the question whether partial agonism rather than full agonism is driving the δOR mediated effects on alcohol intake. The δOR agonist TAN-67 efficaciously reduces alcohol use in the two-bottle choice paradigm, and is a full agonist in the cAMP assay (Chiang et al., 2016) and the [^{35}S]GTPγS assay (Quock et al., 1997). However, a more recent [^{35}S]GTPγS study has suggested TAN-67 may be a partial agonist (Stanczyk et al., 2019), and thus the answer for now is not clear as to whether partial agonism and/or weak β-arrestin recruitment drives reduced alcohol use by δOR agonists.

Given that agonist-bound structures of both the μOR and δOR are available (Huang et al., 2015; Claff et al., 2019), it may be possible to identify strategies by which to enhance 7-hydroxyspeciogynine affinity selectively at δOR and not μOR. Additionally, in vivo characterization of 7-hydroxyspeciogynine for pharmacokinetic parameters including half-life and metabolism (e.g. role of CYP3A4 and CYP2D6) will be insightful. Further behavioral analysis, including modulation of respiratory depression and anxiety-like behavior (van Rijn et al., 2010; Ko et al., 2021) would further establish 7-hydroxyspeciogynine's potential as clinical lead

compound. Similarly, assessing off-target effects in a panel screen could identify other targets, including serotonin receptors (León et al., 2021) that contribute to 7-hydroxyspeciogynine's modulation of alcohol-intake.

In summary, our current and past pharmacological characterization of kratom analogs suggest that alkaloids with sub-micromolar δOR potency, micromolar potency at the μOR, and G-protein bias provide the strongest opportunity to reduce alcohol use in mice with limited side effects. We discovered 7-hydroxyspeciogynine as a novel kratom derived analog that decreases alcohol intake by activating δORs in vitro and in vivo, but with limited μOR in vivo agonist activity, leading to a broadened therapeutic window as evident from a lack of rewarding, locomotive and seizurogenic effects and a MTD of at least 10 $mg \cdot kg^{-1}$. Our findings support the utility of targeting the δOR to reduce volitional alcohol consumption and further demonstrate the effectiveness of using the kratom alkaloids as lead-scaffolds for developing G-protein biased δOR agonists for treatment of AUD.

CHAPTER 4. ISOLATION AND PHARMACOLOGICAL CHARACTERIZATION OF SIX OPIOIDERGIC *PICRALIMA NITIDA* ALKALOIDS

This chapter was previously published in the American Chemical Society (ACS) Journal of Natural Products with the following DOI: 10.1021/acs.jnatprod.0c01036 and citation:
Creed, S.M., Gutridge, A.M., Argade, M.D., Hennessy, M.R., Friesen, J.B., Pauli, G.F., van Rijn, R.M. and Riley, A.P., 2020. Isolation and Pharmacological Characterization of Six Opioidergic Picralima nitida Alkaloids. *Journal of Natural Products*, *84*(1), pp.71-80.
Supplemental data including extensive statistical analyses and chemical characterization is freely available at the following location:
https://pubs.acs.org/doi/10.1021/acs.jnatprod.0c01036?goto=supporting-info

4.1 Introduction

For centuries, morphine and its semi-synthetic derivatives have been integral components of effective pain management (Jones et al., 2018). Opioid analgesics produce their powerful pain-killing effects through the activation of mu opioid receptors (μOR), one of three opioid receptor subtypes found throughout the central and peripheral nervous system (Hylands-White et al., 2017; Volkow and Blanco, 2021). Despite the effectiveness of opioid analgesics in acute and subacute settings, chronic pain remains an escalating and poorly managed health concern, affecting approximately 20% of adults worldwide (Goldberg and McGee, 2011; Ho and Nair, 2018). Over the past two decades, opioid prescriptions for the treatment of chronic pain have risen dramatically despite their reduced effectiveness against chronic pain states (Marshall et al., 2019; Volkow and Blanco, 2021). Unfortunately, the prolonged use of opioid analgesics elicits numerous adverse effects including respiratory depression, tolerance, and dependence (Hylands-White et al., 2017; Jones et al., 2018; Volkow and Blanco, 2021). Increased prescription and duration of use of short and long-acting/extended-release opioids, combined with the side effect profile of opioid medications, has led to the current opioid epidemic characterized by >40,000 opioid overdose deaths per year since 2016 (Wilson et al., 2020b). To counter this trend, in 2016 the Center for Disease Control and Prevention provided new guidelines for the use of opioids in patients suffering from chronic pain with a focus on reducing and replacing opioids when possible (Dowell et al., 2016). This abrupt change has been effective in decreasing opioid prescriptions, but may have come at the expense of patients that were benefitting from their current opioid therapy and are now

left undertreated (Bohnert et al., 2018; Gross and Gordon, 2019). It is within this setting that patients search for non-prescription alternatives such as *Mitragyna speciosa* (kratom) and *Picralima nitida* (akuamma) to self-medicate their pain and opioid withdrawal symptoms (Boyer et al., 2008a; Toce et al., 2018).

Historically, natural products have served as an excellent source of novel scaffolds to initiate drug discovery efforts (Newman and Cragg, 2020). This is particularly true in the arena of pain and other disorders of the nervous system. Beyond the aforementioned analgesics derived from morphine, naturally occurring salicylic acid, capsaicin, and tetrahydrocannabinol have all been exploited for their pain killing effects (Turk et al., 2011; Gouveia et al., 2019). For centuries, the akuamma tree has been used by natives of Western Africa to treat a variety of ailments including malaria, dysmenorrhea, and gastrointestinal disorders (Erharuyi et al., 2014). The seeds in particular have been used for their analgesic and antipyretic properties (Erharuyi et al., 2014). Notably, anecdotal reports indicate that, unlike traditional opioid analgesics, akuamma does not elicit euphoria, tolerance, or dependence. The analgesic effects of *P. nitida* seeds have been generally attributed to a class of indole alkaloids known as the akuamma alkaloids composed of akuammine (**1**), akuammidine (**2**), pseudo-akuammigine (**3**), akuammicine (**4**), akuammiline **(5)**, and picraline (**6**) (**Figure 4.1**) (Menzies et al., 1998). In standard nociception assays, both the ethanolic extract of *P. nitida* and isolated **3** demonstrated antinociceptive properties. While their potency is lower than morphine, the effects of **3** in these assays appeared to be longer lasting (Duwiejua et al., 2002; Dapaah et al., 2016).

Previous investigations indicated the antinociceptive effects of the akuamma alkaloids are produced through their interaction with the opioid receptors (Menzies et al., 1998; Erharuyi et al., 2014). However, the scope of these studies was limited to the opioid receptors, excluded other nervous system receptors, and the rigor of those findings is linked to the suboptimal tools available at the time to study the pharmacology of the akuamma alkaloids. Moreover, several alkaloids found in relatively high abundance in *P. nitida* have remained uninvestigated. Nevertheless, the structural differences between the akuamma alkaloids and traditional opioid analgesics, paired with the reported mild side effect profile, suggests these alkaloids may exhibit unique signaling properties at the opioid receptors, and, therefore, may be promising starting points for the development of new pain management drugs. Thus, to provide additional insight into the effects of akuamma, studies were initiated to identify an effective preparative purification strategy that

permits the resolution of the six main alkaloids found within akuamma seeds to provide a more thorough investigation of their pharmacological activity in vitro and in vivo.

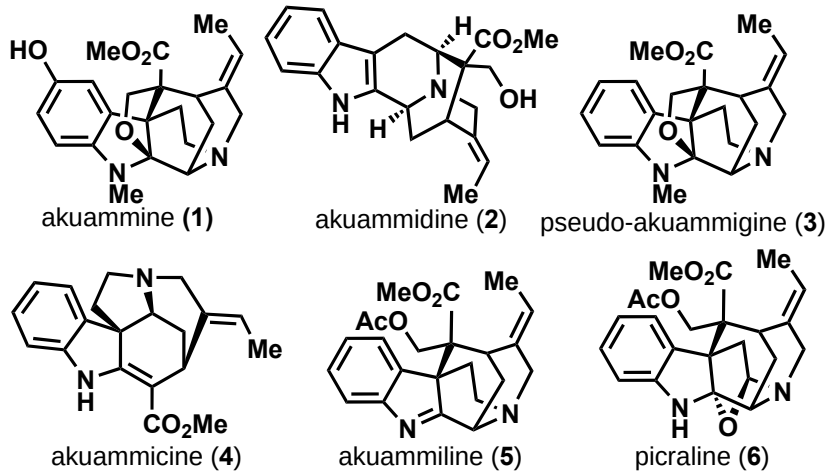

Figure 4.1 Structures of akuamma alkaloids.

Indole alkaloid structures of akuammine (1), akuammidine (2), pseudo-akuammigine (3), akuammicine (4), akuammiline (5), and picraline (6) isolated from *Picralima nitida*.

4.2 Methods

4.2.1 General Experimental Procedures

All solvents and reagents were purchased from commercial sources and used directly without further purification. Akuamma seed powder was purchased from Relax Remedy. ^{1}H and ^{13}C NMR spectra were recorded on Bruker 400 MHz spectrometer and referenced to the residual solvent peaks ($CHCl_3$: ^{1}H δ=7.26, ^{13}C δ=77.16 ppm; D_2HCOD: ^{1}H δ= 3.31, ^{13}C δ=49.00 ppm) High-resolution mass spectra were obtained on a Shimadzu LCMS-IT-TOF and observed values are within 5 ppm of calculated exact masses of the indicated ions. High-performance liquid chromatography was conducted on an Agilent 1260 Infinity II fitted with a DAD detector and a Phenomenex Luna Omega PS-C18 column (100 x 4.6 mm). A gradient of acetonitrile/water (20-45%) each containing 0.1% formic acid with a flow rate of 1 ml/min was used. The purity of all compounds was determined to be >95% as determined by HPLC.

4.2.2 Drugs

Leu-enkephalin, forskolin, and morphine sulfate pentahydrate were purchased from Sigma Aldrich (St. Louis, MO, USA). (2S)-2-[[2-[[(2R) -2- [[(2S)-2-Amino-3- (4-hydroxyphenyl) propanoyl] amino] propanoyl] amino] acetyl] -methylamino] -N- (2-hydroxyethyl) -3-phenylpropanamide (DAMGO), and 2-(3,4-dichlorophenyl)-N-methyl-N-[(1R,2R)-2-pyrrolidin-1-ylcyclohexyl] acetamide (U50,488) were purchased from Tocris Bioscience (Bio-techne Corporation, Minneapolis, MN, USA). [^{3}H]DAMGO (49.2 Ci/mmole, lot#2573313), [^{3}H]U69,593 (60 Ci/mmole, lot#2367921), and [^{3}H]DPDPE (53.7 Ci/mmole, lot#2376538) were purchased from Perkin Elmer (Waltham, MA, USA).

4.2.3 Preparation of Dichloromethane Fraction, Akuammine (1), and Akuammidine (2)

Akuamma seed powder (250 g) was allowed to stir for two hours in methanolic hydrochloride solution (400 mL). Subsequently, the seed powder was filtered, and the filtrate was evaporated to dryness under reduced pressure. The resulting extract was dissolved in aqueous hydrochloric acid (400 mL, 2N), washed with hexanes (3x400 mL), and extracted with dichloromethane (3x400 mL). The combined dichloromethane layers were evaporated to dryness under vacuum to provide the crude dichloromethane fraction (3.356 g). The aqueous layer was brought to pH=12 with 28% ammonium hydroxide, washed with hexanes (1x400 mL), and extracted with ethyl ether (3x400 mL). The combined ethereal layers were dried over magnesium sulfate and concentrated under vacuum to provide a mixture of **1** and **2**. This mixture was treated with cold acetone to precipitate **1** as a white solid (472 mg). The acetone filtrate was concentrated under vacuum and the resulting residue recrystallized in dichloromethane to yield crystalline **2** (15.0 mg).

4.2.4 pH-Zone Refining Countercurrent Chromatography of the Dichloromethane Fraction

The pH-Zone Refining Countercurrent Chromatography was performed on a SCPC-250 (Gilson Incorporated, Middleton, WI USA) chromatograph equipped with a 266 mL rotor. The rotation speed could be adjusted from 500 to 3000 rpm. Samples were injected through a 20 mL sample loop. The detection was performed by a UV-Vis DAD detector. Fractions were collected

with a Gilson-Armen Fraction Collector LS-5600. Chromatographic data were acquired by using the Gilson-Armen Glider CPC Control Software V2.9.2.9 and then transferred to an Excel worksheet for further processing.

The optimal solvent system was determined by evaluation of the acid and base partition coefficients of the alkaloids of interest using guidelines described by Ito (Ito, 2005). Five different solvent system formulations were tested, with triethylamine (TEA) and hydrochloric acid (HCl) added to the upper (organic) and lower (aqueous) phases, respectively. Partition coefficients were determined by comparing the area under the curve for the HPLC peaks produced by akuammicine, akuammiline, pseudo-akuammigine, and picraline (**Table 4.1**).

The pH-zone-refining countercurrent chromatography separation was prepared by thoroughly mixing equal volumes of ethyl acetate and water in a 2 L separatory funnel and allowing the layers to separate. The ethyl acetate layer was basified with TEA to a final concentration of 10 mM to be used as the upper phase. The aqueous lower phase was adjusted to a final concentration of 8 mM with hydrochloric acid. The dichloromethane extract (1.2 g) was dissolved in 10 mL of upper phase with less than 1 mL of the lower phase to aid solubility and loaded into a 20 mL sample loop. An additional 5 mL of upper phase was used to rinse the sample vial and added to the sample loop. The instrument column was filled with the lower phase at a rotation speed of 500 rpm. The rotation speed was increased to 3000 rpm and the sample was introduced into the column. The basified upper layer was pumped through the coil at a flow rate of 10 mL/min with elution in ascending mode. Elution was monitored at 254 nm, 284 nm and 330 nm. Fractions were collected in 7.5 mL quantities. After elution, the pH of each fraction was measured using a benchtop pH meter (Mettler Toledo) and fraction contents were evaluated using TLC. All fractions were dried with sodium sulfate, concentrated under vacuum, and analyzed by ^{1}H NMR. Fractions containing purified, individual alkaloids were combined separately to provide **3** (130 mg) and **4** (145 mg). Fractions containing a mixture of **5** and **6** were combined and further purified by silica gel flash column chromatography eluting with 0-2% MeOH/$CHCl_3$ containing 1% TEA to yield pure samples of **5** (61 mg) and **6** (90 mg).

Table 4.1 Partition Coefficients of Akuamma Alkaloids in CCS Solvent Systems. [a]

Solvent System		Pseudo-akuammigine (3)	Akuammicine (4)	Akuammiline (5)	Picraline (6)
1:1:1:1 Hex/EtOAc/ MeOH/H_2O	K_{acid}	<<0.01	<<0.01	<<0.01	<<0.01
	K_{base}	2.71	1.63	0.23	0.82
3:7:3:7 Hex/EtOAc/ MeOH/H_2O	K_{acid}	<<0.01	<<0.01	<<0.01	0.01
	K_{base}	32.3	28.9	2.53	7.29
1:1 EtOAc/H_2O	K_{acid}	0.10	0.02	0.03	0.03
	K_{base}	51.9	222	28.2	16.09
2:2:3 MTBE/CH_3CN/ H_2O	K_{acid}	2.22	0.61	0.27	0.56
	K_{base}	87.0	27.7	5.61	11.4
3:1.5:4 MTBE/CH_3CN/ H_2O	K_{acid}	0.25	0.14	0.05	0.10
	K_{base}	30.9	64.1	6.82	17.4

[a]The K_{acid} and K_{base} for each akuamma alkaloid were calculated by taking $AUC_{upper\ phase}/AUC_{lower\ phase}$ as observed by HPLC for respective pH conditions.

4.2.5 Primary and Secondary Receptor Screening

Compounds **1** and **3-6**, but unfortunately not **2**, were submitted to the Psychoactive Drug Screening Program (UNC-Chapel Hill) as dry powders to be evaluated using standard protocols. Primary screening was conducted at 10 μM (DMSO) against the "Comprehensive Screen" panel consisting of 37 different GPCR, ion channel, and transporter targets. Assays producing >50% inhibition of radioligand binding were further investigated in secondary binding assays using a 12-point concentration-response curve to determine binding affinity (*K*i).

4.2.6 Cell Culture

HEK293 cells (RRID:CVCL_0045, Life Technologies, Grand Island, NY, USA) were maintained in DMEM supplemented 10% FBS. CHO-K1-human δ opioid receptor (δOR PathHunter β-arrestin 2 cells and CHO-K1-human μ opioid receptor (μOR) PathHunter β-arrestin 2 cells stably expressing the δOR or μOR and β-arrestin 2 (RRID:CVCL_KY70, RRID:CVCL_KY68, DiscoverX, Fremont, CA, USA) were maintained in F12 media supplemented with 10% FBS and containing 800 μg/mL geneticin and 300 μg/mL hygromycin.

U2OS-human κ opioid receptor (κOR) PathHunter β-arrestin 2 cells stably expressing the κOR and β-arrestin 2 (RRID:CVCL_LA97, DiscoverX, Fremont, CA, USA) were maintained in McCoy's 5A media supplemented with 10% FBS and containing 500 µg/mL geneticin and 250 µg/mL hygromycin. All cell lines were maintained in T75 flasks under sterile conditions and kept at 37 °C and 5% CO_2. During passaging, cells were dislodged from the flask following a 3-minute incubation with 0.25% trypsin, and sub cultivated at ratios of 1:10 (HEK293), 1:5 (CHO) and 3:10 (U2OS).

4.2.7 Competitive Radioligand Binding Assay

Binding assays were performed on membranes isolated from CHO cells stably expressing the δOR or µOR and from U2OS cells stably expressing the κOR (DiscoverX) as previously described using tritiated radioligands ([^{3}H]DAMGO, [^{3}H]U69,593, [^{3}H]DPDPE for µOR, κOR, δOR, respectively) (Cassell et al., 2019).

4.2.8 GloSensor cAMP Inhibition Assay

cAMP inhibition assays were performed as previously described in HEK293 cells transiently transfected with pGloSensor22F-cAMP (Promega, Madison, WI, USA) and either FLAG-mouse δOR, HA-mouse µOR, or FLAG-mouse κOR (Chiang et al., 2016).

4.2.9 PathHunter β-arrestin2 Recruitment Assay

β-arrestin recruitment assays were performed as previously described using CHO or U2OS cells (CHO-K1-human δOR, CHO-K1-human µOR, or U2OS-human κOR PathHunter β-arrestin 2 cells, DiscoverX) (Chiang et al., 2016).

4.2.10 Animals

Wildtype C57Bl/6N mice (24 male, 24 female; 7-8-weeks old) were purchased from Envigo (Indianapolis, IN) and were acclimated to the facility and to handling for 1 week prior to any experimental procedures. See Supporting Information for details on subject groups for drug testing (Table S14, Supporting Information). All mice were housed on a 12-hour light (21:30-

9:30)/12-hour dark cycle under controlled temperature (21-23 °C) with ad libitum food access. All experiments were conducted between 10:30-15:00 in a well-lit room. At a minimum, mice were given 2 days between experiments to recover from thermal stimuli. All experimental procedures were approved by the Purdue Animal Care and Use Committee of Purdue University under protocol #1605001408.

4.2.11 Tail Flick Thermal Nociception Assay

Antinociception was measured as previously described (van Rijn et al., 2012b). On the first day of the experiment, mice were habituated to handling restraint; a black washcloth was used to restrain the mice during the experimentation. On the following days of drug testing, a radiant heat tail-flick apparatus (Columbus Instruments, Columbus, OH, USA) was set to a beam intensity of 7-9 as this intensity yielded reproducible responses between 2-3 seconds. On each test day, a baseline tail flick response was first obtained for each mouse. The cutoff time for testing was calculated as 3 times this baseline response time. A saline injection was then administered (s.c. or p.o.) and after 30 minutes, tail flick responses were collected again. Drugs were then administered (s.c. or p.o.), and tail flick responses were collected at various time points following administration. All measurements were collected in duplicate by testing two different regions on the mouse's tail.

4.2.12 Hot Plate Thermal Nociception Assay

On the first day of the experiment, mice were habituated to the hotplate apparatus (Columbus Instruments, Columbus, OH, USA) for 1-2 minutes (while the hotplate was turned off). On the following days of testing, the hot plate was maintained at a temperature of 55 ± 0.5 °C. On each test day, a single baseline time for latency to demonstrate nociceptive behavior was first obtained for each mouse. Behavior considered a positive nociceptive response was fore or hind paw licking, jumping, or non-explorative rearing. Upon demonstrating this behavior, the mouse was immediately removed from the apparatus. The cutoff time for testing was calculated as 3 times the baseline response time. A saline injection was then administered (s.c. or p.o.) and after 30 minutes, hot plate latency responses were collected again. Drugs were then administered (s.c. or p.o.), and hot plate latency responses were collected following administration at various time points. All measurements were collected only once to avoid damage to paws.

4.2.13 Statistics

All data were analyzed using GraphPad 8 (GraphPad Prism software, La Jolla, CA) and is presented as means ± SEM. For in vitro findings, composite figures consisted of one curve averaged from three, independent assays. In these independent assays, PathHunter β-arrestin recruitment and radioligand binding assays were run in duplicate, and GloSensor cAMP assays were run in triplicate. Data from each independent signaling assay was normalized to a positive control before being averaged and added to the composite figure. For nociception assays, significance was calculated via one-way, repeated measures ANOVA with Sidak's multiple comparison's test to compare saline treatment with drug treatment at multiple time points. For any nociception assays where only one time point was tested, a paired t-test was used to assess significance between saline and drug treatment. Nociception data is represented as percent maximal possible effect (%MPE) (calculated as % MPE= (treatment response time – baseline response time)/(cutoff time – baseline response time) * 100) and is normalized (drug treatment %MPE – saline treatment %MPE). Statistical measures and values for all nociception assays are summarized in Tables S15-17 in the online supplement.

4.3 Results and Discussion

4.3.1 Extraction and Isolation of Akuamma Alkaloids

To initiate studies of the akuamma alkaloids, an isolation process capable of providing six alkaloids in high purity and quantities sufficient for in vitro and in vivo studies was needed. Initial efforts revealed **1** and **2** could be easily isolated in >95% purity through liquid-liquid extraction and selective crystallization. However, isolation of the other major alkaloids in this manner proved difficult due to their similar solubilities in organic solvents and their general tendency to form critical pairs, particularly at the preparative scale. Previous studies have employed combinations of normal-phase column chromatography, preparative TLC, high performance liquid chromatography (HPLC) and recrystallization to purify alkaloids present in *P. nitida* extracts (Møller et al., 1972; Ama-Asamoah et al., 1990; Menzies et al., 1998; Tane et al., 2002). In our hands, normal phase chromatography resulted in poor separations of the alkaloids due to their remarkably similar polarities. Furthermore, irreversible adsorption of the alkaloids to the stationary phase severely decreased yields and was particularly problematic for compounds present in minor

quantities (Okunji et al., 2005). Although semi-preparative reversed-phase HPLC proved to be more effective in terms of compound resolution, severe limitation remained in overall efficiency in terms of time and resources for generating the quantities required for our studies.

The shortcomings of standard chromatography techniques led to the investigation of countercurrent separation (CCS) to purify the *P. nitida* alkaloids. By eliminating the use of a solid stationary phase in favor of a continuous flow liquid-liquid partitioning system, both major forms of CCS, high speed countercurrent chromatography (HSCCC) and centrifugal partition chromatography (CPC), avoid the irreversible adsorption of compounds observed in solid phase-based liquid chromatography and allow for quantitative sample recovery (Ito and Ma, 1996; Ito, 2005, 2013). Specifically, pH-zone-refining countercurrent chromatography (pHZR-CCC), which exploits the acid-base interactions of the two immiscible phases, is perfectly matched for the separation of basic alkaloids (Ito and Ma, 1996; Ito, 2005, 2013; Fang et al., 2013; Maurya et al., 2013; Kotland et al., 2016; Zhou et al., 2019). The method provides the benefit of a high loading capacity and produces highly concentrated fractions with minimal compound overlap (Ito and Ma, 1996; Ito, 2005, 2013). Okunji et. al. have applied pHZR-CCC to the fruit rind of *P. nitida*, thus it stood to reason that their method could be adapted to isolate alkaloids found in the ground seeds (Okunji et al., 2005).

As with any liquid chromatography method, the selection of a suitable solvent system is critical to the outcome of the isolation. Solvent systems for pHZR-CCC require two immiscible solvents and typically incorporate the addition of co-solvents to modulate the partition coefficients of the compounds of interest. To select an applicable solvent system, a straightforward partitioning experiment originally developed by Ito was employed (Ito, 2005). Five solvent systems comprised of 2-4 solvents, were modified with the addition of either acid (10 mM HCl) or base (10 mM TEA) and the partition coefficients of **3**-**6** were determined via HPLC to give K_{acid} and K_{base}, respectively (Table 4.1). Suitable *K* values for basic compounds such as the akuamma alkaloids should fit within the parameters $K_{acid} << 1$ and $K_{base} >> 1$.

Generally, pHZR-CCC has relied heavily on hexane-ethyl acetate-methanol-water (HEMWat) and methyl *tert*-butyl ether (MTBE)-acetonitrile-water solvent systems. In particular, these solvent systems have been successfully employed in the separation of several classes of structurally similar indole alkaloids (Okunji et al., 2005; Fang et al., 2013; Maurya et al., 2013; Kotland et al., 2016; Zhou et al., 2019). Initial investigation revealed that the less polar HEMWat

systems were incompatible with the akuamma alkaloids due to the strong retention of compounds in the acidic aqueous phase and unexceptional base partition values for **5** and **6**. Turning to the 2:2:3 MTBE/CH_3CN/H_2O system previously employed by Okunji, K_{acid}>1 was observed for **3** (Okunji et al., 2005). Further alterations to the solvent composition and rations revealed 1:1 EtOAc/H_2O and 3:1.5:4 MTBE/CH_3CN/H_2O systems both proved to be viable solvent systems providing K_{acid} << 1 and K_{base}>> 1 for **3-6**. Of these two, the 1:1 EtOAc/H_2O system was selected as the most appropriate solvent for pHZR-CCC based on the lower acid partition coefficient values and more consistent base partition coefficient values displayed, in addition to exhibiting a larger difference between the K_{acid} and K_{base} of the four alkaloids.

Having identified a promising solvent system, separation of the dichloromethane fraction with pHZR-CCC was first attempted in descending mode using an acidic aqueous mobile phase. Using this method, **4** was first to elute, followed by **3** and subsequently mixed fractions of **5** and **6**. As expected, when performing the run in ascending mode with the basic organic layer as the mobile phase, the order of elution was observed to be the exact opposite of the descending method. Reversing the elution mode facilitated concentration of the fractions due to the use of lower boiling point organic solvent and allowed the alkaloids of interest to elute much earlier in the run.

A plot of the pH values for each fraction produced a series of alternating zones of increasing pH and plateaus which is characteristic of the pHZR-CCC. When overlaid onto the UV-Vis chromatograms, the elution of major alkaloids was observed to coincide with a plateau on the pH curve, presumably at the points where the pH is roughly equal to their isoelectric point (**Figure 4.2).** While initially fractions were collected in 15 mL volumes, reduction of the volume to 7.5 mL led to significant increases in alkaloid purity. From a 1.2 g sample of the dichloromethane fraction, this process directly provided 130 mg of **3** and 145 mg of **4** in high purity. Despite significant attempts to optimize the solvent system and pHZR-CCC conditions, **5** and **6** consistently co-eluted as ~1:1 mixture. Fortunately, this mixture could be easily separated on silica gel via flash chromatography to provide 61 mg of **5** and 90 mg of **6**. Notably, attempts to directly purify the dichloromethane fraction via flash chromatography were unsuccessful due to considerable co-elution of multiple alkaloids, thus highlighting the necessity to first simplify the fraction via pHZR-CCC.

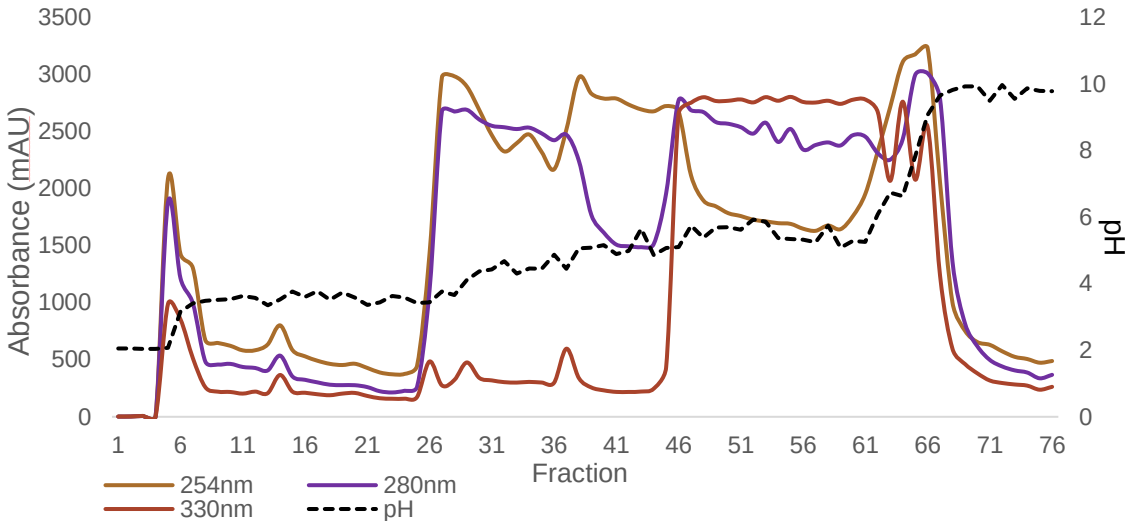

Figure 4.2 pH-zone-refining countercurrent chromatography chromatogram of akuamma alkaloid DCM extract.

Elution of the alkaloids akuammiline (5) and picraline (6) occurred between high pH 3 to low-mid pH 4 range. Elution of pseudo-akuammigine (**3**) occurred between mid pH 4 to low pH 5. Elution of akuammicine (**4**) occurred between low to high pH 5.

Once isolated, the purified alkaloids **1-6** were identified by comparison of the ^{1}H and ^{13}C NMR spectra to literature values (Tables S1-12**,** in the online supplement) (Yamauchi et al., 1990; Jokela and Lounasmaa, 1996; Benayad et al., 2016). In particular, the comparison of the ^{13}C NMR chemical shifts to literature values revealed an average absolute difference of 0.24 ppm, with major differences arising from subtle solvent-dependent changes in chemical shifts. In addition to this agreement with literature values, the spectral data are consistent with previously reported structures.

4.3.2 Identification of Major Drug Targets Through the Psychoactive Drug Screening Program (PDSP).

With the akuamma alkaloids in hand, five of the isolated alkaloids were evaluated via the Psychoactive Drug Screening Program (PDSP) to determine possible receptor targets for their purported biological effects. Alkaloids **1** and **3-6** were first assessed at a single concentration (10 µM) for their ability to displace radiolabeled ligands from a diverse panel of human G-protein coupled receptors, ion channels, and transporters. In this primary screen, all five akuamma alkaloids inhibited [^{3}H]-SCH-23390 from the dopaminergic D_5 receptor and [^{3}H]-U69,593 from

the κOR (**Figure 4.3**). **1**, **3**, and **4** also displaced [^{3}H]-DAMGO from the μOR, whereas **5** and **6** produced significantly less displacement in these assays. All five of the tested alkaloids produced minimal inhibition of [^{3}H]-DADLE binding at the δOR. Although additional displacement was noted for several of the serotonergic and the histaminergic H_3 receptors these were generally low levels of inhibition (<60%). In contrast to **1**, **3**, **5**, and **6**, which appear to be moderately selective for the opioid and D_5 receptors, the primary binding data indicate **4** is considerably more promiscuous.

To validate these potential receptor targets, secondary binding experiments were carried out by the PDSP to determine binding affinities (K_i) for each receptor-ligand pair demonstrating >50% inhibition in the primary screen. Notably, all five alkaloids possess a K_i >10 μM at the D_5, indicating a false positive in the primary screen data (Table S13, in the online supplement). Conversely, **1** and **3** possess considerable affinity at the μOR (K_i = 0.76 μM and 1.0 μM, respectively) while **4** and **5** bind with sub-micromolar affinity to the κOR (K_i = 0.17 μM and 0.40 μM, respectively). These data generated from the cloned human opioid receptors are in good agreement with those reported by Menzies et. al. using guinea pig brain homogenates (Menzies et al., 1998). Furthermore, the data strongly support the hypothesis that any observed biological effects of akuamma likely occur through interactions with the opioid receptors.

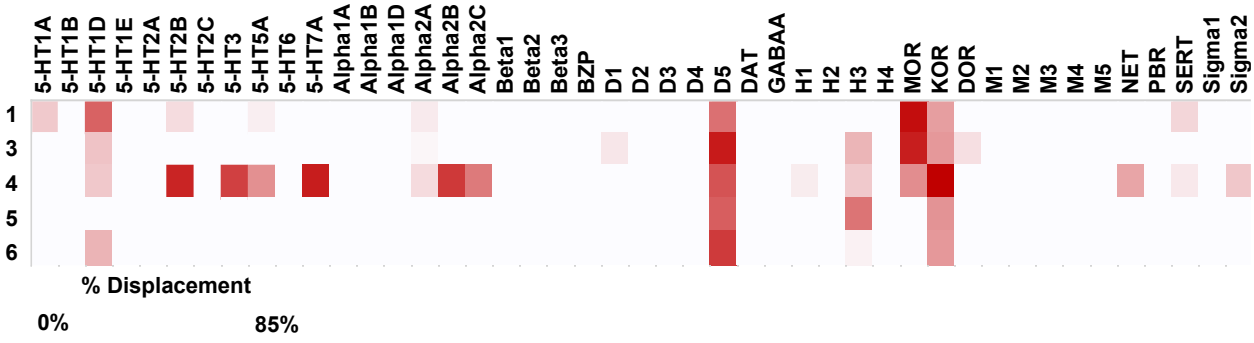

Figure 4.3 Receptor binding profiles of akuamma alkaloids.

The akuamma alkaloids akuammine (**1**), pseudo-akuammigine (**3**), akuammicine (**4**), akuammiline (**5**), and picraline (**6**) were assessed at 10 μM for their ability to displace radiolabeled ligands from membranes expressing individual receptors. The heatmap represents mean displacement of radioligand from four replicates.

4.3.3 Characterization of in vitro Pharmacology of Akuamma Alkaloids.

Having established that the alkaloids target opioids receptors, the affinity and potency of akuamma alkaloids for binding, activation of G-protein and β-arrestin 2 recruitment at the μOR, κOR, and δOR were assessed in cellular assays. In general, the alkaloids had higher affinity and activity at the μOR and κOR, relative to δOR (**Figure 4.4A-I**), confirming the results from the PDSP. For all cellular characterization assays, the alkaloids had weaker affinity, potency and efficacy when compared to reference ligands DAMGO, U50,488, and leu-enkephalin (**Figure 4.4A-I**). More specifically, at the μOR, **1-3** had the highest binding affinities with K_is of 0.30, 0.32 and 0.59 μM, respectively (**Figure 4.4A, Table 4.2**). The binding affinity for these compounds was reflected in their increased potency and efficacy in the cAMP inhibition assay at the μOR, relative to the other alkaloids, with **1** and **2** producing IC_{50}s of 2.6 and 3.14 μM (**Figure 4.4D**, **Table 4.2**). Compounds **4**-**6** exhibited minimal cAMP inhibition at μOR, which is reflective of their relatively lower binding affinity at the receptor (**Figure 4.4A,D**). The alkaloids had non-determinable β-arrestin 2 recruitment at the μOR, but **2** did show minimal recruitment at the highest concentration tested (**Figure 4.4G**). At the κOR, **4** had the highest binding affinity with a K_i of 89 nM, which mirrors its potency in the cAMP assay with an IC_{50} of 240 nM (Figure 3B, 3E, Table 2). Compounds **1**, **3**, **5** and **6** all had similar binding affinities at the κOR, while **2** had the least affinity (**Figure 4.4B, Table 4.2**). Notably, **1** did not inhibit cAMP production, suggesting it possesses antagonistic or inverse agonistic properties at the κOR. Within the tested dose-range, the alkaloids minimally recruited β-arrestin at the κOR but followed the general trend that β-arrestin 2 recruitment was most apparent in alkaloids that display the strongest binding affinity (**Figure 4.4H, Table 4.2**). Compared to the μOR and the κOR, binding affinity, as well as potency and efficacy of the compounds in the cAMP inhibition assay, was lower at the δOR (**Figure 4.4C,F, Table 4.2**). Similar to the other receptors, there was non-determinable β-arrestin recruitment by the alkaloids at the δOR, although **2** did show minimal recruitment at the highest concentration tested (**Figure 4.4I**).

The comparable binding results reported in Menzies et al., in the PDSP screen shown in Figure 2, and in the radioligand binding assays shown in Figure 4.4A-C confirm that the akuamma alkaloids interact with opioid receptors (Menzies et al., 1998). The results from the in vitro signaling assays in Figure 4.4D-I further demonstrate that the alkaloids not only bind to opioid receptors but can elicit intracellular, inhibitory G-protein activity. Furthermore, at the highest

concentrations tested the alkaloids induced β-arrestin 2 recruitment, although the potency for the akuamma alkaloids in the β-arrestin 2 recruitment assay was too weak to calculate bias factors. Inspection of the functional responses at κOR suggests that the efficacy of β-arrestin 2 recruitment correlates with the potency for G-protein mediated cAMP inhibition; **4** is the most efficacious recruiter, while **2** is the weakest. Based on their inherent opioid activity, moving forward, more potent and selective opioids may be discovered using the akuamma alkaloids as a scaffold for drug design.

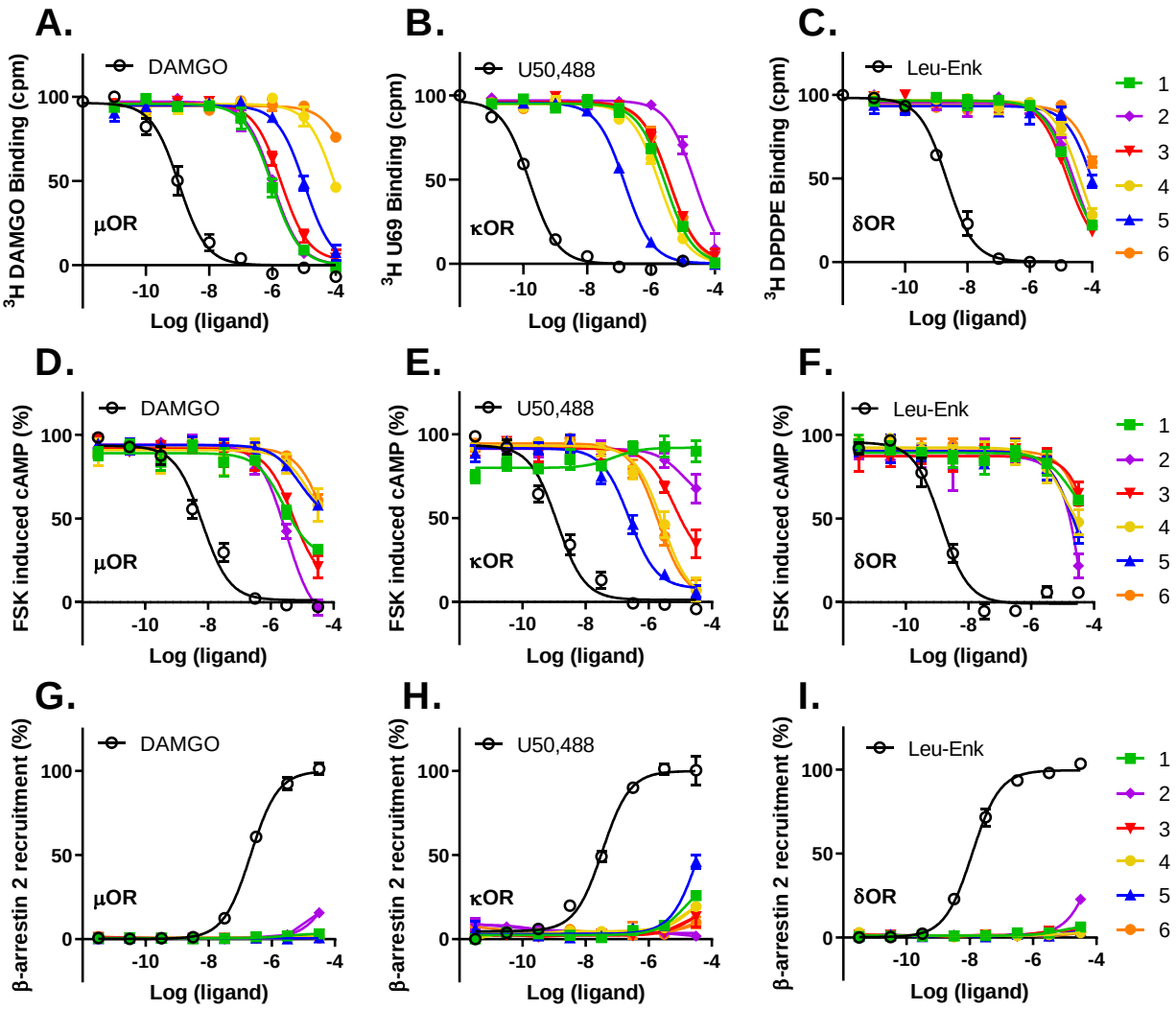

Figure 4.4 Pharmacological characterization of akuamma alkaloids at μOR, κOR, and δORs**.**

The akuamma alkaloids akuammine (**1, AK**), akuammidine (**2, AKD**), pseudo-akuammigine (**3, AKG**), akuammicine (**4, AKC**), akuammiline (**5, AKL**), and picraline (**6, PIC**) were characterized for binding affinity using [^{3}H]DAMGO, [^{3}H]U69,593 and [^{3}H]DPDPE (**A, B, C**), inhibition of forskolin-induced cAMP in a Glo-sensor assay in transfected HEK-293 cells (**D, E, F)** and the ability of the alkaloids to recruit β-arrestin 2 in a PathHunter assay. (**G, H, I**) at μOR (**A, D, G**), κOR (**B, E, H**), and δOR (**C, F, I**). All curves are representative of the averaged values from a minimum of 3 independent assays.

Table 4.2 Summary of Akuamma Alkaloids In Vitro Characterization at Opioid Receptors.

Affinity (pKi, drug concentration at which 50% of receptors is occupied), cAMP inhibition potencies ($pIC_{50,}$ drug concentration at 50% maximal efficacy) and efficacies (α, % inhibition at maximal efficacy normalized to DAMGO [μOR], leu-enkephalin [δOR] or U50,488 [κOR]) for OR agonists to inhibit cAMP production are indicated ± SEM. β-arrestin 2 recruitment potencies (pEC_{50}) and efficacies (α, normalized to DAMGO, leu-enkephalin or U50,488) of OR agonists to recruit β-arrestin 2 are indicated ±SEM. The number of repetitions for each drug is indicated in parentheses. ND = not detectable.

Compounds	**Binding**		**cAMP**			**β-arrestin 2**	
μOR	**pK_i**	**K_i (μM)**	**pIC_{50}**	**IC_{50} (μM)**	**α**	**pEC_{50}**	**α**
DAMGO	9.5 ± 0.1 (1)	0.00035	8.2 ± 0.1 (4)	0.0066	100	6.7 ± 0.1 (3)	100
1, AK	6.5 ± 0.1 (3)	0.30	5.6 ± 0.2 (4)	2.60	62 ± 6	ND (3)	ND
2, AKD	6.5 ± 0.1 (3)	0.32	5.5 ± 0.1 (3)	3.14	94 ± 6	ND (3)	ND
3, AKG	6.2 ± 0.1 (3)	0.59	5.3 ± 0.1 (4)	5.24	82 ± 7	ND (3)	ND
4, AKC	5.5 ± 0.1 (3)	3.31	5.1 ± 0.2 (3)	8.24	45 ± 7	ND (3)	ND
5, AKL	4.5 ± 0.1 (3)	30.7	4.7 ± 0.8 (3)	18.7	50 ± 40	ND (3)	ND
6, PIC	ND (3)	132	ND (3)	45.0	ND	ND (3)	ND
κOR	**pK_i**	**K_i (μM)**	**pIC_{50}**	**IC_{50} (μM)**	**α**	**pEC_{50}**	**α**
U50,488	10.0 ± 0.1(1)	0.000094	8.9 ± 0.1 (6)	0.0015	100	7.5 ± 0.1 (3)	100
1, AK	5.8 ± 0.1 (3)	1.68	ND (4)	0.073	ND	ND (3)	35 ± 6
2, AKD	4.8 ± 0.1 (3)	14.2	ND (5)	ND	ND	ND (3)	ND
3, AKG	5.6 ± 0.1 (3)	2.25	5.2 ± 0.2 (6)	6.46	69 ± 8	ND (3)	20 ± 20
4, AKC	7.1 ± 0.1 (3)	0.089	6.6 ± 0.1 (4)	0.24	84 ± 4	4.4 ± 0.4 (3)	50 ± 10
5, AKL	6.0 ± 0.1 (3)	1.11	5.6 ± 0.1 (4)	2.71	92 ± 6	ND (3)	30 ± 12
6, PIC	5.6 ± 0.1 (3)	2.38	5.7 ± 0.1 (4)	1.97	92 ± 5	ND (3)	ND
δOR	**pK_i**	**K_i (μM)**	**pIC_{50}**	**IC_{50} (μM)**	**α**	**pEC_{50}**	**α**
Leu-Enk	8.9 ± 0.1 (1)	0.0012	8.9 ± 0.1 (4)	0.0014	100	7.9 ± 0.1 (3)	100
1, AK	5.0 ± 0.1 (3)	10.4	4.7 ± 0.8 (3)	20.3	50 ± 35	ND (3)	ND
2, AKD	4.8 ± 0.1 (3)	15.0	4.8 ± 0.4 (3)	15.4	90 ± 30	ND (3)	ND
3, AKG	5.1 ± 0.1 (3)	8.37	ND (3)	95.6	ND	ND (3)	ND
4, AKC	4.6 ± 0.1 (3)	23.2	4.9 ± 0.4 (3)	12.4	60 ± 20	ND (3)	ND
5, AKL	4.2 ± 0.6 (3)	60.3	4.6 ± 0.5 (3)	24.4	90 ± 50	ND (3)	ND
6, PIC	4.0 ± 0.9 (3)	98.8	ND (3)	ND	ND	ND (3)	ND

4.3.4 In vivo Characterization of Antinociceptive Effects of Akuamma Alkaloids.

Given the ability of the akuamma alkaloids to bind to and activate the μOR, we hypothesized that the reported analgesic efficacy of the akuamma plant may be primarily exerted by these μOR-activating akuamma alkaloids. As **3** has previously been demonstrated to be antinociceptive in Wistar rats when administered *per os* (p.o.; 5 mg/kg), experiments were conducted to reproduce these findings in mice (Table S14, in the online supplement) (Duwiejua et al., 2002). Compound **3** did not produce antinociception in mice at 5 mg/kg dose (p.o.) in the tail flick and hot plate assays of thermal nociception at any of the timepoints tested (**Figure 4.5A,B**). In this experiment, subcutaneously (s.c.) administered morphine (6 mg/kg) served as a positive control and produced significant antinociception at the 30 min timepoint. However, when 5 mg/kg **3** was administered subcutaneously, minimal yet statistically significant antinociception was measured at 30 minutes in both nociception assays, as well as at 60 minutes in the tail-flick assay (**Figure 4.5C,D**, Table S15**,** in the online supplement). Notably, a 10 mg/kg dose of **3** (s.c.) also failed to produce antinociception at 30 minutes (**Figure 4.5C, D**).

Because **1** and **2** had slightly higher potencies than **3** at the μOR, they were also tested for antinociceptive properties. Alkaloid **1** was tested at 3, 10, 30, and 60 mg/kg doses (s.c.). In the tail flick assay, minimal yet statistically significant antinociception was measured at 110 minutes for the 3 mg/kg dose, and at 30 minutes for the 60 mg/kg dose (**Figure 4.6A**, Table S16 in the online supplement). In the hotplate assay, minimal yet statistically significant antinociception was measured at 110 minutes for the 3 mg/kg dose, at 60 minutes for the 30 mg/kg dose, and at 30 minutes for the 60 mg/kg dose (**Figure 4.6B**, Table S16 in the online supplement). Alkaloid **2** was tested at 3, 10, and 30 mg/kg doses (s.c.). In the tail flick assay, minimal yet statistically significant antinociception was measured at 50 minutes for the 10 mg/kg dose, and at 30 minutes for the 30 mg/kg dose (**Figure 4.6C**, Table S17 in the online supplement). In the hotplate assay, minimal, yet statistically significant, antinociception was measured at 110 minutes for the 3 mg/kg dose (**Figure 4.6D**, Table S17 in the online supplement). For both **1** and **2**, dose-dependent increases in antinociception were not observed reproducibly between nociception assays, and there was no general trend in the time-course of the antinociceptive effect. To explore whether the route of administration for **1** and **2** would influence the antinociceptive effect, oral dosing was also examined. However, no antinociception was measurable, indicating that metabolism of the

compounds is unlikely to contribute to potential effects as has been previously proposed (data not shown) (Duwiejua et al., 2002).

In a previous study in rats, the antinociceptive effects of **3** differed kinetically from those produced by morphine, with antinociceptive activity for **3** peaking at 180 minutes when administered p.o. (Duwiejua et al., 2002). To account for potential delayed onset in antinociception for akuamma alkaloids, nociception was tested in mice at 50 and 110 minutes following s.c. administration with **1** and **2**. However, with continued testing and after failing to detect convincing levels of antinociception, testing was adjusted to higher doses of 30 and 60-75 minutes in an attempt to capture either a rapid or delayed peak in antinociceptive efficacy. To ensure that the s.c. route of administration was not contributing to the lack of observable antinociception, nociception was measured following p.o. administration of **1**-**3**, yet still convincing levels of antinociception were not observed as was demonstrated by Duwiejua et al (Duwiejua et al., 2002). The lack of antinociception with p.o. administration suggests that metabolism of the akuamma alkaloids does not greatly contribute to their purported antinociceptive effects. The incongruous antinociceptive findings between this study and previous research may be explained by species differences: in this study, C57BL/6 mice were used, whereas Wistar rats were used in the previous study (Duwiejua et al., 2002).

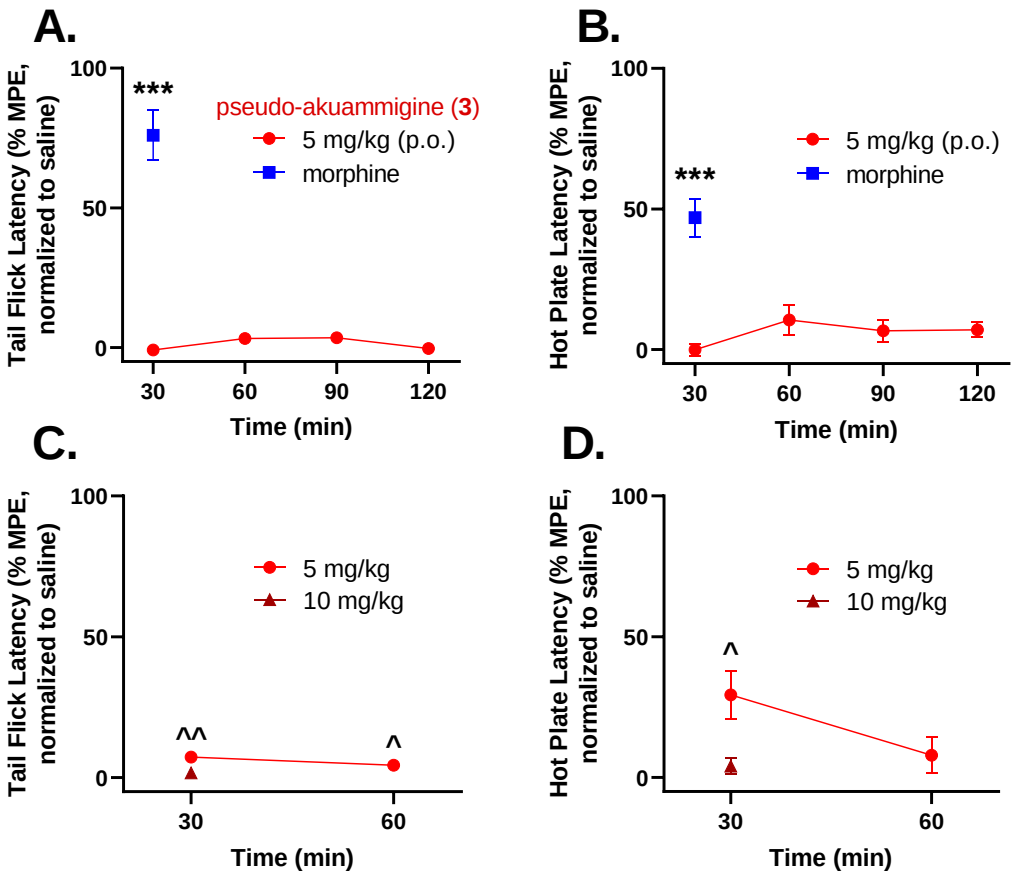

Figure 4.5 Effects of pseudo-akuammigine in mouse models of thermal nociception.

Antinociception by pseudo-akuammigine (**3**) was tested at doses of 5 mg/kg (p.o., n=16) (**A-B**) and 5 and 10 mg/kg (s.c., n=8) (**C-D**) in C57BL/6 mice via the tail flick assay (**A** and **C**) and the hot plate assay (**B** and **D**) at various time points. Morphine (6 mg/kg, s.c., n=8) served as a positive control (**A-B**)**.** All data is expressed as maximum possible effect (%MPE) normalized to a saline baseline (treatment – saline baseline). For the 5 mg/kg doses, ^P < 0.05 vs. vehicle and ^^P < 0.01 vs vehicle. For morphine, ***P < 0.001 vs. vehicle. Morphine and 10 mg/kg alkaloid **3** data was analyzed with a paired t-test. Data for 5 mg/kg alkaloid **3** (p.o. and s.c.) was analyzed with one-way, repeated measures ANOVA followed by Sidak's multiple comparisons post-test.

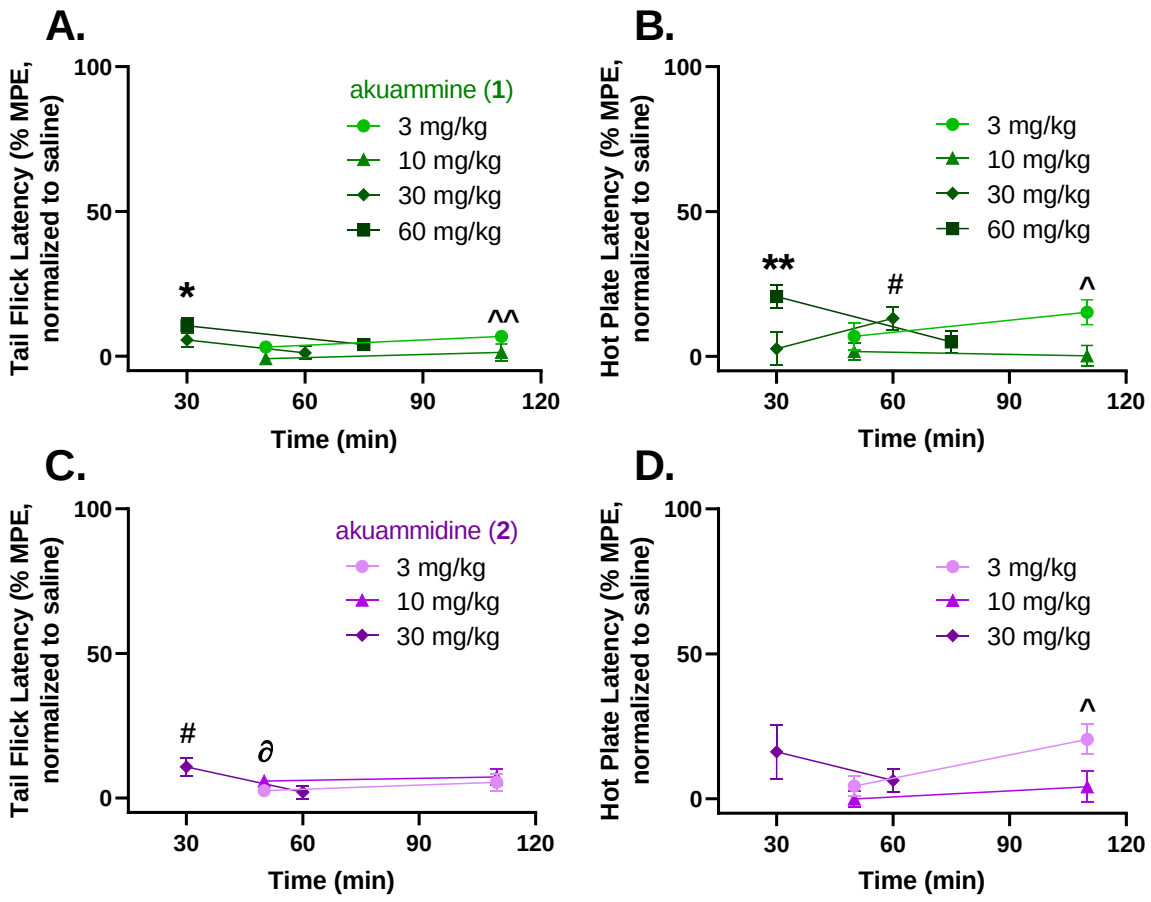

Figure 4.6 Effects of akuammine and akuammidine in mouse models of thermal nociception.

Antinociception by akuammine (1) (3, 10, 30, and 60 mg/kg (s.c.)), A-B) and akuammidine (2) (3, 10, and 30 mg/kg (s.c.)), C-D) was assessed in C57BL/6 mice (n=8, per alkaloid) via the tail flick assay (A and C) and the hot plate assay (B and D) at various time points. All data is expressed as maximum possible effect (%MPE) normalized to a saline baseline (treatment – saline baseline). For the 3 mg/kg doses, ^P < 0.05 vs vehicle and ^^P < 0.01 vs vehicle. For the 10 mg/kg doses, statistical significance is indicated as $^{\partial}$P < 0.05 vs vehicle. For the 30 mg/kg doses, $^{\#}$P < 0.05 vs vehicle. For the 60 mg/kg doses, *P < 0.05 vs vehicle and **P < 0.01 vs vehicle. Data was analyzed with one-way, repeated measures ANOVA followed by Sidak's multiple comparisons post-test.

4.4 Conclusion

Natural products, and in particular plant alkaloids, are a well-known source for medicinal compounds with analgesic potency. Most familiar are the opioids found in *Papaver somniferum*, but more recently *Mitragyna speciosa* has gained recognition in Western society as an alternative source of naturally occurring analgesics. This study provides a detailed investigation of the isolation of six abundant, yet chromatographically very similar, alkaloids from the seeds of *Picralima nitida*, a traditional plant with reported analgesic properties. Using high-purity isolates, this study undertook a detailed characterization of the pharmacology of the isolated akuamma alkaloids in mammalian cells and evaluated their antinociceptive effects in mice.

The cellular signaling characterization of the akuamma alkaloids at the opioid receptors agrees with previous findings but enhances the previous assessment by providing an analysis of intracellular signaling properties, particularly β-arrestin recruitment, at the opioid receptors as well as the binding capability to non-opioid receptors (Menzies et al., 1998). It was observed that the akuamma alkaloids' potency was too weak to accurately determine β-arrestin recruitment, however, several alkaloids display significant recruitment (>25%) at the highest dose that could be tested. The pharmacological profile of the akuamma alkaloids stands in contrast to the kratom alkaloids, particularly 7-hydroxymitragynine, which can be classified as a highly potent and G-protein-biased μOR agonist (Gutridge et al., 2020). Of all the akuamma alkaloids investigated, **4** stands out as being relatively potent at the κOR. The promiscuity of **4** for other receptors is conceivably problematic; however, it has the potential for serving as a scaffold for developing novel κOR agonists.

Analysis of akuamma's antinociceptive properties revealed limited antinociceptive efficacy of three akuamma alkaloids: **1**-**3**. While the observed limited antinociceptive efficacy does not support akuamma's traditional use for pain relief and is not congruous with a previous report of potent antinociception by **3** in rats (Duwiejua et al., 2002), this apparent contradiction is by far not unusual for investigations of ethnomedicinally used plants; as we and others have demonstrated, compound abundance and pharmacological relevance are not necessarily correlated (Case et al., 2006; Inui et al., 2010; Qiu et al., 2013), and even very minor components or impurities can be responsible for the observed biological activity (Choules et al., 2018). Thus, while these studies provide detailed insight into the pharmacology of six highly abundant alkaloids present in the *P. nitida* extracts, other components present in lower abundance may possess potent antinociceptive

activity. Furthermore, it is possible that pharmacokinetic and/or pharmacodynamic differences between rats and mice may account for the discrepant antinociceptive responses for the akuamma alkaloids in Wistar rats and C57BL/6 mice. Future studies should explore the pharmacokinetics of the akuamma opioids and akuamma metabolites in mice, confirm the reported antinociceptive effect in rats, and investigate potential synergistic interaction of the akuamma alkaloids in vivo. Additionally, despite the limited antinociceptive efficacy reported here, the unique structural features of the akuamma alkaloids provide opportunities to study the opioid receptors. By exploring the structure-activity relationships of these scaffolds and developing synthetic analogs, particularly those with improved pharmacokinetic and pharmacodynamic properties, the akuamma alkaloids may be transformed into useful pharmacological probes of the opioid receptors and to gain utility in treating pain and other disorders.

CHAPTER 5. DISCUSSION & FUTURE DIRECTIONS

5.1 Interpretation and investigation of G-protein biased δOR agonists in alcohol abuse therapeutics

5.1.1 Potential mechanism of G-protein biased δOR agonists underlying alcohol consumption effects

In light of the controversial research on G-protein biased μOR agonists detailed in section 1.3.3, it is important to address whether low intrinsic efficacy is driving the alcohol modulating effects of δOR agonists rather than β-arrestin2 recruitment (Gillis et al., 2020; Stahl and Bohn, 2021). The δOR agonists used to correlate heightened alcohol consumption and β-arrestin2 recruitment were all previously reported to display full agonist ability at the δOR in GTPγS binding assays, and displayed similar full agonism in cAMP inhibition assays (Quock et al., 1997; Wei et al., 2000; Jutkiewicz et al., 2004; Nemoto et al., 2013; Chiang et al., 2016). New data from a GTPγS binding experiment suggests TAN-67 may behave as a partial agonist (Stanczyk et al., 2019). This may introduce confusion in how we pharmacologically characterize these δOR agonists— whether as G-protein biased agonists or low efficacy agonists— however both types of agonists poorly promote β-arrestin2 recruitment, and it remains that this property can be a useful parameter for gauging an agonist's ability to modulate alcohol consumption. As far as the mechanism of these G-protein biased δOR agonists in their ability to modulate alcohol consumption, here it is hypothesized that treatment with exogenous G-protein biased δOR agonists replaces the unbiased endogenous δOR peptides that are released upon ethanol consumption (also referred to as "functional antagonism"), thereby reducing β-arrestin2 recruitment at the δOR which drives ethanol consumption. Continued research is necessary to understand how β-arrestin2 recruitment is specifically related to alcohol modulation, although evidence in β-arr2 KO mice demonstrates that β-arrestin2 plays an undefined role in dopamine release and reward following alcohol administration (Björk et al., 2013). Recent findings indicate that ethanol-induced dopamine release is reduced following kratom treatment (Vijeepallam et al., 2019), which supports the hypothesis that G-protein biased kratom compounds act as functional antagonists against endogenous peptides which recruit β-arrestin. The role of β-arrestins in mediating alcohol related effects is reinforced by the finding that in comparison to low-alcohol preferring rats, high-alcohol

preferring rats have elevated levels of β-arrestin2 in several brain regions within the mesolimbic pathway (Björk et al., 2008). Furthermore, β-arrestins are well-studied for their influence in behaviors related to other drugs of abuse, so it is not surprising that their regulation via the δOR can mediate alcohol consumption effects (Porter-Stransky and Weinshenker, 2017). Though the general mechanism of G-protein biased δOR agonists in alcohol modulation is hypothesized here, additional clarification is required to understand the potential downstream effects that mediate this behavior. Below I describe additional pharmacological characterization that would be useful for parsing out these signaling mechanisms.

5.1.2 Further investigation of mechanisms involved in G-protein biased δOR agonism

When tested in βarr2 KO mice, G-protein biased δOR agonist TAN-67 retained its ability to significantly decrease ethanol consumption, confirming its alcohol-modulating ability is independent of β-arrestin2 recruitment (Chiang et al., 2016). This β-arrestin2 independent signaling occurs through inhibitory Gαi/o -proteins, but this class of G-proteins includes Gαi-1, Gαi-2, Gαi-3, GαoA, GαoB and Gαz proteins and it is unclear if a G-protein subtype preferentially couples to δOR to mediate its effects. TAN-67 is known to reduce cAMP production, but both Gαi and Gαo proteins can mediate this effect (Katada et al., 1986; Kobayashi et al., 1990). While Gαi and Gαo proteins are highly homologous and are both expressed extensively throughout the CNS, they can mediate distinct biological functions (Jiang and Bajpayee, 2009). Opioid agonism reduces neurotransmitter release, a process that is dependent on inhibition of Ca_{2+} channels and results in changes to membrane polarization. It has been demonstrated that there are kinetic differences between Gαi and Gαo proteins in regulating the inhibition of calcium channels, with Gαo displaying enhanced coupling relative to Gαi, indicating it may preferentially regulate this effect (Hescheler et al., 1987). As such, though μOR is known to couple to both Gαi and Gαo proteins (Ueda et al., 1988; Gaibelet et al., 1999; Bouchet et al., 2021), μOR analgesia is dependent on the receptor coupling to Gαo and not Gαi (Lamberts et al., 2011, 2013). Thus, while cellular signaling profiles can look similar for these G-proteins, they can facilitate unique behavioral correlates, and it is unclear whether differences between Gαi and Gαo coupling modulate discrepant responses in alcohol intake.

Furthermore, it has been demonstrated that some agonists preferentially bind to μORs coupled to specific G-proteins, and elicit distinct downstream signaling pathways as a result

(Massotte et al., 2002; Clark et al., 2006; Bouchet et al., 2021). Preferential coupling of G proteins to opioid receptors therefore adds another level of functional selectivity to opioid agonists that have important impacts in the mediation of their behaviors. To address these effects, a new BRET-based assay named TRUPATH has been developed to assess ligand activation of multiple G-protein subtypes (Olsen et al., 2020). In this assay, several μOR agonists have displayed differential G-protein signaling patterns (Chakraborty et al., 2021a), supporting the idea that opioid receptors may initiate different signaling mechanisms dependent on G-protein expression in specific regions and cell-types. This concept is not limited to opioid receptors, as other CNS receptors such as cannabinoid and dopamine receptors both display differential activation of G-proteins (Lledo et al., 1992; Obadiah et al., 1999; Preto et al., 2020; Sachdev et al., 2020), further supporting the importance of characterizing differences in this first step of receptor activation.

To better understand G-protein signaling signatures of G-protein biased δOR agonists such as TAN-67 and 7-hydroxyspeciogynine versus non-biased δOR ligands such as DPDPE and leucine enkephalin (among others), the pharmacology of said compounds can be characterized in the TRUPATH assay (Olsen et al., 2020). Based on the information gathered from these experiments, it may be possible to correlate nuanced G-protein signaling signatures of different ligands with their alcohol modulating effects, similar to the β-arrestin2 correlation found in Chiang et al. (Chiang et al., 2016). If a favorable G-protein signature were to exist in regards to alcohol consumption, this would enable an additional parameter besides β-arrestin2 recruitment by which to identity potential therapeutic candidates. Additionally, at the level of receptor activation, β-arrestin2 recruitment is preferentially studied over β-arrestin1 recruitment. While in vivo alcohol-related effects of G-protein biased δOR agonists are not greatly influenced by β-arrestin2 mechanisms as evidenced in βarr2 KO mice (Chiang et al., 2016), β-arrestin1 mechanisms have not been explored. TAN-67 has been shown to weakly recruit β-arrestin1 relative to β-arrestin2 (Chiang et al., 2016; Ko et al., 2021), and β-arrestin1 has been shown to be somewhat protective against alcohol consumption in mice, with female β-arr1 KO mice displaying increased alcohol consumption (Robins et al., 2018a). Therefore, it is possible that mechanisms relating to β-arrestin1 recruitment may confer alcohol modulatory effects. Furthermore, it has been demonstrated that bias towards β-arrestin1 recruitment exists for some compounds at the δOR (Aguila et al., 2012), highlighting the possibility that mechanisms specific to β-arrestin1 recruitment may have behavioral correlates. Therefore, fully characterizing the β-arrestin1

recruitment abilities of δOR agonists may provide insight into the relevance of this property in δOR-mediated alcohol effects. If several G-protein biased δOR ligands recruit β-arrestin1, the role of this protein can be further assessed in β-arr1 KO mice exposed to the same alcohol consumption paradigms described above. To summarize, experiments such as these will provide additional clarification of the δOR signal cascade that promotes a decrease in alcohol consumption in mice, which will support future drug design efforts of signal-biased ligands.

5.2 Relating kratom alkaloid test dosages in mice to kratom use in humans

A concern when assessing novel compounds in mice, especially from natural products, is whether the effective dosages in mice will translate into manageable doses in humans. To estimate human equivalent doses from preclinical data, the FDA has provided guidance for conversion calculations based on body surface area and average body weight between species (Food and Drug Administration, 2005). These conversion calculations rely on correction factors (K_m) determined by the FDA; K_m values for humans and mice are 37 and 3, respectively. Assuming an average body weight of 60 kg for humans and 0.02 kg for mice, these body weights, along with the K_m values, can be used to calculate human and mice equivalent doses using **Equation 5.1** (Food and Drug Administration, 2005; Wilson et al., 2020a):

Equation 5.1 Equivalent dosage conversion

$$\textit{Mouse equivalent dose}\left(\frac{mg}{kg}\right) = \textit{Human equivalent dose}\left(\frac{mg}{kg}\right) * \frac{\textit{human Km}}{\textit{mouse Km}}$$

This equation was used to convert 3, 10, and 30 mg/kg dosages of kratom alkaloids and derivatives to human equivalent doses of 15, 49, and 146 mg, respectively (**Table 5.1**). Importantly, these calculated human equivalent doses only provide an estimate for maximum safe starting doses in early-stage human clinical trials, and do not confirm that the compound of interest is effective at this dose. That being said, a sample of kratom tea for human use has been found to contain 57 mg of mitragynine, a major kratom alkaloid, although amounts may vary greatly across different tea sources and preparations (Singh et al., 2020). The mouse equivalent dose of 57 mg of mitragynine in humans is nearly 12 mg/kg, which is similar to effective dosages of the kratom alkaloids and derivatives in the research presented here (**Table 5.1**). It is difficult to speculate

whether the 57 mg of mitragynine is an "effective dose" in humans due to the conversion of mitragynine to its more potent active metabolite 7-hydroxymitragynine, a process reliant on CYP3A liver enzyme isoforms (Kruegel et al., 2019; Yusof et al., 2019; Kamble et al., 2020). Furthermore, differences in metabolic rates, compound bioavailability, routes of administration, and experimental endpoints between species confounds comparison of mitragynine/7-hydroxymitragynine efficacy in mice and humans. For example, in liver microsomes preparations, the conversion of mitragynine to 7-hydroxymitragynine in humans was more efficient than in mice, suggesting interspecies metabolic differences complicates the understanding of mitragynine's pharmacology (Kruegel et al., 2019).

Table 5.1 Comparison of human and mouse equivalent dosages

Compound/Drug	Mouse Equivalent Dose (mg/kg)	Human Equivalent Dose (mg)*
Disulfiram	51 mg/kg	250 mg**
Acamprosate	137 mg/kg	666 mg**
Naltrexone	10.3 mg/kg	50 mg**
Kratom Alkaloid/ Derivative	3 mg/kg 10 mg/kg 30 mg/kg	15 mg 49 mg 146 mg
Mitragynine	11.7 mg/kg	57 mg***

*based on an average 60 kg body weight
**typical prescription doses for AUD (Holt and Tobin, 2018)
***Mitragynine present in 1 glass of kratom tea (amounts can vary) (Singh et al., 2020)

Nevertheless, the estimated human equivalent doses of 3 and 10 mg/kg of 7-hydroxyspeciogynine (15 and 49 mg, respectively) are both less than the amount of mitragynine found in kratom tea and support the idea that individual kratom alkaloids or derivatives may be a manageable therapeutic option in the future (from a dosage point of view). Kratom contains over 40 individual alkaloids with variable affinity for several different receptor families including opioid receptors, adrenergic receptors, and serotonin receptors (Boyer et al., 2008a; Kruegel et al., 2016; Ellis et al., 2020b; Foss et al., 2020; Obeng et al., 2020b; León et al., 2021). While the pharmacology of several of these alkaloids has been assessed to different degrees at these receptors, many alkaloids have gone under researched. Pharmacological and pharmacokinetic characterization of these alkaloids at the opioid receptors as well as other brain receptors is

necessary to fully appreciate the complex effects of individual compounds and the composite natural product itself.

5.3 Additional concerns with kratom use in humans

In the only clinical trial to assess kratom's effects on pain in humans, one serving of kratom tea was found to significantly increase pain tolerance compared to placebo (ClinicalTrials.gov, NCT03414099) (Vicknasingam et al., 2020). The kratom serving given to participants had "approximat[e] mitragynine concentration levels found in field decoctions," but it is not clear what amount of mitragynine was present per serving. Though in one study, kratom drinks have been shown to contain anywhere from 48.24 to 50.4 mg of mitragynine per glass, which is similar to the value of 57 mg presented above (Singh et al., 2019, 2020; Vicknasingam et al., 2020). Importantly, no withdrawal symptoms or concerning side effects were present following kratom discontinuation, however all participants had previous exposures to kratom which likely influenced this observation. Compared to other therapeutic candidates in clinical trials, kratom provides a unique benefit for evaluation in that it is already in use by humans around the world. Though its wide use does not confirm its safety and tolerability, it should be noted that to date there have only been 6 deaths solely attributed to kratom use in the United States, and risk of overdose deaths is estimated to be greater than 1000-fold less than opioids (Henningfield et al., 2019). This is consistent with lack of kratom overdose reporting in South East Asia, where kratom use originated and is common (Prozialeck et al., 2019). Still, additional research is needed to assess risks associated with kratom use, and to gain further insight of kratom's pharmacokinetics and pharmacodynamics to support its potential in clinical development and/or use. For example, seizure-like side effects have emerged as a major concern with kratom use (Coonan and Tatum, 2021), and in research findings above, kratom alkaloid paynantheine displayed seizure-like side effects in mice. A detailed assessment of individual kratom alkaloids and their associated seizure-like effects would clarify these side effects and potentially aid in preventing them if implicated alkaloids could be removed or reduced in kratom products.

Furthermore, another cause for concern are adverse effects resulting from kratom interaction with medicines or other drugs. As introduced above, kratom has been shown to both promote and inhibit the activities of multiple CYP proteins involved in the metabolism of drugs (Kong et al., 2011; Manda et al., 2017; Kruegel et al., 2019). These metabolic effects have

implicated kratom as a cause of toxicity and some studies have attributed fatalities coinciding with kratom use on these interactions (Ilmie et al., 2015; Hughes, 2019). To further investigate these effects, a pharmacokinetic trial is currently underway to investigate the interaction of kratom on metabolism of opioids (ClinicalTrials.gov, NCT04392011). Results from this study will help elucidate risks involved with co-ingestion of kratom with other drugs that may be helpful in shaping consumer information.

5.4 Comparing alcohol modulation by kratom-based compounds to FDA-approved AUD therapeutics in mice

In the 2-bottle choice voluntary 10% alcohol consumption paradigm, mice administered 7-hydroxymitragynine at 3 and 10 mg/kg doses displayed about 40% and 50% reduction in alcohol consumption, respectively. In the same paradigm, 3 and 10 mg/kg doses of 7-hydroxyspeciogynine decreased alcohol consumption by 20% and 40%. Interpretation of the significance of these results can be difficult as it not clearly defined what constitutes a "meaningful" decrease in alcohol. To aid our understanding, the alcohol modulating effects of FDA approved AUD treatments (naltrexone, acamprosate, and disulfiram) in mice have been summarized in **Table 5.2** for comparison. This summary is non-exhaustive, and several research studies were excluded if they included continuous/repeated dosing or operant, reinforcement, or stress-induced ethanol drinking paradigms which complicate interpretation. Furthermore, only findings conducted in C57Bl/6J mice were included for ease of comparison to our results with 7-hydroxymitrgynine and 7-hydroxyspeciogynine.

The ranges of doses tested for the drugs were 0.5-16 mg/kg for naltrexone (Phillips et al., 1997; Kim et al., 2004; Kamdar et al., 2007; van Rijn and Whistler, 2009; van Rijn et al., 2010; Crabbe et al., 2017), 100-400 mg/kg for acamprosate (Gupta et al., 2008; Lee et al., 2011; Crabbe et al., 2017), and 200 mg/kg for disulfiram (He et al., 1997). Notably, there was a lack of research on disulfiram's alcohol deterrent effects in mice, and only one research paper was found matching the inclusion criteria above. This lack of online, readily available data in mice may be explained by the longtime clinical use of disulfiram, which was first approved by the FDA in 1949. The doses used in our kratom compounds experiments (3, 10, 30 mg/kg) are similar to the mouse equivalent doses of 10.3 mg/kg for naltrexone, 137 mg/kg for acamprosate, and 51 mg/kg for disulfiram which were calculated from typical prescription dosages used in humans, summarized in **Table 5.1** (Holt

and Tobin, 2018). Noted in section 5.2, differences in dosing between these rodent experiments and calculated mouse equivalent doses may arise due to metabolic differences between species and administration routes, which may affect bioavailability.

Naltrexone demonstrated conflicting results between research groups in its ability to modulate alcohol consumption in mice, where some groups saw reductions in alcohol consumption as high as 70%, where others did not detect any noticeable effects (Kamdar et al., 2007; Crabbe et al., 2017). Differences in mouse strains, drinking paradigms, and dosages and may underlie these effects. Similar conflicting results were seen at lower doses of acamprosate, although acamprosate demonstrated an ability to decrease alcohol consumption above 300 mg/kg, with reductions in alcohol consumption as high as 40%. Disulfiram decreased alcohol consumption by 30%, although these findings cannot be corroborated for lack of data. Overall, when taking together the results from these studies, alcohol consumption is decreased about 30-40% by naltrexone, 20-30% by acamprosate, and 30% by disulfiram. These values are similar to the levels of alcohol modulation demonstrated by 7-hydroxymitragynine and 7-hydroxyspeciogynine, 40-50% and 20-40%, respectively. It is not to be inferred that these kratom based compounds are expected to be as equally effective as FDA-approved drugs in treating alcohol abuse, but rather that the decreases in alcohol consumption we see in mice from 7-hydroxymitragynine and 7-hydroxyspeciogynine are relevant and meaningful when compared to the efficacy of these FDA approved drugs in mice.

Table 5.2 Percent decrease in alcohol consumption following pharmacotherapy

Dose	Decrease in alcohol consumption	Experimental Model*	Mouse Strain	Reference
7-hydroxymitragynine				
3 mg/kg 10 mg/kg	~40% ~50%	10% ethanol, limited 2-bottle choice, DID	C57Bl/6 mice	(Gutridge et al., 2020)
7-hydroxyspeciogynine				
3 mg/kg 10 mg/kg	~20% ~40%	10% ethanol, limited 2-bottle choice, DID	C57Bl/6 mice	(Gutridge et al., 2021)
Naltrexone				
1.0 mg/kg 1.5 mg/kg 2.0 mg/kg 4.0 mg/kg 8.0 mg/kg	[no change] ~60% [no change] [no change] [no change]	10% ethanol, limited 2-bottle choice, DID	C57Bl/6 mice	(Phillips et al., 1997)
0.5 mg/kg 1 mg/kg 2 mg/kg 4 8 16	~20% ~30% ~30% ~40% ~60% ~70%	20% ethanol, limited access, DID	C57Bl/6 mice	(Kamdar et al., 2007)
1 mg/kg 4 mg/kg 8 mg/kg 10 mg/kg	[no change for all doses]	20% ethanol, binge, DID	High-ethanol drinking C57Bl/6 mice	(Crabbe et al., 2017)
1.5 mg/kg 5 mg/kg	~50% [no change]	10% ethanol, limited 2-bottle choice, DID	C57Bl/6 mice	(van Rijn and Whistler, 2009; van Rijn et al., 2010)
1.0 mg/kg	~40%	10% ethanol, limited access, DID	C57Bl/6 mice	(Kim et al., 2004)
Acamprosate				
100 mg/kg 200 mg/kg 300 mg/kg 400 mg/kg	[no change] ~10% ~20% ~40%	20% ethanol, intermittent access, DID	C57Bl/6 mice	(Gupta et al., 2008)
300 mg/kg	~40%	20% ethanol, binge, DID	High-ethanol drinking C57Bl/6 mice	(Crabbe et al., 2017)
200 mg/kg	[no change]	10% ethanol, 2-bottle choice, DID	C57Bl/6 mice	(Lee et al., 2011)
Disulfiram				
200 mg/kg	~30%	10% ethanol, 2-bottle choice, DID	C57Bl/6 mice	(He et al., 1997)

*DID: Drinking in the Dark

5.5 Investigation of kratom-based compounds for additional δOR-mediated alcohol related effects

5.5.1 Chronic treatment with kratom compounds in alcohol therapeutics

Importantly, treatment of alcohol abuse in humans usually relies on daily dosing, with disulfiram and naltrexone prescribed for daily use, and acamprosate prescribed for administration three times per day (Holt and Tobin, 2018). This is in contrast to most rodent alcohol models, including those used here to evaluate kratom alkaloids and derivatives, in which drugs are administered only one day per week. Future experiments with kratom and related kratom compounds should probe the effects of daily administration in alcohol-addicted mice to determine if the therapeutic candidate consistently abates alcohol consumption or whether effects wane with repetitive exposure. For instance, tolerance has been shown to develop to repeated administration of 7-hydroxymitragynine as measured by a decrease in antinociceptive action, an effect likely attributed to potent μOR agonism (Matsumoto et al., 2005). Therefore, kratom derivatives with a reduced μOR profile such as 7-hydroxyspeciogynine may produce less tolerance in their therapeutic effects.

However, repeated δOR agonism can also lead to tolerance for some ligands. Analgesic tolerance to potent non-biased δOR agonist SNC80 can develop after 3 days of chronic treatment, and rapid tolerance (<1 day) to SNC80-induced convulsions also occurs (Vicente-Sanchez et al., 2018). A decrease in tolerance to SNC80 behaviors is evident in βarr2 KO mice, indicating a role for β-arrestin2 and downstream mechanisms in the development of δOR-mediated tolerance (Vicente-Sanchez et al., 2018). β-arrestin recruitment is not a reliable indicator of whether a ligand will lead to tolerance upon repeated administration, however. It has been demonstrated that following β-arrestin recruitment and δOR internalization, ligands that promote receptor recycling and re-sensitization, such as deltorphin II and DPDPE, prevent tolerance from developing, similar to findings with μOR (Marie et al., 2003; Lecoq et al., 2004; Beaudry et al., 2009; Pradhan et al., 2009; Audet et al., 2012). In contrast, ligands that do not promote ligand recycling and instead support degradation, such as SNC80, lead to tolerance (Pradhan et al., 2009; Audet et al., 2012; Bagheri Tudashki et al., 2020; Pineyro and Nagi, 2021). In other words, there are two common mechanisms for δORs after internalization, degradation and recycling, and it is not clear why or how one pathway is selected over another. As such, ligands that recruit β-arrestin but display low-

internalizing capability such as ARM390, ADL5747, and ADL5859 bypass these recycling/degradation mechanisms, and thus tolerance is prevented or reduced (Pradhan et al., 2009; Nozaki et al., 2012; Chiang et al., 2016; Ko et al., 2021). Correspondingly, ligands with reduced ability to recruit β-arrestins evade tolerance mechanisms. Compared to SNC80, δOR agonist KNT127 displays reduced β-arrestin2 recruitment and shows no loss of efficacy in hyperemotionality measures following chronic treatment in mice (Chiang et al., 2016; Gotoh et al., 2017). Similarly, G-protein biased δOR agonist PN6047 displays no analgesic tolerance with prolonged treatment (Conibear et al., 2020). The cellular mechanisms underpinning tolerance to δOR agonists are thus very complicated and are still being investigated; ligand specific effects are likely to exist as well as differential tolerance to multiple behaviors. While kratom compound 7-hydroxyspeciogynine is a relatively weak δOR agonist compared to those described above, in vivo interaction at the δOR has been confirmed in our δOR KO studies with regards to alcohol consumption. Based on the G-protein biased profile of 7-hydroxyspeciogynine, one would expect little δOR-mediated tolerance to occur with chronic administration, but this effect should be confirmed in repeated administration alcohol consumption studies. These studies would provide a better understanding of kratom's potential tolerance mechanisms and would support the therapeutic development of δOR agonists for AUD treatments by elucidating their utility in chronic dosing regimens.

5.5.2 Effects of kratom compounds on alcohol withdrawal effects

In addition to evaluating the ability of kratom compounds in decreasing alcohol consumption over time, further research should investigate their ability to mitigate alcohol withdrawal symptoms. In a recent online survey of over 3000 kratom users, 15% indicate that kratom helps to mitigate withdrawal symptoms from opioids (Coe et al., 2019). Supporting this, Wilson et al. have demonstrated that kratom extract and mitragynine both ameliorate symptoms of naloxone-precipitated withdrawal from opioids in mice (Wilson et al., 2020a). Similarly, It has been previously demonstrated that kratom extract can significantly reduce ethanol withdrawal behaviors in rodents such as rearing and hyperactivity (Kumarnsit et al., 2007; Cheaha et al., 2015). However, we have shown that kratom extract can significantly reduce locomotor activity which may confound these alcohol withdrawal behavioral effects. Therefore, in order to determine whether kratom extract or compounds can reduce alcohol withdrawal symptoms, doses that do not

affect locomotor response should first be established. Lead analog 7-hydroxyspeciogynine notably did not affect locomotion, making it an ideal candidate for these investigations. Furthermore, studies have shown that δOR agonists are capable of reducing alcohol withdrawal symptoms (Kotlińska and Langwiński, 1986). To determine whether δOR mechanisms underlie kratom's potential effects on alcohol withdrawal, studies should be carried out in δOR KO mice or with selective δOR antagonists such as naltrindole or naltriben. Antagonism of the δOR and δOR KO are known to increase anxiety like behaviors in mice which may hinder data interpretation due to changes in locomotive behaviors (Filliol et al., 2000; Saitoh et al., 2005; Perrine et al., 2006); therefore, appropriate controls are imperative. In AUD pharmacotherapy, the proposed mechanism of action for FDA approved drug acamprosate is mitigation alcohol withdrawal symptoms (De Witte et al., 2005; Rösner et al., 2010a; Witkiewitz et al., 2012). This is why acamprosate is more useful in treatment of abstinent individuals than in reducing levels of alcohol consumption in heavy drinkers (Maisel et al., 2013). A more thorough characterization of kratom's mechanisms and effects on alcohol withdrawal would thus be relevant to AUD research as reducing withdrawal symptoms can ultimately reduce risk of relapse in alcohol-abstinent individuals (Becker, 2008).

5.6 Probing kratom's κOR-mediated effects

5.6.1 Possible κOR contributions to kratom's alcohol modulating effects

While the μOR and δOR are responsible for alcohol's positively reinforcing effects, the κOR is thought to confer negative reinforcing effects that escalate alcohol use to alcohol dependence (Walker et al., 2011). Generally, κOR antagonists have been investigated as AUD therapeutics (Xuei et al., 2006; Walker et al., 2011; Schank et al., 2012; Domi et al., 2018), with therapeutic effects stemming from their ability to prevent the endogenous κOR ligand, dynorphin, from binding to the receptor and promoting aversive and dysphoric symptoms (Mucha and Herz, 1985). κOR antagonists, therefore, are hypothesized to decrease alcohol consumption in animal models because they reduce alcohol withdrawal negative affect. In contrast, κOR agonism is usually aversive in rodents and humans. However, κOR-induced aversion has been linked to β-arrestin2 signaling (Bruchas et al., 2006, 2007a; Bruchas and Chavkin, 2010); this provides a hypothesis in which G-protein-biased κOR agonists may have therapeutic effects. Indeed, a recent study has bolstered this idea by showing that nalfurafine, a selective G-protein biased κOR agonist,

is able to decrease ethanol consumption in ethanol drinking models (Zhou and Kreek, 2019). Therefore, it is unclear to what degree κOR signaling contributes to the alcohol modulating effects of kratom alkaloids and analogs. To probe κOR contributions in these effects, 2-bottle choice alcohol consumption experiments can be conducted in mice exposed to a selective κOR antagonist as well as kratom compounds at doses previously shown to decrease alcohol consumption. κOR antagonist Nor-binaltophimine (Nor-BNI) is commonly used for blockage of κOR, but it's long-lasting pharmacokinetic profile poses problems for multi-week drinking experiments (Kishioka et al., 2013). Instead, κOR antagonist LY2444296 can be used due to its short in vivo half-life compared to Nor-BNI (Butelman et al., 2019). There is a possibility that κOR antagonist activity will muddle the alcohol consumption effects seen from the kratom compounds themselves, so multiple antagonist doses should be tested in order to select the highest dose that does not reduce alcohol intake. If this strategy does not work, κOR contributions can be evaluated using κOR KO mice. Although 7-hydroxymitragynine's lack of ethanol consumption in δOR KO mice indicates a primary mechanism through δORs, higher doses of kratom analog 7-hydroxyspeciogynine displayed decreases in ethanol consumption in δOR KO mice. To determine if κOR played a role in these findings, a similar ethanol drinking experiment can be conducted in δOR KO mice with and without κOR antagonists. Additionally, antagonists for other adrenergic and serotonin receptors should also be considered in these investigations as kratom alkaloids have been shown to have activity at these receptors (Boyer et al., 2008a; Ellis et al., 2020b; Foss et al., 2020; Obeng et al., 2020b; León et al., 2021). Experiments such as these would help provide a thorough characterization of the receptor contributions in kratom's alcohol modulatory effects which may be useful in directing drug development of ligands with unique polypharmacology for the treatment of alcohol abuse.

5.6.2 Kratom's potential ability to reduce stress via the κOR

Many kratom users indicate that kratom enhances their mood and can relieve anxiety, with 66% reporting that they use kratom to reduce negative moods and mentalities such as anxiety, post-traumatic stress and depression (Grundmann, 2017; Swogger and Walsh, 2018; Garcia-Romeu et al., 2020). As the μOR and κOR systems are well known in modulating positive and negative affective states (Spanagel et al., 1992), with κOR agonism causing dysphoric-like effects for some but not all agonists (Pfeiffer et al., 1986). In a GTPγS assay, mitragynine has been shown

to possess possible antagonistic activity at the κOR (Kruegel et al., 2016), which may promote positive affect by competing with the κOR's endogenous opioid, dynorphin. As such, mitragynine produced anxiolytic effects in rats and mice (Hazim et al., 2014; Yusoff et al., 2016). Importantly, these effects could be antagonized with naloxone, implicating the opioid receptor system in these effects (Hazim et al., 2014). Furthermore, treatment with kratom extract reduced stress-induced analgesia in both wildtype mice and μOR knockout mice, implicating an alternative opioid receptor is involved in kratom's anxiolytic-like effects in rodents (Vázquez López et al., 2017). When this experiment was repeated in μOR knockout mice pre-treated with potent κOR antagonist Nor-BNI, kratom's anxiolytic-like effects were diminished, indicating κOR involvement, although data interpretation is confounded by low responses from control mice treated with Nor-BNI (Vázquez López et al., 2017). While the κOR is highly implicated in the modulation of kratom's effects on mood, data confirming these effects are lacking. To address this, research utilizing well-characterized stress models such as the elevated plus maze or light dark box should be completed using wildtype mice treated with kratom/kratom alkaloids with and without κOR antagonists. These experiments would provide a better understanding of the mechanisms driving kratom's anxiolytic effects which would be useful and informative given that these effects motivate kratom use in many individuals.

5.7 Akuamma alkaloids are useful scaffolds for derivatization

In general, the akuamma analogs characterized in Chapter 4 displayed weak affinity and potency at the opioid receptors. However, akuammicine (AKC, compound 4) stood out as having relatively potent κOR activity compared to the other alkaloids, with a binding pKi of 7.1 ± 0.1 and an pIC50 of 6.6 ± 0.1 in the GloSensor cAMP assay of G-protein activity. Yet, when screened for activity at other CNS receptors, AKC was shown to be very promiscuous. In an effort to discover a compound with improved κOR potency and selectivity, AKC was used as a scaffold to generate several derivatives. Of these derivatives, two compounds stood out as having potent nanomolar κOR affinity and potency (**Figure 5.1**). In radioligand binding assays for κOR affinity, AKC derivatives 1 and 2 had pKi's of 10.1 ± 0.1 and 9.4 ± 0.1, respectively (**Figure 5.1A**). This potent affinity was reflected in pIC50s for 9.0 ± 0.1 and 8.4 ± 0.1 for derivative 1 and 2 in the GloSensor assay (**Figure 5.1B**), as well as the β-arrestin2 recruitment assay with respective pEC50s of 6.4 ± 0.2 and 5.8 ± 0.1 (**Figure 5.1C**).

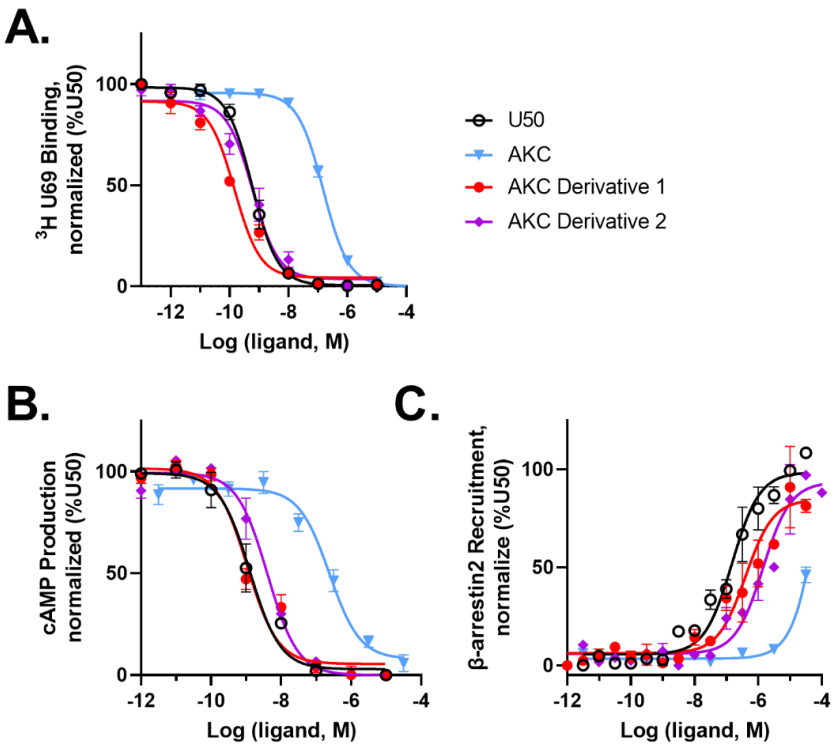

Figure 5.1 Potent κOR pharmacology of akuammicine analogs.

Akuammicine (AKC) derivatives 1 and 2 were characterized for κOR affinity using [^{3}H]U69,593 in a competitive radioligand binding assay (**A**), ability to inhibit forskolin-induced cAMP in the GloSensor assay completed in κOR transfected HEK cells (**B**), and ability to recruit β-arrestin2 at κOR in the PathHunter assay (**C**). For reference, pharmacology of parent compound akuammicine (4, AKC) is shown, as well as positive control U50, 488 (U50).

In future experiments with these compounds, selectivity for the κOR over other opioid receptors needs to be assessed through additional in vitro characterization experiments at δOR and μOR. To determine if receptor promiscuity has been reduced in relation to parent compound AKC, these compounds should also be screened for activity at other CNS receptors via the Psychoactive Drug Screening Program (PDSP), or through another similar resource. Characterization of the signaling profile of these compounds at κOR, μOR, and δOR will provide insight into potential therapeutic application and guide appropriate selection of behavioral paradigms. Based alone on their activity at the κOR, these derivatives should be tested for analgesic and mood-modulating properties. To assess if these compounds create therapeutically limiting dysphoric-like effects via their potent κOR agonism, the conditioned place preference paradigm would be a useful and easy way to measure conditioned place aversion. Furthermore, pain-relieving properties can be

evaluated through a variety of antinociceptive paradigms, including the tail-flick and hot plate assays described in Chapters 2-4. In summary, while the akuamma alkaloids displayed minimal therapeutic potential, the unique scaffolds of the compounds compared to traditional opioids provided an opportunity to develop novel opioids, highlighting the importance of natural products in drug discovery efforts.

5.8 Natural products as a source of novel peptides for pain treatment

This dissertation research explores the therapeutic potential of small molecules derived from natural products. However, a recent study indicated that small molecule drug discovery from natural products is on the decline, whereas peptide drug discovery from natural products has been steadily increasing (Muratspahić et al., 2019). Accordingly, in the last 15 years several reports of novel opioid peptides and derivatives have been reported from natural products such as fungus, spinach, scorpion and rattlesnake venom (Konno et al., 2008; Zhang et al., 2012; Aldrich et al., 2013; Cassell et al., 2019; Dekan et al., 2019; Muratspahić et al., 2019). Yet, several limitations exist for peptides in drug development. For example, peptides tend to be very hydrophilic, limiting their membrane permeability, bioavailability, and biodistribution. This membrane impermeability also lowers the ability of opioid peptides to cross the blood brain barrier, which can limit analgesic potential for centrally mediated pain responses. However, this property can be used as an advantage in the development of analgesics to treat peripheral pain in order limit centrally mediated opioid side effects such as respiratory depression and reward. As such, two peripherally restricted opioids have been approved by the FDA, underscoring their relevance in therapeutic use. Loperamide (Imodium) is a peripherally restricted μOR opioid agonist approved for use as an anti-diarrheal medication. Though it is not used an analgesic in humans, it has displayed antinociceptive properties in rats with nerve injury (Chung et al., 2012). Additionally, difelikefalin (Korsuva) is a recently approved peripherally restricted peptidic κOR agonist used to treat chronic itch, although it has demonstrated analgesic efficacy in several phase II clinical trials. Other peripherally restricted κOR agonists are under investigation for pain treatment, one being peptidic compound CR665, which has displayed efficacy in relieving visceral pain in humans (Arendt-Nielsen et al., 2009). In conclusion, peripherally restricted opioids display an opportunity for growth in opioid analgesic research as they eliminate several centrally mediated side effects that plague clinical development of several small molecule opioids. Additionally, as research and discovery of nature-

based peptides is growing, natural products provide a strong resource for the discovery of novel peripherally restricted peptides.

5.9 Final Conclusions

The research presented in this dissertation contributes to a growing body of work on the pharmacological characterization of kratom, its therapeutic application, and potentially limiting side effects. Many people find kratom helpful in treating opioid abuse, chronic pain, and alcohol abuse, and while extensive research has been completed on kratom's ability to treat opioid abuse and chronic pain, our studies provide an extensive characterization of kratom's ability to modulate alcohol consumption through G-protein biased δOR activation (Chapter 2 and 3). Our findings also align with research indicating that kratom and individual kratom compounds contribute to concerning side-effects such as reward and seizure-like behavior, which may influence potential scheduling of kratom by the Drug Enforcement Agency. We have also demonstrated, along with others, that the lessened side effect profile of kratom alkaloids in comparison to traditional opioids makes them useful scaffolds for derivatization (Chapter 3). Additional investigations into the pharmacology, side effect profiles, and pharmacokinetics of individual alkaloids in kratom would provide a better understanding of kratom's effects in vivo and may also reveal additional "hits" for derivatization in the search for more effective AUD therapeutics. Our studies with akuamma revealed low therapeutic potential for the alkaloids tested (Chapter 4), but high potential for future derivatization (section 5.7). Future akuamma investigations should investigate the therapeutic application of identified high-potency analogs, as well as their promiscuity and side effect profiles. Overall, the findings presented here support the continued development of G-protein biased δOR agonists for AUD pharmacotherapy and underscore the importance of natural products research for the identification of novel opioids and scaffolds.

REFERENCES

Adkins, J. E., Boyer, E. W., and McCurdy, C. R. (2011). Mitragyna speciosa, a psychoactive tree from Southeast Asia with opioid activity. *Curr Top Med Chem* 11, 1165–1175. doi:10.2174/156802611795371305.

Afzal, H., Esang, M., and Rahman, S. (2020). A Case of Kratom-induced Seizures. *Cureus* 12, e6588. doi:10.7759/cureus.6588.

Aguila, B., Coulbault, L., Davis, A., Marie, N., Hasbi, A., Le bras, F., et al. (2012). ßarrestin1-biased agonism at human δ-opioid receptor by peptidic and alkaloid ligands. *Cellular Signalling* 24, 699–707. doi:10.1016/j.cellsig.2011.10.018.

Ahmad, K., and Aziz, Z. (2012). Mitragyna speciosa use in the northern states of Malaysia: A cross-sectional study. *Journal of Ethnopharmacology* 141, 446–450. doi:10.1016/j.jep.2012.03.009.

Akil, H., Mayer, D. J., and Liebeskind, J. C. (1976). Antagonism of stimulation-produced analgesia by naloxone, a narcotic antagonist. *Science* 191, 961–962. doi:10.1126/science.1251210.

Aldrich, J. V., Senadheera, S. N., Ross, N. C., Ganno, M. L., Eans, S. O., and McLaughlin, J. P. (2013). The Macrocyclic Peptide Natural Product CJ-15,208 Is Orally Active and Prevents Reinstatement of Extinguished Cocaine-Seeking Behavior. *J. Nat. Prod.* 76, 433–438. doi:10.1021/np300697k.

Alexander, S. P. H., Christopoulos, A., Davenport, A. P., Kelly, E., Mathie, A., Peters, J. A., et al. (2019). THE CONCISE GUIDE TO PHARMACOLOGY 2019/20: G protein-coupled receptors. *British Journal of Pharmacology* 176, S21–S141. doi:10.1111/bph.14748.

Alhadeff, R., Vorobyov, I., Yoon, H. W., and Warshel, A. (2018). Exploring the free-energy landscape of GPCR activation. *PNAS* 115, 10327–10332. doi:10.1073/pnas.1810316115.

Al-Hasani, R., and Bruchas, M. R. (2011). Molecular Mechanisms of Opioid Receptor-dependent Signaling and Behavior. *Anesthesiology* 115, 1363–1381. doi:10.1097/ALN.0b013e318238bba6.

Alles, S. R. A., and Smith, P. A. (2018). Etiology and Pharmacology of Neuropathic Pain. *Pharmacol Rev* 70, 315–347. doi:10.1124/pr.117.014399.

Alongkronrusmee, D., Chiang, T., and van Rijn, R. M. (2018). Delta Opioid Pharmacology in Relation to Alcohol Behaviors. *Handb Exp Pharmacol* 247, 199–225. doi:10.1007/164_2016_30.

Altarifi, A. A., David, B., Muchhala, K. H., Blough, B. E., Akbarali, H., and Negus, S. S. (2017). Effects of acute and repeated treatment with the biased mu opioid receptor agonist TRV130 (oliceridine) on measures of antinociception, gastrointestinal function, and abuse liability in rodents. *J Psychopharmacol* 31, 730–739. doi:10.1177/0269881116689257.

Alvarez, V. A., Arttamangkul, S., Dang, V., Salem, A., Whistler, J. L., Von Zastrow, M., et al. (2002). mu-Opioid receptors: Ligand-dependent activation of potassium conductance, desensitization, and internalization. *J Neurosci* 22, 5769–5776. doi:20026560.

Ama-Asamoah, R., Kapadia, G. J., Lloyd, H. A., and Sokoloski, E. A. (1990). Picratidine, a New Indole Alkaloid from Picralima nitida Seeds. *J. Nat. Prod.* 53, 975–977. doi:10.1021/np50070a032.

American Psychiatric Association (2013). *Diagnostic and statistical manual of mental disorders (5th ed.)*. Arlington, VA: American Psychiatric Publishing.

Anand, A., and Hosanagar, A. (2021). The Addictive Potential and Challenges With Use of the "Herbal Supplement" Kratom: A Case Report and Literature Review. *Pain Medicine*, pnab126. doi:10.1093/pm/pnab126.

Andersson, G. B. (1999). Epidemiological features of chronic low-back pain. *Lancet* 354, 581–585. doi:10.1016/S0140-6736(99)01312-4.

Angkurawaranon, C., Jiraporncharoen, W., Likhitsathian, S., Thaikla, K., Kanato, M., Perngparn, U., et al. (2018). Trends in the use of illicit substances in Thailand: Results from national household surveys. *Drug Alcohol Rev* 37, 658–663. doi:10.1111/dar.12689.

Arendt-Nielsen, L., Olesen, A. E., Staahl, C., Menzaghi, F., Kell, S., Wong, G. Y., et al. (2009). Analgesic Efficacy of Peripheral κ-Opioid Receptor Agonist CR665 Compared to Oxycodone in a Multi-modal, Multi-tissue Experimental Human Pain Model: Selective Effect on Visceral Pain. *Anesthesiology* 111, 616–624. doi:10.1097/ALN.0b013e3181af6356.

Astra Zeneca Pharmaceuticals (2012). A Phase II, Multi-center, Randomized, Double-bind, Double-dummy, Active and Placebo Controlled, Parallel Group Study to Assess the Efficacy and Safety of AZD7268 in Patients With Major Depressive Disorder. clinicaltrials.gov Available at: https://clinicaltrials.gov/ct2/show/results/NCT01020799 [Accessed October 20, 2021].

Atanasov, A. G., Zotchev, S. B., Dirsch, V. M., and Supuran, C. T. (2021). Natural products in drug discovery: advances and opportunities. *Nat Rev Drug Discov* 20, 200–216. doi:10.1038/s41573-020-00114-z.

Attramadal, H., Arriza, J. L., Aoki, C., Dawson, T. M., Codina, J., Kwatra, M. M., et al. (1992). Beta-arrestin2, a novel member of the arrestin/beta-arrestin gene family. *J Biol Chem* 267, 17882–17890.

Audet, N., Charfi, I., Mnie-Filali, O., Amraei, M., Chabot-Doré, A.-J., Millecamps, M., et al. (2012). Differential Association of Receptor-Gβγ Complexes with β-Arrestin2 Determines Recycling Bias and Potential for Tolerance of Delta Opioid Receptor Agonists. *J. Neurosci.* 32, 4827–4840. doi:10.1523/JNEUROSCI.3734-11.2012.

Austin Zamarripa, C., Edwards, S. R., Qureshi, H. N., Yi, J. N., Blough, B. E., and Freeman, K. B. (2018). The G-protein biased mu-opioid agonist, TRV130, produces reinforcing and antinociceptive effects that are comparable to oxycodone in rats. *Drug and Alcohol Dependence* 192, 158–162. doi:10.1016/j.drugalcdep.2018.08.002.

Bagheri Tudashki, H., Haddad, Y., Charfi, I., Couture, R., and Pineyro, G. (2020). Ligand-specific recycling profiles determine distinct potential for chronic analgesic tolerance of delta-opioid receptor (DOPr) agonists. *J Cell Mol Med*. doi:10.1111/jcmm.15234.

Ballantyne, J. C., Loach, A. B., and Carr, D. B. (1988). Itching after epidural and spinal opiates. *PAIN* 33, 149–160. doi:10.1016/0304-3959(88)90085-1.

Ballas, S. K., Kanter, J., Agodoa, I., Howard, R., Wade, S., Noxon, V., et al. (2018). Opioid utilization patterns in United States individuals with sickle cell disease. *American Journal of Hematology* 93, E345–E347. doi:10.1002/ajh.25233.

Banks, M. L. (2020). THE RISE AND FALL OF KAPPA-OPIOID RECEPTORS IN DRUG ABUSE RESEARCH. *Handb Exp Pharmacol* 258, 147–165. doi:10.1007/164_2019_268.

Bardo, M. T., and Neisewander, J. L. (1986). Single-trial conditioned place preference using intravenous morphine. *Pharmacology Biochemistry and Behavior* 25, 1101–1105. doi:10.1016/0091-3057(86)90092-4.

Barrett, L. F., and Bliss-Moreau, E. (2009). Affect as a Psychological Primitive. *Adv Exp Soc Psychol* 41, 167–218. doi:10.1016/S0065-2601(08)00404-8.

Beaudry, H., Proteau-Gagné, A., Li, S., Dory, Y., Chavkin, C., and Gendron, L. (2009). Differential noxious and motor tolerance of chronic delta opioid receptor agonists in rodents. *Neuroscience* 161, 381–391. doi:10.1016/j.neuroscience.2009.03.053.

Becker, A., Grecksch, G., Brödemann, R., Kraus, J., Peters, B., Schroeder, H., et al. (2000). Morphine self-administration in μ-opioid receptor-deficient mice. *Naunyn-Schmied Arch Pharmacol* 361, 584–589. doi:10.1007/s002100000244.

Becker, H. C. (2008). Alcohol dependence, withdrawal, and relapse. *Alcohol Res Health* 31, 348–361.

Belknap, J. K., Crabbe, J. C., and Young, E. R. (1993). Voluntary consumption of ethanol in 15 inbred mouse strains. *Psychopharmacology* 112, 503–510. doi:10.1007/BF02244901.

Benarroch, E. E. (2012). Endogenous opioid systems: current concepts and clinical correlations. *Neurology* 79, 807–814. doi:10.1212/WNL.0b013e3182662098.

Benayad, S., Ahamada, K., Lewin, G., Evanno, L., and Poupon, E. (2016). Preakuammicine: A Long-Awaited Missing Link in the Biosynthesis of Monoterpene Indole Alkaloids. *European Journal of Organic Chemistry* 2016, 1494–1499. doi:10.1002/ejoc.201600102.

Benjamin, D., Grant, E. R., and Pohorecky, L. A. (1993). Naltrexone reverses ethanol-induced dopamine release in the nucleus accumbens in awake, freely moving rats. *Brain Res* 621, 137–140. doi:10.1016/0006-8993(93)90309-b.

Benyamin, R., Trescot, A. M., Datta, S., Buenaventura, R., Adlaka, R., Sehgal, N., et al. (2008). Opioid Complications and Side Effects. *Pain Physician*, 16.

Berg, K. A., and Clarke, W. P. (2018). Making Sense of Pharmacology: Inverse Agonism and Functional Selectivity. *International Journal of Neuropsychopharmacology* 21, 962–977. doi:10.1093/ijnp/pyy071.

Berger, A. C., and Whistler, J. L. (2011). Morphine-induced mu opioid receptor trafficking enhances reward yet prevents compulsive drug use. *EMBO Mol Med* 3, 385–397. doi:10.1002/emmm.201100144.

Bergese, S. D., Brzezinski, M., Hammer, G. B., Beard, T. L., Pan, P. H., Mace, S. E., et al. (2019). ATHENA: A Phase 3, Open-Label Study Of The Safety And Effectiveness Of Oliceridine (TRV130), A G-Protein Selective Agonist At The μ-Opioid Receptor, In Patients With Moderate To Severe Acute Pain Requiring Parenteral Opioid Therapy. *J Pain Res* 12, 3113–3126. doi:10.2147/JPR.S217563.

Berquist, M. D., and Fantegrossi, W. E. (2021). Effects of 5-HT2A receptor agonist 2,5-dimethoxy-4-iodoamphetamine on alcohol consumption in Long–Evans rats. *Behavioural Pharmacology* Publish Ahead of Print. doi:10.1097/FBP.0000000000000628.

Bhowmik, S., Galeta, J., Havel, V., Nelson, M., Faouzi, A., Bechand, B., et al. (2021). Site selective C–H functionalization of Mitragyna alkaloids reveals a molecular switch for tuning opioid receptor signaling efficacy. *Nat Commun* 12, 3858. doi:10.1038/s41467-021-23736-2.

Bidlack, J. M., Knapp, B. I., Deaver, D. R., Plotnikava, M., Arnelle, D., Wonsey, A. M., et al. (2018). In Vitro Pharmacological Characterization of Buprenorphine, Samidorphan, and Combinations Being Developed as an Adjunctive Treatment of Major Depressive Disorder. *J Pharmacol Exp Ther* 367, 267–281. doi:10.1124/jpet.118.249839.

Bie, B., Zhu, W., and Pan, Z. Z. (2009). Ethanol-induced delta-opioid receptor modulation of glutamate synaptic transmission and conditioned place preference in central amygdala. *Neuroscience* 160, 348–358. doi:10.1016/j.neuroscience.2009.02.049.

Bigal, M. E., and Lipton, R. B. (2009). Excessive opioid use and the development of chronic migraine. *PAIN* 142, 179–182. doi:10.1016/j.pain.2009.01.013.

Björk, K., Rimondini, R., Hansson, A. C., Terasmaa, A., Hyytiä, P., Heilig, M., et al. (2008). Modulation of voluntary ethanol consumption by beta-arrestin 2. *FASEB J* 22, 2552–2560. doi:10.1096/fj.07-102442.

Björk, K., Tronci, V., Thorsell, A., Tanda, G., Hirth, N., Heilig, M., et al. (2013). β-Arrestin 2 knockout mice exhibit sensitized dopamine release and increased reward in response to a low dose of alcohol. *Psychopharmacology* 230, 439–449. doi:10.1007/s00213-013-3166-x.

Blanco, C., and Volkow, N. D. (2019). Management of opioid use disorder in the USA: present status and future directions. *The Lancet* 393, 1760–1772. doi:10.1016/S0140-6736(18)33078-2.

Bohn, L. M., Gainetdinov, R. R., Lin, F.-T., Lefkowitz, R. J., and Caron, M. G. (2000). μ-Opioid receptor desensitization by β-arrestin-2 determines morphine tolerance but not dependence. *Nature* 408, 720–723. doi:10.1038/35047086.

Bohn, L. M., Gainetdinov, R. R., Sotnikova, T. D., Medvedev, I. O., Lefkowitz, R. J., Dykstra, L. A., et al. (2003). Enhanced rewarding properties of morphine, but not cocaine, in beta(arrestin)-2 knock-out mice. *J Neurosci* 23, 10265–10273.

Bohn, L. M., Lefkowitz, R. J., Gainetdinov, R. R., Peppel, K., Caron, M. G., and Lin, F.-T. (1999). Enhanced Morphine Analgesia in Mice Lacking β-Arrestin 2. *Science* 286, 2495–2498. doi:10.1126/science.286.5449.2495.

Bohnert, A. S. B., Guy, G. P., and Losby, J. L. (2018). Opioid Prescribing in the United States Before and After the Centers for Disease Control and Prevention's 2016 Opioid Guideline. *Ann Intern Med* 169, 367–375. doi:10.7326/M18-1243.

Bouchet, C. A., McPherson, K. B., Li, M., Traynor, J. R., and Ingram, S. L. (2021). RGS-insensitive mice define roles of mu opioid receptor (MOR)-Gαo and Gαi subunit coupling in inhibition of presynaptic GABA release. *Mol Pharmacol*. doi:10.1124/molpharm.121.000249.

Boyer, E. W., Babu, K. M., Adkins, J. E., McCurdy, C. R., and Halpern, J. H. (2008a). Self-treatment of opioid withdrawal using kratom (Mitragynia speciosa korth). *Addiction* 103, 1048–1050. doi:10.1111/j.1360-0443.2008.02209.x.

Boyer, E. W., Babu, K. M., Adkins, J. E., McCurdy, C. R., and Halpern, J. H. (2008b). Self-treatment of opioid withdrawal using kratom (Mitragynia speciosa korth). *Addiction* 103, 1048–1050. doi:10.1111/j.1360-0443.2008.02209.x.

Boyer, E. W., Babu, K. M., Macalino, G. E., and Compton, W. (2007). Self-treatment of opioid withdrawal with a dietary supplement, Kratom. *Am J Addict* 16, 352–356. doi:10.1080/10550490701525368.

Brandt, M. R., Furness, M. S., Rice, K. C., Fischer, B. D., and Negus, S. S. (2001). Studies of tolerance and dependence with the delta-opioid agonist SNC80 in rhesus monkeys responding under a schedule of food presentation. *J Pharmacol Exp Ther* 299, 629–637.

Broom, D. C., Nitsche, J. F., Pintar, J. E., Rice, K. C., Woods, J. H., and Traynor, J. R. (2002). Comparison of Receptor Mechanisms and Efficacy Requirements for δ-Agonist-Induced Convulsive Activity and Antinociception in Mice. *J Pharmacol Exp Ther* 303, 723–729. doi:10.1124/jpet.102.036525.

Brown, P. N., Lund, J. A., and Murch, S. J. (2017). A botanical, phytochemical and ethnomedicinal review of the genus Mitragyna korth: Implications for products sold as kratom. *Journal of Ethnopharmacology* 202, 302–325. doi:10.1016/j.jep.2017.03.020.

Browne, C. A., and Lucki, I. (2019). Targeting opioid dysregulation in depression for the development of novel therapeutics. *Pharmacol Ther* 201, 51–76. doi:10.1016/j.pharmthera.2019.04.009.

Bruchas, M. R., and Chavkin, C. (2010). Kinase cascades and ligand-directed signaling at the kappa opioid receptor. *Psychopharmacology* 210, 137–147. doi:10.1007/s00213-010-1806-y.

Bruchas, M. R., Land, B. B., Aita, M., Xu, M., Barot, S. K., Li, S., et al. (2007a). Stress-induced p38 mitogen-activated protein kinase activation mediates kappa-opioid-dependent dysphoria. *J Neurosci* 27, 11614–11623. doi:10.1523/JNEUROSCI.3769-07.2007.

Bruchas, M. R., Land, B. B., Aita, M., Xu, M., Barot, S. K., Li, S., et al. (2007b). Stress-Induced p38 Mitogen-Activated Protein Kinase Activation Mediates -Opioid-Dependent Dysphoria. *Journal of Neuroscience* 27, 11614–11623. doi:10.1523/JNEUROSCI.3769-07.2007.

Bruchas, M. R., Macey, T. A., Lowe, J. D., and Chavkin, C. (2006). Kappa opioid receptor activation of p38 MAPK is GRK3- and arrestin-dependent in neurons and astrocytes. *J Biol Chem* 281, 18081–18089. doi:10.1074/jbc.M513640200.

Burke, D., Shearer, A., and Cott, A. V. (2019). Two Cases of Provoked Seizure Associated With Kratom Ingestion (P4.5-030). *Neurology* 92. Available at: https://n.neurology.org/content/92/15_Supplement/P4.5-030 [Accessed May 7, 2021].

Buse, D. C., Pearlman, S. H., Reed, M. L., Serrano, D., Ng-Mak, D. S., and Lipton, R. B. (2012). Opioid use and dependence among persons with migraine: results of the AMPP study. *Headache* 52, 18–36. doi:10.1111/j.1526-4610.2011.02050.x.

Butelman, E. R., McElroy, B. D., Prisinzano, T. E., and Kreek, M. J. (2019). Impact of Pharmacological Manipulation of the κ-Opioid Receptor System on Self-grooming and Anhedonic-like Behaviors in Male Mice. *J Pharmacol Exp Ther* 370, 1–8. doi:10.1124/jpet.119.256354.

Cabrera-Vera, T. M., Vanhauwe, J., Thomas, T. O., Medkova, M., Preininger, A., Mazzoni, M. R., et al. (2003). Insights into G Protein Structure, Function, and Regulation. *Endocrine Reviews* 24, 765–781. doi:10.1210/er.2000-0026.

Cahill, C. M., Morinville, A., Hoffert, C., O'Donnell, D., and Beaudet, A. (2003). Up-regulation and trafficking of delta opioid receptor in a model of chronic inflammation: implications for pain control. *Pain* 101, 199–208. doi:10.1016/s0304-3959(02)00333-0.

Cahill, C. M., Walwyn, W., Taylor, A. M. W., Pradhan, A. A. A., and Evans, C. J. (2016). Allostatic Mechanisms of Opioid Tolerance Beyond Desensitization and Downregulation. *Trends in Pharmacological Sciences* 37, 963–976. doi:10.1016/j.tips.2016.08.002.

Cai, N.-S., Quiroz, C., Bonaventura, J., Bonifazi, A., Cole, T. O., Purks, J., et al. (2019). Opioid-galanin receptor heteromers mediate the dopaminergic effects of opioids. *J Clin Invest* 129, 2730–2744. doi:10.1172/JCI126912.

Cao, D., Huang, P., Chiu, Y.-T., Chen, C., Wang, H., Li, M., et al. (2020). Comparison of Pharmacological Properties between the Kappa Opioid Receptor Agonist Nalfurafine and 42B, Its 3-Dehydroxy Analogue: Disconnect between in Vitro Agonist Bias and in Vivo Pharmacological Effects. *ACS Chem. Neurosci.* 11, 3036–3050. doi:10.1021/acschemneuro.0c00407.

Case, R. J., Franzblau, S. G., Wang, Y., Cho, S. H., Soejarto, D. D., and Pauli, G. F. (2006). Ethnopharmacological evaluation of the informant consensus model on anti-tuberculosis claims among the Manus. *J Ethnopharmacol* 106, 82–89. doi:10.1016/j.jep.2005.12.005.

Cassell, R. J., Mores, K. L., Zerfas, B. L., Mahmoud, A. H., Lill, M. A., Trader, D. J., et al. (2019). Rubiscolins are naturally occurring G protein-biased delta opioid receptor peptides. *European Neuropsychopharmacology* 29, 450–456. doi:10.1016/j.euroneuro.2018.12.013.

Centers for Disease Control (2020). Overdose Deaths Accelerating During COVID-19. *Centers for Disease Control and Prevention*. Available at: https://www.cdc.gov/media/releases/2020/p1218-overdose-deaths-covid-19.html [Accessed October 11, 2021].

Centers for Disease Control (2021). Drug Overdose Deaths in the U.S. Up 30% in 2020. Available at: https://www.cdc.gov/nchs/pressroom/nchs_press_releases/2021/20210714.htm [Accessed October 11, 2021].

Chakraborty, S., DiBerto, J. F., Faouzi, A., Bernhard, S. M., Gutridge, A. M., Ramsey, S., et al. (2021a). A Novel Mitragynine Analog with Low-Efficacy Mu Opioid Receptor Agonism Displays Antinociception with Attenuated Adverse Effects. *J. Med. Chem.* 64, 13873–13892. doi:10.1021/acs.jmedchem.1c01273.

Chakraborty, S., and Majumdar, S. (2021). Natural Products for the Treatment of Pain: Chemistry and Pharmacology of Salvinorin A, Mitragynine, and Collybolide. *Biochemistry* 60, 1381–1400. doi:10.1021/acs.biochem.0c00629.

Chakraborty, S., Uprety, R., Daibani, A. E., Rouzic, V. L., Hunkele, A., Appourchaux, K., et al. (2021b). Kratom Alkaloids as Probes for Opioid Receptor Function: Pharmacological Characterization of Minor Indole and Oxindole Alkaloids from Kratom. *ACS Chem. Neurosci.* doi:10.1021/acschemneuro.1c00149.

Charles, A., and Pradhan, A. A. (2016). Delta-opioid receptors as targets for migraine therapy. *Current Opinion in Neurology* 29, 314–319. doi:10.1097/WCO.0000000000000311.

Chavkin, C. (2011). The therapeutic potential of κ-opioids for treatment of pain and addiction. *Neuropsychopharmacology* 36, 369–370. doi:10.1038/npp.2010.137.

Chavkin, C., James, I. F., and Goldstein, A. (1982). Dynorphin is a specific endogenous ligand of the kappa opioid receptor. *Science* 215, 413–415. doi:10.1126/science.6120570.

Che, T., Majumdar, S., Zaidi, S. A., Ondachi, P., McCorvy, J. D., Wang, S., et al. (2018). Structure of the Nanobody-Stabilized Active State of the Kappa Opioid Receptor. *Cell* 172, 55-67.e15. doi:10.1016/j.cell.2017.12.011.

Cheaha, D., Keawpradub, N., Sawangjaroen, K., Phukpattaranont, P., and Kumarnsit, E. (2015). Effects of an alkaloid-rich extract from Mitragyna speciosa leaves and fluoxetine on sleep profiles, EEG spectral frequency and ethanol withdrawal symptoms in rats. *Phytomedicine* 22, 1000–1008. doi:10.1016/j.phymed.2015.07.008.

Chen, Y., Mestek, A., Liu, J., Hurley, J. A., and Yu, L. (1993). Molecular cloning and functional expression of a mu-opioid receptor from rat brain. *Mol Pharmacol* 44, 8–12.

Chiang, T., Sansuk, K., and Rijn, R. M. van (2016). β-Arrestin 2 dependence of δ opioid receptor agonists is correlated with alcohol intake. *British Journal of Pharmacology* 173, 332–343. doi:10.1111/bph.13374.

Chick, J. (1999). Safety issues concerning the use of disulfiram in treating alcohol dependence. *Drug Saf* 20, 427–435. doi:10.2165/00002018-199920050-00003.

Choules, M. P., Klein, L. L., Lankin, D. C., McAlpine, J. B., Cho, S.-H., Cheng, J., et al. (2018). Residual Complexity Does Impact Organic Chemistry and Drug Discovery: The Case of Rufomyazine and Rufomycin. *J Org Chem* 83, 6664–6672. doi:10.1021/acs.joc.8b00988.

Chu Sin Chung, P., Boehrer, A., Stephan, A., Matifas, A., Scherrer, G., Darcq, E., et al. (2015). Delta opioid receptors expressed in forebrain GABAergic neurons are responsible for SNC80-induced seizures. *Behavioural Brain Research* 278, 429–434. doi:10.1016/j.bbr.2014.10.029.

Chu Sin Chung, P., and Kieffer, B. L. (2013). Delta opioid receptors in brain function and diseases. *Pharmacology & Therapeutics* 140, 112–120. doi:10.1016/j.pharmthera.2013.06.003.

Chung, C., Carteret, A. F., McKelvy, A. D., Ringkamp, M., Yang, F., Hartke, T. V., et al. (2012). Analgesic properties of loperamide differ following systemic and local administration to rats after spinal nerve injury. *Eur J Pain* 16, 1021–1032. doi:10.1002/j.1532-2149.2012.00148.x.

Ciaraldi, T. P., and Maisel, A. (1989). Role of guanine nucleotide regulatory proteins in insulin stimulation of glucose transport in rat adipocytes. Influence of bacterial toxins. *Biochem J* 264, 389–396. doi:10.1042/bj2640389.

Cicero, T. J., Ellis, M. S., Surratt, H. L., and Kurtz, S. P. (2014). Factors contributing to the rise of buprenorphine misuse: 2008-2013. *Drug Alcohol Depend* 142, 98–104. doi:10.1016/j.drugalcdep.2014.06.005.

Cinosi, E., Martinotti, G., Simonato, P., Singh, D., Demetrovics, Z., Roman-Urrestarazu, A., et al. (2015). Following "the Roots" of Kratom (Mitragyna speciosa): The Evolution of an Enhancer from a Traditional Use to Increase Work and Productivity in Southeast Asia to a Recreational Psychoactive Drug in Western Countries. *Biomed Res Int* 2015. doi:10.1155/2015/968786.

Claff, T., Yu, J., Blais, V., Patel, N., Martin, C., Wu, L., et al. (2019). Elucidating the active δ-opioid receptor crystal structure with peptide and small-molecule agonists. *Science Advances* 5, eaax9115. doi:10.1126/sciadv.aax9115.

Claing, A., Laporte, S. A., Caron, M. G., and Lefkowitz, R. J. (2002). Endocytosis of G protein-coupled receptors: roles of G protein-coupled receptor kinases and beta-arrestin proteins. *Prog Neurobiol* 66, 61–79. doi:10.1016/s0301-0082(01)00023-5.

Clark, A. M. (1996). Natural products as a resource for new drugs. *Pharm Res* 13, 1133–1144. doi:10.1023/a:1016091631721.

Clark, M. J., Furman, C. A., Gilson, T. D., and Traynor, J. R. (2006). Comparison of the relative efficacy and potency of mu-opioid agonists to activate Galpha(i/o) proteins containing a pertussis toxin-insensitive mutation. *J Pharmacol Exp Ther* 317, 858–864. doi:10.1124/jpet.105.096818.

Coe, M. A., Pillitteri, J. L., Sembower, M. A., Gerlach, K. K., and Henningfield, J. E. (2019). Kratom as a substitute for opioids: Results from an online survey. *Drug and Alcohol Dependence* 202, 24–32. doi:10.1016/j.drugalcdep.2019.05.005.

Compton, W. M., Jones, C. M., Stein, J. B., and Wargo, E. M. (2019). Promising roles for pharmacists in addressing the U.S. opioid crisis. *Research in Social and Administrative Pharmacy* 15, 910–916. doi:10.1016/j.sapharm.2017.12.009.

Cong, X., Maurel, D., Déméné, H., Vasiliauskaité-Brooks, I., Hagelberger, J., Peysson, F., et al. (2021). Molecular insights into the biased signaling mechanism of the μ-opioid receptor. *Molecular Cell* 81, 4165-4175.e6. doi:10.1016/j.molcel.2021.07.033.

Conibear, A. E., Asghar, J., Hill, R., Henderson, G., Borbely, E., Tekus, V., et al. (2020). A Novel G Protein–Biased Agonist at the δ Opioid Receptor with Analgesic Efficacy in Models of Chronic Pain. *J Pharmacol Exp Ther* 372, 224–236. doi:10.1124/jpet.119.258640.

Conner, K. R., Gamble, S. A., Bagge, C. L., He, H., Swogger, M. T., Watts, A., et al. (2014). Substance-induced depression and independent depression in proximal risk for suicidal behavior. *J Stud Alcohol Drugs* 75, 567–572. doi:10.15288/jsad.2014.75.567.

Connor, M., and Christie, M. D. (1999). Opioid receptor signalling mechanisms. *Clin Exp Pharmacol Physiol* 26, 493–499. doi:10.1046/j.1440-1681.1999.03049.x.

Coonan, E., and Tatum, W. (2021). Kratom: The safe legal high? *Epilepsy & Behavior* 117, 107882. doi:10.1016/j.yebeh.2021.107882.

Corder, G., Castro, D. C., Bruchas, M. R., and Scherrer, G. (2018). Endogenous and Exogenous Opioids in Pain. *Annu Rev Neurosci* 41, 453–473. doi:10.1146/annurev-neuro-080317-061522.

Crabbe, J. C., Ozburn, A. R., Metten, P., Barkley-Levenson, A., Schlumbohm, J. P., Spence, S. E., et al. (2017). High Drinking in the Dark (HDID) mice are sensitive to the effects of some clinically relevant drugs to reduce binge-like drinking. *Pharmacology Biochemistry and Behavior* 160, 55–62. doi:10.1016/j.pbb.2017.08.002.

Creed, S. M., Gutridge, A. M., Argade, M. D., Hennessy, M. R., Friesen, J. B., Pauli, G. F., et al. (2021). Isolation and Pharmacological Characterization of Six Opioidergic Picralima nitida Alkaloids. *J. Nat. Prod.* 84, 71–80. doi:10.1021/acs.jnatprod.0c01036.

Crombie, A., Arezzo, J., Dewire, S., Gowen-MacDonald, W., Jutkiewicz, E. M., Kramer, M., et al. (2015). TRV250: a novel G protein-biased ligand at the delta receptor for the potential treatment of migraine. *Postgraduate Medicine*. doi:10.1080/00325481.2015.1086533.

Curtis, M. J., Alexander, S., Cirino, G., Docherty, J. R., George, C. H., Giembycz, M. A., et al. (2018). Experimental design and analysis and their reporting II: updated and simplified guidance for authors and peer reviewers. *British Journal of Pharmacology* 175, 987–993. doi:10.1111/bph.14153.

Dahan, A., Dam, C. J. van, Niesters, M., Velzen, M. van, Fossler, M. J., Demitrack, M. A., et al. (2020). Benefit and Risk Evaluation of Biased μ-Receptor Agonist Oliceridine versus Morphine. *Anesthesiology*. doi:10.1097/ALN.0000000000003441.

Dapaah, G., Koffuor, G. A., Mante, P. K., and Ben, I. O. (2016). Antitussive, expectorant and analgesic effects of the ethanol seed extract of Picralima nitida (Stapf) Th. & H. Durand. *Res Pharm Sci* 11, 100–112.

Das, G. (1993). Cocaine abuse in North America: a milestone in history. *J Clin Pharmacol* 33, 296–310. doi:10.1002/j.1552-4604.1993.tb04661.x.

Davis, M. P. (2012). Twelve reasons for considering buprenorphine as a frontline analgesic in the management of pain. *J Support Oncol* 10, 209–219. doi:10.1016/j.suponc.2012.05.002.

Day, R., Schäfer, M. K., Collard, M. W., Weihe, E., and Akil, H. (1993). Prodynorphin gene expression in the rat intermediate pituitary lobe: gender differences and postpartum regulation. *Endocrinology* 133, 2652–2659. doi:10.1210/endo.133.6.8243288.

De Sarro, G. B., Marra, R., Spagnolo, C., and Nisticò, G. (1992). Delta opioid receptors mediate seizures produced by intrahippocampal injection of ala-deltorphin in rats. *Funct Neurol* 7, 235–238.

De Witte, P., Littleton, J., Parot, P., and Koob, G. (2005). Neuroprotective and Abstinence-Promoting Effects of Acamprosate. *CNS Drugs* 19, 517–537. doi:10.2165/00023210-200519060-00004.

DEA (2016). Schedules of Controlled Substances: Temporary Placement of Mitragynine and 7-Hydroxymitragynine Into Schedule I. *Federal Register*. Available at: https://www.federalregister.gov/documents/2016/08/31/2016-20803/schedules-of-controlled-substances-temporary-placement-of-mitragynine-and-7-hydroxymitragynine-into [Accessed August 24, 2021].

Décaillot, F. M., Befort, K., Filliol, D., Yue, S., Walker, P., and Kieffer, B. L. (2003). Opioid receptor random mutagenesis reveals a mechanism for G protein-coupled receptor activation. *Nat Struct Biol* 10, 629–636. doi:10.1038/nsb950.

Deeks, E. D. (2021). Difelikefalin: First Approval. *Drugs*. doi:10.1007/s40265-021-01619-6.

Dekan, Z., Sianati, S., Yousuf, A., Sutcliffe, K. J., Gillis, A., Mallet, C., et al. (2019). A tetrapeptide class of biased analgesics from an Australian fungus targets the μ-opioid receptor. *PNAS* 116, 22353–22358. doi:10.1073/pnas.1908662116.

DeWire, S. M., Yamashita, D. S., Rominger, D. H., Liu, G., Cowan, C. L., Graczyk, T. M., et al. (2013). A G Protein-Biased Ligand at the μ-Opioid Receptor Is Potently Analgesic with Reduced Gastrointestinal and Respiratory Dysfunction Compared with Morphine. *J Pharmacol Exp Ther* 344, 708–717. doi:10.1124/jpet.112.201616.

Di Chiara, G. (1998). A motivational learning hypothesis of the role of mesolimbic dopamine in compulsive drug use. *J Psychopharmacol* 12, 54–67. doi:10.1177/026988119801200108.

Dietis, N., Rowbotham, D. J., and Lambert, D. G. (2011). Opioid receptor subtypes: fact or artifact? *Br J Anaesth* 107, 8–18. doi:10.1093/bja/aer115.

DiVito, A. J., and Leger, R. F. (2020). Psychedelics as an emerging novel intervention in the treatment of substance use disorder: a review. *Mol Biol Rep* 47, 9791–9799. doi:10.1007/s11033-020-06009-x.

Do Carmo, G. P., Folk, J. E., Rice, K. C., Chartoff, E., Carlezon, W. A., and Negus, S. S. (2009). The selective non-peptidic delta opioid agonist SNC80 does not facilitate intracranial self-stimulation in rats. *Eur J Pharmacol* 604, 58–65. doi:10.1016/j.ejphar.2008.12.021.

Domi, E., Barbier, E., Augier, E., Augier, G., Gehlert, D., Barchiesi, R., et al. (2018). Preclinical evaluation of the kappa-opioid receptor antagonist CERC-501 as a candidate therapeutic for alcohol use disorders. *Neuropsychopharmacol* 43, 1805–1812. doi:10.1038/s41386-018-0015-y.

Dowell, D., Haegerich, T. M., and Chou, R. (2016). CDC Guideline for Prescribing Opioids for Chronic Pain—United States, 2016. *JAMA* 315, 1624–1645. doi:10.1001/jama.2016.1464.

Dowell, D., Noonan, R. K., and Houry, D. (2017). Underlying Factors in Drug Overdose Deaths. *JAMA* 318, 2295. doi:10.1001/jama.2017.15971.

Dripps, I. J., Boyer, B. T., Neubig, R. R., Rice, K. C., Traynor, J. R., and Jutkiewicz, E. M. (2018). Role of signalling molecules in behaviours mediated by the δ opioid receptor agonist SNC80. *British Journal of Pharmacology* 175, 891–901. doi:https://doi.org/10.1111/bph.14131.

Duwiejua, M., Woode, E., and Obiri, D. D. (2002). Pseudo-akuammigine, an alkaloid from Picralima nitida seeds, has anti-inflammatory and analgesic actions in rats. *Journal of Ethnopharmacology* 81, 73–79. doi:10.1016/S0378-8741(02)00058-2.

Eggleston, W., Stoppacher, R., Suen, K., Marraffa, J. M., and Nelson, L. S. (2019). Kratom Use and Toxicities in the United States. *Pharmacotherapy: The Journal of Human Pharmacology and Drug Therapy* 39, 775–777. doi:10.1002/phar.2280.

Eguchi, M. (2004). Recent advances in selective opioid receptor agonists and antagonists. *Medicinal Research Reviews* 24, 182–212. doi:https://doi.org/10.1002/med.10059.

Ehrich, E., Turncliff, R., Du, Y., Leigh-Pemberton, R., Fernandez, E., Jones, R., et al. (2015). Evaluation of opioid modulation in major depressive disorder. *Neuropsychopharmacology* 40, 1448–1455. doi:10.1038/npp.2014.330.

Eisinger, D. A., and Ammer, H. (2008). δ-Opioid receptors activate ERK/MAP kinase via integrin-stimulated receptor tyrosine kinases. *Cellular Signalling* 20, 2324–2331. doi:10.1016/j.cellsig.2008.09.002.

Ellis, C. R., Racz, R., Kruhlak, N. L., Kim, M. T., Zakharov, A. V., Southall, N., et al. (2020a). Evaluating kratom alkaloids using PHASE. *PLOS ONE* 15, e0229646. doi:10.1371/journal.pone.0229646.

Ellis, C. R., Racz, R., Kruhlak, N. L., Kim, M. T., Zakharov, A. V., Southall, N., et al. (2020b). Evaluating kratom alkaloids using PHASE. *PLOS ONE* 15, e0229646. doi:10.1371/journal.pone.0229646.

Erharuyi, O., Falodun, A., and Langer, P. (2014). Medicinal uses, phytochemistry and pharmacology of Picralima nitida (Apocynaceae) in tropical diseases: A review. *Asian Pacific Journal of Tropical Medicine* 7, 1–8. doi:10.1016/S1995-7645(13)60182-0.

Erspamer, V., Melchiorri, P., Falconieri-Erspamer, G., Negri, L., Corsi, R., Severini, C., et al. (1989). Deltorphins: a family of naturally occurring peptides with high affinity and selectivity for delta opioid binding sites. *Proc Natl Acad Sci U S A* 86, 5188–5192. doi:10.1073/pnas.86.13.5188.

Evans, C. J., Keith, D. E., Morrison, H., Magendzo, K., and Edwards, R. H. (1992). Cloning of a delta opioid receptor by functional expression. *Science* 258, 1952–1955. doi:10.1126/science.1335167.

Fang, L., Zhou, J., Lin, Y., Wang, X., Sun, Q., Li, J.-L., et al. (2013). Large-scale separation of alkaloids from Gelsemium elegans by pH-zone-refining counter-current chromatography with a new solvent system screening method. *J Chromatogr A* 1307, 80–85. doi:10.1016/j.chroma.2013.07.069.

Faouzi, A., Varga, B. R., and Majumdar, S. (2020). Biased Opioid Ligands. *Molecules* 25, 4257. doi:10.3390/molecules25184257.

Ferdousi, M., and Finn, D. P. (2018). "Chapter 4 - Stress-induced modulation of pain: Role of the endogenous opioid system," in *Progress in Brain Research* The Opioid System as the Interface between the Brain's Cognitive and Motivational Systems., ed. S. O'Mara (Elsevier), 121–177. doi:10.1016/bs.pbr.2018.07.002.

Ferrari, A., Coccia, C. P. R., Bertolini, A., and Sternieri, E. (2004). Methadone—metabolism, pharmacokinetics and interactions. *Pharmacological Research* 50, 551–559. doi:10.1016/j.phrs.2004.05.002.

Field, M. J., Carnell, A. J., Gonzalez, M. I., McCleary, S., Oles, R. J., Smith, R., et al. (1999). Enadoline, a selective kappa-opioid receptor agonist shows potent antihyperalgesic and antiallodynic actions in a rat model of surgical pain. *Pain* 80, 383–389. doi:10.1016/s0304-3959(98)00237-1.

Fields, H. L., and Margolis, E. B. (2015). Understanding opioid reward. *Trends Neurosci* 38, 217–225. doi:10.1016/j.tins.2015.01.002.

Filliol, D., Ghozland, S., Chluba, J., Martin, M., Matthes, H. W. D., Simonin, F., et al. (2000). Mice deficient for δ- and μ-opioid receptors exhibit opposing alterations of emotional responses. *Nat Genet* 25, 195–200. doi:10.1038/76061.

Finn, A. K., and Whistler, J. L. (2001). Endocytosis of the mu opioid receptor reduces tolerance and a cellular hallmark of opiate withdrawal. *Neuron* 32, 829–839. doi:10.1016/s0896-6273(01)00517-7.

Fishbain, D. A., Goldberg, M., Robert Meagher, B., Steele, R., and Rosomoff, H. (1986). Male and female chronic pain patients categorized by DSM-III psychiatric diagnostic criteria. *Pain* 26, 181–197. doi:10.1016/0304-3959(86)90074-6.

Food and Drug Administration (2005). Guidance for industry: estimating the maximum safe starting dose in initial clinical trials for therapeutics in adult healthy volunteers.idance for Industry. *Center for Drug Evaluation and Research (CDER)*, 7.

Food and Drug Administration (2020). FDA Approves New Opioid for Intravenous Use in Hospitals, Other Controlled Clinical Settings. *FDA*. Available at: https://www.fda.gov/news-events/press-announcements/fda-approves-new-opioid-intravenous-use-hospitals-other-controlled-clinical-settings [Accessed October 14, 2021].

Foss, J. D., Nayak, S. U., Tallarida, C. S., Farkas, D. J., Ward, S. J., and Rawls, S. M. (2020). Mitragynine, bioactive alkaloid of kratom, reduces chemotherapy-induced neuropathic pain in rats through α-adrenoceptor mechanism. *Drug Alcohol Depend* 209, 107946. doi:10.1016/j.drugalcdep.2020.107946.

Fossler, M. J., Schmith, V., Greene, S. A., Lohmer, L., Kramer, M. S., Arscott, K., et al. (2020). A Phase I, Randomized, Single-Blind, Placebo-Controlled, Single Ascending Dose Study of the Safety, Tolerability, and Pharmacokinetics of Subcutaneous and Oral TRV250, a G Protein-Selective Delta Receptor Agonist, in Healthy Subjects. *CNS Drugs* 34, 853–865. doi:10.1007/s40263-020-00738-0.

Franck, J., and Jayaram-Lindström, N. (2013). Pharmacotherapy for alcohol dependence: status of current treatments. *Current Opinion in Neurobiology* 23, 692–699. doi:10.1016/j.conb.2013.05.005.

Fredriksson, R., Lagerström, M. C., Lundin, L.-G., and Schiöth, H. B. (2003). The G-Protein-Coupled Receptors in the Human Genome Form Five Main Families. Phylogenetic Analysis, Paralogon Groups, and Fingerprints. *Mol Pharmacol* 63, 1256–1272. doi:10.1124/mol.63.6.1256.

Gaibelet, G., Meilhoc, E., Riond, J., Saves, I., Exner, T., Liaubet, L., et al. (1999). Nonselective coupling of the human mu-opioid receptor to multiple inhibitory G-protein isoforms. *Eur J Biochem* 261, 517–523. doi:10.1046/j.1432-1327.1999.00301.x.

Galandrin, S., Oligny-Longpré, G., and Bouvier, M. (2007). The evasive nature of drug efficacy: implications for drug discovery. *Trends Pharmacol Sci* 28, 423–430. doi:10.1016/j.tips.2007.06.005.

Gallantine, E. L., and Meert, T. F. (2005). A comparison of the antinociceptive and adverse effects of the mu-opioid agonist morphine and the delta-opioid agonist SNC80. *Basic Clin Pharmacol Toxicol* 97, 39–51. doi:10.1111/j.1742-7843.2005.pto_97107.x.

Garcia-Romeu, A., Cox, D. J., Smith, K. E., Dunn, K. E., and Griffiths, R. R. (2020). Kratom (Mitragyna speciosa): User demographics, use patterns, and implications for the opioid epidemic. *Drug and Alcohol Dependence* 208, 107849. doi:10.1016/j.drugalcdep.2020.107849.

Gaskin, D. J., and Richard, P. (2012). The Economic Costs of Pain in the United States. *The Journal of Pain* 13, 715–724. doi:10.1016/j.jpain.2012.03.009.

Gavériaux-Ruff, C., Karchewski, L. A., Hever, X., Matifas, A., and Kieffer, B. L. (2008). Inflammatory pain is enhanced in delta opioid receptor-knockout mice. *Eur J Neurosci* 27, 2558–2567. doi:10.1111/j.1460-9568.2008.06223.x.

Gianoulakis, C. (2001). Influence of the endogenous opioid system on high alcohol consumption and genetic predisposition to alcoholism. *Journal of Psychiatry & Neuroscience* 26, 304–318.

Gillis, A., Gondin, A. B., Kliewer, A., Sanchez, J., Lim, H. D., Alamein, C., et al. (2020). Low intrinsic efficacy for G protein activation can explain the improved side effect profiles of new opioid agonists. *Sci. Signal.* 13. doi:10.1126/scisignal.aaz3140.

Goldberg, D. S., and McGee, S. J. (2011). Pain as a global public health priority. *BMC Public Health* 11, 770. doi:10.1186/1471-2458-11-770.

Gonzales, R. A., and Weiss, F. (1998). Suppression of ethanol-reinforced behavior by naltrexone is associated with attenuation of the ethanol-induced increase in dialysate dopamine levels in the nucleus accumbens. *J Neurosci* 18, 10663–10671.

Gostin, L. O., Hodge, J. G., and Noe, S. A. (2017). Reframing the Opioid Epidemic as a National Emergency. *JAMA* 318, 1539–1540. doi:10.1001/jama.2017.13358.

Gotoh, L., Saitoh, A., Yamada, M., Fujii, H., Nagase, H., and Yamada, M. (2017). Effects of repeated treatment with a delta opioid receptor agonist KNT-127 on hyperemotionality in olfactory-bulbectomized rats. *Behavioural Brain Research* 323, 11–14. doi:10.1016/j.bbr.2016.11.008.

Gouveia, D. N., Guimarães, A. G., Santos, W. B. da R., and Quintans-Júnior, L. J. (2019). Natural products as a perspective for cancer pain management: A systematic review. *Phytomedicine* 58, 152766. doi:10.1016/j.phymed.2018.11.026.

Granier, S., Manglik, A., Kruse, A. C., Kobilka, T. S., Thian, F. S., Weis, W. I., et al. (2012). Structure of the δ-opioid receptor bound to naltrindole. *Nature* 485, 400–404. doi:10.1038/nature11111.

Grant, B. F., Stinson, F. S., Dawson, D. A., Chou, S. P., Dufour, M. C., Compton, W., et al. (2004). Prevalence and co-occurrence of substance use disorders and independent mood and anxiety disorders: results from the National Epidemiologic Survey on Alcohol and Related Conditions. *Arch Gen Psychiatry* 61, 807–816. doi:10.1001/archpsyc.61.8.807.

Greenfield, S. F., Weiss, R. D., Muenz, L. R., Vagge, L. M., Kelly, J. F., Bello, L. R., et al. (1998). The effect of depression on return to drinking: a prospective study. *Arch Gen Psychiatry* 55, 259–265. doi:10.1001/archpsyc.55.3.259.

Greengard, P., Jen, J., Nairn, A. C., and Stevens, C. F. (1991). Enhancement of the glutamate response by cAMP-dependent protein kinase in hippocampal neurons. *Science* 253, 1135–1138. doi:10.1126/science.1716001.

Griffin, O. H., and Webb, M. E. (2018). The Scheduling of Kratom and Selective Use of Data. *Journal of Psychoactive Drugs* 50, 114–120. doi:10.1080/02791072.2017.1371363.

Gross, J., and Gordon, D. B. (2019). The Strengths and Weaknesses of Current US Policy to Address Pain. *Am J Public Health* 109, 66–72. doi:10.2105/AJPH.2018.304746.

Grundmann, O. (2017). Patterns of Kratom use and health impact in the US-Results from an online survey. *Drug Alcohol Depend* 176, 63–70. doi:10.1016/j.drugalcdep.2017.03.007.

Grundmann, O., Brown, P. N., Henningfield, J., Swogger, M., and Walsh, Z. (2018). The therapeutic potential of kratom. *Addiction* 113, 1951–1953. doi:10.1111/add.14371.

Gupta, A., Gomes, I., Bobeck, E. N., Fakira, A. K., Massaro, N. P., Sharma, I., et al. (2016). Collybolide is a novel biased agonist of κ-opioid receptors with potent antipruritic activity. *PNAS* 113, 6041–6046. doi:10.1073/pnas.1521825113.

Gupta, T., Syed, Y. M., Revis, A. A., Miller, S. A., Martinez, M., Cohn, K. A., et al. (2008). Acute Effects of Acamprosate and MPEP on Ethanol Drinking-in-the-Dark in Male C57BL/6J Mice. *Alcoholism: Clinical and Experimental Research* 32, 1992–1998. doi:https://doi.org/10.1111/j.1530-0277.2008.00787.x.

Gurevich, E. V., Benovic, J. L., and Gurevich, V. V. (2002). Arrestin2 and arrestin3 are differentially expressed in the rat brain during postnatal development. *Neuroscience* 109, 421–436. doi:10.1016/s0306-4522(01)00511-5.

Gutridge, A. M., Chakraborty, S., Varga, B. R., Rhoda, E. S., French, A. R., Blaine, A. T., et al. (2021). Evaluation of Kratom Opioid Derivatives as Potential Treatment Option for Alcohol Use Disorder. *Frontiers in Pharmacology* 12, 2943. doi:10.3389/fphar.2021.764885.

Gutridge, A. M., Robins, M. T., Cassell, R. J., Uprety, R., Mores, K. L., Ko, M. J., et al. (2020). G protein-biased kratom-alkaloids and synthetic carfentanil-amide opioids as potential treatments for alcohol use disorder. *British Journal of Pharmacology* 177, 1497–1513. doi:https://doi.org/10.1111/bph.14913.

Guy, G. P. (2017). Vital Signs: Changes in Opioid Prescribing in the United States, 2006–2015. *MMWR Morb Mortal Wkly Rep* 66. doi:10.15585/mmwr.mm6626a4.

Haass-Koffler, C. L., Swift, R. M., and Leggio, L. (2018). Noradrenergic targets for the treatment of alcohol use disorder. *Psychopharmacology* 235, 1625–1634. doi:10.1007/s00213-018-4843-6.

Haffmans, J., and Dzoljic, M. R. (1983). Differential epileptogenic potentials of selective mu and delta opiate receptor agonists. *J Neural Transm* 57, 1–11. doi:10.1007/BF01250043.

Harding, S. D., Sharman, J. L., Faccenda, E., Southan, C., Pawson, A. J., Ireland, S., et al. (2018). The IUPHAR/BPS Guide to PHARMACOLOGY in 2018: updates and expansion to encompass the new guide to IMMUNOPHARMACOLOGY. *Nucleic Acids Res* 46, D1091–D1106. doi:10.1093/nar/gkx1121.

Harvey, A. L., Edrada-Ebel, R., and Quinn, R. J. (2015). The re-emergence of natural products for drug discovery in the genomics era. *Nat Rev Drug Discov* 14, 111–129. doi:10.1038/nrd4510.

Hasin, D., Liu, X., Nunes, E., McCloud, S., Samet, S., and Endicott, J. (2002). Effects of major depression on remission and relapse of substance dependence. *Arch Gen Psychiatry* 59, 375–380. doi:10.1001/archpsyc.59.4.375.

Hassan, Z., Muzaimi, M., Navaratnam, V., Yusoff, N. H. M., Suhaimi, F. W., Vadivelu, R., et al. (2013). From Kratom to mitragynine and its derivatives: physiological and behavioural effects related to use, abuse, and addiction. *Neurosci Biobehav Rev* 37, 138–151. doi:10.1016/j.neubiorev.2012.11.012.

Hauser, A. S., Attwood, M. M., Rask-Andersen, M., Schiöth, H. B., and Gloriam, D. E. (2017). Trends in GPCR drug discovery: new agents, targets and indications. *Nat Rev Drug Discov* 16, 829–842. doi:10.1038/nrd.2017.178.

Havemann-Reinecke, U. (2011). P01-50-Kratom and alcohol dependence: Clinical symptoms, withdrawal treatment and pharmacological mechanisms- A case report. *European Psychiatry* 26, 50. doi:10.1016/S0924-9338(11)71761-8.

Hayhurst, C. J., and Durieux, M. E. (2016). Differential Opioid Tolerance and Opioid-induced Hyperalgesia: A Clinical Reality. *Anesthesiology* 124, 483–488. doi:10.1097/ALN.0000000000000963.

Hazim, A. I., Ramanathan, S., Parthasarathy, S., Muzaimi, M., and Mansor, S. M. (2014). Anxiolytic-like effects of mitragynine in the open-field and elevated plus-maze tests in rats. *J Physiol Sci* 64, 161–169. doi:10.1007/s12576-014-0304-0.

He, L., Gooding, S. W., Lewis, E., Felth, L. C., Gaur, A., and Whistler, J. L. (2021). Pharmacological and genetic manipulations at the μ-opioid receptor reveal arrestin-3 engagement limits analgesic tolerance and does not exacerbate respiratory depression in mice. *Neuropsychopharmacol.*, 1–9. doi:10.1038/s41386-021-01054-x.

He, X. X., Nebert, D. W., Vasiliou, V., Zhu, H., and Shertzer, H. G. (1997). Genetic differences in alcohol drinking preference between inbred strains of mice. *Pharmacogenetics* 7, 223–233. doi:10.1097/00008571-199706000-00007.

Hedegaard, H. B., Warner, M., and Miniño, A. M. (2017). Drug Overdose Deaths in the United States, 1999-2016. *NCHS data brief* 294, 1–8.

Heilig, M., Thorsell, A., Sommer, W. H., Hansson, A. C., Ramchandani, V. A., George, D. T., et al. (2010). Translating the neuroscience of alcoholism into clinical treatments: from blocking the buzz to curing the blues. *Neurosci Biobehav Rev* 35, 334–344. doi:10.1016/j.neubiorev.2009.11.018.

Hemby, S. E., McIntosh, S., Leon, F., Cutler, S. J., and McCurdy, C. R. (2019). Abuse liability and therapeutic potential of the Mitragyna speciosa (kratom) alkaloids mitragynine and 7-hydroxymitragynine. *Addiction Biology* 24, 874–885. doi:10.1111/adb.12639.

Henningfield, J. E., Fant, R. V., and Wang, D. W. (2018). The abuse potential of kratom according the 8 factors of the controlled substances act: implications for regulation and research. *Psychopharmacology (Berl)* 235, 573–589. doi:10.1007/s00213-017-4813-4.

Henningfield, J. E., Grundmann, O., Babin, J. K., Fant, R. V., Wang, D. W., and Cone, E. J. (2019). Risk of death associated with kratom use compared to opioids. *Preventive Medicine* 128, 105851. doi:10.1016/j.ypmed.2019.105851.

Henry, A. G., White, I. J., Marsh, M., von Zastrow, M., and Hislop, J. N. (2011). The role of ubiquitination in lysosomal trafficking of δ-opioid receptors. *Traffic* 12, 170–184. doi:10.1111/j.1600-0854.2010.01145.x.

Herz, A. (1997). Endogenous opioid systems and alcohol addiction. *Psychopharmacology* 129, 99–111. doi:10.1007/s002130050169.

Hescheler, J., Rosenthal, W., Trautwein, W., and Schultz, G. (1987). The GTP-binding protein, Go, regulates neuronal calcium channels. *Nature* 325, 445–447. doi:10.1038/325445a0.

Hill, R., Disney, A., Conibear, A., Sutcliffe, K., Dewey, W., Husbands, S., et al. (2018). The novel μ-opioid receptor agonist PZM21 depresses respiration and induces tolerance to antinociception. *British Journal of Pharmacology* 175, 2653–2661. doi:10.1111/bph.14224.

Hill, R., Lyndon, A., Withey, S., Roberts, J., Kershaw, Y., MacLachlan, J., et al. (2016). Ethanol Reversal of Tolerance to the Respiratory Depressant Effects of Morphine. *Neuropsychopharmacology* 41, 762–773. doi:10.1038/npp.2015.201.

Hill, S. J. (2006). G-protein-coupled receptors: past, present and future. *Br J Pharmacol* 147, S27–S37. doi:10.1038/sj.bjp.0706455.

Ho, A., and Nair, S. (2018). “Global Chronic Pain: Public and Population Health Responses,” in *Developments in Neuroethics and Bioethics* Pain Neuroethics and Bioethics., eds. D. Z. Buchman and K. D. Davis (Academic Press), 171–189. doi:10.1016/bs.dnb.2018.08.009.

Holt, S. R., and Tobin, D. G. (2018). Pharmacotherapy for Alcohol Use Disorder. *The Medical clinics of North America* 102, 653–666. doi:10.1016/j.mcna.2018.02.008.

Hong, E. J., Rice, K. C., Calderon, S., Woods, J. H., and Traynor, J. R. (1998). Convulsive Behavior of Nonpeptide δ-Opioid Ligands:Comparison of SNC80 and BW373U86 in Mice. *Analgesia* 3, 269–276. doi:10.3727/107156998819565947.

Huang, W., Manglik, A., Venkatakrishnan, A. J., Laeremans, T., Feinberg, E. N., Sanborn, A. L., et al. (2015). Structural insights into μ-opioid receptor activation. *Nature* 524, 315–321. doi:10.1038/nature14886.

Hughes, J., Smith, T. W., Kosterlitz, H. W., Fothergill, L. A., Morgan, B. A., and Morris, H. R. (1975). Identification of two related pentapeptides from the brain with potent opiate agonist activity. *Nature* 258, 577–579. doi:10.1038/258577a0.

Hughes, R. L. (2019). Fatal combination of mitragynine and quetiapine - a case report with discussion of a potential herb-drug interaction. *Forensic Sci Med Pathol* 15, 110–113. doi:10.1007/s12024-018-0049-9.

Hurley, R. W., and Hammond, D. L. (2000). The analgesic effects of supraspinal mu and delta opioid receptor agonists are potentiated during persistent inflammation. *J Neurosci* 20, 1249–1259.

Hylands-White, N., Duarte, R. V., and Raphael, J. H. (2017). An overview of treatment approaches for chronic pain management. *Rheumatol Int* 37, 29–42. doi:10.1007/s00296-016-3481-8.

Ilmie, M. U., Jaafar, H., Mansor, S. M., and Abdullah, J. M. (2015). Subchronic toxicity study of standardized methanolic extract of Mitragyna speciosa Korth in Sprague-Dawley Rats. *Front Neurosci* 9, 189. doi:10.3389/fnins.2015.00189.

Institute of Medicine (US) Committee on Advancing Pain Research, Care, and Education (2011). *Relieving Pain in America: A Blueprint for Transforming Prevention, Care, Education, and Research*. Washington (DC): National Academies Press (US) Available at: http://www.ncbi.nlm.nih.gov/books/NBK91497/ [Accessed October 31, 2021].

Inui, T., Wang, Y., Nikolic, D., Smith, D. C., Franzblau, S. G., and Pauli, G. F. (2010). Sesquiterpenes from Oplopanax horridus. *J Nat Prod* 73, 563–567. doi:10.1021/np900674d.

Ito, Y. (2005). Golden rules and pitfalls in selecting optimum conditions for high-speed counter-current chromatography. *J Chromatogr A* 1065, 145–168. doi:10.1016/j.chroma.2004.12.044.

Ito, Y. (2013). pH-zone-refining counter-current chromatography: origin, mechanism, procedure and applications. *J Chromatogr A* 1271, 71–85. doi:10.1016/j.chroma.2012.11.024.

Ito, Y., and Ma, Y. (1996). pH-zone-refining countercurrent chromatography. *J Chromatogr A* 753, 1–36. doi:10.1016/s0021-9673(96)00565-1.

Jiang, M., and Bajpayee, N. S. (2009). Molecular Mechanisms of Go Signaling. *Neurosignals* 17, 23–41. doi:10.1159/000186688.

Jiang, Q., Mosberg, H. I., and Porreca, F. (1990). Antinociceptive effects of [D-Ala2]deltorphin II, a highly selective δ agonist invivo. *Life Sciences* 47, PL43–PL47. doi:10.1016/0024-3205(90)90545-3.

Jokela, R., and Lounasmaa, M. (1996). [1]H- and [13]C-NMR Spectral Data of Five Sarpagine-type Alkaloids. *Heterocycles* 43, 1015–1020.

Jonas, D. E., Amick, H. R., Feltner, C., Bobashev, G., Thomas, K., Wines, R., et al. (2014). Pharmacotherapy for adults with alcohol use disorders in outpatient settings: a systematic review and meta-analysis. *JAMA* 311, 1889–1900. doi:10.1001/jama.2014.3628.

Jones, M. R., Viswanath, O., Peck, J., Kaye, A. D., Gill, J. S., and Simopoulos, T. T. (2018). A Brief History of the Opioid Epidemic and Strategies for Pain Medicine. *Pain Ther* 7, 13–21. doi:10.1007/s40122-018-0097-6.

Jutkiewicz, E. M., Baladi, M. G., Folk, J. E., Rice, K. C., and Woods, J. H. (2006). The Convulsive and Electroencephalographic Changes Produced by Nonpeptidic δ-Opioid Agonists in Rats: Comparison with Pentylenetetrazol. *J Pharmacol Exp Ther* 317, 1337–1348. doi:10.1124/jpet.105.095810.

Jutkiewicz, E. M., Eller, E. B., Folk, J. E., Rice, K. C., Traynor, J. R., and Woods, J. H. (2004). δ-Opioid Agonists: Differential Efficacy and Potency of SNC80, Its 3-OH (SNC86) and 3-Desoxy (SNC162) Derivatives in Sprague-Dawley Rats. *J Pharmacol Exp Ther* 309, 173–181. doi:10.1124/jpet.103.061242.

Jutkiewicz, E. M., Traynor, J. R., Woods, J. H., and Rice, K. C. (2005). Separation of the convulsions and antidepressant-like effects produced by the delta-opioid agonist SNC80 in rats. *Psychopharmacology (Berl)* 182, 588–596. doi:10.1007/s00213-005-0138-9.

Kakidani, H., Furutani, Y., Takahashi, H., Noda, M., Morimoto, Y., Hirose, T., et al. (1982). Cloning and sequence analysis of cDNA for porcine beta-neo-endorphin/dynorphin precursor. *Nature* 298, 245–249. doi:10.1038/298245a0.

Kamble, S. H., Berthold, E. C., King, T. I., Raju Kanumuri, S. R., Popa, R., Herting, J. R., et al. (2021). Pharmacokinetics of Eleven Kratom Alkaloids Following an Oral Dose of Either Traditional or Commercial Kratom Products in Rats. *J. Nat. Prod.* 84, 1104–1112. doi:10.1021/acs.jnatprod.0c01163.

Kamble, S. H., León, F., King, T. I., Berthold, E. C., Lopera-Londoño, C., Siva Rama Raju, K., et al. (2020). Metabolism of a Kratom Alkaloid Metabolite in Human Plasma Increases Its Opioid Potency and Efficacy. *ACS Pharmacol. Transl. Sci.* doi:10.1021/acsptsci.0c00075.

Kamdar, N. K., Miller, S. A., Syed, Y. M., Bhayana, R., Gupta, T., and Rhodes, J. S. (2007). Acute effects of Naltrexone and GBR 12909 on ethanol drinking-in-the-dark in C57BL/6J mice. *Psychopharmacology* 192, 207–217. doi:10.1007/s00213-007-0711-5.

Kane, B. E., Svensson, B., and Ferguson, D. M. (2006). Molecular recognition of opioid receptor ligands. *AAPS J* 8, E126-137. doi:10.1208/aapsj080115.

Kapoor, A., Provasi, D., and Filizola, M. (2020). Atomic-Level Characterization of the Methadone-Stabilized Active Conformation of μ-Opioid Receptor. *Mol Pharmacol* 98, 475–486. doi:10.1124/mol.119.119339.

Katada, T., Oinuma, M., and Ui, M. (1986). Two guanine nucleotide-binding proteins in rat brain serving as the specific substrate of islet-activating protein, pertussis toxin. Interaction of the alpha-subunits with beta gamma-subunits in development of their biological activities. *J Biol Chem* 261, 8182–8191.

Keith, D. E., Anton, B., Murray, S. R., Zaki, P. A., Chu, P. C., Lissin, D. V., et al. (1998). μ-Opioid Receptor Internalization: Opiate Drugs Have Differential Effects on a Conserved Endocytic Mechanism In Vitro and in the Mammalian Brain. *Mol Pharmacol* 53, 377–384. doi:10.1124/mol.53.3.377.

Keith, D. E., Murray, S. R., Zaki, P. A., Chu, P. C., Lissin, D. V., Kang, L., et al. (1996). Morphine Activates Opioid Receptors without Causing Their Rapid Internalization *. *Journal of Biological Chemistry* 271, 19021–19024. doi:10.1074/jbc.271.32.19021.

Kelly, B., Hollingsworth, S. A., Blakemore, D. C., Owen, R. M., Storer, R. I., Swain, N. A., et al. (2021). Delineating the Ligand–Receptor Interactions That Lead to Biased Signaling at the μ-Opioid Receptor. *J. Chem. Inf. Model.* 61, 3696–3707. doi:10.1021/acs.jcim.1c00585.

Kenakin, T. (2001). Inverse, protean, and ligand-selective agonism: matters of receptor conformation. *The FASEB Journal* 15, 598–611. doi:10.1096/fj.00-0438rev.

Kenakin, T. (2004). Principles: Receptor theory in pharmacology. *Trends in Pharmacological Sciences* 25, 186–192. doi:10.1016/j.tips.2004.02.012.

Kenakin, T. (2011). Functional selectivity and biased receptor signaling. *J Pharmacol Exp Ther* 336, 296–302. doi:10.1124/jpet.110.173948.

Kenakin, T. (2015). The Effective Application of Biased Signaling to New Drug Discovery. *Mol Pharmacol* 88, 1055–1061. doi:10.1124/mol.115.099770.

Kenakin, T., and Christopoulos, A. (2013). Signalling bias in new drug discovery: detection, quantification and therapeutic impact. *Nat Rev Drug Discov* 12, 205–216. doi:10.1038/nrd3954.

Kenakin, T., Watson, C., Muniz-Medina, V., Christopoulos, A., and Novick, S. (2012). A Simple Method for Quantifying Functional Selectivity and Agonist Bias. *ACS Chem Neurosci* 3, 193–203. doi:10.1021/cn200111m.

Khan, S. M., Sleno, R., Gora, S., Zylbergold, P., Laverdure, J.-P., Labbé, J.-C., et al. (2013). The expanding roles of Gβγ subunits in G protein-coupled receptor signaling and drug action. *Pharmacol Rev* 65, 545–577. doi:10.1124/pr.111.005603.

Kieffer, B. L., Befort, K., Gaveriaux-Ruff, C., and Hirth, C. G. (1992). The delta-opioid receptor: isolation of a cDNA by expression cloning and pharmacological characterization. *PNAS* 89, 12048–12052. doi:10.1073/pnas.89.24.12048.

Kilkenny, C., Browne, W., Cuthill, I. C., Emerson, M., and Altman, D. G. (2010a). Animal research: Reporting in vivo experiments: The ARRIVE guidelines: Animal research: reporting in vivo experiments the ARRIVE guidelines. *British Journal of Pharmacology* 160, 1577–1579. doi:10.1111/j.1476-5381.2010.00872.x.

Kilkenny, C., Browne, W. J., Cuthill, I. C., Emerson, M., and Altman, D. G. (2010b). Improving Bioscience Research Reporting: The ARRIVE Guidelines for Reporting Animal Research. *PLOS Biology* 8, e1000412. doi:10.1371/journal.pbio.1000412.

Killgore, W. D. S., Cloonan, S. A., Taylor, E. C., Lucas, D. A., and Dailey, N. S. (2021). Alcohol dependence during COVID-19 lockdowns. *Psychiatry Research* 296, 113676. doi:10.1016/j.psychres.2020.113676.

Kim, J. A., Bartlett, S., He, L., Nielsen, C. K., Chang, A. M., Kharazia, V., et al. (2008). Morphine-Induced Receptor Endocytosis in a Novel Knockin Mouse Reduces Tolerance and Dependence. *Current Biology* 18, 129–135. doi:10.1016/j.cub.2007.12.057.

Kim, S.-G., Han, B.-D., Park, J.-M., Kim, M.-J., and Stromberg, M. F. (2004). Effect of the combination of naltrexone and acamprosate on alcohol intake in mice. *Psychiatry Clin Neurosci* 58, 30–36. doi:10.1111/j.1440-1819.2004.01189.x.

Kishioka, S., Kiguchi, N., Kobayashi, Y., Yamamoto, C., Saika, F., Wakida, N., et al. (2013). Pharmacokinetic evidence for the long-lasting effect of nor-binaltorphimine, a potent kappa opioid receptor antagonist, in mice. *Neuroscience Letters* 552, 98–102. doi:10.1016/j.neulet.2013.07.040.

Kivell, B., and Prisinzano, T. E. (2010). Kappa opioids and the modulation of pain. *Psychopharmacology (Berl)* 210, 109–119. doi:10.1007/s00213-010-1819-6.

Kliewer, A., Gillis, A., Hill, R., Schmiedel, F., Bailey, C., Kelly, E., et al. (2020). Morphine-induced respiratory depression is independent of β-arrestin2 signalling. *Br J Pharmacol* 177, 2923–2931. doi:10.1111/bph.15004.

Kliewer, A., Schmiedel, F., Sianati, S., Bailey, A., Bateman, J. T., Levitt, E. S., et al. (2019). Phosphorylation-deficient G-protein-biased μ-opioid receptors improve analgesia and diminish tolerance but worsen opioid side effects. *Nature Communications* 10, 1–11. doi:10.1038/s41467-018-08162-1.

Ko, M. J., Chiang, T., Mukadam, A. A., Mulia, G. E., Gutridge, A. M., Lin, A., et al. (2021). β-Arrestin-dependent ERK signaling reduces anxiety-like and conditioned fear-related behaviors in mice. *Sci Signal* 14, eaba0245. doi:10.1126/scisignal.aba0245.

Kobayashi, I., Shibasaki, H., Takahashi, K., Tohyama, K., Kurachi, Y., Ito, H., et al. (1990). Purification and characterization of five different alpha subunits of guanine-nucleotide-binding proteins in bovine brain membranes. Their physiological properties concerning the activities of adenylate cyclase and atrial muscarinic K+ channels. *Eur J Biochem* 191, 499–506. doi:10.1111/j.1432-1033.1990.tb19149.x.

Kong, W. M., Chik, Z., Ramachandra, M., Subramaniam, U., Aziddin, R. E. R., and Mohamed, Z. (2011). Evaluation of the effects of Mitragyna speciosa alkaloid extract on cytochrome P450 enzymes using a high throughput assay. *Molecules* 16, 7344–7356. doi:10.3390/molecules16097344.

Konno, K., Picolo, G., Gutierrez, V. P., Brigatte, P., Zambelli, V. O., Camargo, A. C. M., et al. (2008). Crotalphine, a novel potent analgesic peptide from the venom of the South American rattlesnake Crotalus durissus terrificus. *Peptides* 29, 1293–1304. doi:10.1016/j.peptides.2008.04.003.

Koob, G. F. (2003). Alcoholism: allostasis and beyond. *Alcohol Clin Exp Res* 27, 232–243. doi:10.1097/01.ALC.0000057122.36127.C2.

Koob, G. F., and Volkow, N. D. (2016). Neurobiology of addiction: a neurocircuitry analysis. *Lancet Psychiatry* 3, 760–773. doi:10.1016/S2215-0366(16)00104-8.

Kosterlitz, H. W. (1985). The Wellcome Foundation lecture, 1982. Opioid peptides and their receptors. *Proc R Soc Lond B Biol Sci* 225, 27–40. doi:10.1098/rspb.1985.0048.

Kotland, A., Chollet, S., Diard, C., Autret, J.-M., Meucci, J., Renault, J.-H., et al. (2016). Industrial case study on alkaloids purification by pH-zone refining centrifugal partition chromatography. *J Chromatogr A* 1474, 59–70. doi:10.1016/j.chroma.2016.10.039.

Kotlińska, J., and Langwiński, R. (1986). Audiogenic seizures during ethanol withdrawal can be blocked by a delta opioid agonist. *Drug Alcohol Depend* 18, 361–367. doi:10.1016/0376-8716(86)90100-6.

Kovoor, A., Nappey, V., Kieffer, B. L., and Chavkin, C. (1997). Mu and delta opioid receptors are differentially desensitized by the coexpression of beta-adrenergic receptor kinase 2 and beta-arrestin 2 in xenopus oocytes. *J Biol Chem* 272, 27605–27611. doi:10.1074/jbc.272.44.27605.

Kozasa, T., Jiang, X., Hart, M. J., Sternweis, P. M., Singer, W. D., Gilman, A. G., et al. (1998). p115 RhoGEF, a GTPase activating protein for Galpha12 and Galpha13. *Science* 280, 2109–2111. doi:10.1126/science.280.5372.2109.

Kranzler, H. R., and Soyka, M. (2018). Diagnosis and Pharmacotherapy of Alcohol Use Disorder: A Review. *JAMA* 320, 815–824. doi:10.1001/jama.2018.11406.

Kreek, M. J., Borg, L., Ducat, E., and Ray, B. (2010). Pharmacotherapy in the Treatment of Addiction: Methadone. *J Addict Dis* 29, 200–216. doi:10.1080/10550881003684798.

Krishnan-Sarin, S., Jing, S. L., Kurtz, D. L., Zweifel, M., Portoghese, P. S., Li, T. K., et al. (1995a). The delta opioid receptor antagonist naltrindole attenuates both alcohol and saccharin intake in rats selectively bred for alcohol preference. *Psychopharmacology (Berl)* 120, 177–185. doi:10.1007/BF02246191.

Krishnan-Sarin, S., Portoghese, P. S., Li, T. K., and Froehlich, J. C. (1995b). The delta 2-opioid receptor antagonist naltriben selectively attenuates alcohol intake in rats bred for alcohol preference. *Pharmacol Biochem Behav* 52, 153–159. doi:10.1016/0091-3057(95)00080-g.

Kruegel, A. C., Gassaway, M. M., Kapoor, A., Váradi, A., Majumdar, S., Filizola, M., et al. (2016). Synthetic and Receptor Signaling Explorations of the Mitragyna Alkaloids: Mitragynine as an Atypical Molecular Framework for Opioid Receptor Modulators. *J. Am. Chem. Soc.* 138, 6754–6764. doi:10.1021/jacs.6b00360.

Kruegel, A. C., and Grundmann, O. (2018). The medicinal chemistry and neuropharmacology of kratom: A preliminary discussion of a promising medicinal plant and analysis of its potential for abuse. *Neuropharmacology* 134, 108–120. doi:10.1016/j.neuropharm.2017.08.026.

Kruegel, A. C., Uprety, R., Grinnell, S. G., Langreck, C., Pekarskaya, E. A., Le Rouzic, V., et al. (2019). 7-Hydroxymitragynine Is an Active Metabolite of Mitragynine and a Key Mediator of Its Analgesic Effects. *ACS Cent. Sci.* 5, 992–1001. doi:10.1021/acscentsci.9b00141.

Krystal, A. D., Pizzagalli, D. A., Smoski, M., Mathew, S. J., Nurnberger, J., Lisanby, S. H., et al. (2020). A randomized proof-of-mechanism trial applying the 'fast-fail' approach to evaluating κ-opioid antagonism as a treatment for anhedonia. *Nat Med* 26, 760–768. doi:10.1038/s41591-020-0806-7.

Kumagai, H., Ebata, T., Takamori, K., Muramatsu, T., Nakamoto, H., and Suzuki, H. (2010). Effect of a novel kappa-receptor agonist, nalfurafine hydrochloride, on severe itch in 337 haemodialysis patients: a Phase III, randomized, double-blind, placebo-controlled study. *Nephrol Dial Transplant* 25, 1251–1257. doi:10.1093/ndt/gfp588.

Kumarnsit, E., Keawpradub, N., and Nuankaew, W. (2007). Effect of Mitragyna speciosa aqueous extract on ethanol withdrawal symptoms in mice. *Fitoterapia* 78, 182–185. doi:10.1016/j.fitote.2006.11.012.

Lagerström, M. C., and Schiöth, H. B. (2008). Structural diversity of G protein-coupled receptors and significance for drug discovery. *Nat Rev Drug Discov* 7, 339–357. doi:10.1038/nrd2518.

Lambert, D. G. (2008). The nociceptin/orphanin FQ receptor: a target with broad therapeutic potential. *Nat Rev Drug Discov* 7, 694–710. doi:10.1038/nrd2572.

Lamberts, J. T., Jutkiewicz, E. M., Mortensen, R. M., and Traynor, J. R. (2011). μ-Opioid receptor coupling to Gα(o) plays an important role in opioid antinociception. *Neuropsychopharmacology* 36, 2041–2053. doi:10.1038/npp.2011.91.

Lamberts, J. T., Smith, C. E., Li, M.-H., Ingram, S. L., Neubig, R. R., and Traynor, J. R. (2013). Differential control of opioid antinociception to thermal stimuli in a knock-in mouse expressing regulator of G-protein signaling-insensitive Gαo protein. *J Neurosci* 33, 4369–4377. doi:10.1523/JNEUROSCI.5470-12.2013.

Land, B. B., Bruchas, M. R., Schattauer, S., Giardino, W. J., Aita, M., Messinger, D., et al. (2009). Activation of the kappa opioid receptor in the dorsal raphe nucleus mediates the aversive effects of stress and reinstates drug seeking. *Proc Natl Acad Sci U S A* 106, 19168–19173. doi:10.1073/pnas.0910705106.

Le Merrer, J., Becker, J. A. J., Befort, K., and Kieffer, B. L. (2009). Reward Processing by the Opioid System in the Brain. *Physiological Reviews* 89, 1379–1412. doi:10.1152/physrev.00005.2009.

Lecoq, I., Marie, N., Jauzac, Ph., and Allouche, S. (2004). Different Regulation of Human δ-Opioid Receptors by SNC-80 [(+)-4-[(α *R*)-α-((2 *S* ,5 *R*)-4-Allyl-2,5-dimethyl-1-piperazinyl)-3-methoxybenzyl]- *N* , *N* -diethylbenzamide] and Endogenous Enkephalins. *J Pharmacol Exp Ther* 310, 666–677. doi:10.1124/jpet.103.063958.

Lee, M. R., Hinton, D. J., Wu, J., Mishra, P. K., Port, J. D., Macura, S. I., et al. (2011). Acamprosate reduces ethanol drinking behaviors and alters the metabolite profile in mice lacking ENT1. *Neurosci Lett* 490, 90–95. doi:10.1016/j.neulet.2010.12.033.

Lefkowitz, R. J. (2013). A Brief History of G-Protein Coupled Receptors (Nobel Lecture). *Angew. Chem. Int. Ed.* 52, 6366–6378. doi:10.1002/anie.201301924.

Lemel, L., Lane, J. R., and Canals, M. (2020). GRKs as Key Modulators of Opioid Receptor Function. *Cells* 9, 2400. doi:10.3390/cells9112400.

León, F., Obeng, S., Mottinelli, M., Chen, Y., King, T. I., Berthold, E. C., et al. (2021). Activity of Mitragyna speciosa ("Kratom") Alkaloids at Serotonin Receptors. *J. Med. Chem.* 64, 13510–13523. doi:10.1021/acs.jmedchem.1c00726.

Lett, B. T. (1989). Repeated exposures intensify rather than diminish the rewarding effects of amphetamine, morphine, and cocaine. *Psychopharmacology (Berl)* 98, 357–362. doi:10.1007/BF00451687.

Li, Y., Liu, X., Liu, C., Kang, J., Yang, J., Pei, G., et al. (2009). Improvement of morphine-mediated analgesia by inhibition of β-arrestin2 expression in mice periaqueductal gray matter. *Int J Mol Sci* 10, 954–963. doi:10.3390/ijms10030954.

Ling, G. S., Paul, D., Simantov, R., and Pasternak, G. W. (1989). Differential development of acute tolerance to analgesia, respiratory depression, gastrointestinal transit and hormone release in a morphine infusion model. *Life Sci* 45, 1627–1636. doi:10.1016/0024-3205(89)90272-5.

Litten, R. Z., Egli, M., Heilig, M., Cui, C., Fertig, J. B., Ryan, M. L., et al. (2012). Medications development to treat alcohol dependence: a vision for the next decade. *Addict Biol* 17, 513–527. doi:10.1111/j.1369-1600.2012.00454.x.

Lledo, P. M., Homburger, V., Bockaert, J., and Vincent, J.-D. (1992). Differential G protein-mediated coupling of D2 dopamine receptors to K+ and Ca2+ currents in rat anterior pituitary cells. *Neuron* 8, 455–463. doi:10.1016/0896-6273(92)90273-G.

Lovell, K. M., Frankowski, K. J., Stahl, E. L., Slauson, S. R., Yoo, E., Prisinzano, T. E., et al. (2015). Structure–Activity Relationship Studies of Functionally Selective Kappa Opioid Receptor Agonists that Modulate ERK 1/2 Phosphorylation While Preserving G Protein Over βArrestin2 Signaling Bias. *ACS Chem. Neurosci.* 6, 1411–1419. doi:10.1021/acschemneuro.5b00092.

Lovell, K. M., Simpson, D. S., Cunningham, C. W., and Prisinzano, T. E. (2009). Utilizing nature as a source of new probes for opioid pharmacology. *Future Med Chem* 1, 285–301. doi:10.4155/fmc.09.22.

Lutz, P.-E., and Kieffer, B. L. (2013). Opioid receptors: distinct roles in mood disorders. *Trends in Neurosciences* 36, 195–206. doi:10.1016/j.tins.2012.11.002.

Macey, T. A., Lowe, J. D., and Chavkin, C. (2006). Mu opioid receptor activation of ERK1/2 is GRK3 and arrestin dependent in striatal neurons. *J Biol Chem* 281, 34515–34524. doi:10.1074/jbc.M604278200.

Mafi, A., Kim, S.-K., and Goddard, W. A. (2020a). Mechanism of β-arrestin recruitment by the μ-opioid G protein-coupled receptor. *PNAS* 117, 16346–16355. doi:10.1073/pnas.1918264117.

Mafi, A., Kim, S.-K., and Goddard, W. A. (2020b). The atomistic level structure for the activated human κ-opioid receptor bound to the full Gi protein and the MP1104 agonist. *PNAS* 117, 5836–5843. doi:10.1073/pnas.1910006117.

Maisel, N. C., Blodgett, J. C., Wilbourne, P. L., Humphreys, K., and Finney, J. W. (2013). Meta-analysis of naltrexone and acamprosate for treating alcohol use disorders: when are these medications most helpful? *Addiction* 108, 275–293. doi:10.1111/j.1360-0443.2012.04054.x.

Majumdar, S., and Devi, L. A. (2018). Strategy for making safer opioids bolstered. *Nature* 553, 286–288. doi:10.1038/d41586-018-00045-1.

Makary, M. A., Overton, H. N., and Wang, P. (2017). Overprescribing is major contributor to opioid crisis. *BMJ* 359. doi:10.1136/bmj.j4792.

Manda, V. K., Avula, B., Dale, O. R., Ali, Z., Khan, I. A., Walker, L. A., et al. (2017). PXR mediated induction of CYP3A4, CYP1A2, and P-gp by Mitragyna speciosa and its alkaloids. *Phytother Res* 31, 1935–1945. doi:10.1002/ptr.5942.

Manglik, A., Kruse, A. C., Kobilka, T. S., Thian, F. S., Mathiesen, J. M., Sunahara, R. K., et al. (2012). Crystal structure of the μ-opioid receptor bound to a morphinan antagonist. *Nature* 485, 321–326. doi:10.1038/nature10954.

Manglik, A., Lin, H., Aryal, D. K., McCorvy, J. D., Dengler, D., Corder, G., et al. (2016). Structure-based discovery of opioid analgesics with reduced side effects. *Nature* 537, 185–190. doi:10.1038/nature19112.

Manhapra, A., Quinones, L., and Rosenheck, R. (2016). Characteristics of veterans receiving buprenorphine vs. methadone for opioid use disorder nationally in the Veterans Health Administration. *Drug Alcohol Depend* 160, 82–89. doi:10.1016/j.drugalcdep.2015.12.035.

Manhapra, A., Rosenheck, R., and Fiellin, D. A. (2017). Opioid substitution treatment is linked to reduced risk of death in opioid use disorder. *BMJ* 357, j1947. doi:10.1136/bmj.j1947.

Manning, B. H., Morgan, M. J., and Franklin, K. B. (1994). Morphine analgesia in the formalin test: evidence for forebrain and midbrain sites of action. *Neuroscience* 63, 289–294. doi:10.1016/0306-4522(94)90023-x.

Margolis, E. B., Fields, H. L., Hjelmstad, G. O., and Mitchell, J. M. (2008). δ-Opioid Receptor Expression in the Ventral Tegmental Area Protects Against Elevated Alcohol Consumption. *J. Neurosci.* 28, 12672–12681. doi:10.1523/JNEUROSCI.4569-08.2008.

Margolis, E. B., Fujita, W., Devi, L. A., and Fields, H. L. (2017). Two delta opioid receptor subtypes are functional in single ventral tegmental area neurons, and can interact with the mu opioid receptor. *Neuropharmacology* 123, 420–432. doi:10.1016/j.neuropharm.2017.06.019.

Marie, N., Lecoq, I., Jauzac, P., and Allouche, S. (2003). Differential sorting of human delta-opioid receptors after internalization by peptide and alkaloid agonists. *J Biol Chem* 278, 22795–22804. doi:10.1074/jbc.M300084200.

Marmolejo-Valencia, A. F., Madariaga-Mazón, A., and Martinez-Mayorga, K. (2021). Bias-inducing allosteric binding site in mu-opioid receptor signaling. *SN Applied Sciences* 3, undefined-undefined. doi:10.1007/s42452-021-04505-8.

Marshall, B., Bland, M. K., Hulla, R., and Gatchel, R. J. (2019). Considerations in addressing the opioid epidemic and chronic pain within the USA. *Pain Manag* 9, 131–138. doi:10.2217/pmt-2018-0070.

Massotte, D., Brillet, K., Kieffer, B., and Milligan, G. (2002). Agonists activate Gi1 alpha or Gi2 alpha fused to the human mu opioid receptor differently. *J Neurochem* 81, 1372–1382. doi:10.1046/j.1471-4159.2002.00946.x.

Matsumoto, K., Hatori, Y., Murayama, T., Tashima, K., Wongseripipatana, S., Misawa, K., et al. (2006). Involvement of mu-opioid receptors in antinociception and inhibition of gastrointestinal transit induced by 7-hydroxymitragynine, isolated from Thai herbal medicine Mitragyna speciosa. *Eur J Pharmacol* 549, 63–70. doi:10.1016/j.ejphar.2006.08.013.

Matsumoto, K., Horie, S., Ishikawa, H., Takayama, H., Aimi, N., Ponglux, D., et al. (2004). Antinociceptive effect of 7-hydroxymitragynine in mice: Discovery of an orally active opioid analgesic from the Thai medicinal herb Mitragyna speciosa. *Life Sciences* 74, 2143–2155. doi:10.1016/j.lfs.2003.09.054.

Matsumoto, K., Horie, S., Takayama, H., Ishikawa, H., Aimi, N., Ponglux, D., et al. (2005). Antinociception, tolerance and withdrawal symptoms induced by 7-hydroxymitragynine, an alkaloid from the Thai medicinal herb Mitragyna speciosa. *Life Sci* 78, 2–7. doi:10.1016/j.lfs.2004.10.086.

Matsumoto, K., Takayama, H., Narita, M., Nakamura, A., Suzuki, M., Suzuki, T., et al. (2008). MGM-9 [(E)-methyl 2-(3-ethyl-7a,12a-(epoxyethanoxy)-9-fluoro-1,2,3,4,6,7,12,12b-octahydro-8-methoxyindolo[2,3-a]quinolizin-2-yl)-3-methoxyacrylate], a derivative of the indole alkaloid mitragynine: a novel dual-acting mu- and kappa-opioid agonist with potent antinociceptive and weak rewarding effects in mice. *Neuropharmacology* 55, 154–165. doi:10.1016/j.neuropharm.2008.05.003.

Matthes, H. W. D., Maldonado, R., Simonin, F., Valverde, O., Slowe, S., Kitchen, I., et al. (1996). Loss of morphine-induced analgesia, reward effect and withdrawal symptoms in mice lacking the μ-opioid-receptor gene. *Nature* 383, 819–823. doi:10.1038/383819a0.

Mattick, R. P., Breen, C., Kimber, J., and Davoli, M. (2009). Methadone maintenance therapy versus no opioid replacement therapy for opioid dependence. *Cochrane Database Syst Rev*, CD002209. doi:10.1002/14651858.CD002209.pub2.

Maurya, A., Gupta, S., and Srivastava, S. K. (2013). Large-scale separation of antipsychotic alkaloids from Rauwolfia tetraphylla L. by pH-zone-refining fast centrifugal partition chromatography. *J Sep Sci* 36, 407–413. doi:10.1002/jssc.201200273.

May, C. N., Dashwood, M. R., Whitehead, C. J., and Mathias, C. J. (1989). Differential cardiovascular and respiratory responses to central administration of selective opioid agonists in conscious rabbits: correlation with receptor distribution. *Br J Pharmacol* 98, 903–913. doi:10.1111/j.1476-5381.1989.tb14620.x.

McDonald, J., and Lambert, D. (2015). Opioid receptors. *BJA Education* 15, 219–224. doi:10.1093/bjaceaccp/mku041.

McHugh, R. K., and Weiss, R. D. (2019). Alcohol Use Disorder and Depressive Disorders. *Alcohol Res* 40, arcr.v40.1.01. doi:10.35946/arcr.v40.1.01.

McNally, G. P., and Akil, H. (2002). *Opioid peptides and their receptors: overview and function in pain modulation.* Philadelphia: Lippincott Williams & Wilkins.

McWhirter, L., and Morris, S. (2010). A case report of inpatient detoxification after kratom (Mitragyna speciosa) dependence. *Eur Addict Res* 16, 229–231. doi:10.1159/000320288.

Menzies, J. R. W., Paterson, S. J., Duwiejua, M., and Corbett, A. D. (1998). Opioid activity of alkaloids extracted from Picralima nitida (fam. Apocynaceae). *European Journal of Pharmacology* 350, 101–108. doi:10.1016/s0014-2999(98)00232-5.

Mercadante, S., Casuccio, A., Tirelli, W., and Giarratano, A. (2009). Equipotent doses to switch from high doses of opioids to transdermal buprenorphine. *Support Care Cancer* 17, 715–718. doi:10.1007/s00520-008-0546-6.

Merskey, H., Bond, M. R., Boyd, D. B., Carmon, A., Deathe, A. B., Dehen, H., et al. (1986). International Association for the Study of Pain, Subcommittee on Taxonomy. *Classification of Chronic Pain: Descriptions of Chronic Pain Syndromes and Definitions of Pain Terms*.

Middaugh, L. D., and Bandy, A. L. (2000). Naltrexone effects on ethanol consumption and response to ethanol conditioned cues in C57BL/6 mice. *Psychopharmacology (Berl.)* 151, 321–327. doi:10.1007/s002130000479.

Millan, M. J. (1999). The induction of pain: an integrative review. *Prog Neurobiol* 57, 1–164. doi:10.1016/s0301-0082(98)00048-3.

Millan, M. J. (2002). Descending control of pain. *Prog Neurobiol* 66, 355–474. doi:10.1016/s0301-0082(02)00009-6.

Minami, M., and Satoh, M. (1995). Molecular biology of the opioid receptors: structures, functions and distributions. *Neurosci Res* 23, 121–145. doi:10.1016/0168-0102(95)00933-k.

Minami, M., Toya, T., Katao, Y., Maekawa, K., Nakamura, S., Onogi, T., et al. (1993). Cloning and expression of a cDNA for the rat kappa-opioid receptor. *FEBS Lett* 329, 291–295. doi:10.1016/0014-5793(93)80240-u.

Minneman, K. P., and Iversen, I. L. (1976). Enkephalin and opiate narcotics increase cyclic GMP accumulation in slices of rat neostriatum. *Nature* 262, 313–314. doi:10.1038/262313a0.

Møller, B. L., Seedorff, L., and Nartey, F. (1972). Alkaloids of Picralima nitida. *Phytochemistry* 11, 2620–2621. doi:10.1016/S0031-9422(00)88556-8.

Mollereau, C., Parmentier, M., Mailleux, P., Butour, J.-L., Moisand, C., Chalon, P., et al. (1994). ORL1, a novel member of the opioid receptor family: Cloning, functional expression and localization. *FEBS Letters* 341, 33–38. doi:10.1016/0014-5793(94)80235-1.

Mores, K. L., Cummins, B. R., Cassell, R. J., and van Rijn, R. M. (2019). A Review of the Therapeutic Potential of Recently Developed G Protein-Biased Kappa Agonists. *Front. Pharmacol.* 10. doi:10.3389/fphar.2019.00407.

Morgan, M. M., and Christie, M. J. (2011). Analysis of opioid efficacy, tolerance, addiction and dependence from cell culture to human: Opioid efficacy, tolerance and addiction. *British Journal of Pharmacology* 164, 1322–1334. doi:10.1111/j.1476-5381.2011.01335.x.

Mori, T., Shibasaki, Y., Matsumoto, K., Shibasaki, M., Hasegawa, M., Wang, E., et al. (2013). Mechanisms that underlie μ-opioid receptor agonist-induced constipation: differential involvement of μ-opioid receptor sites and responsible regions. *J Pharmacol Exp Ther* 347, 91–99. doi:10.1124/jpet.113.204313.

Moye, L. S., Tipton, A. F., Dripps, I., Sheets, Z., Crombie, A., Violin, J. D., et al. (2019). Delta opioid receptor agonists are effective for multiple types of headache disorders. *Neuropharmacology* 148, 77–86. doi:10.1016/j.neuropharm.2018.12.017.

Mucha, R. F., and Herz, A. (1985). Motivational properties of kappa and mu opioid receptor agonists studied with place and taste preference conditioning. *Psychopharmacology* 86, 274–280. doi:10.1007/BF00432213.

Mudge, A. W., Leeman, S. E., and Fischbach, G. D. (1979). Enkephalin inhibits release of substance P from sensory neurons in culture and decreases action potential duration. *Proc Natl Acad Sci U S A* 76, 526–530. doi:10.1073/pnas.76.1.526.

Munro, T. A., Berry, L. M., Van't Veer, A., Béguin, C., Carroll, F. I., Zhao, Z., et al. (2012). Long-acting κ opioid antagonists nor-BNI, GNTI and JDTic: pharmacokinetics in mice and lipophilicity. *BMC Pharmacol* 12, 5. doi:10.1186/1471-2210-12-5.

Muratspahić, E., Freissmuth, M., and Gruber, C. W. (2019). Nature-Derived Peptides: A Growing Niche for GPCR Ligand Discovery. *Trends in Pharmacological Sciences* 40, 309–326. doi:10.1016/j.tips.2019.03.004.

Nadal, X., Baños, J.-E., Kieffer, B. L., and Maldonado, R. (2006). Neuropathic pain is enhanced in delta-opioid receptor knockout mice. *Eur J Neurosci* 23, 830–834. doi:10.1111/j.1460-9568.2006.04569.x.

Nagi, K., and Piñeyro, G. (2011). Regulation of opioid receptor signalling: Implications for the development of analgesic tolerance. *Mol Brain* 4, 25. doi:10.1186/1756-6606-4-25.

Nakanishi, S., Inoue, A., Kita, T., Nakamura, M., Chang, A. C., Cohen, S. N., et al. (1979). Nucleotide sequence of cloned cDNA for bovine corticotropin-beta-lipotropin precursor. *Nature* 278, 423–427. doi:10.1038/278423a0.

National Institute on Drug Abuse (2021). Overdose Death Rates. *National Institute on Drug Abuse*. Available at: https://www.drugabuse.gov/drug-topics/trends-statistics/overdose-death-rates [Accessed October 11, 2021].

Negus, S. S., Gatch, M. B., Mello, N. K., Zhang, X., and Rice, K. (1998). Behavioral effects of the delta-selective opioid agonist SNC80 and related compounds in rhesus monkeys. *J Pharmacol Exp Ther* 286, 362–375.

Negus, S. S., Henriksen, S. J., Matrox, A., Pasternak, G. W., Portoghese, P. S., Takemori, A. E., et al. (1993). *Effect of antagonists selective for mu, delta and kappa opioid receptors on the reinforcing effects of heroin in rats*.

Nelsen, J. L., Lapoint, J., Hodgman, M. J., and Aldous, K. M. (2010). Seizure and Coma Following Kratom (Mitragynina speciosa Korth) Exposure. *J. Med. Toxicol.* 6, 424–426. doi:10.1007/s13181-010-0079-5.

Nemoto, T., Ida, Y., Iihara, Y., Nakajima, R., Hirayama, S., Iwai, T., et al. (2013). The most effective influence of 17-(3-ethoxypropyl) substituent on the binding affinity and the agonistic activity in KNT-127 derivatives, δ opioid receptor agonists. *Bioorganic & Medicinal Chemistry* 21, 7628–7647. doi:10.1016/j.bmc.2013.10.032.

Newman, D. J., and Cragg, G. M. (2016). Natural Products as Sources of New Drugs from 1981 to 2014. *J Nat Prod* 79, 629–661. doi:10.1021/acs.jnatprod.5b01055.

Newman, D. J., and Cragg, G. M. (2020). Natural Products as Sources of New Drugs over the Nearly Four Decades from 01/1981 to 09/2019. *J. Nat. Prod.* 83, 770–803. doi:10.1021/acs.jnatprod.9b01285.

Nielsen, C. K., Simms, J. A., Li, R., Mill, D., Yi, H., Feduccia, A. A., et al. (2012a). -Opioid Receptor Function in the Dorsal Striatum Plays a Role in High Levels of Ethanol Consumption in Rats. *Journal of Neuroscience* 32, 4540–4552. doi:10.1523/JNEUROSCI.5345-11.2012.

Nielsen, C. K., Simms, J. A., Li, R., Mill, D., Yi, H., Feduccia, A. A., et al. (2012b). δ-Opioid Receptor Function in the Dorsal Striatum Plays a Role in High Levels of Ethanol Consumption in Rats. *J. Neurosci.* 32, 4540–4552. doi:10.1523/JNEUROSCI.5345-11.2012.

Nocjar, C., Middaugh, L. D., and Tavernetti, M. (1999). Ethanol consumption and place-preference conditioning in the alcohol-preferring C57BL/6 mouse: relationship with motor activity patterns. *Alcohol Clin Exp Res* 23, 683–692.

Noronha, A., Cui, C., Harris, R. A., and Crabbe, J. C. (2014). *Neurobiology of Alcohol Dependence*. Elsevier Inc. doi:10.1016/C2012-0-02501-X.

North, R. A., and Williams, J. T. (1985). On the potassium conductance increased by opioids in rat locus coeruleus neurones. *J Physiol* 364, 265–280. doi:10.1113/jphysiol.1985.sp015743.

Nozaki, C., Le Bourdonnec, B., Reiss, D., Windh, R. T., Little, P. J., Dolle, R. E., et al. (2012). δ-Opioid mechanisms for ADL5747 and ADL5859 effects in mice: analgesia, locomotion, and receptor internalization. *J Pharmacol Exp Ther* 342, 799–807. doi:10.1124/jpet.111.188987.

Obadiah, J., Avidor-Reiss, T., Fishburn, C. S., Carmon, S., Bayewitch, M., Vogel, Z., et al. (1999). Adenylyl Cyclase Interaction with the D2 Dopamine Receptor Family; Differential Coupling to Gi, Gz, and Gs. *Cell Mol Neurobiol* 19, 653–664. doi:10.1023/A:1006988603199.

Obeng, S., Kamble, S. H., Reeves, M. E., Restrepo, L. F., Patel, A., and Behnke, M. (2020a). Investigation of the Adrenergic and Opioid Binding Affinities, Metabolic Stability, Plasma Protein Binding Properties, and Functional Effects of Selected Indole-Based Kratom Alkaloids. *J. Med. Chem.*, 7.

Obeng, S., Kamble, S. H., Reeves, M. E., Restrepo, L. F., Patel, A., Behnke, M., et al. (2020b). Investigation of the Adrenergic and Opioid Binding Affinities, Metabolic Stability, Plasma Protein Binding Properties, and Functional Effects of Selected Indole-Based Kratom Alkaloids. *J. Med. Chem.* 63, 433–439. doi:10.1021/acs.jmedchem.9b01465.

Obeng, S., Wilkerson, J. L., León, F., Reeves, M. E., Restrepo, L. F., Gamez-Jimenez, L. R., et al. (2021). Pharmacological Comparison of Mitragynine and 7-Hydroxymitragynine: In Vitro Affinity and Efficacy for μ-Opioid Receptor and Opioid-Like Behavioral Effects in Rats. *J Pharmacol Exp Ther* 376, 410–427. doi:10.1124/jpet.120.000189.

Odlaug, B. L., Gual, A., DeCourcy, J., Perry, R., Pike, J., Heron, L., et al. (2016). Alcohol Dependence, Co-occurring Conditions and Attributable Burden. *Alcohol Alcohol* 51, 201–209. doi:10.1093/alcalc/agv088.

Okunji, C. O., Iwu, M. M., Ito, Y., and Smith, P. L. (2005). Preparative Separation of Indole Alkaloids from the Rind of Picralima nitida (Stapf) T. Durand & H. Durand by pH-Zone-Refining Countercurrent Chromatography. *Journal of Liquid Chromatography & Related Technologies* 28, 775–783. doi:10.1081/JLC-200048915.

Oldham, W. M., and Hamm, H. E. (2008). Heterotrimeric G protein activation by G-protein-coupled receptors. *Nat Rev Mol Cell Biol* 9, 60–71. doi:10.1038/nrm2299.

Olsen, R. H. J., DiBerto, J. F., English, J. G., Glaudin, A. M., Krumm, B. E., Slocum, S. T., et al. (2020). TRUPATH, an open-source biosensor platform for interrogating the GPCR transducerome. *Nat Chem Biol* 16, 841–849. doi:10.1038/s41589-020-0535-8.

O'Neill, S. J., Collins, M. A., Pettit, H. O., McNutt, R. W., and Chang, K. J. (1997). Antagonistic modulation between the delta opioid agonist BW373U86 and the mu opioid agonist fentanyl in mice. *J Pharmacol Exp Ther* 282, 271–277.

Orio, L., Alexandru, L., Cravotto, G., Mantegna, S., and Barge, A. (2012). UAE, MAE, SFE-CO2 and classical methods for the extraction of Mitragyna speciosa leaves. *Ultrasonics Sonochemistry* 19, 591–595. doi:10.1016/j.ultsonch.2011.10.001.

Ortega, A., Blount, J. F., and Manchand, P. S. (1982). Salvinorin, a new trans-neoclerodane diterpene from Salvia divinorum(Labiatae). *J. Chem. Soc., Perkin Trans. 1*, 2505–2508. doi:10.1039/P19820002505.

Ossipov, M. H., Dussor, G. O., and Porreca, F. (2010). Central modulation of pain. *J Clin Invest* 120, 3779–3787. doi:10.1172/JCI43766.

Palamar, J. J. (2021). Past-Year Kratom Use in the U.S.: Estimates From a Nationally Representative Sample. *American Journal of Preventive Medicine*. doi:10.1016/j.amepre.2021.02.004.

Pastor, R., Sanchis-Segura, C., and Aragon, C. M. G. (2005). Effect of selective antagonism of mu(1)-, mu(1/2)-, mu(3)-, and delta-opioid receptors on the locomotor-stimulating actions of ethanol. *Drug and Alcohol Dependence* 78, 289–295. doi:10.1016/j.drugalcdep.2004.11.007.

Pei, G., Kieffer, B. L., Lefkowitz, R. J., and Freedman, N. J. (1995). Agonist-dependent phosphorylation of the mouse delta-opioid receptor: involvement of G protein-coupled receptor kinases but not protein kinase C. *Mol Pharmacol* 48, 173–177.

Pepper, C. M., and Henderson, G. (1980). Opiates and opioid peptides hyperpolarize locus coeruleus neurons in vitro. *Science* 209, 394–395. doi:10.1126/science.7384811.

Perrine, S. A., Hoshaw, B. A., and Unterwald, E. M. (2006). Delta opioid receptor ligands modulate anxiety-like behaviors in the rat. *Br J Pharmacol* 147, 864–872. doi:10.1038/sj.bjp.0706686.

Pert, C. B., and Snyder, S. H. (1973). Opiate Receptor: Demonstration in Nervous Tissue. *Science* 179, 1011–1014. doi:10.1126/science.179.4077.1011.

Petry, N., Ledgerwood, D., and McKay, J. (2014). "Chapter 10. Treatment of substance use disorders," in *Clinical Manual of Addiction Psychopharmacology* (Washington, D.C.: American Psychiatric Publishing), 387–412. Available at: https://psychiatryonline.org/doi/abs/10.1176/appi.books.9781585625284 [Accessed October 31, 2021].

Pezalla, E. J., Rosen, D., Erensen, J. G., Haddox, J. D., and Mayne, T. J. (2017). Secular trends in opioid prescribing in the USA. *J Pain Res* 10, 383–387. doi:10.2147/JPR.S129553.

Pfeiffer, A., Brantl, V., Herz, A., and Emrich, H. M. (1986). Psychotomimesis mediated by kappa opiate receptors. *Science* 233, 774–776. doi:10.1126/science.3016896.

Phillips, T. J., Wenger, C. D., and Dorow, J. D. (1997). Naltrexone effects on ethanol drinking acquisition and on established ethanol consumption in C57BL/6J mice. *Alcohol Clin Exp Res* 21, 691–702.

Phillipson, J. D., Roberts, M. F., Zenk, M. H., and Phytochemical Society of Europe (1985). The Chemistry and biology of isoquinoline alkaloids. in Proceedings in life sciences. (Berlin: Springer-Verlag).

Piekielna-Ciesielska, J., Artali, R., Azzam, A. A. H., Lambert, D. G., Kluczyk, A., Gentilucci, L., et al. (2021). Pharmacological Characterization of μ-Opioid Receptor Agonists with Biased G Protein or β-Arrestin Signaling, and Computational Study of Conformational Changes during Receptor Activation. *Molecules* 26, 13. doi:10.3390/molecules26010013.

Piepponen, T. P., Kivastik, T., Katajamäki, J., Zharkovsky, A., and Ahtee, L. (1997). Involvement of Opioid μ1 Receptors in Morphine-Induced Conditioned Place Preference In Rats. *Pharmacology Biochemistry and Behavior* 58, 275–279. doi:10.1016/S0091-3057(96)00567-9.

Pierce, K. L., Premont, R. T., and Lefkowitz, R. J. (2002). Seven-transmembrane receptors. *Nat Rev Mol Cell Biol* 3, 639–650. doi:10.1038/nrm908.

Pineyro, G., and Nagi, K. (2021). Signaling diversity of mu- and delta- opioid receptor ligands: Re-evaluating the benefits of β-arrestin/G protein signaling bias. *Cellular Signalling* 80, 109906. doi:10.1016/j.cellsig.2020.109906.

Pizzagalli, D. A., Smoski, M., Ang, Y.-S., Whitton, A. E., Sanacora, G., Mathew, S. J., et al. (2020). Selective kappa-opioid antagonism ameliorates anhedonic behavior: evidence from the Fast-fail Trial in Mood and Anxiety Spectrum Disorders (FAST-MAS). *Neuropsychopharmacol.* 45, 1656–1663. doi:10.1038/s41386-020-0738-4.

Pollard, M. S., Tucker, J. S., and Green, H. D., Jr (2020). Changes in Adult Alcohol Use and Consequences During the COVID-19 Pandemic in the US. *JAMA Network Open* 3, e2022942–e2022942. doi:10.1001/jamanetworkopen.2020.22942.

Poole, H., White, S., Blake, C., Murphy, P., and Bramwell, R. (2009). Depression in Chronic Pain Patients: Prevalence and Measurement. *Pain Practice* 9, 173–180. doi:10.1111/j.1533-2500.2009.00274.x.

Porreca, F., Filla, A., and Burks, T. F. (1983). Studies in vivo with dynorphin-(1-9): analgesia but not gastrointestinal effects following intrathecal administration to mice. *Eur J Pharmacol* 91, 291–294. doi:10.1016/0014-2999(83)90481-8.

Porreca, F., Mosberg, H. I., Hurst, R., Hruby, V. J., and Burks, T. F. (1984). Roles of mu, delta and kappa opioid receptors in spinal and supraspinal mediation of gastrointestinal transit effects and hot-plate analgesia in the mouse. *J Pharmacol Exp Ther* 230, 341–348.

Porter-Stransky, K. A., and Weinshenker, D. (2017). Arresting the Development of Addiction: The Role of β-Arrestin 2 in Drug Abuse. *J Pharmacol Exp Ther* 361, 341–348. doi:10.1124/jpet.117.240622.

Pradhan, A. A. A., Becker, J. A. J., Scherrer, G., Tryoen-Toth, P., Filliol, D., Matifas, A., et al. (2009). In vivo delta opioid receptor internalization controls behavioral effects of agonists. *PLoS One* 4, e5425. doi:10.1371/journal.pone.0005425.

Pradhan, A. A. A., Walwyn, W., Nozaki, C., Filliol, D., Erbs, E., Matifas, A., et al. (2010). Ligand-directed trafficking of the δ-opioid receptor in vivo: two paths toward analgesic tolerance. *J Neurosci* 30, 16459–16468. doi:10.1523/JNEUROSCI.3748-10.2010.

Pradhan, A. A., Befort, K., Nozaki, C., Gavériaux-Ruff, C., and Kieffer, B. L. (2011). The delta opioid receptor: an evolving target for the treatment of brain disorders. *Trends Pharmacol Sci* 32, 581–590. doi:10.1016/j.tips.2011.06.008.

Pradhan, A. A., Smith, M. L., Kieffer, B. L., and Evans, C. J. (2012). Ligand-directed signalling within the opioid receptor family. *British Journal of Pharmacology* 167, 960–969. doi:10.1111/j.1476-5381.2012.02075.x.

Preto, A. J., Barreto, C. A. V., Baptista, S. J., Almeida, J. G. de, Lemos, A., Melo, A., et al. (2020). Understanding the Binding Specificity of G-Protein Coupled Receptors toward G-Proteins and Arrestins: Application to the Dopamine Receptor Family. *J. Chem. Inf. Model.* 60, 3969–3984. doi:10.1021/acs.jcim.0c00371.

Prozialeck, W. C. (2016). Update on the Pharmacology and Legal Status of Kratom. *J Am Osteopath Assoc* 116, 802–809. doi:10.7556/jaoa.2016.156.

Prozialeck, W. C., Avery, B. A., Boyer, E. W., Grundmann, O., Henningfield, J. E., Kruegel, A. C., et al. (2019). Kratom policy: The challenge of balancing therapeutic potential with public safety. *Int J Drug Policy* 70, 70–77. doi:10.1016/j.drugpo.2019.05.003.

Prozialeck, W. C., Jivan, J. K., and Andurkar, S. V. (2012). Pharmacology of kratom: an emerging botanical agent with stimulant, analgesic and opioid-like effects. *J Am Osteopath Assoc* 112, 792–799.

Qiu, F., Cai, G., Jaki, B. U., Lankin, D. C., Franzblau, S. G., and Pauli, G. F. (2013). Quantitative purity-activity relationships of natural products: the case of anti-tuberculosis active triterpenes from Oplopanax horridus. *J Nat Prod* 76, 413–419. doi:10.1021/np3007809.

Quock, R. M., Hosohata, Y., Knapp, R. J., Burkey, T. H., Hosohata, K., Zhang, X., et al. (1997). Relative efficacies of δ-opioid receptor agonists at the cloned human δ-opioid receptor. *European Journal of Pharmacology* 326, 101–104. doi:10.1016/S0014-2999(97)83488-7.

Raehal, K. M., Walker, J. K. L., and Bohn, L. M. (2005). Morphine Side Effects in β-Arrestin 2 Knockout Mice. *J Pharmacol Exp Ther* 314, 1195–1201. doi:10.1124/jpet.105.087254.

Rajagopal, S., Rajagopal, K., and Lefkowitz, R. J. (2010). Teaching old receptors new tricks: biasing seven-transmembrane receptors. *Nat Rev Drug Discov* 9, 373–386. doi:10.1038/nrd3024.

Raman, M., Chen, W., and Cobb, M. H. (2007). Differential regulation and properties of MAPKs. *Oncogene* 26, 3100–3112. doi:10.1038/sj.onc.1210392.

Raynor, K., Kong, H., Chen, Y., Yasuda, K., Yu, L., Bell, G. I., et al. (1994). Pharmacological characterization of the cloned kappa-, delta-, and mu-opioid receptors. *Mol Pharmacol* 45, 330–334.

Reiter, E., Ahn, S., Shukla, A. K., and Lefkowitz, R. J. (2012). Molecular mechanism of β-arrestin-biased agonism at seven-transmembrane receptors. *Annu Rev Pharmacol Toxicol* 52, 179–197. doi:10.1146/annurev.pharmtox.010909.105800.

Renthal, W. (2016). Seeking Balance Between Pain Relief and Safety: CDC Issues New Opioid-Prescribing Guidelines. *JAMA Neurol* 73, 513. doi:10.1001/jamaneurol.2016.0535.

Reuben, D. B., Alvanzo, A. A. H., Ashikaga, T., Bogat, G. A., Callahan, C. M., Ruffing, V., et al. (2015). National Institutes of Health Pathways to Prevention Workshop: the role of opioids in the treatment of chronic pain. *Ann Intern Med* 162, 295–300. doi:10.7326/M14-2775.

Rhee, S. G., and Bae, Y. S. (1997). Regulation of phosphoinositide-specific phospholipase C isozymes. *J Biol Chem* 272, 15045–15048. doi:10.1074/jbc.272.24.15045.

Rhodes, J. S., Best, K., Belknap, J. K., Finn, D. A., and Crabbe, J. C. (2005). Evaluation of a simple model of ethanol drinking to intoxication in C57BL/6J mice. *Physiology & Behavior* 84, 53–63. doi:10.1016/j.physbeh.2004.10.007.

Richards, E. M., Mathews, D. C., Luckenbaugh, D. A., Ionescu, D. F., Machado-Vieira, R., Niciu, M. J., et al. (2016). A randomized, placebo-controlled pilot trial of the delta opioid receptor agonist AZD2327 in anxious depression. *Psychopharmacology (Berl)* 233, 1119–1130. doi:10.1007/s00213-015-4195-4.

Ritter, S. L., and Hall, R. A. (2009). Fine-tuning of GPCR activity by receptor-interacting proteins. *Nat Rev Mol Cell Biol* 10, 819–830. doi:10.1038/nrm2803.

Roberts, A. J., McDonald, J. S., Heyser, C. J., Kieffer, B. L., Matthes, H. W., Koob, G. F., et al. (2000). mu-Opioid receptor knockout mice do not self-administer alcohol. *J Pharmacol Exp Ther* 293, 1002–1008.

Robins, M., Chiang, T., Berry, J., Ko, M., Ha, J., and Van Rijn, R. (2018a). Behavioral Characterization of β-Arrestin 1 Knockout Mice in Anxiety-Like and Alcohol Behaviors. *Frontiers in Behavioral Neuroscience*. doi:10.3389/fnbeh.2018.00054.

Robins, M. T., Chiang, T., Mores, K. L., Alongkronrusmee, D., and Van Rijn, R. M. (2018b). Critical Role for Gi/o-Protein Activity in the Dorsal Striatum in the Reduction of Voluntary Alcohol Intake in C57Bl/6 Mice. *Frontiers in psychiatry* 9, 112. doi:10.3389/fpsyt.2018.00112.

Rosenbaum, D. M., Rasmussen, S. G. F., and Kobilka, B. K. (2009). The structure and function of G-protein-coupled receptors. *Nature* 459, 356–363. doi:10.1038/nature08144.

Rösner, S., Hackl-Herrwerth, A., Leucht, S., Lehert, P., Vecchi, S., and Soyka, M. (2010a). Acamprosate for alcohol dependence. *Cochrane Database Syst Rev*, CD004332. doi:10.1002/14651858.CD004332.pub2.

Rösner, S., Hackl-Herrwerth, A., Leucht, S., Vecchi, S., Srisurapanont, M., and Soyka, M. (2010b). Opioid antagonists for alcohol dependence. *Cochrane Database Syst Rev*, CD001867. doi:10.1002/14651858.CD001867.pub2.

Roth, B. L., Baner, K., Westkaemper, R., Siebert, D., Rice, K. C., Steinberg, S., et al. (2002). Salvinorin A: A potent naturally occurring nonnitrogenous κ opioid selective agonist. *PNAS* 99, 11934–11939. doi:10.1073/pnas.182234399.

Ruiz-Garcia, V., and Lopez-Briz, E. (2008). Morphine remains gold standard in breakthrough cancer pain. *BMJ* 337, a3104. doi:10.1136/bmj.a3104.

Rush, B. (1784). *An inquiry into the effects of ardent spirits upon the human body and mind: with an account of the means of preventing, and of the remedies for curing them*. 8th ed. E. Merriam & Co. Available at: https://collections.nlm.nih.gov/catalog/nlm:nlmuid-2569025R-bk [Accessed October 31, 2021].

Rusin, K. I., Giovannucci, D. R., Stuenkel, E. L., and Moises, H. C. (1997). Kappa-opioid receptor activation modulates Ca2+ currents and secretion in isolated neuroendocrine nerve terminals. *J Neurosci* 17, 6565–6574.

Sachdev, S., Banister, S. D., Santiago, M., Bladen, C., Kassiou, M., and Connor, M. (2020). Differential activation of G protein-mediated signaling by synthetic cannabinoid receptor agonists. *Pharmacology Research & Perspectives* 8, e00566. doi:10.1002/prp2.566.

Sacks, J. J., Gonzales, K. R., Bouchery, E. E., Tomedi, L. E., and Brewer, R. D. (2015). 2010 National and State Costs of Excessive Alcohol Consumption. *Am J Prev Med* 49, e73–e79. doi:10.1016/j.amepre.2015.05.031.

Saitoh, A., Kimura, Y., Suzuki, T., Kawai, K., Nagase, H., and Kamei, J. (2004). Potential anxiolytic and antidepressant-like activities of SNC80, a selective delta-opioid agonist, in behavioral models in rodents. *J Pharmacol Sci* 95, 374–380. doi:10.1254/jphs.fpj04014x.

Saitoh, A., Yoshikawa, Y., Onodera, K., and Kamei, J. (2005). Role of δ-opioid receptor subtypes in anxiety-related behaviors in the elevated plus-maze in rats. *Psychopharmacology* 182, 327–334. doi:10.1007/s00213-005-0112-6.

SAMHSA (2015). 2015 National Survey on Drug Use and Health: Detailed Tables. Available at: https://www.samhsa.gov/data/sites/default/files/NSDUH-ServiceUseAdult-2015/NSDUH-ServiceUseAdult-2015/NSDUH-ServiceUseAdult-2015.htm.

SAMHSA (2019). 2019 National Survey on Drug Use and Health (NSDUH). Available at: https://www.samhsa.gov/data/release/2019-national-survey-drug-use-and-health-nsduh-releases.

Saref, A., Suraya, S., Singh, D., Grundmann, O., Narayanan, S., Swogger, M. T., et al. (2019). Self-reported prevalence and severity of opioid and kratom (Mitragyna speciosa korth.) side effects. *Journal of Ethnopharmacology* 238, 111876. doi:10.1016/j.jep.2019.111876.

Schank, J. R., Goldstein, A. L., Rowe, K. E., King, C. E., Marusich, J. A., Wiley, J. L., et al. (2012). The kappa opioid receptor antagonist JDTic attenuates alcohol seeking and withdrawal anxiety. *Addiction Biology* 17, 634–647. doi:10.1111/j.1369-1600.2012.00455.x.

Schappert, S. M., and Burt, C. W. (2006). Ambulatory care visits to physician offices, hospital outpatient departments, and emergency departments: United States, 2001-02. *Vital Health Stat 13*, 1–66.

Schattauer, S. S., Kuhar, J. R., Song, A., and Chavkin, C. (2017). Nalfurafine is a G-protein biased agonist having significantly greater bias at the human than rodent form of the kappa opioid receptor. *Cellular Signalling* 32, 59–65. doi:10.1016/j.cellsig.2017.01.016.

Schmid, C. L., Kennedy, N. M., Ross, N. C., Lovell, K. M., Yue, Z., Morgenweck, J., et al. (2017). Bias Factor and Therapeutic Window Correlate to Predict Safer Opioid Analgesics. *Cell* 171, 1165-1175.e13. doi:10.1016/j.cell.2017.10.035.

Schmitz, R. (1985). Friedrich Wilhelm Sertürner and the discovery of morphine. *Pharm Hist* 27, 61–74.

Schröder, W., Lambert, D. G., Ko, M. C., and Koch, T. (2014). Functional plasticity of the N/OFQ-NOP receptor system determines analgesic properties of NOP receptor agonists. *Br J Pharmacol* 171, 3777–3800. doi:10.1111/bph.12744.

Schuckit, M. A. (2014). Recognition and management of withdrawal delirium (delirium tremens). *N Engl J Med* 371, 2109–2113. doi:10.1056/NEJMra1407298.

Scott, J. (1969). *The White Poppy - a History of Opium.* New York, NY: Funk & Wagnalls.

Sessa, B., Higbed, L., O'Brien, S., Durant, C., Sakal, C., Titheradge, D., et al. (2021). First study of safety and tolerability of 3,4-methylenedioxymethamphetamine-assisted psychotherapy in patients with alcohol use disorder. *J Psychopharmacol* 35, 375–383. doi:10.1177/0269881121991792.

Seyedabadi, M., Gharghabi, M., Gurevich, E. V., and Gurevich, V. V. (2021). Receptor-Arrestin Interactions: The GPCR Perspective. *Biomolecules* 11, 218. doi:10.3390/biom11020218.

Shippenberg, T. S., Stein, C., Huber, A., Millan, M. J., and Herz, A. (1988). Motivational effects of opioids in an animal model of prolonged inflammatory pain: alteration in the effects of kappa- but not of mu-receptor agonists. *Pain* 35, 179–186. doi:10.1016/0304-3959(88)90225-4.

Simon, E. J., Hiller, J. M., and Edelman, I. (1973). Stereospecific Binding of the Potent Narcotic Analgesic [3H]Etorphine to Rat-Brain Homogenate. *PNAS* 70, 1947–1949. doi:10.1073/pnas.70.7.1947.

Singh, D., Müller, C. P., and Vicknasingam, B. K. (2014). Kratom (Mitragyna speciosa) dependence, withdrawal symptoms and craving in regular users. *Drug Alcohol Depend* 139, 132–137. doi:10.1016/j.drugalcdep.2014.03.017.

Singh, D., Narayanan, S., Müller, C. P., Swogger, M. T., Chear, N. J. Y., Dzulkapli, E. B., et al. (2019). Motives for using Kratom (Mitragyna speciosa Korth.) among regular users in Malaysia. *Journal of Ethnopharmacology* 233, 34–40. doi:10.1016/j.jep.2018.12.038.

Singh, D., Narayanan, S., and Vicknasingam, B. (2016). Traditional and non-traditional uses of Mitragynine (Kratom): A survey of the literature. *Brain Research Bulletin* 126, 41–46. doi:10.1016/j.brainresbull.2016.05.004.

Singh, D., Yeou Chear, N. J., Narayanan, S., Leon, F., Sharma, A., McCurdy, C. R., et al. (2020). Patterns and reasons for kratom (Mitragyna speciosa) use among current and former opioid poly-drug users. *Journal of Ethnopharmacology* 249, 112462. doi:10.1016/j.jep.2019.112462.

Singla, N. K., Skobieranda, F., Soergel, D. G., Salamea, M., Burt, D. A., Demitrack, M. A., et al. (2019). APOLLO-2: A Randomized, Placebo and Active-Controlled Phase III Study Investigating Oliceridine (TRV130), a G Protein–Biased Ligand at the μ-Opioid Receptor, for Management of Moderate to Severe Acute Pain Following Abdominoplasty. *Pain Practice* 19, 715–731. doi:10.1111/papr.12801.

Singla, N., Minkowitz, H. S., Soergel, D. G., Burt, D. A., Subach, R. A., Salamea, M. Y., et al. (2017). A randomized, Phase IIb study investigating oliceridine (TRV130), a novel μ-receptor G-protein pathway selective (μ-GPS) modulator, for the management of moderate to severe acute pain following abdominoplasty. *J Pain Res* 10, 2413–2424. doi:10.2147/JPR.S137952.

Sinha, R., and Li, C. S. R. (2007). Imaging stress- and cue-induced drug and alcohol craving: association with relapse and clinical implications. *Drug Alcohol Rev* 26, 25–31. doi:10.1080/09595230601036960.

Sittl, R., Nuijten, M., and Nautrup, B. P. (2005). Changes in the prescribed daily doses of transdermal fentanyl and transdermal buprenorphine during treatment of patients with cancer and noncancer pain in Germany: results of a retrospective cohort study. *Clin Ther* 27, 1022–1031. doi:10.1016/j.clinthera.2005.06.024.

Skinner, M. D., Lahmek, P., Pham, H., and Aubin, H.-J. (2014). Disulfiram efficacy in the treatment of alcohol dependence: a meta-analysis. *PLoS One* 9, e87366. doi:10.1371/journal.pone.0087366.

Smith, K. E., and Lawson, T. (2017). Prevalence and motivations for kratom use in a sample of substance users enrolled in a residential treatment program. *Drug Alcohol Depend* 180, 340–348. doi:10.1016/j.drugalcdep.2017.08.034.

Smrcka, A. V. (2008). G protein βγ subunits: Central mediators of G protein-coupled receptor signaling. *Cell Mol Life Sci* 65, 2191–2214. doi:10.1007/s00018-008-8006-5.

Snyder, S. H., and Pasternak, G. W. (2003). Historical review: Opioid receptors. *Trends in Pharmacological Sciences* 24, 198–205. doi:10.1016/S0165-6147(03)00066-X.

Soergel, D. G., Ann Subach, R., Sadler, B., Connell, J., Marion, A. S., Cowan, C. L., et al. (2014a). First Clinical Experience With TRV130: Pharmacokinetics and Pharmacodynamics in Healthy Volunteers: The Journal of Clinical Pharmacology. *The Journal of Clinical Pharmacology* 54, 351–357. doi:10.1002/jcph.207.

Soergel, D. G., Subach, R. A., Burnham, N., Lark, M. W., James, I. E., Sadler, B. M., et al. (2014b). Biased agonism of the μ-opioid receptor by TRV130 increases analgesia and reduces on-target adverse effects versus morphine: A randomized, double-blind, placebo-controlled, crossover study in healthy volunteers: *Pain* 155, 1829–1835. doi:10.1016/j.pain.2014.06.011.

Sorkin, A., and von Zastrow, M. (2009). Endocytosis and signalling: intertwining molecular networks. *Nat Rev Mol Cell Biol* 10, 609–622. doi:10.1038/nrm2748.

Spanagel, R., Herz, A., and Shippenberg, T. S. (1992). Opposing tonically active endogenous opioid systems modulate the mesolimbic dopaminergic pathway. *Proc Natl Acad Sci U S A* 89, 2046–2050. doi:10.1073/pnas.89.6.2046.

Spetea, M., Eans, S. O., Ganno, M. L., Lantero, A., Mairegger, M., Toll, L., et al. (2017). Selective κ receptor partial agonist HS666 produces potent antinociception without inducing aversion after i.c.v. administration in mice. *British Journal of Pharmacology* 174, 2444–2456. doi:10.1111/bph.13854.

Stahl, E. L., and Bohn, L. M. (2021). Low Intrinsic Efficacy Alone Cannot Explain the Improved Side Effect Profiles of New Opioid Agonists. *Biochemistry*. doi:10.1021/acs.biochem.1c00466.

Stanciu, C. N., Gnanasegaram, S. A., Ahmed, S., and Penders, T. (2019). Kratom Withdrawal: A Systematic Review with Case Series. *J Psychoactive Drugs* 51, 12–18. doi:10.1080/02791072.2018.1562133.

Stanczyk, M. A., Livingston, K. E., Chang, L., Weinberg, Z. Y., Puthenveedu, M. A., and Traynor, J. R. (2019). The δ-opioid receptor positive allosteric modulator BMS 986187 is a G-protein-biased allosteric agonist. *Br J Pharmacol* 176, 1649–1663. doi:10.1111/bph.14602.

Standifer, K. M., and Pasternak, G. W. (1997). G proteins and opioid receptor-mediated signalling. *Cell Signal* 9, 237–248. doi:10.1016/s0898-6568(96)00174-x.

Sternini, C., Spann, M., Anton, B., Keith, D. E., Bunnett, N. W., Zastrow, M. von, et al. (1996). Agonist-selective endocytosis of mu opioid receptor by neurons in vivo. *PNAS* 93, 9241–9246. doi:10.1073/pnas.93.17.9241.

Stevenson, G. W., Folk, J. E., Rice, K. C., and Negus, S. S. (2005). Interactions between delta and mu opioid agonists in assays of schedule-controlled responding, thermal nociception, drug self-administration, and drug versus food choice in rhesus monkeys: studies with SNC80 [(+)-4-[(alphaR)-alpha-((2S,5R)-4-allyl-2,5-dimethyl-1-piperazinyl)-3-methoxybenzyl]-N,N-diethylbenzamide] and heroin. *J Pharmacol Exp Ther* 314, 221–231. doi:10.1124/jpet.104.082685.

Substance Abuse Center for Behavioral Health Statistics and Quality (2020). Results from the 2019 National Survey on Drug Use and Health: Detailed Tables. *SAMHSA*, 2472.

Sufka, K. J., Loria, M. J., Lewellyn, K., Zjawiony, J. K., Ali, Z., Abe, N., et al. (2014). The effect of Salvia divinorum and Mitragyna speciosa extracts, fraction and major constituents on place aversion and place preference in rats. *J Ethnopharmacol* 151, 361–364. doi:10.1016/j.jep.2013.10.059.

Suhaimi, F. W., Hassan, Z., Mansor, S. M., and Müller, C. P. (2021). The effects of chronic mitragynine (Kratom) exposure on the EEG in rats. *Neuroscience Letters* 745, 135632. doi:10.1016/j.neulet.2021.135632.

Suhaimi, F. W., Yusoff, N. H. M., Hassan, R., Mansor, S. M., Navaratnam, V., Müller, C. P., et al. (2016). Neurobiology of Kratom and its main alkaloid mitragynine. *Brain Research Bulletin* 126, 29–40. doi:10.1016/j.brainresbull.2016.03.015.

Sunahara, R. K., Dessauer, C. W., and Gilman, A. G. (1996). Complexity and diversity of mammalian adenylyl cyclases. *Annu Rev Pharmacol Toxicol* 36, 461–480. doi:10.1146/annurev.pa.36.040196.002333.

Suwanlert, S. (1975). A study of kratom eaters in Thailand. *Bull Narc* 27, 21–27.

Swift, R. M., and Aston, E. R. (2015). Pharmacotherapy for Alcohol Use Disorder: Current and Emerging Therapies. *Harv Rev Psychiatry* 23, 122–133. doi:10.1097/HRP.0000000000000079.

Swogger, M. T., and Walsh, Z. (2018). Kratom use and mental health: A systematic review. *Drug and Alcohol Dependence* 183, 134–140. doi:10.1016/j.drugalcdep.2017.10.012.

Syrovatkina, V., Alegre, K. O., Dey, R., and Huang, X.-Y. (2016). Regulation, Signaling, and Physiological Functions of G-Proteins. *Journal of Molecular Biology* 428, 3850–3868. doi:10.1016/j.jmb.2016.08.002.

Takayama, H. (2004). Chemistry and Pharmacology of Analgesic Indole Alkaloids from the Rubiaceous Plant, Mitragyna speciosa. 52, 13.

Takayama, H., Ishikawa, H., Kurihara, M., Kitajima, M., Aimi, N., Ponglux, D., et al. (2002). Studies on the synthesis and opioid agonistic activities of mitragynine-related indole alkaloids: discovery of opioid agonists structurally different from other opioid ligands. *J. Med. Chem.* 45, 1949–1956. doi:10.1021/jm010576e.

Takemori, A. E., and Portoghese, P. S. (1984). Comparative antagonism by naltrexone and naloxone of μ, κ, and δ agonists. *European Journal of Pharmacology* 104, 101–104. doi:10.1016/0014-2999(84)90374-1.

Tane, P., Tene, M., and Sterner, O. (2002). Picranitine, a new indole alkaloid from picralima nitida (APOCYNACEAE). *Bulletin of the Chemical Society of Ethiopia* 16, 165–168. doi:10.4314/bcse.v16i2.20939.

Tatum, W. O., Hasan, T. F., Coonan, E. E., and Smelick, C. P. (2018). Recurrent seizures from chronic kratom use, an atypical herbal opioid. *Epilepsy & Behavior Case Reports* 10, 18–20. doi:10.1016/j.ebcr.2018.04.002.

Terenius, L. (1973). Characteristics of the "Receptor" for Narcotic Analgesics in Synaptic Plasma Membrane Fraction from Rat Brain. *Acta Pharmacologica et Toxicologica* 33, 377–384. doi:10.1111/j.1600-0773.1973.tb01539.x.

The Nielsen Company (2020). Rebalancing the 'COVID-19 Effect' on alcohol sales. Available at: https://nielseniq.com/global/en/insights/2020/rebalancing-the-covid-19-effect-on-alcohol-sales/.

Theriot, J., Sabir, S., and Azadfard, M. (2021). "Opioid Antagonists," in *StatPearls* (Treasure Island (FL): StatPearls Publishing). Available at: http://www.ncbi.nlm.nih.gov/books/NBK537079/ [Accessed October 11, 2021].

Thompson, R. C., Mansour, A., Akil, H., and Watson, S. J. (1993). Cloning and pharmacological characterization of a rat μ opioid receptor. *Neuron* 11, 903–913. doi:10.1016/0896-6273(93)90120-G.

Toce, M. S., Chai, P. R., Burns, M. M., and Boyer, E. W. (2018). Pharmacologic Treatment of Opioid Use Disorder: a Review of Pharmacotherapy, Adjuncts, and Toxicity. *J. Med. Toxicol.* 14, 306–322. doi:10.1007/s13181-018-0685-1.

Torrecilla, M., Marker, C. L., Cintora, S. C., Stoffel, M., Williams, J. T., and Wickman, K. (2002). G-protein-gated potassium channels containing Kir3.2 and Kir3.3 subunits mediate the acute inhibitory effects of opioids on locus ceruleus neurons. *J Neurosci* 22, 4328–4334. doi:20026414.

Tseng, P.-Y., and Hoon, M. A. (2020). Molecular Genetics of Kappa Opioids in Pain and Itch Sensations. *Handb Exp Pharmacol*. doi:10.1007/164_2020_397.

Tsui, J. I., Burt, R., Thiede, H., and Glick, S. N. (2018). Utilization of buprenorphine and methadone among opioid users who inject drugs. *Subst Abus* 39, 83–88. doi:10.1080/08897077.2017.1363844.

Turk, D. C., Wilson, H. D., and Cahana, A. (2011). Treatment of chronic non-cancer pain. *Lancet* 377, 2226–2235. doi:10.1016/S0140-6736(11)60402-9.

Tzschentke, T. M. (2007). Measuring reward with the conditioned place preference (CPP) paradigm: update of the last decade. *Addict Biol* 12, 227–462. doi:10.1111/j.1369-1600.2007.00070.x.

Ueda, H., Harada, H., Nozaki, M., Katada, T., Ui, M., Satoh, M., et al. (1988). Reconstitution of rat brain mu opioid receptors with purified guanine nucleotide-binding regulatory proteins, Gi and Go. *Proc Natl Acad Sci U S A* 85, 7013–7017. doi:10.1073/pnas.85.18.7013.

Unterwald, E., Sasson, S., and Kornetsky, C. (1987). Evaluation of the supraspinal analgesic activity and abuse liability of ethylketocyclazocine. *Eur J Pharmacol* 133, 275–281. doi:10.1016/0014-2999(87)90023-9.

Uprety, R., Che, T., Zaidi, S. A., Grinnell, S. G., Varga, B. R., Faouzi, A., et al. (2021). Controlling opioid receptor functional selectivity by targeting distinct subpockets of the orthosteric site. *Elife* 10, e56519. doi:10.7554/eLife.56519.

Urban, J. D., Clarke, W. P., von Zastrow, M., Nichols, D. E., Kobilka, B., Weinstein, H., et al. (2007). Functional selectivity and classical concepts of quantitative pharmacology. *J. Pharmacol. Exp. Ther.* 320, 1–13. doi:10.1124/jpet.106.104463.

Urbano, M., Guerrero, M., Rosen, H., and Roberts, E. (2014). Antagonists of the kappa opioid receptor. *Bioorganic & Medicinal Chemistry Letters* 24, 2021–2032. doi:10.1016/j.bmcl.2014.03.040.

Vaidehi, N., and Kenakin, T. (2010). The role of conformational ensembles of seven transmembrane receptors in functional selectivity. *Curr Opin Pharmacol* 10, 775–781. doi:10.1016/j.coph.2010.09.004.

Valdés, L. J., Hatheld, G. M., Koreeda, M., and Paul, A. G. (1987). Studies ofSalvia divinorum (Lamiaceae), an Hallucinogenic mint from the Sierra Mazateca in Oaxaca, Central Mexico. *Econ Bot* 41, 283–291. doi:10.1007/BF02858975.

Valenti, E., Pettersson, D., and Motika, P. (2021). Kratom-Induced Seizures Associated With Reversible Basal Ganglia T1 Hyperintensities on MRI (1562). *Neurology* 96. Available at: https://n.neurology.org/content/96/15_Supplement/1562 [Accessed May 12, 2021].

Valentino, R. J., and Volkow, N. D. (2018). Untangling the complexity of opioid receptor function. *Neuropsychopharmacol* 43, 2514–2520. doi:10.1038/s41386-018-0225-3.

van der Westhuizen, E. T., Breton, B., Christopoulos, A., and Bouvier, M. (2014). Quantification of Ligand Bias for Clinically Relevant β_2 -Adrenergic Receptor Ligands: Implications for Drug Taxonomy. *Mol Pharmacol* 85, 492–509. doi:10.1124/mol.113.088880.

van Rijn, R. M., Brissett, D. I., and Whistler, J. L. (2010). Dual efficacy of delta opioid receptor-selective ligands for ethanol drinking and anxiety. *J Pharmacol Exp Ther* 335, 133–139. doi:10.1124/jpet.110.170969.

van Rijn, R. M., Brissett, D. I., and Whistler, J. L. (2012a). Distinctive modulation of ethanol place preference by delta opioid receptor-selective agonists. *Drug and Alcohol Dependence* 122, 156–159. doi:10.1016/j.drugalcdep.2011.09.024.

van Rijn, R. M., Brissett, D. I., and Whistler, J. L. (2012b). Emergence of Functional Spinal Delta Opioid Receptors After Chronic Ethanol Exposure. *Biological Psychiatry* 71, 232–238. doi:10.1016/j.biopsych.2011.07.015.

van Rijn, R. M., Defriel, J. N., and Whistler, J. L. (2013). Pharmacological traits of delta opioid receptors: pitfalls or opportunities. *Psychopharmacology (Berl)* 228, 1–18. doi:10.1007/s00213-013-3129-2.

van Rijn, R. M., and Whistler, J. L. (2009). The δ1 opioid receptor is a heterodimer that opposes the actions of the δ2 receptor on alcohol intake. *Biol Psychiatry* 66, 777–784. doi:10.1016/j.biopsych.2009.05.019.

Váradi, A., Marrone, G. F., Eans, S. O., Ganno, M. L., Subrath, J. J., Le Rouzic, V., et al. (2015a). Synthesis and Characterization of a Dual Kappa-Delta Opioid Receptor Agonist Analgesic Blocking Cocaine Reward Behavior. *ACS Chem. Neurosci.* 6, 1813–1824. doi:10.1021/acschemneuro.5b00153.

Váradi, A., Marrone, G. F., Palmer, T. C., Narayan, A., Szabó, M. R., Le Rouzic, V., et al. (2016). Mitragynine/Corynantheidine Pseudoindoxyls As Opioid Analgesics with Mu Agonism and Delta Antagonism, Which Do Not Recruit β-Arrestin-2. *J. Med. Chem.* 59, 8381–8397. doi:10.1021/acs.jmedchem.6b00748.

Váradi, A., Palmer, T. C., Haselton, N., Afonin, D., Subrath, J. J., Le Rouzic, V., et al. (2015b). Synthesis of Carfentanil Amide Opioids Using the Ugi Multicomponent Reaction. *ACS Chem. Neurosci.* 6, 1570–1577. doi:10.1021/acschemneuro.5b00137.

Vaughan, C. W., and Christie, M. J. (1997). Presynaptic inhibitory action of opioids on synaptic transmission in the rat periaqueductal grey in vitro. *J Physiol* 498 (Pt 2), 463–472. doi:10.1113/jphysiol.1997.sp021872.

Vázquez López, J. L., Schild, L., Günther, T., Schulz, S., Neurath, H., and Becker, A. (2017). The effects of kratom on restraint–stress-induced analgesia and its mechanisms of action. *Journal of Ethnopharmacology* 205, 178–185. doi:10.1016/j.jep.2017.05.008.

Vicente-Sanchez, A., Dripps, I. J., Tipton, A. F., Akbari, H., Akbari, A., Jutkiewicz, E. M., et al. (2018). Tolerance to high-internalizing δ opioid receptor agonist is critically mediated by arrestin 2. *British Journal of Pharmacology* 175, 3050–3059. doi:https://doi.org/10.1111/bph.14353.

Vicknasingam, B., Chooi, W. T., Rahim, A. A., Ramachandram, D., Singh, D., Ramanathan, S., et al. (2020). Kratom and Pain Tolerance: A Randomized, Placebo-Controlled, Double-Blind Study. *Yale J Biol Med* 93, 229–238.

Vijeepallam, K., Pandy, V., Murugan, D. D., and Naidu, M. (2019). Methanolic extract of Mitragyna speciosa Korth leaf inhibits ethanol seeking behaviour in mice: involvement of antidopaminergic mechanism. *Metab Brain Dis* 34, 1713–1722. doi:10.1007/s11011-019-00477-2.

Viscusi, E. R., Skobieranda, F., Soergel, D. G., Cook, E., Burt, D. A., and Singla, N. (2019). APOLLO-1: a randomized placebo and active-controlled phase III study investigating oliceridine (TRV130), a G protein-biased ligand at the μ-opioid receptor, for management of moderate-to-severe acute pain following bunionectomy. *J Pain Res* 12, 927–943. doi:10.2147/JPR.S171013.

Viscusi, E. R., Webster, L., Kuss, M., Daniels, S., Bolognese, J. A., Zuckerman, S., et al. (2016). A randomized, phase 2 study investigating TRV130, a biased ligand of the μ-opioid receptor, for the intravenous treatment of acute pain. *Pain* 157, 264–272. doi:10.1097/j.pain.0000000000000363.

Volkow, N., Benveniste, H., and McLellan, A. T. (2018). Use and Misuse of Opioids in Chronic Pain. *Annual Review of Medicine* 69, 451–465. doi:10.1146/annurev-med-011817-044739.

Volkow, N. D., and Blanco, C. (2021). The changing opioid crisis: development, challenges and opportunities. *Mol Psychiatry* 26, 218–233. doi:10.1038/s41380-020-0661-4.

Vowles, K. E., McEntee, M. L., Julnes, P. S., Frohe, T., Ney, J. P., and van der Goes, D. N. (2015). Rates of opioid misuse, abuse, and addiction in chronic pain: a systematic review and data synthesis. *Pain* 156, 569–576. doi:10.1097/01.j.pain.0000460357.01998.f1.

Walker, B. M., and Koob, G. F. (2008). Pharmacological evidence for a motivational role of kappa-opioid systems in ethanol dependence. *Neuropsychopharmacology* 33, 643–652. doi:10.1038/sj.npp.1301438.

Walker, B. M., Valdez, G. R., McLaughlin, J. P., and Bakalkin, G. (2012). Targeting dynorphin/kappa opioid receptor systems to treat alcohol abuse and dependence. *Alcohol* 46, 359–370. doi:10.1016/j.alcohol.2011.10.006.

Walker, B. M., Zorrilla, E. P., and Koob, G. F. (2011). Systemic κ-opioid receptor antagonism by nor-binaltorphimine reduces dependence-induced excessive alcohol self-administration in rats. *Addiction Biology* 16, 116–119. doi:10.1111/j.1369-1600.2010.00226.x.

Wang, J. B., Imai, Y., EPPLERt, C. M., Gregor, P., Spivak, C. E., and Uhl, G. R. (1993). ,u opiate receptor: cDNA cloning and expression. *Proc. Natl. Acad. Sci. USA*, 5.

Wei, Z. Y., Brown, W., Takasaki, B., Plobeck, N., Delorme, D., Zhou, F., et al. (2000). N,N-Diethyl-4-(phenylpiperidin-4-ylidenemethyl)benzamide: a novel, exceptionally selective, potent delta opioid receptor agonist with oral bioavailability and its analogues. *J Med Chem* 43, 3895–3905. doi:10.1021/jm000229p.

Wettschureck, N., and Offermanns, S. (2005). Mammalian G Proteins and Their Cell Type Specific Functions. *Physiological Reviews* 85, 1159–1204. doi:10.1152/physrev.00003.2005.

Whalen, E. J., Rajagopal, S., and Lefkowitz, R. J. (2011). Therapeutic potential of β-arrestin- and G protein-biased agonists. *Trends in Molecular Medicine* 17, 126–139. doi:10.1016/j.molmed.2010.11.004.

Whistler, J. L., Chuang, H., Chu, P., Jan, L. Y., and von Zastrow, M. (1999). Functional Dissociation of μ Opioid Receptor Signaling and Endocytosis: Implications for the Biology of Opiate Tolerance and Addiction. *Neuron* 23, 737–746. doi:10.1016/S0896-6273(01)80032-5.

Whistler, J. L., and Zastrow, M. von (1998). Morphine-activated opioid receptors elude desensitization by β-arrestin. *PNAS* 95, 9914–9919. doi:10.1073/pnas.95.17.9914.

White, K. L., Robinson, J. E., Zhu, H., DiBerto, J. F., Polepally, P. R., Zjawiony, J. K., et al. (2015). The G Protein–Biased κ-Opioid Receptor Agonist RB-64 Is Analgesic with a Unique Spectrum of Activities In Vivo. *J Pharmacol Exp Ther* 352, 98–109. doi:10.1124/jpet.114.216820.

Williams, J. T., Egan, T. M., and North, R. A. (1982). Enkephalin opens potassium channels on mammalian central neurones. *Nature* 299, 74–77. doi:10.1038/299074a0.

Wilson, L. L., Chakraborty, S., Eans, S. O., Cirino, T. J., Stacy, H. M., Simons, C. A., et al. (2021). Kratom Alkaloids, Natural and Semi-Synthetic, Show Less Physical Dependence and Ameliorate Opioid Withdrawal. *Cell Mol Neurobiol*. doi:10.1007/s10571-020-01034-7.

Wilson, L. L., Harris, H. M., Eans, S. O., Brice-Tutt, A. C., Cirino, T. J., Stacy, H. M., et al. (2020a). Lyophilized Kratom Tea as a Therapeutic Option for Opioid Dependence. *Drug and Alcohol Dependence* 216, 108310. doi:10.1016/j.drugalcdep.2020.108310.

Wilson, N., Kariisa, M., Seth, P., Smith, H., and Davis, N. L. (2020b). Drug and Opioid-Involved Overdose Deaths - United States, 2017-2018. *MMWR Morb Mortal Wkly Rep* 69, 290–297. doi:10.15585/mmwr.mm6911a4.

Witkiewitz, K., Litten, R. Z., and Leggio, L. (2019). Advances in the science and treatment of alcohol use disorder. *Sci Adv* 5, eaax4043. doi:10.1126/sciadv.aax4043.

Witkiewitz, K., Saville, K., and Hamreus, K. (2012). Acamprosate for treatment of alcohol dependence: mechanisms, efficacy, and clinical utility. *Ther Clin Risk Manag* 8, 45–53. doi:10.2147/TCRM.S23184.

Witkin, L. R., Zylberger, D., Mehta, N., Hindenlang, M., Johnson, C., Kean, J., et al. (2017). Patient-Reported Outcomes and Opioid Use in Outpatients With Chronic Pain. *J Pain* 18, 583–596. doi:10.1016/j.jpain.2016.12.018.

Wu, H., Wacker, D., Mileni, M., Katritch, V., Han, G. W., Vardy, E., et al. (2012). Structure of the human κ-opioid receptor in complex with JDTic. *Nature* 485, 327–332. doi:10.1038/nature10939.

Xuei, X., Dick, D., Flury-Wetherill, L., Tian, H.-J., Agrawal, A., Bierut, L., et al. (2006). Association of the κ -opioid system with alcohol dependence. *Molecular Psychiatry* 11, 1016–1024. doi:10.1038/sj.mp.4001882.

Yaksh, T. L., Yeung, J. C., and Rudy, T. A. (1976). Systematic examination in the rat of brain sites sensitive to the direct application of morphine: observation of differential effects within the periaqueductal gray. *Brain Res* 114, 83–103. doi:10.1016/0006-8993(76)91009-x.

Yalcin, I., and Barrot, M. (2014). The anxiodepressive comorbidity in chronic pain. *Curr Opin Anaesthesiol* 27, 520–527. doi:10.1097/ACO.0000000000000116.

Yamauchi, T., Abe, F., Chen, R., Nonaka, G.-I., Santisuk, T., and Padolina, W. G. (1990). Alkaloids from the leaves of Alstonia scholaris in Taiwan, Thailand, Indonesia and the Philippines. *Phytochemistry* 29, 3547–3552. doi:10.1016/0031-9422(90)85273-I.

Yang, C.-H., Huang, H.-W., Chen, K.-H., Chen, Y.-S., Sheen-Chen, S.-M., and Lin, C.-R. (2011). Antinociceptive potentiation and attenuation of tolerance by intrathecal β-arrestin 2 small interfering RNA in rats. *Br J Anaesth* 107, 774–781. doi:10.1093/bja/aer291.

Yudin, Y., and Rohacs, T. (2019). The G-protein-biased agents PZM21 and TRV130 are partial agonists of μ-opioid receptor-mediated signalling to ion channels. *Br J Pharmacol*, bph.14702. doi:10.1111/bph.14702.

Yue, K., Kopajtic, T. A., and Katz, J. L. (2018). Abuse liability of mitragynine assessed with a self-administration procedure in rats. *Psychopharmacology (Berl)* 235, 2823–2829. doi:10.1007/s00213-018-4974-9.

Yusof, S. R., Mohd Uzid, M., Teh, E.-H., Hanapi, N. A., Mohideen, M., Mohamad Arshad, A. S., et al. (2019). Rate and extent of mitragynine and 7-hydroxymitragynine blood–brain barrier transport and their intra-brain distribution: the missing link in pharmacodynamic studies. *Addiction Biology* 24, 935–945. doi:10.1111/adb.12661.

Yusoff, N. H. M., Suhaimi, F. W., Vadivelu, R. K., Hassan, Z., Rümler, A., Rotter, A., et al. (2016). Abuse potential and adverse cognitive effects of mitragynine (kratom). *Addiction Biology* 21, 98–110. doi:10.1111/adb.12185.

Zadina, J. E., Martin-Schild, S., Gerall, A. A., Kastin, A. J., Hackler, L., Ge, L.-J., et al. (1999). Endomorphins: Novel Endogenous μ-Opiate Receptor Agonists in Regions of High μ-Opiate Receptor Density. *Annals of the New York Academy of Sciences* 897, 136–144. doi:10.1111/j.1749-6632.1999.tb07885.x.

Zhang, Y., Xu, J., Wang, Z., Zhang, X., Liang, X., and Civelli, O. (2012). BmK-YA, an Enkephalin-Like Peptide in Scorpion Venom. *PLOS ONE* 7, e40417. doi:10.1371/journal.pone.0040417.

Zhou, J., Du, S.-Y., Dong, H.-J., Fang, L., and Feng, J.-H. (2019). Preparative Separation of Monoterpenoid Indole Alkaloid Epimers from Ervatamia yunnanensis Tsiang by pH-Zone-Refining Counter-Current Chromatography Combined with Preparative High-Performance Liquid Chromatography. *Molecules* 24, E1316. doi:10.3390/molecules24071316.

Zhou, Y., and Kreek, M. J. (2019). Combination of Clinically Utilized Kappa-Opioid Receptor Agonist Nalfurafine With Low-Dose Naltrexone Reduces Excessive Alcohol Drinking in Male and Female Mice. *Alcoholism: Clinical and Experimental Research* 43, 1077–1090. doi:10.1111/acer.14033.

Zhou, Y., Ramsey, S., Provasi, D., El Daibani, A., Appourchaux, K., Chakraborty, S., et al. (2021). Predicted Mode of Binding to and Allosteric Modulation of the μ-Opioid Receptor by Kratom's Alkaloids with Reported Antinociception In Vivo. *Biochemistry* 60, 1420–1429. doi:10.1021/acs.biochem.0c00658.

VITA

Anna Marie Gutridge was born to Kent and Michelle (nee Ferland) Gutridge in Zanesville, Ohio. Upon graduation at the top of her class from West Muskingum High School in 2013, she attended Wittenberg University with a full-tuition scholarship to earn her Bachelor of Science in Biochemistry and Molecular Biology with University and departmental honors. During her undergraduate education she participated in two summer research internships funded by the National Science Foundation at West Virginia State University and Central State University. She was also heavily involved in community service, spending nearly every spring break on Habitat for Humanity service trips, and leading the college Habitat for Humanity/Fuller Center for Housing chapter as president her senior year. Eager to continue her science education and earn a Ph.D., she joined the research lab of Dr. Richard van Rijn at Purdue University. Here she studied natural products and opioid pharmacology for application in alcohol abuse and pain therapeutics. During her graduate studies, Anna's research was supported by the Purdue University Ross fellowship, the Chaney Research Award, and multiple Purdue travel and research grants. She also had the honored distinction of being awarded a nationally competitive fellowship from the American Foundation of Pharmaceutical Education which partially funded her graduate studies. While at Purdue, she also had the opportunity to participate in an Applied Management Principles program and serve on the organizing committee for a large research symposium for graduate students at Purdue. With her Ph.D. in hand, Dr. Gutridge will be utilizing her preclinical pharmacology background in her to transition into clinical pharmaceutical research.

PUBLICATIONS

Hennessy MR[1], **Gutridge AM**[1], French AR, van Rijn RM, Riley, AP. Investigating the structure-activity relationships of akuammine, an alkaloid from Picralima nitida. (*Manuscript in final preparation*). [1]contributed equally.

French AR, **Gutridge AM**, Royer QH, Yuan J, van Rijn RM. Minor role for beta-arrestin 2 in kappa opioid receptor agonist modulation of voluntary alcohol consumption and locomotion. (*Manuscript under review*).

Meqbil YJ, Su H, Cassell RJ, Mores KL, **Gutridge AM**, Cummins BR, Chen L, van Rijn RM. Identification of a novel delta opioid receptor agonist chemotype with negative allosteric modulator capabilities. (2021) *Molecules.*

Gutridge AM[1], Chakraborty S[1], Varga BR[1], Rhoda ES, French AR, Blaine AT, Royer QH, Cui H, Yuan J, Cassell RJ, Szabo, M, Majumdar S, van Rijn RM. Evaluation of kratom opioid derivatives as potential treatment option for alcohol use disorder. (2021) *Frontiers in Pharmacology.* [1]contributed equally.

Sharifi, F, Meqbil, YJ, Otte, A, **Gutridge, AM**, Blaine, AT, van Rijn, RM, Park, K. Engineering Quick- and Long-acting Naloxone Delivery Systems for Treating Opioid Overdose. (2021) *Pharmaceutical Research*.

Chakraborty S, Dibertov J, Faouziv A, Bernhard SM, **Gutridge AM**, Ramsey S, Zhou Y, Provasi D, Nuthikattu N, Jilakia R, Nelson MF, Asher WB, Eans SO, Wilson L, Chintala S, Filizola M, van Rijn RM, Margolis EB, Roth B, McLaughlin JP, Che T, Sames D, Javitch J, Majumdar S. A novel mitragynine analog with low efficacy mu-opioid receptor agonism displays antinociception with attenuated adverse effects. (2021) *Journal of Medicinal Chemistry.*

Ko MJ, Chiang T, Mukadam AM, Mulia GE, **Gutridge AM**, Chester JA, van Rijn RM. β-arrestin-dependent ERK signaling positively correlates with reduced anxiety-like and conditioned fear-related behavior in mice. (2021) *Science Signaling*.

Creed SM[1], **Gutridge AM**[1], Argade MD, Hennessy MR, Friesen JB, Pauli GF, van Rijn RM, Riley AP. Isolation and Pharmacological Characterization of Six Opioidergic Picralima nitida Alkaloids. (2020) *ACS Journal of Natural Products*. [1]contributed equally.

Gutridge AM[1], Robins MT[1], Cassell RJ[1], Uprety R[1], Mores KL, Ko MJ, Pasternak GW, Majumdar S, van Rijn RM. Signal-biased kratom and -carfentanil-amide opioids as potential treatment for alcohol use disorder. (2020) *British Journal of Pharmacology*. [1]contributed equally.